CONTENT

1 INTRODUCTION

2 BASIC CONCEPTS

2 1 THE PHASE RULE OF GIBBS

2 2 PROJECTIONS AND SECTIONS

2 3 MONOVARIANT EQUILIBRIA PHASE TRANSFORMATIONS

3 TYPES OF FLUID PHASE BEHAVIOUR

3 1 THE CLASSIFICATION OF VAN KONYNENBURG AND SCOTT

3 2 TYPE I PHASE BEHAVIOUR

3 3 TYPE II PHASE BEHAVIOUR

3 4 TYPE V PHASE BEHAVIOUR

3 5 TYPE IV PHASE BEHAVIOUR

3 6 TYPE III PHASE BEHAVIOUR

3 7 TYPE VI PHASE BEHAVIOUR

3 8 INTERFERENCE WITH THE SOLID PHASE

4 DISCUSSION

REFERENCES

UNDERSTANDING PHASE DIAGRAMS

Th W DE LOOS
Delft University of Technology
Laboratory of Applied Thermodynamics and Phase Equilibria
Julianalaan 136 2628 BL Delft
The Netherlands

ABSTRACT The basic principles of phase diagrams are treated in such a way that they can be used as a tool to construct schematic phase diagrams based on limited information This tool can be used by the engineer for the interpretation of often limited experimental data and by the experimentalist to design experiments By means of the phase rule of Gibbs it is shown how phase equilibria are represented in P T x projections and P x- and T x sections The six basic types of fluid phase behaviour according to the classification of van Konynenburg and Scott are discussed In addition an example of a system is given where the formation of a solid phase interferes with critical phenomena

1 Introduction

For an understanding of the fundamentals of processing with near critical fluids and for the design of supercritical extraction processes a thorough knowledge of the phase behaviour of the mixtures involved is necessary Often one is dealing with two phase equilibria i e solid fluid or liquid-vapour equilibria but also multiphase equilibria like solid liquid vapour or liquid-liquid-vapour equilibria play an important role These equilibria are strongly influenced by pressure temperature and composition of these mixtures The ideal situation is that complete knowledge of the phase behaviour is available either from experiments or from a quantitative thermodynamic model This ideal situation is hardly ever met

Based on limited experimental information, however, it is often possible to predict qualitatively the phase behaviour of the system of interest at other than the experimental conditions These predictions can help to design additional experiments or to perform the right type of phase equilibrium calculations In order to make these qualitative predictions one should master the basic concepts of phase diagrams and one should be aware of the different possible types of phase behaviour

In this contribution the basic concepts of phase diagrams are treated Many of the features of phase diagrams can be derived from the phase rule of Gibbs [1] The representation of phase equilibria in P T- and T x projections and in T x and P x sections is discussed Special attention will be paid to special points in phase diagrams, like critical points and also to monovariant equilibria These monovariant equilibria and special points border the regions of extension of two phase equilibria The six basic types of fluid phase behaviour according to the classification

of van Konynenburg and Scott [2-4] will be discussed together with relevant P x and T x sections This treatment of phase equilibria will be restricted to binary systems Extensions to multicomponent systems can be found in older textbooks on phase equilibria [5-6]

2 Basic Concepts

2 1 THE PHASE RULE OF GIBBS

An equilibrium of Π phases in a system of N components is fully described by $2+\Pi(N\ 1)$ variables P T and the independent composition variables of each phase e g (N 1) mole fractions x_i The equilibrium conditions for this equilibrium can be expressed in $(\Pi\ 1)N$ equilibrium equat ons

$$\mu_i^{\alpha} = \mu_i^{\beta} = \quad = \mu_i^{\pi}\ , for\ i = 1,\ 2,\quad ,\ N \tag{1}$$

μ_i^{α} is the chemical potential of component i in phase α The difference between the number of variables and the number of equilibrium conditions is the number of degrees of freedom F

$$F = N - \Pi + 2 - \phi \tag{2}$$

Equation 2 is the famous phase rule of Gibbs In special cases one has to account for extra relations between the variables other than given by equation 1 This number of additional relations is ϕ For instance in the case of a binary azeotrope the composition of the liquid phase L and the vapour phase V are equal So $x_1^L = x_1^V$ and $\phi = 1$ The critical state a state in a phase diagram where two phases become identical can be counted as one phase with $\phi = 2$ See for instance the contribution of Heidemann [7] and of Peters [8] in these Proceedings

The phase rule can be used to classify the different types of systems and equilibria A system with one component is called a unary system, a system with two components a binary system, a system with three components a ternary system, etc The minimum number of phases $\Pi = 1$ so the maximum value of F is given by

$$F_{max} = N + 1 \tag{3}$$

Equation 3 gives the dimension of the space needed to represent the complete phase behaviour of an N component system For a unary system $F_{max} = 2$ and the phase behaviour of such a system can be represented in a two-dimensional P T-plane For $N=2$, $F_{max} = 3$ and we need a three-dimensional P T x_2-space to represent the system For a ternary system we need a four dimensional P,T x_2,x_3-space etc x_i is the mole fraction of component i The mole fraction of component 1 is a dependent variable and can be obtained from $\Sigma\, x_i = 1$ An equilibrium with $F=0$ is called nonvariant, an equilibrium with $F=1$ monovariant, an equilibrium with $F=2$ bivariant etc Since the minimum value of $F=0$ it can be concluded from equation 2 that the maximum number of phases that can coexist in a system with N components is

$$\Pi_{max} = N + 2 \tag{4}$$

For a unary system the phase rule gives

$$F = 3 - \Pi - \phi \tag{5}$$

and $\Pi_{max}=3$ According to equation 5 a three phase equilibrium is represented by a point in the P T plane the triple point More triple points are possible i e solid liquid vapour (SLV) or solid-solid-liquid ($S^{\alpha}S^{\beta}L$) S^{α} and S^{β} are different modification of the same solid compound Two phase equilibria are represented by a curve in the P T plane Examples are the melting curve (SL) the sublimation curve (SV) and the vapour pressure curve (LV) Equilibria of one homogeneous phase (S L or V) are represented by a region in the P T plane The regions of homogeneous phases are separated by the corresponding two phase curves and a triple point is found at the intersection of three two phase curves So the vapour-pressure curve starts in the triple point SLV and ends at the critical point L=V which is nonvariant according to equation 5 An example of a phase diagram of a unary system showing two solid modifications is given in Figure 1

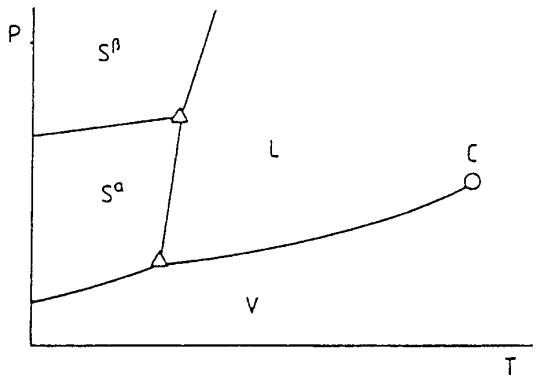

Figure 1 P T-diagram of an unary system showing two solid modifications

The phase rule for a binary system is given by

$$F = 4 - \Pi - \phi \tag{6}$$

In this case the maximum number of phases that can coexist is $\Pi_{max}=4$ The phase behaviour of binary systems is not only much more complicated because one needs three dimensions to represent the equilibria (P T x space) but also because many more phases are possible Solids can not only form many different solid modifications but solids of different compounds can also form one phase (mixed crystals) or do not mix at all or only mix partially Also one has to deal with more fluid phases For instance liquid water and liquid butan 2-ol are not completely miscible at all conditions Two liquid phases are formed one liquid is relatively more rich in

water the other liquid contains relatively more butan 2-ol In extreme cases the two liquids are almost pure components i e in the system mercury + water at room temperature The two liquid phases are often referred to as L_1 and L_2 If the mutual solubility of the two liquids increases for instance with increasing temperatures at constant pressure the two liquid components can become miscible in all proportions and the region of liquid liquid immiscibility is bordered by a liquid liquid critical point ($L = L_1$) The different types of phase equilibria and their representation in P T x space are given in Table 1

Table 1 Phase equilibria in binary systems and their representation in P T x space with $x = x_2$

		representation in P T x	examples
$\Pi = 1$	$F = 3$	region	S_1/S /L/V/L_1/L_2/S
$\Pi = 2$	$F = 2$	two surfaces $x^\alpha(P,T)$ $x^\beta(P\ T)$	LV/S_1L/L_2L_1
$\Pi = 3$	$F = 1$	three curves $x^\alpha[P(T)]$, $x^\beta[P(T)]$ $x^\gamma[P(T)]$	S_1LV/S_2S_1L/L_2L_1V
critical curve	$F = 1$	$x^c[P(T)]$	$L = V/L_2 = L_1$
azeotropic curve	$F = 1$	$x^{az}[P(T)]$	
$\Pi = 4$	$F = 0$	four points at one P and T	S S_1LV/$S_2L_2L_1$V
critical endpoint	$F = 0$	two points at one P and T	$L_2 = L_1V/L_2L_1 = V/SL = V$
critical azeotrope	$F = 0$	one point	

In a critical endpoint two phases of a three-phase equilibrium become identical and the two corresponding curves in the P,T,x space merge in one point From that point also a critical curve emerges A critical azeotrope is an endpoint of the azeotropic curve At this point the azeotropic curve is tangent to the critical curve $L = V$

As an example in Figure 2 the fluid phase behaviour of a binary system showing a L_2L_1V equilibrium with a critical endpoint $L_2 = L_1V$ and a critical endpoint $L_2L_1 = V$ is given in P,T x-space The critical endpoint $L_2 = L_1V$ is the low temperature limit of the three phase equilibrium and is for that reason called lower critical endpoint (LCEP) In this endpoint the phases L_2 and L_1 become identical The critical endpoint $L_2L_1 = V$ is the upper temperature limit of the three phase equilibrium and it is called an upper critical endpoint (UCEP) In this critical endpoint the phases L_1 and V become identical In the planes x = 0 and x = 1 the vapour pressure curves of the two pure components are found From the critical point of component 1 (x = 0) a critical curve $L_1 = V$ runs to the point $L_1 = V$ of the upper critical endpoint

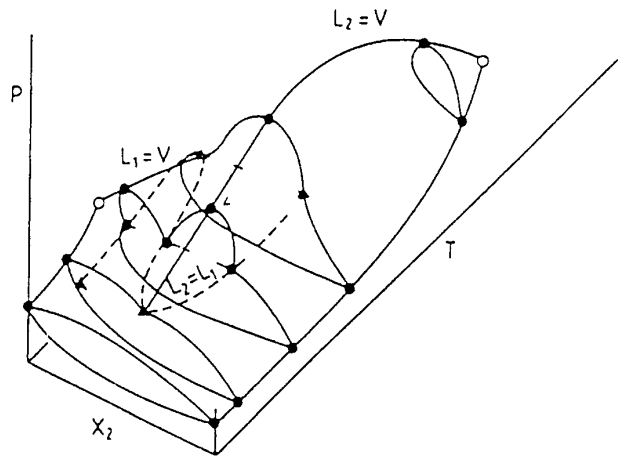

Figure 2 P T x-diagram of a binary system showing type V fluid phase behaviour

$L_2L_1=V$ and from the point $L_2=L_1$ of the lower critical endpoint $L_2=L_1V$ a critical curve $L_2=L_1$ runs to the critical point of pure component 2 (x = 1) At higher temperature the nature of this critical curve changes to $L_2=V$

For a ternary system the phase rule gives

$$F = 5 - \Pi - \phi \tag{7}$$

and one needs four dimensions (P T x_2 x_3 space) to represent all equilibria Since it is very hard to visualize a four dimensional space, it is common practice to represent the phase equilibria of a ternary system at constant pressure and temperature in a Gibbs triangle (see Figure 3) or at

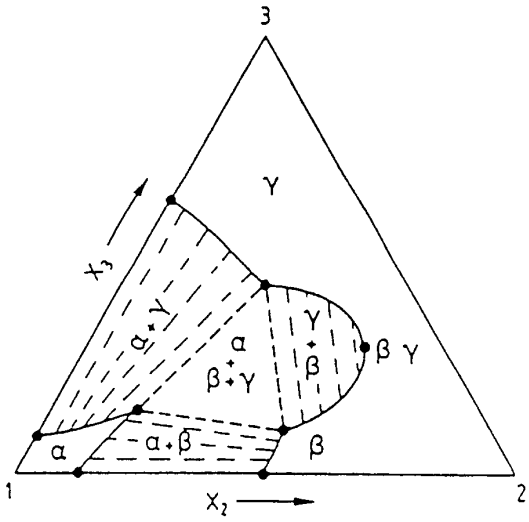

Figure 3 Reprensentation of ternary two phase and three phase equilibria at constant P and T in a Gibbs triangle _____ binodals _ _ _ tie lines

constant pressure or temperature in T x_2 x_3 or P x_2 x_3 prism Figure 3 shows a Gibbs triangle for a ternary system 1+2+3 The mole fractions x_2 and x_3 are chosen as the independent concentration variables A three-phase equilibrium $\alpha\beta\gamma$ is found in a three phase triangle whose vertices represent the compositions of the three phases Three two phase regions $\alpha\beta$ $\alpha\gamma$ and $\beta\gamma$ are grouped around the three phase triangle These two phase equilibria are represented by two curves i e $x_3^\alpha(x_2^\alpha)$ and $x_3^\beta(x_2^\beta)$ in the case of the $\alpha\beta$ equilibrium and tie lines which connect corresponding (=coexisting) points on these two curves The diagram also shows three one phase regions α, β and γ and a critical point $\beta=\gamma$ In the critical point the length of the tie line is zero and the coexisting phases have equal composition

2 2 PROJECTIONS AND SECTIONS

In practice mainly two-dimensional diagrams are used to represent phase equilibria and not the multi-dimensional P T $\underline{x}$ space representations like Figure 2 Most commonly used are projections of monovariant and nonvariant states on the P,T plane and sections of the P T,$\underline{x}$ space keeping one or more variables constant For instance Figure 3 is a ternary x_2,x_3 section at constant P and T For binary systems mainly P x sections at constant T and T x sections at constant P are used

Figure 4 gives the combined P T and T,x-*projections* which corresponds to the P,T x space of Figure 2 Since in these projections only monovariant and nonvariant equilibria can be shown the information on the details of the two-phase equilibria is lost in the projections

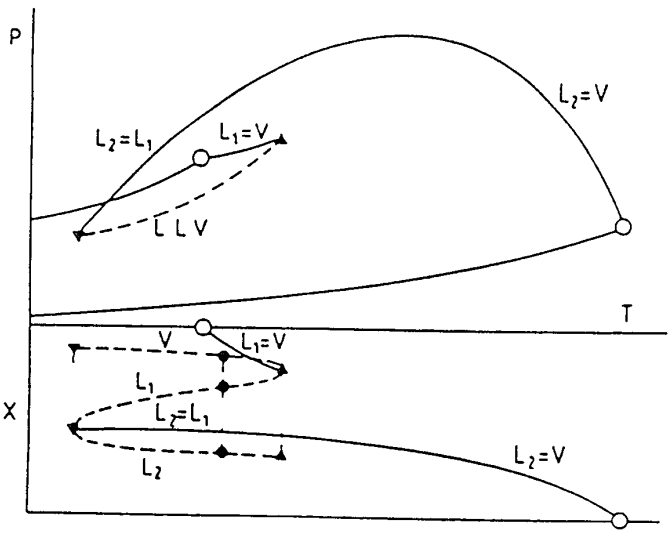

Figure 4 Combined P T and T x projections of type V fluid phase behaviour

The three phase equilibria which in P T x space are represented by three curves are represented by one curve in the P T projection and by three curves in the T x projection The reason for this is that at one temperature the three phases have different compositions but the same pressure so in P T projection the three curves coincide The P,T- projection also shows the two vapour pressure curves of the two pure components In the T x projection these curves are found along the axes x = 0 and x = 1 The critical curves are represented by a curve in both projections and the pure component critical points by a point The critical endpoints are

represented by one point in the P T projection and by two points in the T x projection

In a P,x or T x *section* a three phase equilibrium is represented by three points These points are found from the P T x-space from respectively the intersection of the plane T = constant or P = constant with the three curves representing the three phase equilibrium These points are also easily found from the P T- and T,x projection Two phase equilibria are represented by two curves in a P x or T x-section These curves are found from respectively the intersection of the plane T = constant or P = constant with the two surfaces representing the two phase equilibrium in P T x space

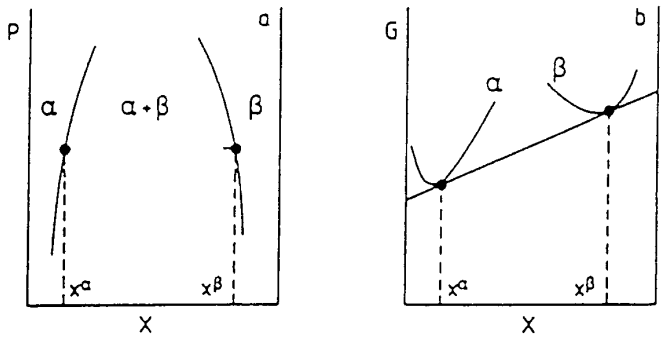

Figure 5 a P x section of a two phase equilibrium $\alpha\beta$ Schematic b G x-diagram for phases α and β at constant P and T

Figure 5a represents schematically a two-phase equilibrium $\alpha\beta$ in a P x section The figure shows two curves the composition of phase α and of phase β as a function of pressure In Figure 5b the Gibbs energy as function of composition is plotted for phase α and phase β at constant P and T A common tangent can be drawn to both curves These tangent points represent the coexisting phases α and β It can easily be shown that for the tangent points the equilibrium condition $\mu_i^\alpha = \mu_i^\beta$ for i = 1,2 is fulfilled [4] In the left part of Figure 5b phase α is the stable phase since it has a lower Gibbs energy than phase β In the right part of the diagram phase β is stable Between the two common tangent points an equilibrium of phase α and phase β is more stable than homogeneous phase α or homogeneous phase β The Gibbs energy of the two phase equilibrium $\alpha\beta$ is represented by the straight line through the two common tangent points, so the two phase equilibrium always has a lower Gibbs energy than phase α or phase β The consequence of this is that a mixture with a composition in between that of phase α and that of phase β will split into two phases with composition given by the curves $P(x^\alpha)$ and $P(x^\beta)$ To the left of the curve $P(x^\alpha)$ there will be a region with the homogeneous phase α to the right of the curve $P(x^\beta)$ there will be a region with the homogeneous phase β

The amounts of the phases α and β in case of a two phase equilibrium $\alpha\beta$ can easily be read from Figure 5a Suppose one mole of mixture with mole fraction x^0 splits in a moles of phase α and b moles of phase β From mass balances for the two components it is easily derived that

$$a = \frac{(x^{\beta} - x^{0})}{(x^{\beta} - x^{\alpha})} \quad and \quad b = \frac{(x^{0} - x^{\alpha})}{(x^{\beta} - x^{\alpha})} \tag{8}$$

Equation 8 is known as the lever rule

The compositions of the phases α and β can become equal in three different ways [4] The curves can intersect at x = 0 or x = 1 This is shown in Figure 6a which shows a liquid vapour equilibrium LV where the curve that represents the composition of phase L intersects the curve for phase V in the boiling points of both pure components Also the curves can merge in a horizontal tangent point $(\partial T/\partial x)_P = 0$ or $(\partial P/\partial x)_T = 0$ This type of point is a critical point where not only the compositions but all the thermodynamic properties of the two phases become identical A diagram with a critical point is shown in Figure 6b The third possibility is that the two curves have a common horizontal tangent In this case only the compositions of the two phases are equal but not the other thermodynamic properties An example is an azeotropic point (Figure 6c)

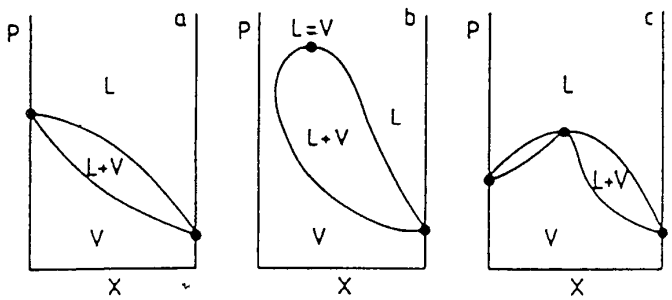

Figure 6 Three cases where the compositions of the two phases of a two phase equilibrium are equal a Pure component boiling points b Critical point c Azeotropic point

2 3 MONOVARIANT EQUILIBRIA PHASE TRANSFORMATIONS

For monovariant equilibria F=1, therefore these equilibria are represented by a curve in the P T projection The slope of this curve dP/dT is given by the equation of Clapeyron

$$T\left(\frac{dP}{dT}\right) = \frac{\Delta H}{\Delta V} \tag{9}$$

ΔH and ΔV are respectively the changes in enthalpy and volume of a so called phase transformation For instance in a unary system the two phase equilibria are monovariant In the case of the vapour pressure curve an LV equilibrium curve, the phase transformation is

$$1 \ mole \ L \rightarrow 1 \ mole \ V \tag{10}$$

and ΔH and ΔV are respectively the molar enthalpy (H^V H^L) and molar volume (V^V V^L) of

vaporization

The nature of the phase transformation can be derived from the Gibbs Duhem equation applied to all phases in equilibrium For a three phase equilibrium $\alpha\beta\gamma$ in a binary system these equations are

$$-(1-x^{\alpha})\,d\mu_1^{\alpha} - x^{\alpha}\,d\mu_2^{\alpha} + V^{\alpha}\,dP - S^{\alpha}\,dT = 0 \tag{11}$$

$$-(1-x^{\beta})\,d\mu_1^{\beta} - x^{\beta}\,d\mu_2^{\beta} + V^{\beta}\,dP - S^{\beta}\,dT = 0 \tag{12}$$

$$-(1-x^{\gamma})\,d\mu_1^{\gamma} - x^{\gamma}\,d\mu_2^{\gamma} + V^{\gamma}\,dP - S^{\gamma}\,dT = 0 \tag{13}$$

If one moves along the equilibrium curve from a state (P T) to a state (P+dP T+dT) the equilibrium condition

$$\mu_i^{\alpha} = \mu_i^{\beta} = \mu_i^{\gamma} \qquad for\ i = 1,2 \tag{14}$$

requires that

$$d\mu_i^{\alpha} = d\mu_i^{\beta} = d\mu_i^{\gamma} \qquad for\ i = 1,2 \tag{15}$$

so we can omit the superscripts of the $d\mu$ s in equations 11 13 After division by dT and rearranging these equations we get

$$-(1-x^{\alpha})\frac{d\mu_1}{dT} - x^{\alpha}\frac{d\mu_2}{dT} + V^{\alpha}\frac{dP}{dT} = S^{\alpha} \tag{16}$$

$$-(1-x^{\beta})\frac{d\mu_1}{dT} - x^{\beta}\frac{d\mu_2}{dT} + V^{\beta}\frac{dP}{dT} = S^{\beta} \tag{17}$$

$$-(1-x^{\gamma})\frac{d\mu_1}{dT} - x^{\gamma}\frac{d\mu_2}{dT} + V^{\gamma}\frac{dP}{dT} = S^{\gamma} \tag{18}$$

Equations 16 18 are three linear equations in $d\mu_1/dT$ $d\mu_2/dT$ and dP/dT According to Cramer s

rule the solution for dP/dT is

$$\frac{dP}{dT} = \frac{\begin{vmatrix} S^{\alpha} & (1-x^{\alpha}) & x^{\alpha} \\ S^{\beta} & (1-x^{\beta}) & x^{\beta} \\ S^{\gamma} & (1-x^{\gamma}) & x^{\gamma} \end{vmatrix}}{\begin{vmatrix} V^{\alpha} & (1-x^{\alpha}) & x^{\alpha} \\ V^{\beta} & (1-x^{\beta}) & x^{\beta} \\ V^{\gamma} & (1-x^{\gamma}) & x^{\gamma} \end{vmatrix}} = \frac{\Delta S}{\Delta V} \tag{19}$$

If we choose the phases α β and γ in such a way that $x^{\alpha} < x^{\beta} < x^{\gamma}$ than the phase transformation is

$$1 \ mole \ \beta \rightarrow a \ mole \ \alpha + c \ mole \ \gamma \tag{20}$$

with

$$a = \frac{(x^{\gamma} - x^{\beta})}{(x^{\gamma} - x^{\alpha})} \qquad and \qquad c = \frac{(x^{\beta} - x^{\alpha})}{(x^{\gamma} - x^{\alpha})} \tag{21}$$

and

$$\Delta S = a S^{\alpha} + c S^{\gamma} - S^{\beta} \tag{22}$$

$$\Delta V = a V^{\alpha} + c V^{\gamma} - V^{\beta} \tag{23}$$

Equation 21 is identical with equation 8, so at the P and T of the three phase equilibrium the phase with the middle mole fraction can transform into the phases with the lowest and with the highest mole fraction and the relative amounts of these phases are given by the lever rule It can be shown that for this transformation $\Delta G=0$ and since $\Delta G=\Delta H \ T\Delta S$ equation 19 is identical with equation 9 For monovariant equilibria in systems with more than two components similar equations can be derived

If at constant P and T on the vapour pressure curve of an unary system heat is added to the system an equivalent amount of liquid is vapourized into the vapour phase and the volume will change accordingly If heat is withdrawn the reverse process takes place This can be done until one of the phases has disappeared and the system ends up either in homogeneous vapour region or in the homogeneous liquid region A similar process takes place at a three phase equilibrium in a binary system at constant P and T However the final situation is now also dependent on the overall composition x^0 of the mixture If the transformation represented by equation 20 goes to the right the final situation is always a region of $(\alpha+\gamma)$ because one starts with $(\alpha+\beta+\gamma)$ and β disappears For the reverse transformation there are three possible final

states depending on which phase(s) disappear(s) first $(\alpha+\beta)$ if $x^{\alpha}<x^{0}<x^{\beta}$ (β) if $x^{0}=x^{\beta}$ and $(\beta+\gamma)$ if $x^{\beta}<x^{0}<x^{\gamma}$ The consequence of this is that the location of the one phase regions and of the two phase regions around a three phase equilibrium in a P x section or in a T x section are always as given in Figure 7 and Figure 8 Note that the topology of Figures 7a 8a and that of Figures 7b 8b is mirrored with respect to the line representing the three phase equilibrium

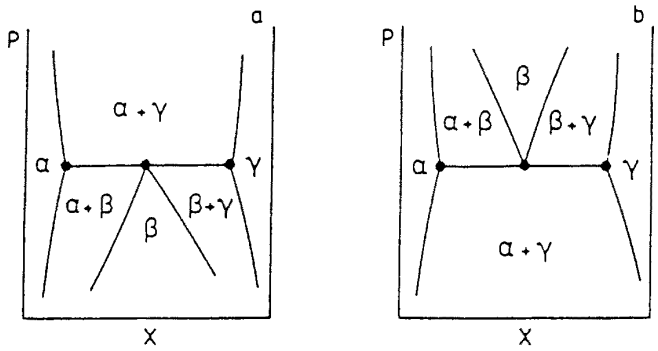

Figure 7 Possible locations of one and two phase equilibria around a three phase equilibrium in a P x section

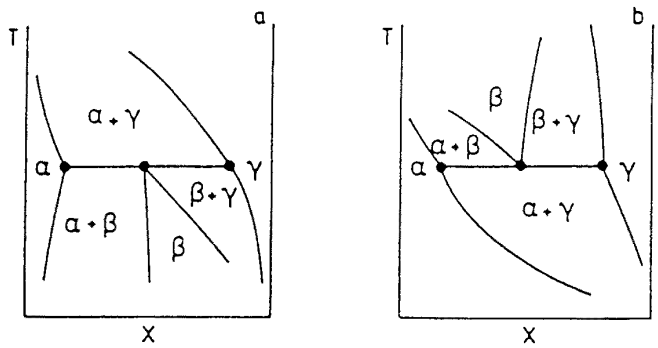

Figure 8 Possible locations of one and two phase equilibria around a three phase equilibrium in a T x section

3 Types of Fluid Phase Behaviour

3 1 THE CLASSIFICATION OF VAN KONYNENBURG AND SCOTT

According to the classification of van Konynenburg and Scott [2-4] one can distinguish between six main types of fluid phase behaviour which all have been found experimentally With exception of type VI the existence of these types of phase behaviour can be predicted with a

simple equation of state such as the van der Waals equation The occurrence of azeotropy leads to a subdivision of these six main types but we will not deal with that detail here Other equations of state than the van der Waals equation [9 10] can also produce type VI phase behaviour Many more types of fluid phase behaviour have been found computationally from different equations of state [11] but up till now all experimentally studied systems fit in the original classification of van Konynenburg and Scott with the exception of the systems butan-2-ol + water and butan 1-ol + water [12] that show a liquid liquid critical curve with a pressure minimum and a pressure maximum Also the transition in type of phase behaviour that has been reported in the family of systems of water + n alkanes [13] can not be explained by the van Konynenburg and Scott classification scheme Only the P T- and T x projections of the six main types of phase behaviour of Scott and van Konynenburg are discussed below together with relevant P x- and T x sections All diagrams are schematic

The best way to construct P x and T x-sections from given P T and T x projections is to plot first the information (pressure or temperature and phase compositions) on nonvariant and monovariant equilibria respectively at the given temperature or given pressure The location of the different one and two phase regions can than be found from general rules as discussed in sections 2 2 and 2 3 Figure 9 gives two sections with the same monovariant equilibria Figure 9a is incorrect In the critical point $\gamma=\delta$, dP/dx (or dT/dx) is not zero Also the curve running

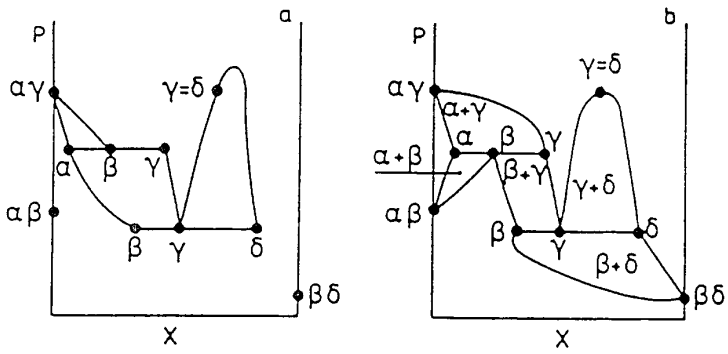

Figure 9 Two examples of a P x section with the same location of the monovariant equilibria a Incorrect See text b Correct

from the point β on the $\beta\gamma\delta$ equilibrium to the point α of the $\alpha\beta\gamma$ equilibrium is incorrect because this curve should represent the composition of the β phase in equilibrium with the γ-phase and can only connect points representing β phases To construct the correct diagram which is given in Figure 9b one can start with one of the three phase equilibria i e $\beta\gamma\delta$ According to Figure 7 and 8 there are only two possible arrangements of two phase equilibria around this three phase equilibrium It is clear that the two-phase region $\beta\delta$ can only end in the unary $\beta\delta$-equilibrium point at x = 1 since it is the only other $\beta\delta$ equilibrium possible The conclusion is that we have a two phase arrangement as in Figure 7b or Figure 8b For similar reasons as for the $\beta\delta$ region the $\gamma\delta$ region must end in the critical point $\gamma=\delta$ and the $\beta\gamma$ region must be the same two phase region as the $\beta\gamma$ region of the $\alpha\beta\gamma$ three phase equilibrium Now we can conclude that the location of the two-phase regions around the $\alpha\beta\gamma$ three phase equilibrium must be that of Figure 7a or Figure 8a It is now clear that the $\alpha\gamma$ and $\alpha\beta$ regions

found around the $\alpha\beta\gamma$ three phase equilibrium should end in the unary two phase points $\alpha\gamma$ and $\alpha\beta$ at $x = 0$ respectively

3 2 TYPE I PHASE BEHAVIOUR

In Figure 10 the combined P T and T x projections of type I phase behaviour are shown In a type I system only one critical curve is found This is the liquid vapour critical curve L = V which runs continuously from the critical point of component 1 to the critical point of component 2 Type I phase behaviour is found for instance in the binaries of methane with n alkanes up to n-pentane [4]

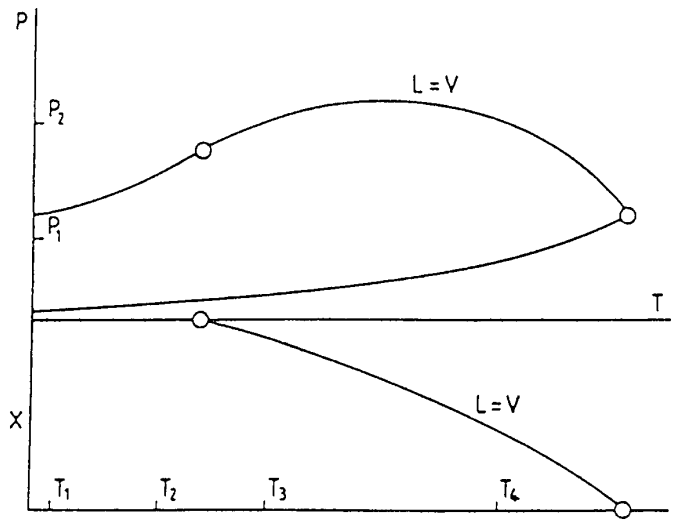

Figure 10 Combined P T and T x projections of type I fluid phase behaviour

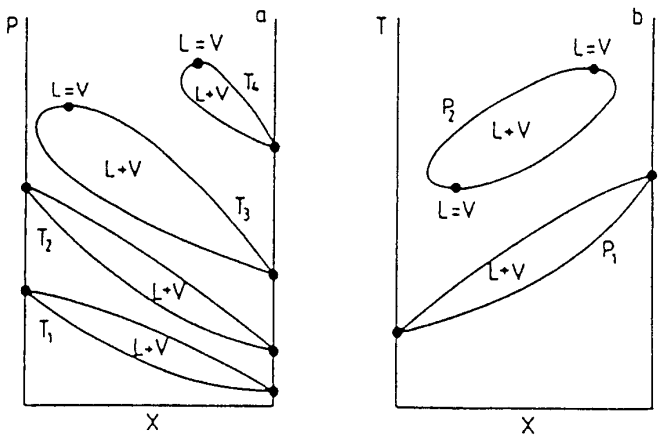

Figure 11 Type I fluid phase behaviour a P x sections at constant T See Figure 10 b T x sections at constant P See Figure 10

In Figure 11 some P x and T x sections are shown The P x sections at T1 and T2 have the shape of Figure 6a At T3 and T4 component 1 is supercritical and the P x sections show a binary critical point as in Figure 6b In the T x sections the two phase LV region has a reversed position compared with the P x section Note that the T x section at P2 shows two critical points which is a consequence of the pressure maximum of the critical curve in the P T projection These pressure maxima are often found in type I systems

3 3 TYPE II PHASE BEHAVIOUR

Type II fluid phase behaviour has a continuous liquid vapour critical curve just as in the case of type I In addition systems of this type show a liquid liquid critical curve $L_2=L_1$ and a three phase equilibrium L_2L_1V See Figure 12 which shows the P T and T x projection of a type II system In the P T projection the curves $L_2=L_1$ and L_2L_1V intersect in a UCEP $L_2=L_1V$ In

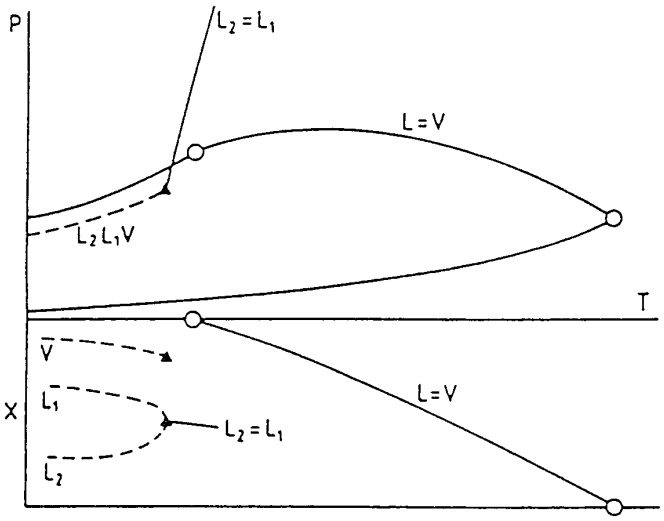

Figure 12 Combined P T and T x-projections of type II fluid phase behaviour

the diagram shown the liquid-liquid critical curve has a positive slope in the P T projection but this curve can also have a negative slope or a temperature minimum If not interrupted by the formation of a solid phase, the $L_2=L_1$ curve runs to infinite pressure Both the $L_2=L_1$ curve and the L_2L_1V curve can be completely hidden by a solid liquid equilibrium surface so in practice it may be impossible to distinguish between type I and type II fluid phase behaviour For instance, in the binary systems of carbon dioxide + n alkanes for carbon number n $6<n<13$ type II phase behaviour is found [14] For lower values of n no stable liquid-liquid equilibria are found but it is very likely that the system carbon dioxide + n pentane for instance is also of type II

In Figure 13 four characteristic P x sections are shown At low temperature the P x sections show a L_2L_1V equilibrium At higher pressure than the three phase pressure the L_1V and L_2L_1 two phase regions are found and at lower pressure the two phase region L_2V With increasing temperature the compositions of the two liquid phases of the L_2L_1V equilibrium approach each other as can be seen from the T x projection in Figure 12 At the temperature of

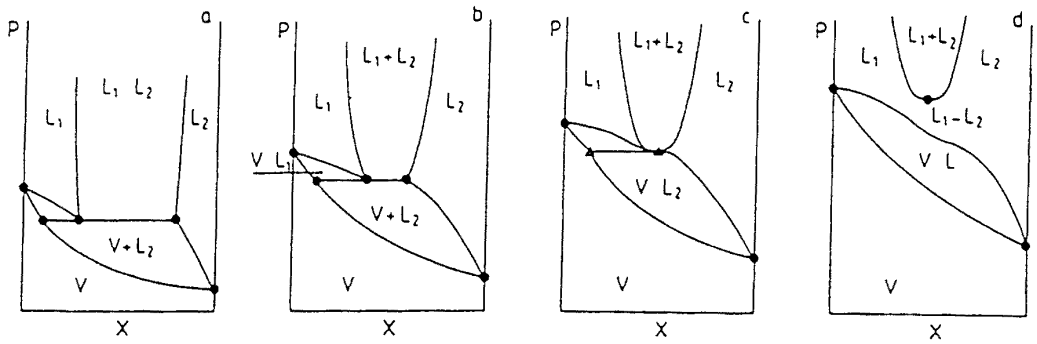

Figure 13 Type II fluid phase behaviour P x sections at constant T a b $T<T(L=L_1V)$ c $T=T(L_2=L_1V)$ d $T(L_2=L_1V)<T<T(L=V)$ $_{-0}$ See Figure 12

the UCEP a critical phase $L_2=L_1$ is in equilibrium with a vapour phase and as a consequence the L_1V and L_2V regions join in one two-phase region LV which shows a horizontal point of inflection at the $L_2=L_1$ critical point At higher temperatures the LV region and the L_2L_1 region are separated by a region of a homogeneous liquid phase At even higher temperatures the L_2L_1 region shifts to higher pressures and the LV region may detach on the left hand side as shown in Figure 11

3 4 TYPE V PHASE BEHAVIOUR

The phase behaviour of type V systems is the example we discussed earlier it is represented in P T x space in Figure 2 The corresponding P T and T x projections are given in Figure 4 Characteristic for this type of phase behaviour is a three phase equilibrium L_2L_1V with a LCEP $L_2=L_1V$ and a UCEP $L_2L_1=V$ and a discontinuous critical curve The first branch of the critical curve connects the critical point of the more volatile component with the UCEP The second branch runs from the LCEP to the critical point of the less volatile component Examples of type V systems are the systems methane + n hexane [15] and ethane + n eicosane [16] although there are reasons to believe that these systems are in reality type IV systems (see section 3 5)

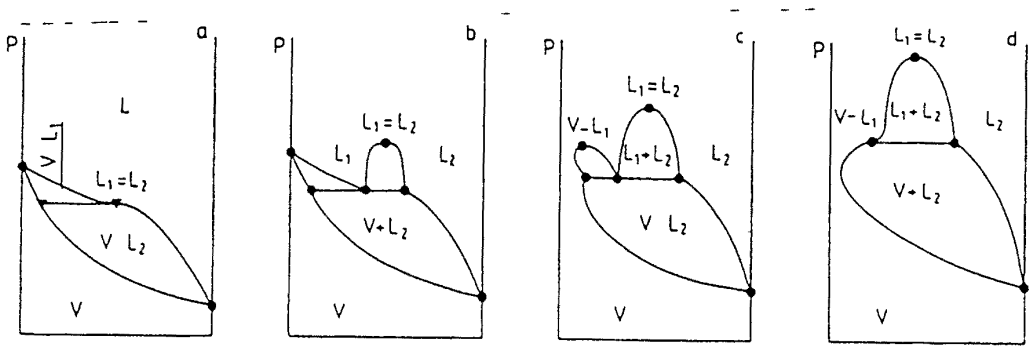

Figure 14 Type V fluid phase behaviour P x sections at constant T a $T=T(L=L_1V)$ b $T(L_2=L_1V)<T<T(L=V)$ $_{-0}$ c $T(L=V)$ $_{-0}<T<T(L_2L_1=V)$ d $T=T(L_2L_1=V)$ See Figure 4

In Figure 14 four P x sections are shown at temperatures $T(L_2=L_1V) \leq T \leq T(L_2L_1=V)$ At lower and at higher temperatures the P x sections are comparable with those of type I systems In Figure 14b a P,x section is shown at a temperature between the LCEP and the critical pointof the more volatile component This P x section is comparable with Figure 13a On lowering the temperature the composition of the L_2 phase and of the L_1 phase of the L_2L_1V equilibrium approach each other and the pressure of the $L_2=L_1$ critical point approaches the three phase pressure At the temperature of the LCEP (see Figure 14a) the L_2 and L_1 points of the three phase equilibrium and the critical point $L_2=L_1$ coincide The L_2L_1 two-phase region disappears and the L_1V and L_2V two phase regions join in one LV two phase region The LV region shows a horizontal point of inflection at the $L_2=L_1$ critical point At higher temperatures than the temperature of Figure 14b the L_1V region will detach from the axis $x=0$ (Figure 14c) and at even higher temperatures the composition of the L_1 phase and of the vapour phase of the L_2L_1V equilibrium approach each other At the temperature of the UCEP the L_1 and V points of the three phase equilibrium and the $L_1=V$ critical point coincide See Figure 14d At this temperature the L_1V two-phase region disappears and the L_2V and L_2L_1 two phase regions again join in one LV two phase region Now the LV region shows a horizontal point of inflection at the $L_1=V$ critical point

3 5 TYPE IV PHASE BEHAVIOUR

The combined P T- and T x projections of a type IV system are given in Figure 15 In this type of phase behaviour the three phase equilibrium L_2L_1V consist of two branches The low temperature branch shows a UCEP $L_2=L_1V$ and is comparable with the L_2L_1V equilibrium

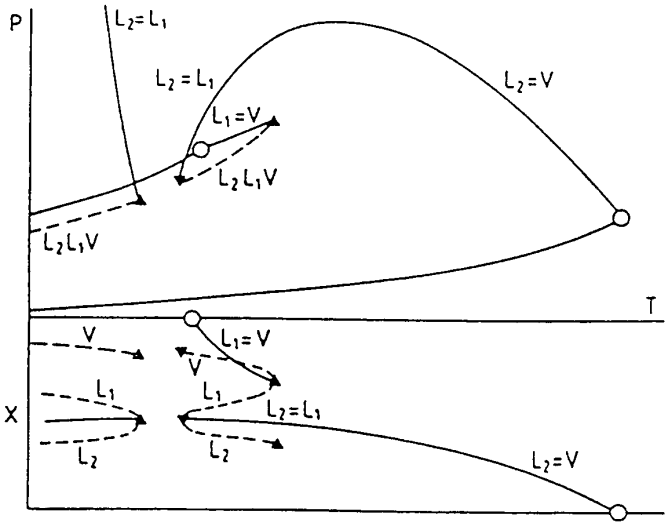

Figure 15 Combined P T and T x projections of type IV fluid phase behaviour

that is found in type II systems The high-temperature branch shows a LCEP $L_2=L_1V$ and a UCEP $L_2L_1=V$ and is comparable with the L_2L_1V equilibrium that is found in type V systems Not many binary type IV systems are known but for similar reasons as mentioned for type II phase behaviour it is likely that many systems that are supposed to show type V phase behaviour

in fact are of type IV and the low-temperature branch of the L_2L_1V equilibrium is masked by the solidification surface The system carbon dioxide + tridecane [17 18] is an example of a system showing type IV fluid phase behaviour

Since type II and type V phase behaviour is combined in type IV phase behaviour the P x sections at low temperatures are those of type II (Figure 13) and at high temperature those of type V (Figure 14) However phase diagrams at constant temperature can show two separated regions of liquid liquid immiscibility An example of a T x section is given in Figure 16 At this pressure the high temperature branch of the L_2L_1V curve is intersected in the P T projection The T x section shows three critical points At low temperature a critical point $L_2=L_1$ is the maximum

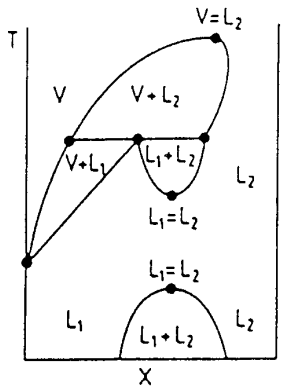

Figure 16 Type IV fluid phase behaviour T x section at constant P for $P(LCEP) < P < P(L=V)_{-0}$ See Figure 15

temperature of a L_2L_1 two phase region This kind of critical point is called upper critical solution temperature (UCST) The other $L_2=L_1$ critical point is the minimum temperature of a second L_2L_1 two-phase region, which ends at higher temperature at the L_2L_1V equilibrium This critical point is called a lower critical solution temperature (LCST) The third critical point is a liquid vapour critical point $L_2=V$

3 6 TYPE III PHASE BEHAVIOUR

In type III phase behaviour the two branches of the L_2L_1V equilibrium of type IV phase behaviour are combined and also two of the three branches of the critical curve that are found for type IV Only the UCEP $L_2L_1=V$ remains The P T and T x projection of type III phase behaviour are given in Figure 17 In the example shown the branch of the critical curve that runs from high pressure to the critical point of the less volatile component shows a pressure minimum and a pressure maximum An example of this behaviour is found in the system propane + triphenylmethane [19] This branch of the critical curve can also show a temperature minimum combined with a pressure minimum and a pressure maximum (i e carbon dioxide + tetradecane [20]) or only a temperature minimum (i e propane + water [21]) or can have a positive value of $(dP/dT)_c$ in the critical point of the less volatile component (i e He + Xe [22]) See Figure 18 Since in the latter two types of systems two phase equilibria can exist at higher temperatures than the critical temperature of the less volatile component these equilibria are often referred to

as gas gas equilibria The system He + Xe is said to show gas gas equilibria of the first kind (no minimum critical temperature) the system propane water gas gas equilibria of the second kind (the critical line passes through a minimum in temperature)

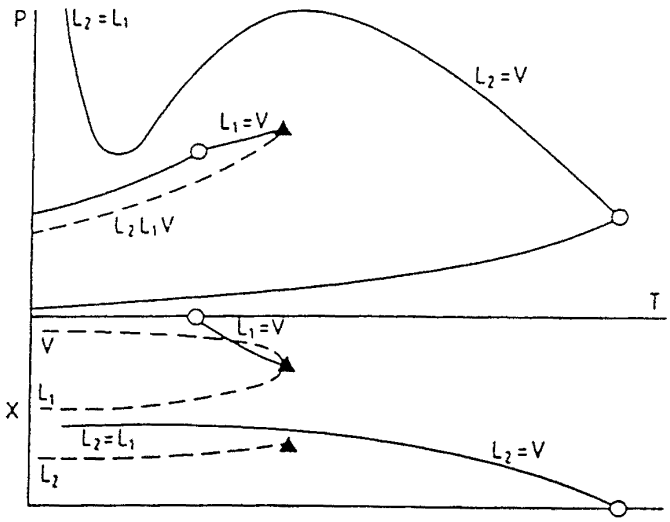

Figure 17 Combined P T and T x projections of type III fluid phase behaviour

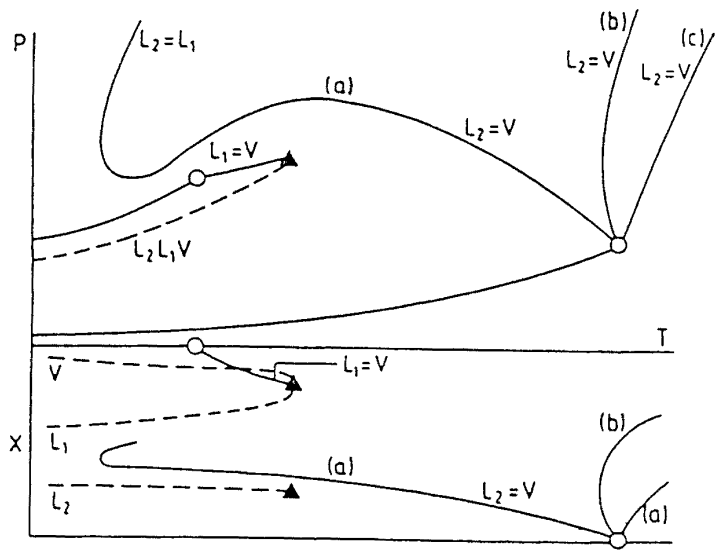

Figure 18 Combined P T and T x projections of type III fluid phase behaviour a Critical curve with a pressure maximum a pressure minimum and a temperature minimum b Critical curve with a temperature minimum (gas gas equilibria of the second kind) c Critical curve without a pressure maximum and a temperature minimum (gas gas equilibria of the first kind)

At temperatures lower than the UCEP $L_2L_1=V$ the P x sections corresponding to Figure 17 resemble those in Figure 14b At the temperature of the UCEP a P x section such as that in Figure 14c is found In Figure 19 some P x sections of a system showing gas gas equilibria of the second kind are shown in Figure 20 P x sections of a system showing gas gas equilibria of the first kind

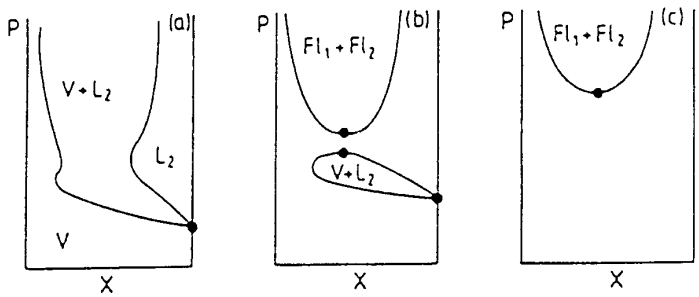

Figure 19 Gas gas equilibria of the second kind P x sections at constant T a $T(UCEP)<T<T_{min}(L_2=V)$ b $T_{min}(L_2=V)<T<T(L=V)_{-1}$ c $T>T(L=V)_{-1}$

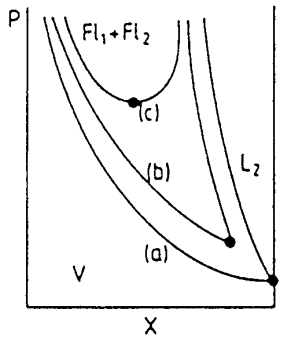

Figure 20 Gas gas equilibria of the first kind P x sections at constant T a $T=T(L=V)_1$ $T(a)<T(b)<T(c)$

3 7 TYPE VI PHASE BEHAVIOUR

Type VI phase behaviour is found in systems with specific chemical interactions i e water + 2-butoxyethanol [23] In the P T projection a three phase equilibrium L_2L_1V is found with a LCEP $L_2=L_1V$ and a UCEP $L_2=L_1V$ In Figure 21 the LCEP and UCEP are connected by a $L_2=L_1$ critical curve which shows a pressure maximum Another possibility is the existence of a second $L_2=L_1$ critical curve at high pressure with a pressure minimum This phenomenon is called high pressure immiscibility Also the low pressure immiscibility region and the high pressure immiscibility region can be combined in one uninterrupted L_2L_1 region [14]

At temperatures between the temperature of the LCEP and of the UCEP the P x sections which correspond to Figure 21 resemble those of Figure 14b At the temperature of the LCEP and the UCEP the P x section is like that in Figure 14a A typical T x section is shown in Figure 22 At the pressure of this T x-section two separate two-phase regions LV and L_2L_1 are found The L_2L_1 two phase region is a closed loop with a LCST and a UCST

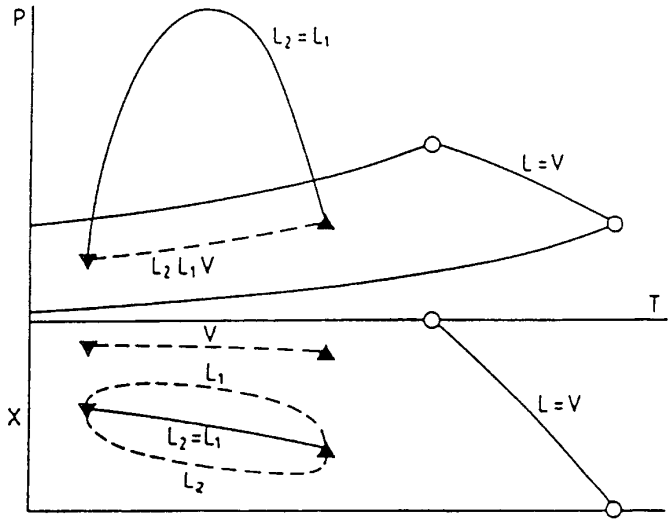

Figure 21 Combined P T and T x projections of type VI fluid phase behaviour

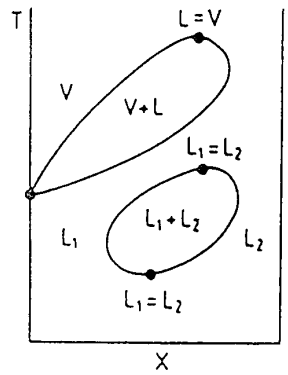

Figure 22 Type VI fluid phase behaviour T x section at P(UCEP) < P < P(L = V)

3 8 INTERFERENCE WITH THE SOLID PHASE

In practice the L_2L_1V equilibrium in type III systems ends at lower temperature in a four phase equilibrium $S_2L_2L_1V$, a quadruple point With increasing molecular weight of the less volatile component this quadruple point shifts to higher temperature and even passes the UCEP $LL_1 = V$

See also the contribution of Peters [8] The result is a P T and T x projection as given in Figure 23 Again the critical curve shows two branches One branch runs in the P T projection from the critical point of the more volatile component to a point of intersection with a three phase curve S_2LV This point of intersection is called the first critical endpoint of the S_2LV equilibrium The second branch of the critical curve runs from a point of intersection with a second branch of the S_2LV equilibrium to the critical point of the less volatile component This intersection point is called the second critical endpoint of the S_2LV equilibrium The second branch of this three phase equilibrium starts in the triple point of the pure less volatile component and can show a temperature minimum as is the case in Figure 23 As a consequence the curves in the T x projection representing the composition of the liquid phase and of the vapour phase along the

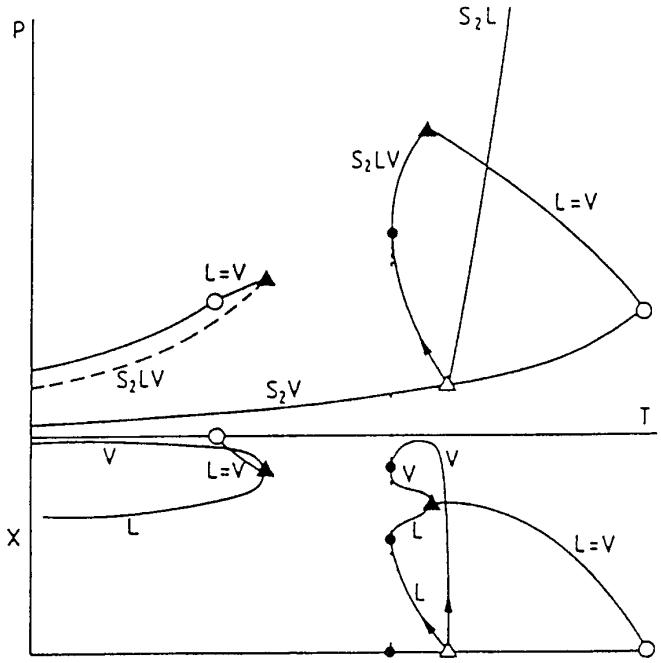

Figure 23 Interference of the solid phase Type III fluid phase behaviour The L_1L_2V curve is masked by solid fluid equilibria

three-phase equilibrium also show a temperature minimum With increasing pressure the mole fraction of component 2 in the liquid decreases as indicated by the arrows in the P T- and T x-projection, because component 1 the supercritical fluid will dissolve better at high pressure The mole fraction of component 2 in the vapour phase is one in the triple point of 2 but in the binary system the vapour is at low pressure almost pure component 1 So the vapour mole fraction approaches zero at low pressure but will increase again with increasing pressure due to the increasing density of the vapour phase and as a consequence its increasing solvent power The melting curve of component 2 S_2L, coincides in the T x projection with the axis $x=1$

This type of phase behaviour is displayed by the system carbon dioxide + naphthalene

[24] In the system ethylene + naphthalene [25] dP/dT of the second branch of the S-LV equilibrium is negative from triple point to second critical endpoint In the system nitrogen + naphthalene [26] this slope is always positive

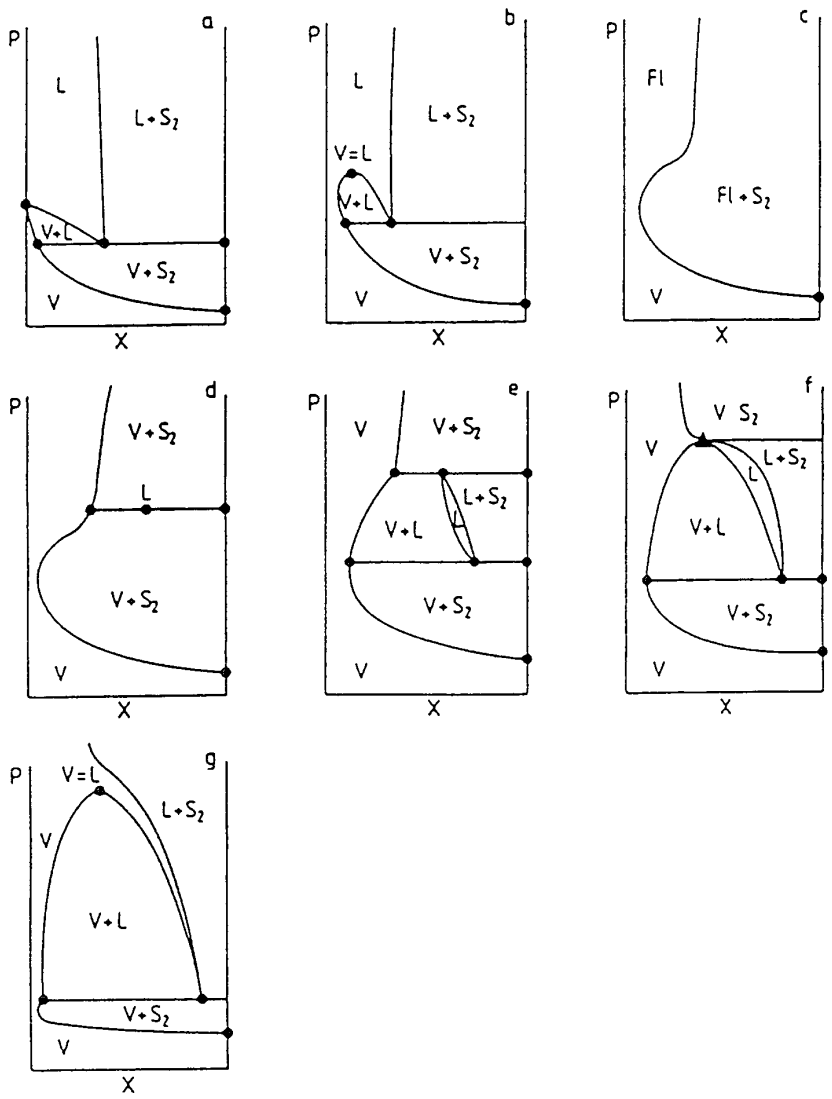

Figure 24 P x sections for the phase behaviour shown in Figure 23 See text

In Figure 24 a series of P x sections corresponding to Figure 23 is shown At temperatures below the critical point of the more volatile component (Figure 24a) a two phase region S_2V is separated from a S_2L region a homogeneous liquid region and a LV region by the

three phase equilibrium S_2LV Between the critical temperature of the more volatile component and the temperature of the first critical endpoint $S_2L=V$ the LV region ends at high pressure in a L=V critical point (Figure 24b) At the temperature of this critical endpoint the L point and the V point of the three phase equilibrium coincide with the L=V critical point The LV region disappears and the S_2V region and the S_2L region merge into one solid fluid two phase region which shows a horizontal point of inflection at the L=V critical point As a consequence of this horizontal point of inflection the mole fraction of component 2 in the fluid in equilibrium with S_2 increases strongly with increasing pressure This strong increase in solubility can also be seen at temperatures higher than the temperature of the first critical endpoint (Figure 24c) The P x section of Figure 24d is at the temperature of the temperature minimum of the second branch of the S_2LV equilibrium In the middle of the solid fluid region region a S_2LV equilibrium comes into existence At a somewhat higher temperature the S_2LV curve is intersected twice in the P T-projection and the solid vapour (fluid) region is divided into two parts separated by a LV region a homogeneous liquid region and a S_2L region (Figure 24e) At the temperature of the second critical endpoint the L and V points of the three phase equilibrium with the highest pressure coincide in a L=V critical point (Figure 24f) This point is a pressure maximum of the LV two-phase region The solid fluid two phase region shows a horizontal point of inflection in this point now, the mole fraction of component 2 in the fluid decreases strongly with pressure For temperatures between the temperature of the second critical endpoint and the triple point of the less volatile component the P x-section is given in Figure 24g In systems with a negative value of dP/dT for the second branch of the S_2LV curve, also a strong enhancement in solubility occurs at the temperature of the second critical end point

4 Discussion

In application of near and supercritical fluids principally type II and type III phase behaviour is encountered, complicated by the presence of solid phases, although also the other types of fluid phase behaviour can play a role Since processes with near-critical fluids are often performed in a relatively narrow window of pressure and temperature around the critical point of the near-critical gas not only liquid vapour and solid vapour equilibria are important, but also liquid-liquid-vapour and solid liquid vapour three phase equilibria and liquid- liquid and solid-fluid two-phase equilibria may occur at process conditions Often use is made of the strong enhancement in solubility which occurs close to a critical endpoint of a three phase equilibrium and which can be explained by the occurrence of a horizontal point of inflection on the two phase boundary liquid vapour or solid vapour in P,x sections like Figure 14c and Figure 24c

The manufacturing of Low Density Polyethylene (LDPE) is frequently mentioned as the only large-scale chemical process where use is made of the enhanced solubility of a low volatile component, in this case polyethylene in a supercritical fluid here ethylene It can be questioned however, if in this process use is made of the special effects in solubility that occur close to the critical point of the solvent or close to critical endpoints The type of phase behaviour of the system ethylene + polyethylene is of the type discussed in section 3 8 [27] and the process is carried out at temperatures higher than 450 K [28] The melting temperature of polyethylene is 360-390 K and the temperature of the second critical endpoint is lower than 405 K So the process occurs at conditions in the right hand side of Figure 23 while the temperature is at least 170 K higher than the critical temperature of ethylene and 45 K higher than the temperature of the second critical endpoint

The design engineer is often faced with the fact that no or almost no information is available on the phase behaviour of the systems of interest However often it is possible to predict the type of phase behaviour from information on other similar systems For instance in the family of binary systems of carbon dioxide with n alkanes systematic changes in the type of phase behaviour occur [14 29] For carbon number n $1 \leq n \leq 6$ this family shows type I phase behaviour for $7 \leq n \leq 12$ type II phase behaviour for $n = 13$ type IV phase behaviour and for $14 \leq n \leq 21$ type III phase behaviour For $n \geq 22$ the solid phase interferes in the phase diagram as discussed in section 3 8 In other families similar trends are found

If a single P x- or T,x section is available for a certain system it is in general not possible to decide what type of phase behaviour is displayed by that system because for the different types of phase behaviour these sections can be very much alike More detailed information on the course of the critical curve or the nature of critical endpoint(s) of the L_1L_2V equilibrium curve is necessary Knowledge of the basic principles of phase diagrams can be of great help in completing only partly known phase diagrams and for detecting experimental errors

REFERENCES

[1] Gibbs, J W *The Scientific Papers Vol I*, Dover Publications New York, 1961

[2] Van Konynenburg P H *Critical Lines and Phase Equilibria* PhD Thesis UCLA Los Angeles, 1968

[3] Van Konynenburg, P H , Scott, R L *Phil Trans* 1980, 298A 495

[4] Rowlinson J S Swinton F L *Liquids and Liquid Mixtures* 3rd ed Butterworth Scientific London, 1982

[5] Vogel, R *Die Heterogenen Gleichgewichte* 2nd ed Geest & Portig Leipzig 1959

[6] Zernike J *Chemical Phase Theory*, Kluwer Deventer 1955

[7] Heidemann, R A *Lecture presented at this meeting*

[8] Peters C J *Lecture presented at this meeting*

[9] Boshkov L Z *Dokl Akad Nauk SSSR* 1987, 294, 901

[10] Van Pelt A , Peters C J De Swaan Arons, J *J Chem Phys* 1991 95 7569

[11] Bolz, A *Vergleichende Untersuchung Globaler Phasendiagramme*, PhD Thesis Ruhr-Unversität Bochum Bochum, 1992

[12] Ochel, H , Becker, H , Maag, K , Schneider, G M *J Chem Thermodynamics* 1993 25 667

[13] Brunner, E *J Chem Thermodynamics* 1990, 22, 220

[14] Schneider, G M *In Chemical Thermodynamics Vol 2*, McGlashan M L Ed The Chemical Society London 1978 Chapter 4

[15] Davenport A J Rowlinson J S *Trans Farad Soc* 1963 59 78

[16] Kohn, J P Kim, Y J Pan Y C *J Chem Eng Data* 1966 11 33

[17] Enick R Holder G D Morsi B I *Fluid Phase Equilibria* 1985 22 209

[18] Fall D J , Luks K D *J Chem Eng Data* 1985, 30 276

[19] De Roo J L Peters C J De Swaan Arons J *To be published*

[20] Hottovy J D Luks K D , Kohn J P *J Chem Eng Data* 1981, 26 256

[21] De Loos Th W Wijen A J M Diepen G A M *J Chem Thermodynamics* 1980 12 193

[22] De Swaan Arons J Diepen G A M *J Chem Phys* 1966 44 2322
[23] Ellis C M *J Chem Ed* 1967 44 405
[24] Lamb D M Barbara T M , Jonas J *J Phys Chem* 1986 90 4210
[25] Van Welie G S A Diepen G A M *Rec Trav Chim Pays Bas* 1961 80 673
[26] De Leeuw V V Poot W De Loos Th W De Swaan Arons J *Fluid Phase Equilibria* 1989 49 75
[27] De Loos, Th W *Evenwichten Tussen Fluide Fasen in Systemen van Lineair Polyetheen en Etheen* PhD Thesis Delft University of Technology Delft 1981
[28] Luft G *Chem Ing Tech* 1979 51, 960
[29] Van der Steen J De Loos Th W De Swaan Arons J *Fluid Phase Equilibria* 1989 51 353

Binary Phase Equilibria

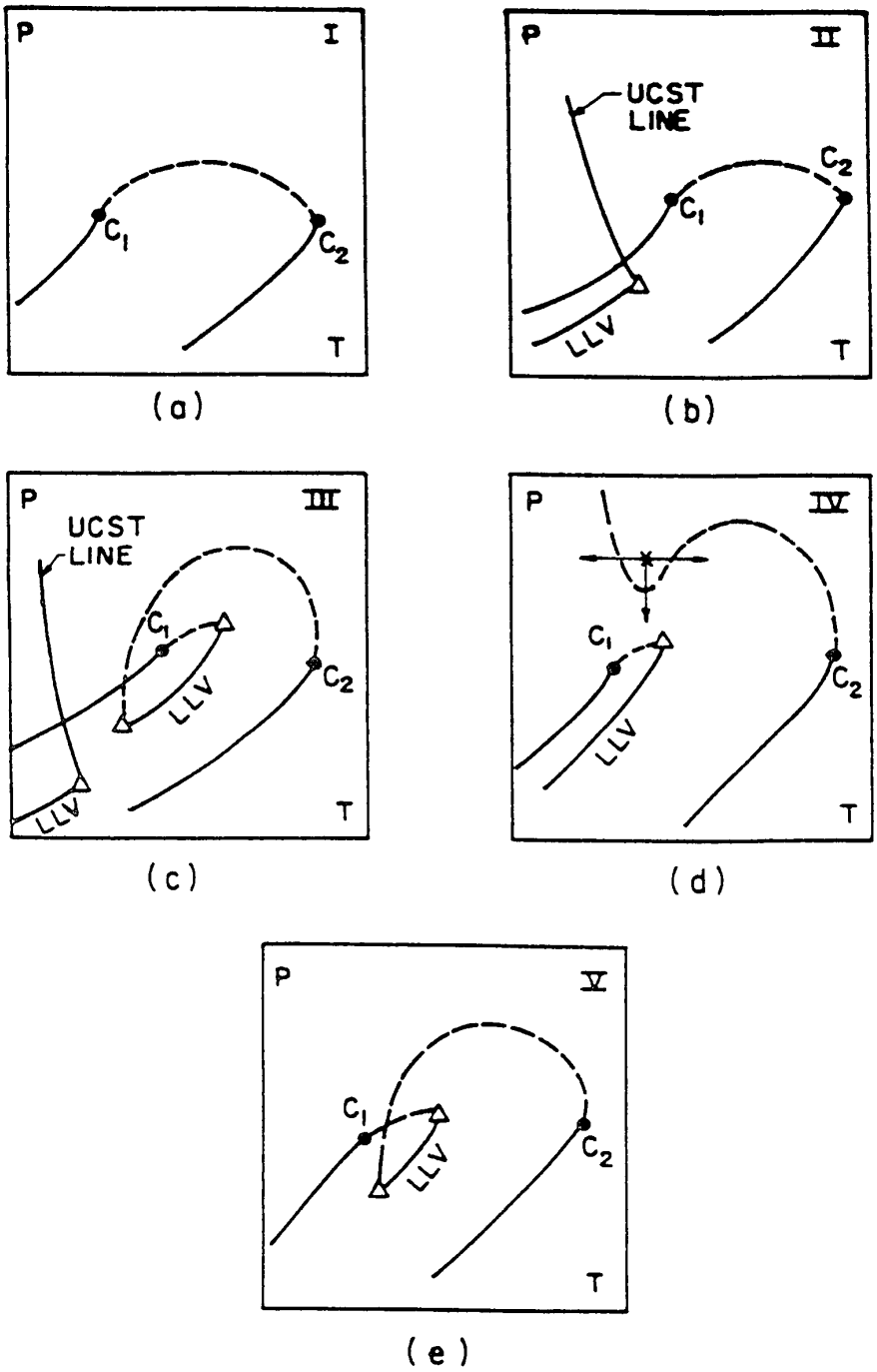

Binary Phase Equilibria

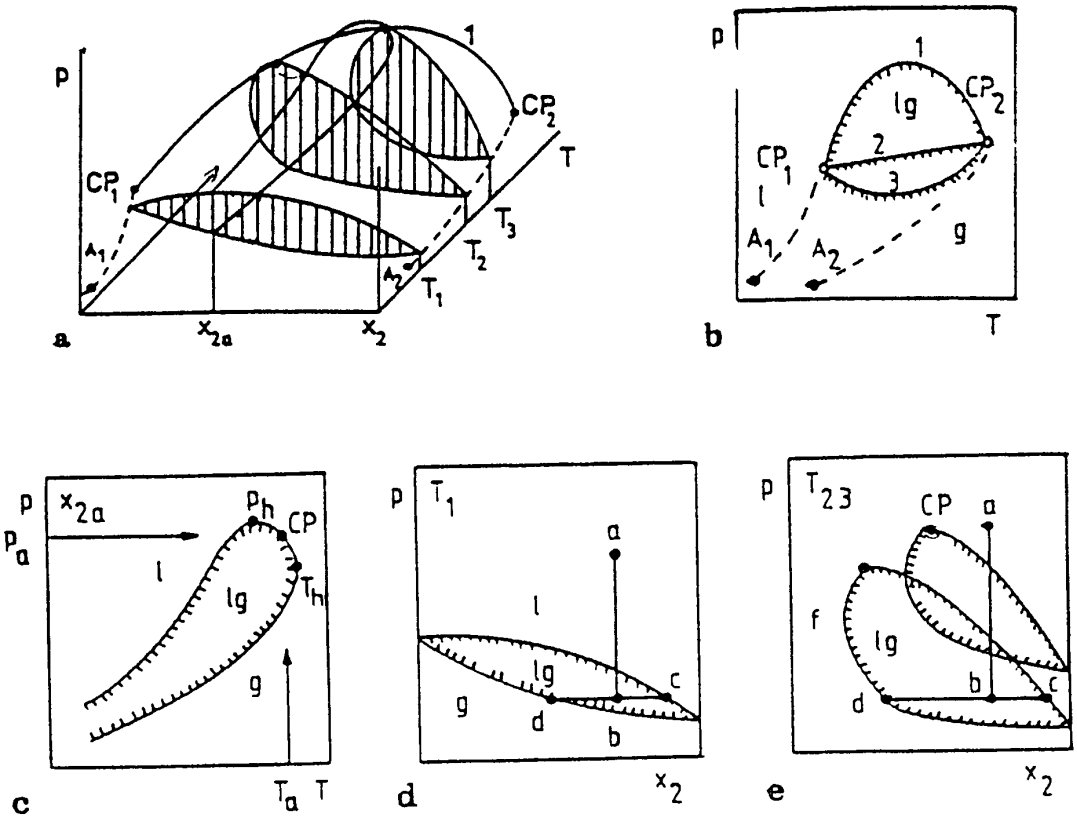

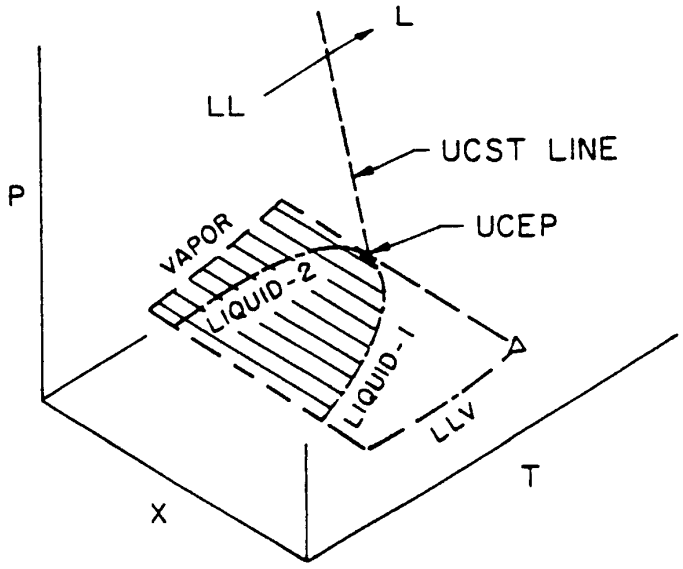

A-27

Ternary Phase Equilibria

Type I

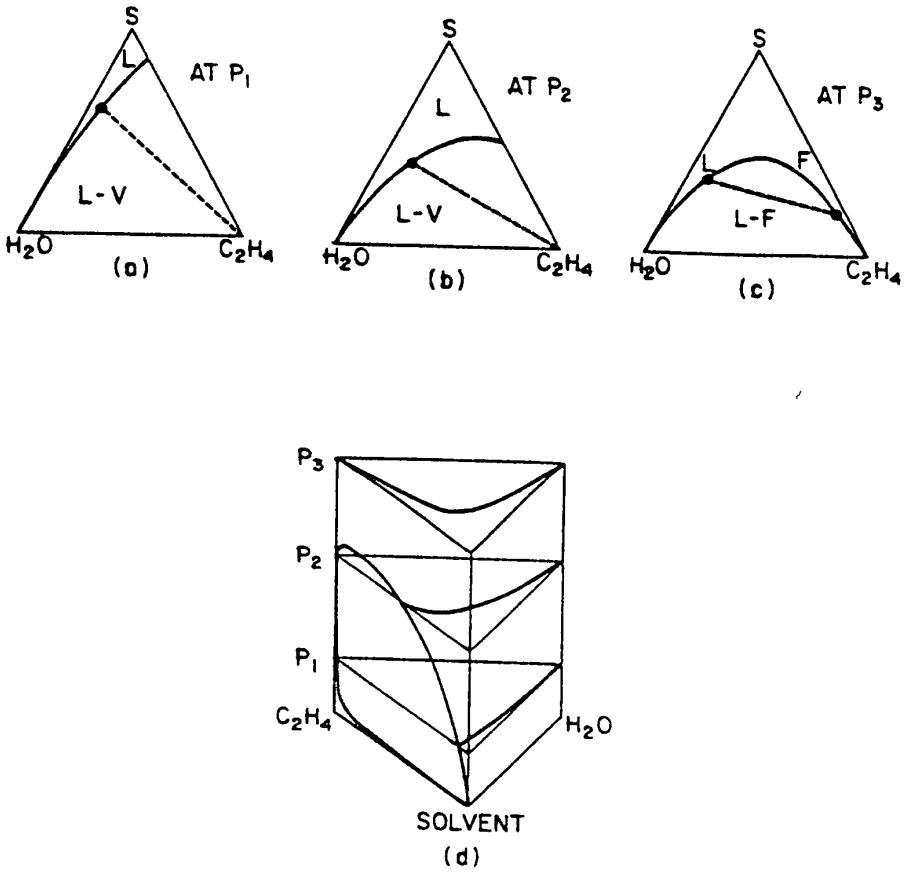

Ternary Phase Equilibria

Type II

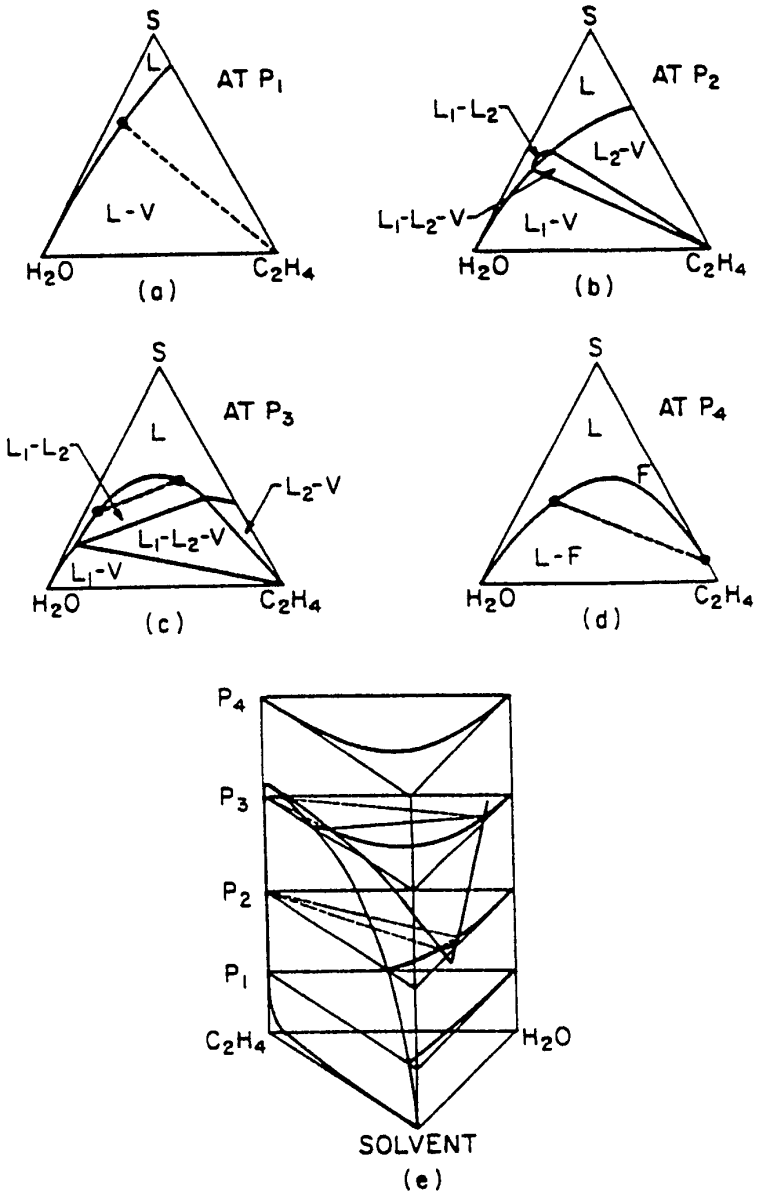

Ternary Phase Equilibria

Type III

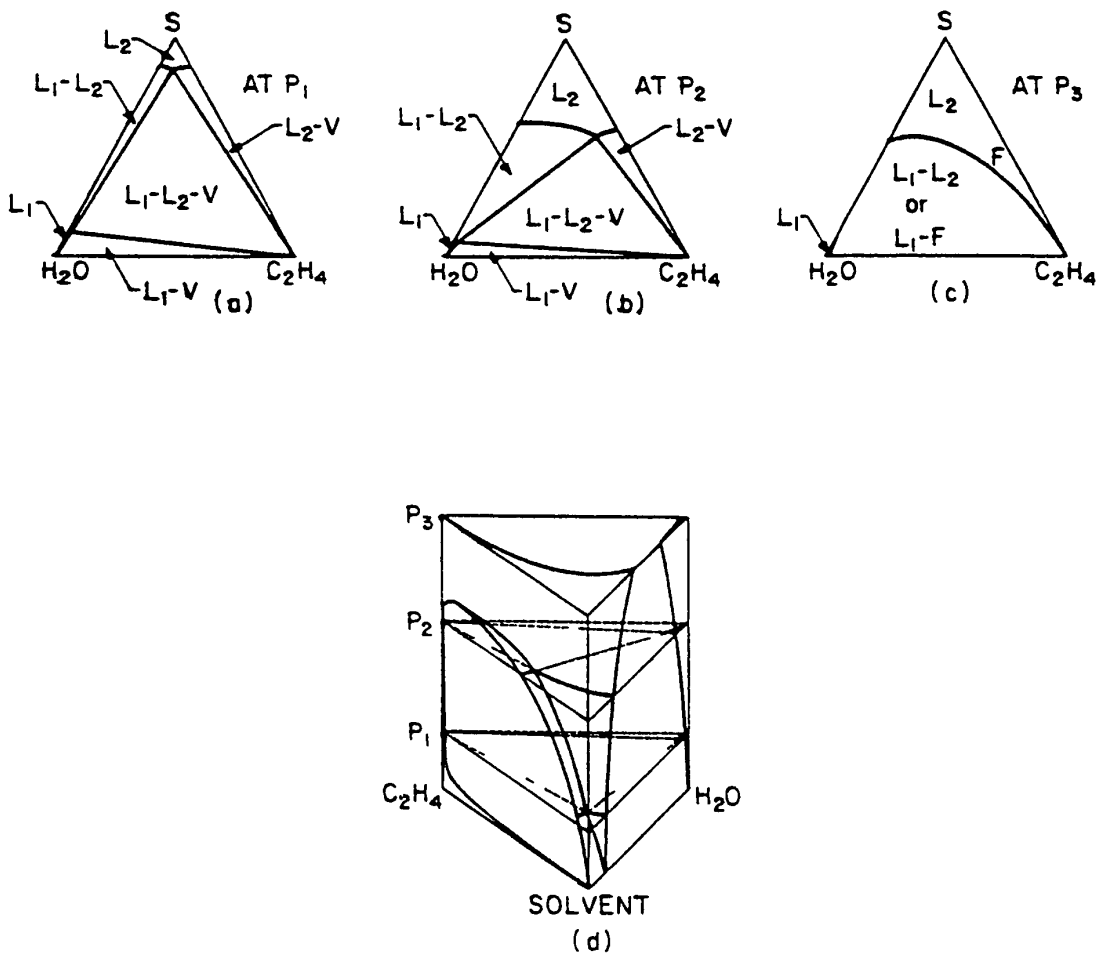

Natex Prozesstechnologie GesmbH

Basic-Course

of

Supercritical Fluid Extraction Process

Metal Industries Research & Development Center

Kaohsiung, Taiwan, ROC

Mr TZU-CHEN KUO

THERMODYNAMIC PROPERTIES PHASE EQUILIBRIA

EXPERIMENTAL METHODS

Possibilities for determination of high pressure phase equilibria

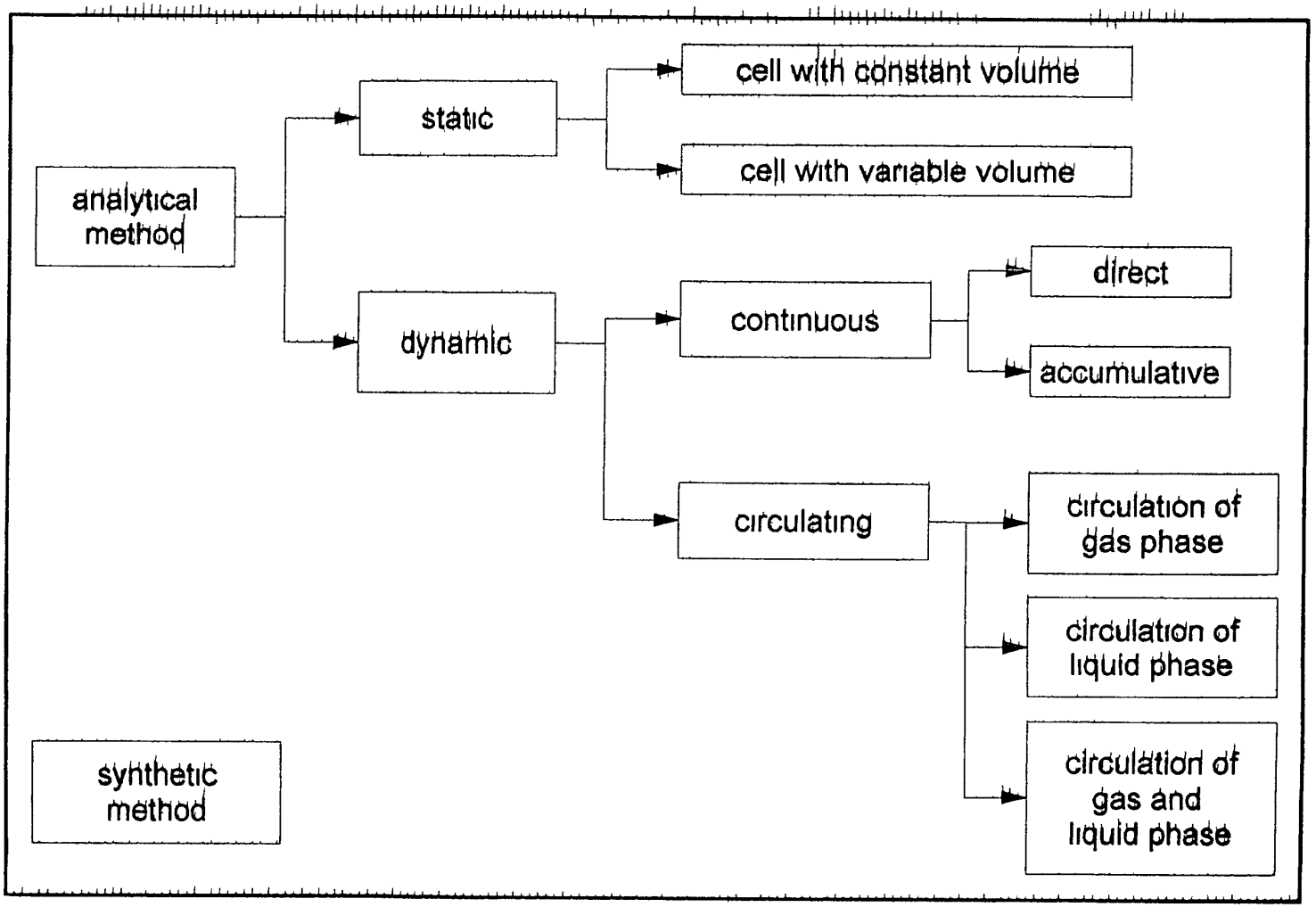

CONTENT

INTRODUCTION

1 STATIC METHODS

2 RECIRCULATION METHODS

3 FLOW METHODS

4 SATURATION (TRANSPIRATION) METHODS

5 DEW AND BUBBLE POINT METHODS

6 SUPERCRITICAL FLUID CHROMATOGRAPHY

6 1 DETERMINATION OF PARTIAL MOLAR VOLUMES

7 REFERENCES

1 INTRODUCTION

A comprehensive review on experimental methods in high pressure fluid phase equilibria was presented by Fornari et al (1990) and updated by Dohrn and Brunner (1995)

In the following there is a particular description of experimental methods used in connections with measurement of solubility in supercritical fluids

We should keep in mind that the understanding of complicated phase behaviour and the possibility of the prediction of temperature and pressure effects is of crucial importance for the experimentalists As an example a typical solubility behaviour can be presented as that shown in Figure 1 (Paulaitis et al, 1983) In the vicinity of critical point very small changes in temperature and pressure have enormous effects on solubility The effect of temperature is not so dramatic, but as it can be seen from the same Figure 1, there are still problems to deal with. Namely, at relatively low pressure the solubility can fall by over an order of magnitude when temperature is raised which is the opposite of the behaviour at higher pressures This indicates the sensitivity of the solubility to small changes in temperature and pressure as well as the additional complexity which is seen from the crossing of the curves, which is a result of mutual competition of the solvent density and solute vapour pressure effects Because of all this, special care should be taken in the area, close to the critical points, where even small disturbances caused by pumping pressure or temperature control, may cause changes in the state of the determined systems

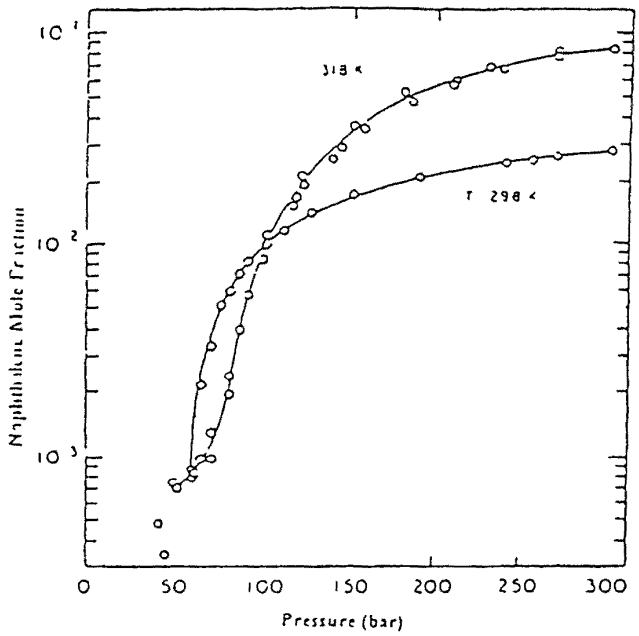

Figure 1 Solubility of naphthalene at 298 and 318 K

Some examples of experimental work are given in Table 1 The examples are recent and are not included in the above mentioned review The abbreviations related to the experimental techniques and to the analytical methods used are as follows

Experimental techniques
- S static
- CF continuous flow
- R recirculation

Analytical methods
- SFC supercritical fluid chromatographic
- G gravimetric
- SP spectroscopic
- HPLC high pressure liquid chromatographic

Alessi and Cortesi (1988) have reviewed the measurements of solubility in dense gases Although there are different classifications for the methods for determining solubility in supercritical fluids (e g analytic and synthetic methods) a recent classification is presented here

- static methods
- dynamic methods
  - recirculation methods
  - flow methods
  - saturation (transpiration) methods
- dew and bubble point methods
- supercritical fluid chromatographic methods

There is not any general rule for the choice of the method which should be applied to a certain problem. All of them have advantages and disadvantages, regarding building up, handling, consumption of investigated substances, visual observation of the system, experimental duration, pressure and temperature determination, low-cost equipment etc

1 STATIC METHODS

A very simple basics of the static method can be seen in the Figure 2 The mixture is placed into an evacuated cell located in a constant temperature bath (usually a liquid or air bath although metal block thermostats have been used) The content of the cell, at least two separated phases of different density, is brought to equilibrium by shaking, stirring or agitation and the equilibrium pressure is measured The sample remains closed in the cell and no phase or a part of the system is a subject to flow with respect to the others Because dealing with the closed systems, this requires careful evacuation of the cell and tubing, degassing of the materials in order to avoid errors in the reading of the equilibrium pressure, although the problem is not so crucial as at low pressures

We generally distinguish between two methods when the determination of composition of the equilibrium phases is taking place

In the first method, known amounts of pure substances are introduced into the cell, so that the overall composition of the mixture contained in the cell is known The compositions of the coexisting equilibrium phases may then be recalculated by an iterative procedure from the known overall composition and equilibrium temperature and pressure data, provided that at the system state conditions the pressure volume-

Table 1 Experimental techniques for supercritical fluid phase equilibria.

Authors	Solute	Method/Analysis	T (K)	P(bar)
Nakatani et al 1989 1991	Indole 3-Aldehyde Indole 3 Carboxylic acid 2 Mercaptopyrimidine 2 Chloro-pyrimidine 5 Aminoindole 5 Hydroxyindole 4 Hydroxypyrimidine 2 Aminopyrazine, Oxindole Pyrazine 2 carboxylic acid	S SFC	308	63 198
Liong 1991 Liong et al 1992	Arachidonic acid (C20 4) Ethyl ester (liq) Eicosa trienoic acid (C20 3) Ethyl ester (liq) Oleic acid (C18 1) Ethyl ester	CF G	313 373	90 250
Hamdi et al 1991	Copper acetylacetonate Barium hexafluoroacetyl acetonate Yttrium acetyl acetonate, Yttrium hexa fluoroacetylacetonate	CF G	423-453	120 220
Schmitt and Reid, 1988	Brassylic acid, Di N-dodecylamine Di N dodecyl amine (liq) Didodecyl phosphine Didodecyl thoether (liq) Dioctyl ether (liq) Docosane (liq) Eicosane (liq) Nonadecane (liq) Nonadecanenitrile (liq) 2 Nonadecanone (liq) Octa-decane (liq) 1 Octadecanol Octadecylmercaptan (liq), Squalane Steric acid, Tetracosane Tetracosane (liq) Trihexylamine (liq), Trioctylamine Trioctylphosphine (liq) Trioctylphosphine oxide (liq) Triphenylamine Triphenylphosphate Triphenyphosphine	CF G	110-364	150-364
Cygnarowicz et al 1990	β-Carotene	R, SP	313 343	212-439
Sakaki 1992	β Carotene	CF SFC	308-323	99 298
Yun et al 1991	Cholesterol	CF G	313 333	100 250

Table 1 (continued)

Authors	Solute	Method/Analysis	T (K)	P(bar)
Laintz et al 1991	Cobalt diethydithio-carbamate $Co(DDC)_3$ Co-balt (trifluoroethyl) dithio-carbamate $Co(FDDC)_3$ Copper diethyldithiocarba mate $Cu(DDC)_2$ Copper (trifluoroethyl) dithiocarba mate $Cu(FDDC)_2$ Bismuth diethyldithiocarbamate $Bi(DDC)_3$ Bismuth (trifluoroethyl) dithiocarba mate $Bi(FDDC)_3$ Nickel diethyldithiocarbamate Ni(DDC) Nickel (trifluoroethyl) dithiocarba mate Ni(FDDC) Sodium diethyldithiocarbamate Na(DDC) Sodium (trifluoroethyl) dithiocarba mate Na(FDDC)	S SP	323	101 153
Mitra et al 1988	Dibenzothiophene Naphthalene	CF G	309 338	75-277
Bartle et al 1990	Fluorene Phenanthrene Pyrene	CF CR	308 328	78 254
Kramer and Thodos 1988	1 Hexadecanoic acid, 1-Hexadecanol 1 Octadecanol Steric acid,	CF G	318-338	140 575
Iwai et al 1991	1 Hexadecanoic acid, 1 Hexadecanol 2 5-Xylenols 2 6-Xylenols Tetradecanoic acid	CF G	308	74-267
Gurdial and Foster 1990	o-Hydroxybenzoic acid, p-Hydroxybenzoic acid	CF G	308 328	81-409
Sako et al 1988 1989	Indole 5 Methoxyindole	S SFC	308	54 208
Warzinski et al 1992	Molybdenum Hexacarbonyl	S O	313-333	78 116
Maxwell et al 1992	Monensin, Salinomycin Narasin	R, SP	353	141-408
Schaeffer et al 1988	Monocrotaline	CF G	308 328	89-274
Ko et al 1991	Penicillin V	CF SP	315-335	80 280
Wells et al 1990	Phenylacetic acid, Vanillan	CF G	308-318	83 195
Billoni et al 1988	Vanillan	CF HPLC	315 329	80-200

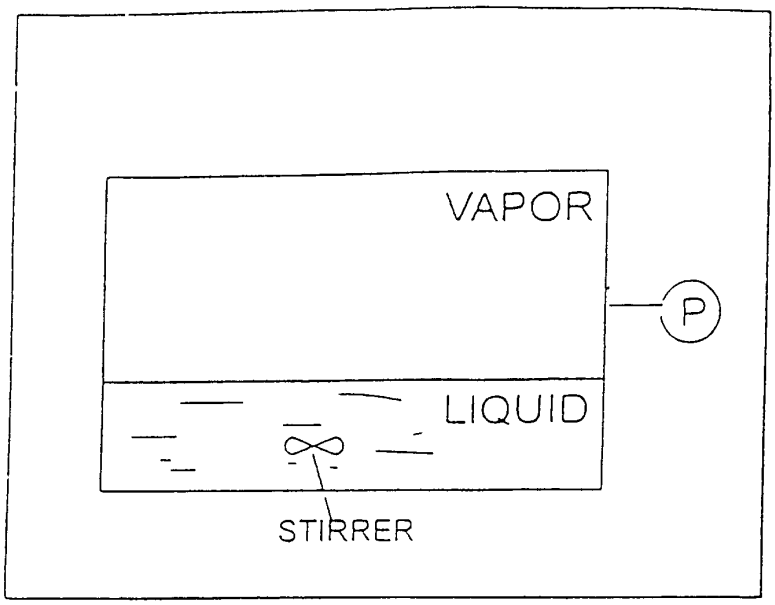

Figure 2 Principle of static method

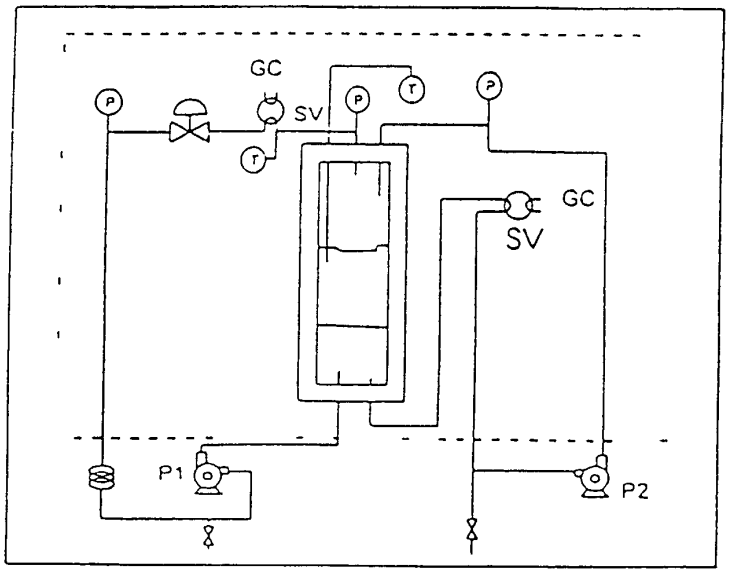

Figure 3 The scheme of a recirculation apparatus

temperature (PVT) behaviour as a function of the composition is known to a sufficient accuracy in the form of a mathematical model for all the phases present in the system. This is very difficult to achieve when dealing with systems at high pressures Here the need arises for additional experimentally determined information One possibility is the determination of the bubble or dew point either optically or by studying the pressure volume relations The main problem associated with this method is the preparation of the mixture of known composition in the cell

The second method is employed more frequently In this case the initial overall composition of the mixture charged into the cell is established only approximately just to pre determine the location of the measured equilibrium data point in the phase diagram The major difficulty with this method lies in withdrawal of the samples of the equilibrium phase or phases from the cell without disturbing the system equilibrium and with their transport to analytical devices This is usually accompanied by the depressurization but any changes in the homogeneity and composition of the phases must be avoided

The advantage of the static method is that only small amounts of substances are needed for determinations A simple apparatus was developed in the nineteen-fifties (Depen and Sheffer (1953)) and since then the method has become widespread and employed for many purposes (Chrastil, (1982) Hollar and Ehrlich, (1990)) It should be pointed out, that the method could be used for measurements of relatively good soluble substances, while it can be very inaccurate for low soluble substances

2 RECIRCULATION METHODS

These methods were developed from the static methods The main part of the recirculation apparatus is a thermostated equilibrium cell The scheme of the recirculation apparatus is shown in Figure 3 It can be seen, that the equilibrium cell has the facility for mechanically driven circulation through external loop(s) of either the lighter (i e the top) phase or the heavier (the bottom) phase or of both phases Magnetically operated high-pressure pumps usually achieve the circulation

The reason for introducing the external circulation of phases is to achieve more efficient equilibrating of the phases through stirring and contacting and thereby to improve the process of equilibration and to reduce the time required Another reason is the facilitation of the sampling After the equilibration has been achieved, the phases circulated through an external loop in a steady state regime already represent a separated equilibrium phase A portion of such a phase may be trapped in a sampling cell and taken for analysis or the phase may be temporarily circulated through an in-line sampling loop such as an injection valve and then analyzed off-line On line analysis can also be performed in this case without disturbing the phase stream in the circulation loop

The following is a typical experimental procedure After purging and evacuating the equipment, the cell is loaded with the mixture of roughly known composition and pressurized by pumping in the solvent to a desired pressure value The operation of magnetically driven pump(s) is started and one or two phases are recirculated so that the lighter phase exits the cell at the top and is returned at the bottom, bubbling through the heavier phase, whereas the heavier phase leaves at the bottom and returns at the top of the cell being sprayed into the lighter phase The process of approaching equilibrium is

followed by examining the stability of pressure and sometimes of density and/or composition After approximately 10 to 15 minutes, the equilibrium state is reached and the phases are sampled and analysed

The system examined in a recirculation apparatus is still a closed thermodynamic system and so the limitations and precautions related to this feature, particularly the degassing of the system, mentioned in Static method section, have to be observed

It should be noted that problem associated with sample withdrawal arises here, namely the danger of entrainment of droplets or bubbles of a second phase with the circulated stream of the phase to be sampled for analysis

The method was first described in the beginning of the seventies (Besserer and Robinson, (1971) The great advantage for this method lies in visual equilibrium cells The necessity to observe the phase behaviour becomes more important as the complexity of the behaviour of the investigated systems increases

3 FLOW METHODS

In the nomenclature adopted here flow methods are considered the class of experimental techniques, in which a pre heated mixture of constant and only approximately known overall composition continuously flows to the equilibrium cell, wherein it separates into two phases differing in density The separated single phases then continuously flow out of the cell (lighter phase at the top, heavier at the bottom) and are sampled for analysis

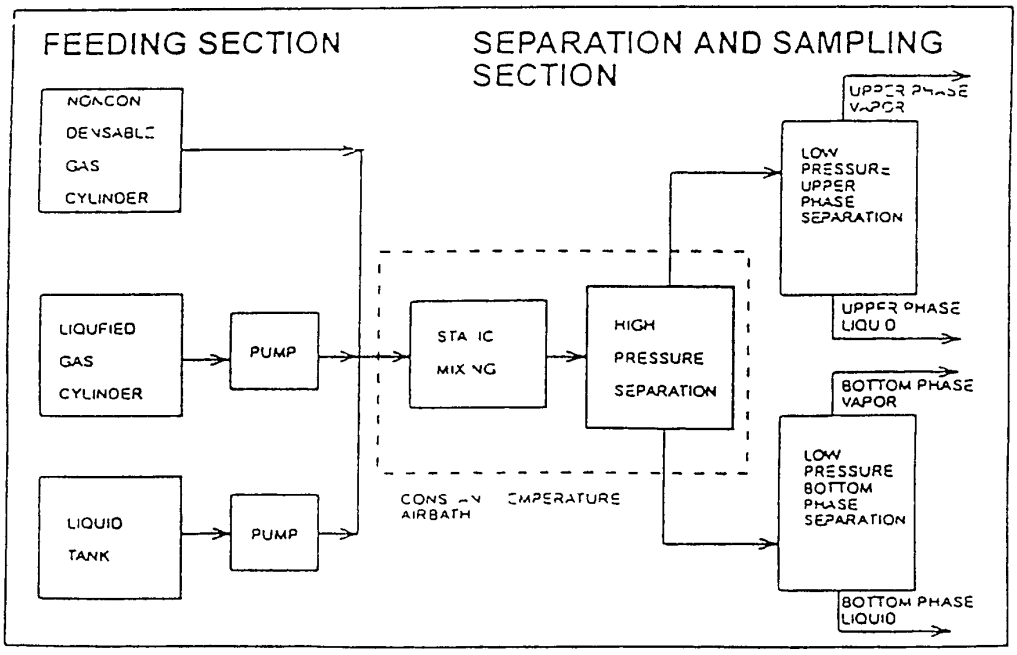

Figure 4 The scheme of a flow apparatus

Flow methods are employed for systems containing thermally unstable compounds and reacting systems The main reasons for designing this technique is to reduce the time required to attain the required state conditions and to reduce the residence time of the studied mixture in the high temperature compartment of the apparatus

The scheme of this type of the apparatus is shown in Figure 4 High-pressure pumps are used to deliver in a continuous manner the components in a fluid state to form a steady mixture stream of constant composition at a desired pressure The stream passes through a pre-heater where it approaches the desired system temperature and then is fed into an equilibrium chamber The function of this part of the apparatus is to immediately separate the two coexistent fluid phases differing in density For a given feed, the samples of equilibrium phases to be analyzed can be collected in sufficiently large amounts and quite rapidly The possibility of getting samples of large enough size (depending on duration of the sample collecting period) is particularly valuable for investigations of dilute regions

The flow technique is applicable to systems where the equilibrium phases as well as the pure components are fluids at all conditions encountered in the flow system of the experimental set-up So this technique is also applicable to liquid-liquid equilibrium systems provided that the difference in densities of the equilibrium phases is sufficiently large

The disadvantages of the flow method are relatively large consumption of the studied substances and the fact that pressure fluctuations may be a problem, which makes a precise pressure control more difficult when compared to other methods

This type of experimental equipment was described in detail in the late seventies (Simnick et al , (1977)) Here some articles to cover this subject can be mentioned (Iwai et al (1989) Iwai et al. (1990) Barber et al (1991) Jennings et al (1991) Weng and Lee (1992))

4 SATURATION (TRANSPIRATION) METHODS

This is perhaps the most frequently applied technique for determining the solubility of solids and highly viscous heavy liquids in supercritical solvents The principle of this class of methods is quite simple as shown in Figure 5 In the saturation technique the nonvolatile, heavy phase is loaded batchwise in a saturator, or in a battery of two or even more saturators connected in series and remains there as a stationary phase during the experiment In most cases the saturator has the form of a packed column.

Under a measured constant pressure a steady stream of supercritical fluid passes through a preheater where it reaches the desired system temperature Then it is continuously fed to the saturator at its bottom, it strips the solute of the stationary heavy phase residing in the column and, saturated by the solute it leaves the saturator at its top

The solubility of the heavy phase in supercritical fluid may be determined either by a direct sampling and analysis of the effluent stream or from the total volume of gas (i.e of supercritical fluid after expansion) passed through the saturator and from the known mass of solute extracted during a sample collecting period To this end, the effluent stream is expanded from the experimental pressure to atmospheric pressure across a metering valve then it passes through a cold trap where the extract is quantitatively precipitated or condensed, and finally it proceeds to a dry test or a wet test gas meter or other device

where the total amount of the passed gas is measured The amount of extracted solute is usually determined by weighing the sample collected in the cold trap

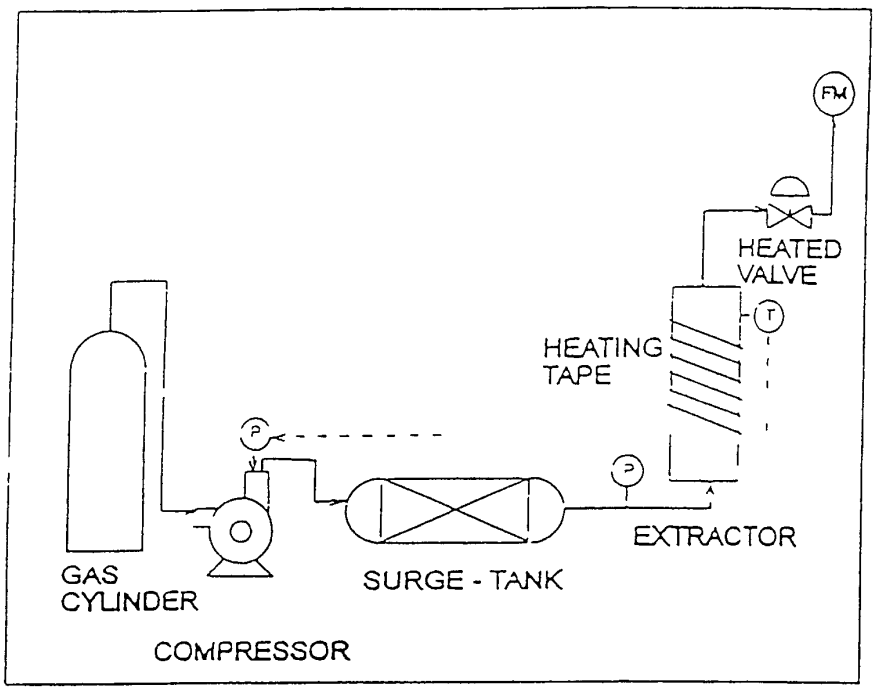

Figure 5 The scheme of a saturation apparatus

The method is applicable only to two phase systems Since only the supercritical fluid rich effluent phase is sampled, the composition of the equilibrium heavy phase cannot be determined But there are some pitfalls in this technique, which the experimentalist should be aware of

- the danger of unnoticed phase changes occurring in the saturators they can be avoided by using a view cell
- necessity to avoid any entrainment of the particles or drops of the stationary heavy phase with the stream of the supercritical fluid rich phase by using a filter
  the saturation of the supercritical fluid rich phase with the solute can be achieved by adjusting the flow rate
- necessity to avoid the precipitation or condensation and subsequent deposition of the extracted solute from the effluent stream during the expansion in the metering valve and also in the section of tubing before the stream reaches the collecting trap Weighing the valve can overcome this problem.

As mentioned before the saturation method is by far the most often used technique for determining the solubility of low volatile solutes in supercritical fluid solvents originally

used in the late fifties (Prausnitz and Benson, (1959)) From then a lot of authors had employed this kind of technique in their investigations (Czicoryt et al (1970), Van Leer and Paulaitis (1980) McHugh and Paulaitis (1980) Johnston et al (1982) Masuoka et al (1982) Kurnik and Reid (1982) Kim and Lentz (1988) Kramer and Thodos (1988 1989) Dimitrelis and Prausnitz, (1989) Tsai and Yau, (1990) Lemert and Johnston, (1990) Suzuki et al (1991) Gurdial and Foster (1991) Iwai et al (1991) Yau and Tsai (1992 a b), Mori at al (1992), Madras et al (1993), Reverchon et al (1993c) Macnaughton (1993))

5 DEW AND BUBBLE POINT METHODS

These methods are normally employed for the complete measurement of the phase behaviour although important examples of application of the method are also found in the literature for the direct determination of the solubility in dense gases as a function of pressure and temperature

In the dew and bubble point method a mixture of known composition is isothermally expanded or isobarically heated until a phase change is detected In the dew and bubble-point method the visual location of a phase transition is used a pressure value is established at which the composition of one of the present phases is equal to the known total composition at a given temperature

The usual way of determining dew and bubble points at high pressure is the following the sample volume or pressure is varied by injection or removal of mercury and the saturation point is visually observed as a phase formation or disappearance Bubble points can sometimes be detected as a break point in a pressure versus volume curve The relative large sample volumes that are used in such cells make the re-establishment of equilibrium time consuming after a temperature or pressure change and the visual detection technique is in itself operator deperdent and difficult to automate

The main advantage of the method is that no sampling and analysis are required

The main difficulty in running the apparatus lies in the preparation of a mixture of known composition in the cell

As mentioned before the solubility in dense fluid is rarely the only data measured with this group of apparatus The example of measuring the solubility data by this method is reported (Fall and Luks, (1984))

6 SUPERCRITICAL FLUID CHROMATOGRAPHY

This approach is very promising because chromatographic measurements are rapid, require little amount of solute and inherently separates impurities from the solute This method is not used only for determination of solubility data, but also for determination of cosolvent effects in the solubility of organic in supercritical fluids, and for the determination of partial molar volumes at infinite dilution, etc

The principle of operation of supercritical fluid chromatograph is very simple The supercritical fluid flows at high pressure through a column in which the stationary phase is loaded The solute is injected at the beginning of the column and it is distributed between the mobile and the stationary phases

Major disadvantage of the method is that solubility data can not be actually measured but should be calculated For calculating solubility in supercritical fluids the following Equation can be used

$$S = C / k \qquad (1)$$

where S is the solubility (per unit volume) k is the chromatographic capacity factor and C is a constant for a particular column, solute and temperature Solubilities in supercritical fluids may be achieved in favorable circumstances more rapidly than by conventional methods, provided that the constant C in Equation 19 can be determined
Five possible methods for achieving constant C are available (Bartle et al. (1990a))

- from the vapour pressure of the solute
- from at least one solubility measured by other methods at the required temperature
- from solubility measurements obtained by other methods at two temperatures at least close to the required temperature
- from solubilities obtained by other techniques in another supercritical fluid
- from solubilities in liquids by comparing the retention in supercritical chromatograph and high pressure liquid chromatograph with the same solute and column

Examples of the use of this technique for determining solubility in supercritical fluids are reported by (Sako et al , (1988), Bartle et al , (1990a,b))
The experimental methods for determining solubility data are numerous and the choice for using one of them depends mainly on the system to be investigated Regardless the techniques that are used, it is important for the experimentalist to perform the experiments with a great deal of care, since a wide variety of phase behavior can occur at high pressures However it is possible to reduce the amount of experimental work on supercritical fluid-solute systems by modeling the resultant phase behavior

6 1 DETERMINATION OF PARTIAL MOLAR VOLUMES

Among the thermodynamic properties that can be measured to understand the behavior of mixtures in the vicinity of the critical point, partial molar volume is important in describing the pressure dependence of the fugacity coefficient (and consequently solubility), which is the basis for many separation processes The large negative partial molar volumes of solutes at infinite dilution in SF physically indicate a large volume decrease when a molecule of a solute is added to the pure solvent
Using classical methods or using SFC may perform measurements of partial molar volumes Generally speaking the experimental methods employed may be roughly divided in two categories direct and indirect methods The direct methods are normally based on density or volume determinations and the partial molar properties are derived directly from their definitions This group of methods requires very precise measurements and special care is needed when operating in the vicinity of the critical point
Indirect methods are all based measuring the variation of a given equilibrium property (*e g* , solubility, K factor) with pressure In this respect the determination is easier, but requires a very accurate method for the determination of the equilibrium property over a wide range of pressures, since the partial molar property is obtained from a slope measurement

A possible choice for experimentally determining thermodynamic properties and partial molar properties is inverse chromatography which has been widely used at low to moderate pressures Supercritical fluid chromatography (SFC) may be used at high pressure in almost the same fashion as inverse chromatography This technique has several advantages with respect to static or dynamic methods for the determination of thermodynamic properties in the vicinity of the critical point small quantities of the solute are required the method is rapid and it uses standard equipment

Among others, van Wasen and Schneider (employed supercritical fluid chromatography to determine $\bar{v}^{\infty}$ of naphthalene and fluorene in supercritical CO_2 based on an adsorption retention mechanism. The same approach has been used also by Erkey and Akgerman (1990) who calculated the partial molar volumes of naphthalene at infinite dilution in supercritical CO_2 Shim and Johnston (Shim and Johston (1991)) used SFC to measure K factors partial molar volumes and partial molar enthalpies of naphthalene and phenanthrene in supercritical CO_2

K factors (partitition coefficients defined as the ratio of the concentration in the liquid over the concentration in the fluid phase) have been determined by Olesik (Olesik et al (1987))

The theoretical background for applying the SFC technique for the determination of $\bar{v}^{\infty}$ is briefly reviewed in this section According to standard chromatographic terminology, the capacity factor k_i is defined (per unit of bed volume) as follows

$$k_i = \frac{t_i - t_0}{t_0} \qquad (2)$$

where t_i is the retention time of component i and t_0 is the retention time of an unretained solute The capacity factor is related to the equilibrium compositions in the mobile phase (y) and in the stationary phase (x) through the relationship

$$k_i = \frac{x V_s v_m}{y_i V_m v_s} \qquad (3)$$

where V_m and V_s represent the total volumes of the mobile and stationary phases respectively, and v_m and v_s are the molar volumes

If the fugacity in each phase is expressed by means of the well-known relationship

$$f_i = x_i \phi_i P \qquad (4)$$

at equilibrium

$$k_i = \frac{\phi_m V_s v_m}{\phi_{is} v_m v_s} \qquad (5)$$

The effect of temperature and pressure on k_i are given by the following derivatives expressed in terms of partial molar quantities (in the hypothesis of infinite dilution)

$$\left(\frac{\partial \ln k}{\partial P}\right)_T = \frac{\bar{v}_{im}^{\infty} - \bar{v}_{is}^{\infty}}{RT} - \kappa \qquad (6)$$

$$\left(\frac{\partial \ln k_i}{\partial T}\right)_T = -\frac{\bar{h}_{im} - \bar{h}_{is}}{RT^2} + \beta \qquad (7)$$

where κ is the mobile phase isothermal compressibility and β the isobaric thermal expansion coefficient All the derivatives are taken at infinite dilution of the solute
The derivative of the capacity factor with respect to the density is expressed still at infinite dilution, by the following relationship

$$\left(\frac{\partial \ln k}{\partial \rho}\right)_T = \left(\frac{\partial P}{\partial \rho}\right)_T \left(\frac{\bar{v}_{im}^{\infty} - \bar{v}_{is}^{\infty}}{RT} - \kappa\right) \qquad (8)$$

Transforming the above expression we achieve

$$\left(\frac{\partial \ln k}{\partial \ln \rho}\right)_T = \left(\frac{\bar{v}_{im}^{\infty} - \bar{v}_{is}^{\infty}}{RT\kappa} - 1\right) \qquad (9)$$

Near the solvent critical point $\bar{v}_{im}^{\infty}$ is much larger than $\bar{v}_{is}^{\infty}$ and consequently the latter can be neglected, thus giving the following relationship

$$\left(\frac{\partial \ln k_i}{\partial \ln \rho}\right)_T = -\left(1 - \frac{\bar{v}_{im}^{\infty}}{RT\kappa}\right) \qquad (10)$$

This equation has been derived by Chimowitz (Chimowitz and Kelley (1989)) on the basis of theoretical developments of Kumar (Kumar and Johnston (1988)) and it is strictly valid only very close to the solvent critical point Rearranging this relationship the partial molar volume can be easily obtained The behaviour of the derivative in Equation 28 with density, in the regime of interest is determined by the variation of the ratio of the partial molar volume and isothermal compressibility with density It has been shown (Kumar and Johnston (1988)) that on the critical isotherm, very close to the solvent s critical point, this ratio is independent of density since both, the partial molar volume and the isothermal compressibility, have the same scaling

However by looking at the different terms of this equation, it appears that the derivative strictly depends upon the properties of the mobile phase (κ) and of the mixture of the solute and the mobile phase The derivative is independent of the stationary phase used and this can be confirmed using data reported in literature (Jinno and Numi (1988))

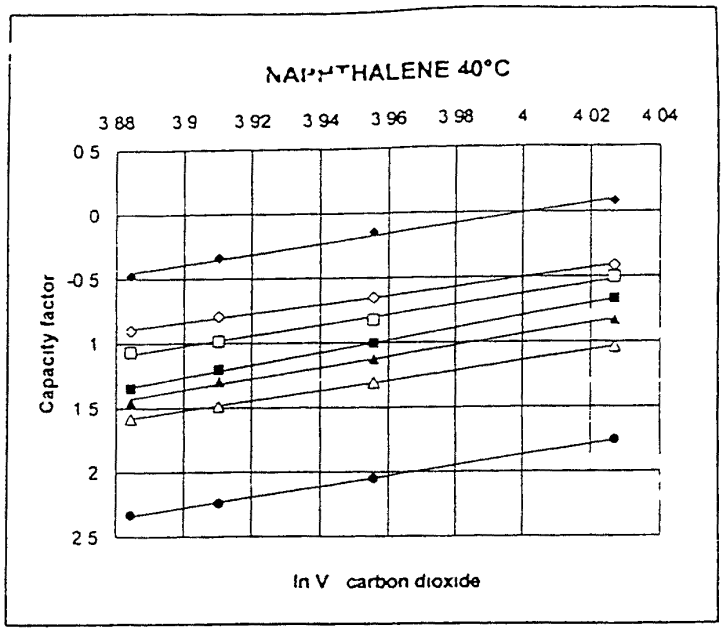

Figure 6 Slope ln k / ln V for different stationary phases

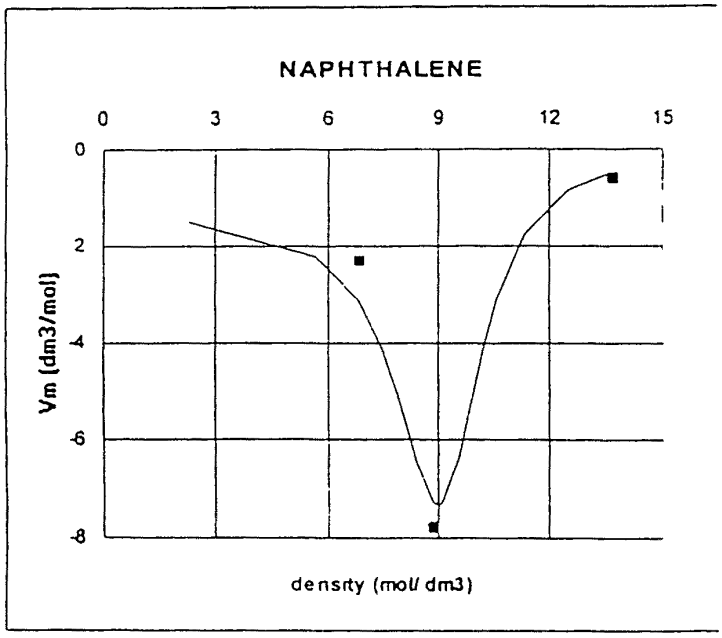

Figure 7 Partial molar volumes of naphthalene at infinite dilution versus molar density of carbon dioxide (■ data from the literature at 35 23°C -- the line represents the calculated data at 313 15 K)

Figure 6 illustrates retention data of naphthalene at 313 15 K as a function of density for several different stationary phases (Jinno and Niimi (1988)) and the parallel lines indicate that the derivative is independent of the stationary phase

Equation 10 is strictly valid only in proximity of the critical point However, Chimowitz (Chimowitz and Kelly (1989)) presents capacity factor data and conclude that the linear relationship is still valid across a broader range of conditions and not only along the critical isotherm

Since κ is a function of the pure mobile phase and it is easily calculated from experimental data for pure CO_2, isothermal capacity factor data at different densities can be successfully used for the determination of the partial molar volumes of the solute in the mobile phase The partial molar volumes of naphthalene in supercritical CO_2 were calculated on the basis of the above mentioned theory using published retention data The results obtained are illustrated in Figure 30 and are in good agreement with existing partial molar volume data (Eckert et al (1986))

The experimental uncertainty of the reported $\bar{v}^{\infty}$ data has been estimated as 15% This value is calculated using statistical analysis of the experimental data and taking into account the uncertainties in the direct measured variables This is in agreement with the accuracy of other experimental determinations of partial molar volumes

A comparison with literature results may be done for the benzaldehyde - carbon dioxide system (Foster et al (1989))

Figure 8 shows the data measured at University of Trieste (at 313 15 K) compared with literature results at 314 95 K (graphical data only) The agreement is good considering the difference in temperature (1 8 K) of the two sets of data.

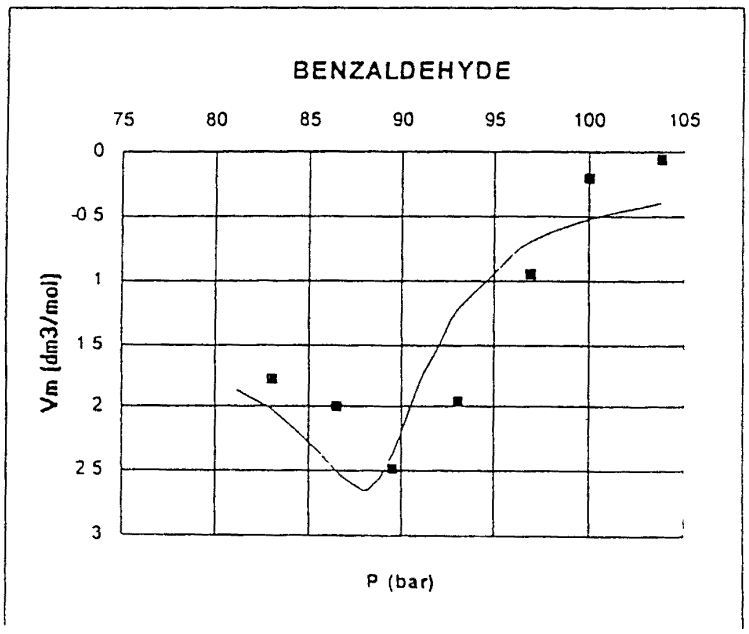

Figure 8 Comparison of the $\bar{v}^{\infty}$ data for benzaldehyde (the line represents data measured with SFC the symbols are literature data)

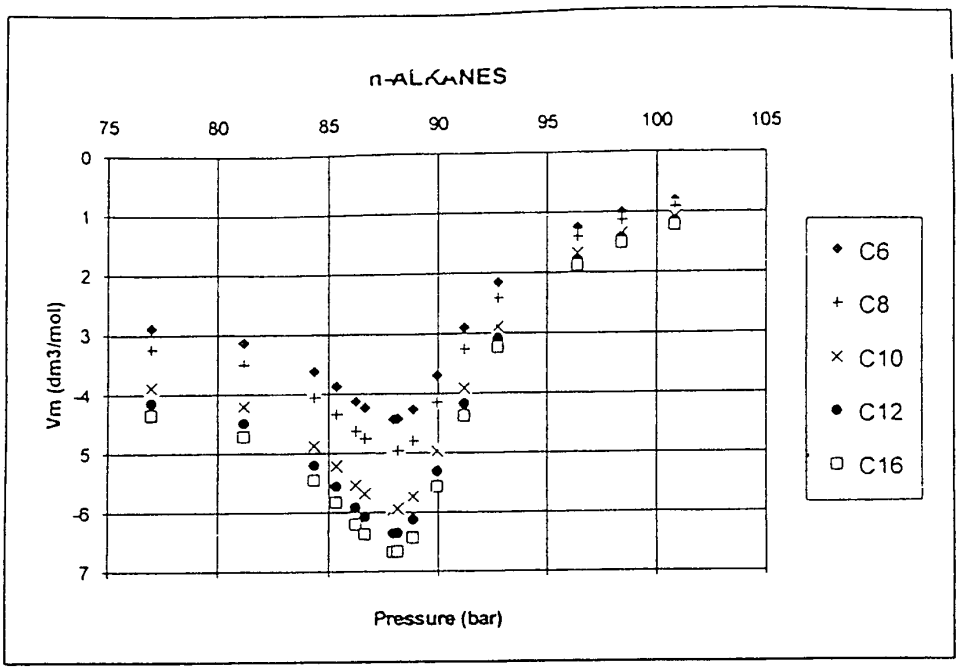

Figure 9 $\bar{v}^{\infty}$ data for n-alkanes in the vicinity of the critical point

Figure 9 illustrates the measured partial molar volume data for a series of normal alkanes ranging from hexane to hexadecane as a function of pressure in the vicinity of the critical point As expected the absolute magnitude of the partial molar volume increases with increasing carbon chain length.

7 REFERENCES

Alessi P Cortesi, A Solubility Measurements in Dense Gases Experimental Methods 'Summer School on Experimental Methods in the Thermodynamics of Fluids", Zakopane (Poland) 11-17 September 1988 137

Barber T A Cochran, H D Bienkovski, P R Solubility of Solid CCl_4 in Supercritical CF_4, *J Chem Eng Data* **1991** *36*, (1) 99

Bartle K.D Clifford, A A Jafar S A Measurement of Solubility in Supercritical Fluids Using Chromatographic Retention the Solubility of Fluorene Phenantrene and Pyrene in Carbon Dioxide *J Chem Eng Data* **1990a**, *35*, (3), 355

Bartle, K D , Clifford, A A Jafar S A Relationship between Retention of a Solid Solute in Liquid and Supercritical Fluid Chromatography and its Solubility in the Mobile Phase *J Chem Soc Faraday Trans* **1990b** *86* (5) 855

Besserer G J Robinson D B A High Pressure Autocooling Refractometer for Determining Coexisting Liquid and Vapor Phase Densities, *Can. J Chem Eng* **1971** *49* 651

Billoni N Jose, J Merlin J C Solubilities of Heavy Components in Supercritical CO_2 Using Directly Coupled Supercritical Fluid Extraction-High Performance Liquid Chromatograpy, Presented at the *International Symposium on Supercritical Fluids* Nice France October **1988**, 373

Chimowitz E H , Kelley F D *J Supercritical Fluids*, **1989**, *2*, 106

Chrastil, J , Solubility of Solids and Liquids in Supercritical Gases, *J Phys Chem* **1982**, *86* (15), 3016

Cygnarowicz, M L , Seider W D Effects of Retrograde Solubility on the Design Optimization of Supercritical Extraction Processes *Ind. Eng Chem Res* **1989** *28*, (10) 1497

Czubryt, J J , Myers, M N Giddings, J C , Solubility Phenomena in Dense Carbon Dioxide Gas in the Range 270-1900 Atmospheres, *J Phys Chem.* **1970**, *74*, (24), 4260

Diepen, G A M Scheffer, F E C , The Solubility of Naphthalene in Supercritical Ethylene, *J Phys Chem* , **1953** *57* 575

Dimitrelis, D , Prausnitz, J M Solubilities of *n*-Octadecane, Phenantrene, and *n*-Octadecane-Phenantrene Mixtures in Supercritical Propane at 390 and 420 K and at Pressures to 60 bar, *J Chem Eng Data* **1989**, *34*, (3), 286

Dohrn, R Brunner G High Pressure Fluid Phase Equilibria Experimental Methods and Systems Investigated (1988-1993) *Fluid Phase Equilibria* **1995**, 106 213-282

Eckert C A., Ziger D H , Johnston K.P , Kim S , *J Phys Chem* , **1986**, *90*, 2738

Erkey C Akgerman A *AIChE J* 1990 *36* 1715

Fall D J , Lucks, D , Phase Equilibria Behavior of the System Carbon Dioxide + n-dotriacontane and Carbon Dioxide + n-docosane, *J Chem Eng Data* **1984**, *29*, 413

Fornari, R E , Alessi, P , Kikic, I High Pressure Fluid Phase Equilibria. Experimental Methods and Systems Investigated (1978 1987), *Fluid Phase Equilibria* **1990**, *57*, 1-33

Foster N R Macnaughton S J Chaplin R P Wells P T *Ind.Eng Chem Res* **1989**, *28* 1903

Gangadhara Rao V S Mukhopadhyay M Solid Solubilities in Supercritical Fluids from Group Contributions *J Supercritical Fluids* **1990** *3* (2) 66
Gurdial, G S Foster N R. Solubility of o-Hydroxybenzoic Acid in Supercritical Carbon Dioxide *Ind. Eng Chem Res* **1991** *30* (3) 575
Hamdi, R. M Bocquet J F Chhor, K Pommier, C Solubility and Decomposition Studies on Metal Chelates in Supercritical Fluids for Ceramic Precursor Powders Synthesis, *J Supercrit Fluids* **1991** *4* 55
Hollar, W E , Ehrlich, P Solubility of Naphthalene in Mixtures of Carbon Dioxide and Ethane, *J Chem Eng Data* **1990**, *35* (3) 271
Iwai, Y Yamamoto, H , Sohda, M Tanaka, Y Shimizu, T Arai, Y A Flow-Type Apparatus for Measurements of Solubilities of Coal-Derived Component in Supercritical Fluids *Memoirs of the Faculty of Engineering Kyushu University* **1989** *49*, (3) 175
Iwai Y Yamamoto H Tanaka, Y Arai Y Solubilities of 2 5 and 2 6-Xylenols in Supercritical Carbon Dioxide, *J Chem Eng Data* **1990**, *35*, (2) 174
Iwai, Y Fukuda, T Koga, Y Arai, Y Solubilities of Myristic Acid, Palmitic Acid, and Cetyl Alcohol in Supercritical Carbon Dioxide at 35°C *J Chem Eng Data* **1991**, *36* (4), 430
Jennings, D W Lee, R -J Teja, A S Vapor-Liquid Equilibria in the Carbon Dioxide + Ethanol and Carbon Dioxide + 1-Butanol Systems, *J Chem Eng Data* **1991** *36* (3) 303
Jinno K., Niimi S , *J Chromatogr* , **1988** *453* 29
Johnston, K.P , Zieger, D H , Eckert, C A , Solubilities of Hydrocarbon Solids in Supercritical Fluids The Augmented van der Waals Treatment *Ind. Eng Chem Fundam.* **1982** *21* (3) 191
Kim, J R., Lentz, H , Solubilities and Second Cross-Virial Coefficients of Caffeine in Ammonia, *Fluid Phase Equilibria* **1988**, *41* 295
Knez, Z , Skerget, M , Sencar-Bozic, P , Rizner, A , *J Chem Eng Data* **1995** 8, 40
Ko, M , Shah, V , Bienskowski, P R., Cochran, H D "Solubility of the Antibiotic Penicillin V in Supercritical CO_2," *J Supercrit Fluids* **1991** 4 32
Kramer, A , Thodos, G Solubility of 1-Hexadecanol and Palmitic Acid in Supercritical Carbon Dioxide, *J Chem Eng Data* **1988** *33* 230
Kramer, A., Thodos, G Solubility of 1-Octadecanol and Stearic Acid in Supercritical Carbon Dioxide *J Chem Eng Data* **1989** *34* (2), 184
Kumar S K , Johnston K.P , *J Supercritical Fluids* **1988**, *1* 15
Kurnik, R T Reid, R C , Solubilities of Solid Mixtures in Supercritical Fluids, *Fluid Phase Equilibria* **1982**, *8*, 93
Laintz, K. E Wai, C M , Yonker C R Smith, R. D Solubility of Fluorinated Metal Diethyldithiocarbamates in Supercritical Carbon Dioxide *J Supercrit Fluids* **1991**, *4* 194
Lemert, R.M , Johnston, K.P Solubilities and Selectivities in Supercritical Fluid Mixtures Near Critical End Points *Fluid Phase Equilibria* **1990** *59* 31
Liong, K. K , Foster N R., Ting S S Solubility of Fatty Acid Esters in Supercritical Carbon Dioxide *Ind Eng Chem Res* 1992 31 400

Liong K K *A Fundamental Investigation of the Phase Behavior of Fatty Acid Esters in Supercritical Carbon Dioxide* Dissertation University of New South Wales Australia, 1991
Macnaughton, S J *Solubility in Supercritical Fluids* Dissertation, School of Chemical Engineering & Industrial Chemistry University of New South Wales Kensington, NSW, Australia, 1993
Madras G Erkey C Akgerman, A A New Technique for Measuring Solubilities of Organics in Supercritical Fluids *J Chem Eng Data* 1993 *38*, (3) 422
Masuoka, H Yorizane M Solubility of Solid Naphthalene in Gaseous Ethylene at High Pressures *J Chem Eng Japan* 1982 *15* (1) 5
Maxwell, R J Hampson, J W Cygnarowicz-Provost, M L Comparison of the Solubility in Supercritical Fluids of Polycyclic Ether Antibiotics Lasalocid Monensin Narasin, and Slinomysin, *J Supercrit Fluids* 1992, 5 31
McHugh M Paulaitis M E, Solid Solubilities of Naphthalene and Biphenyl in Supercritical Carbon Dioxide, *J Chem Eng Data* 1980, *25* (4) 326
Mitra, S Chen, J W Viswanath, D S Solubility and Partial Molar Volumes of Heavy Aromatic Hydrocarbons in Supercritical CO_2 *J Chem Eng Data* 1988 *33* (1) 35
Mosca, T, Thesis, 1995, DICAMP University of Trieste Italy
Olesik S V, Steger J L Kiba N Roth M Novotny M V *J Chromatogr* 1987, *392* 165
Paulaitis M E Krukonis V J Kurnik R T Reid, R.C, Supercritical Fluid Extraction *Rev Chem. Eng* 1983 *1* (2) 179
Prausnitz, J M, Benson, P R., Solubility of Liquids in Compressed Hydrogen, Nitrogen and Carbon Dioxide, *AIChE Journal* 1959 *5* 161
Reverchon, E Russo P Stassi, A Solubilities of Solid Octacosane and Triacontane in Supercritical Carbon Dioxide *J Chem Eng Data* 1993, *38*, (3), 458
Sakaki, K., Solubility of β-Carotene in Dense Carbon Dioxide and Nitrous Oxide from 308 to 323 K and from 9 6 to 30 MPa, *J Chem Eng Data*, 1992 *37* 249
Sako S Ohgaki K, Katayama, T Solubilities of Naphthalene and Indole in Supercritical Fluids *J Supercritical Fluids* 1988, *1* (1), 1
Sako S, Shibata, K, Ohgaki, K, Katayama, T Solubilities of Indole Skatole, and 5-Methoxyindole in Supercritical Fluids *J Supercrit Fluids* 1989 *2* 3
Schaeffer, S T Zalkow, L H, Teja, A S Solubility of Monocrotaline in Supercritical Carbon Dioxide and Carbon Dioxide Ethanol Mixtures ' *Fluid Phase Equilib* 1988, 43, 45
Schmitt, W J Reid, R. C, The Solubility of Paraffinic Hydrocarbons and Their Derivatives in Supercritical Carbon Dioxide *Chem Eng Comm* 1988 *64* 155
Shim J -J, Johnston K P *J Phys Chem* 1991 *95* 353
Schuchardt, A, Thesis, 1995, DICAMP University of Trieste Italy
Simnick, J J Lawson, C C Lin, M Chao K.C Vapor-Liquid Equilibrium of Hydrogen/Tetralin System at Elevated Temperatures and Pressures *AIChE Journal* 1977 *23* 469
Suzuki, K, Sue H Itou, M Smith R L Inomata, H, Arai K Saito S Isothermal Vapor-Liquid Equilibrium Data for Binary Systems at High Pressures Carbon Dioxide Methanol Carbon Dioxide Ethanol Carbon Dioxide-1 Propanol Methane-Ethanol

Methane-1-Propanol, Ethane-Ethanol and Ethane 1-Propanol Systems, *J Chem. Eng Data* **1990a** *35* 63
Tsai, F -N Yau, J S Solubility of Carbon Dioxide in *n*-Tetracosane and in *n*-Dotriacontane, *J Chem Eng Data* **1990**, *35* 43
Valli M Thesis **1994**, DICAMP University of Trieste Italy
Van Leer, R A Paulaitis, M E Solubilities of Phenol and Chlorinated Phenols in Supercritical Carbon Dioxide, *J Chem Eng Data* **1980** *25*, (3) 257
van Wasen U Schneider G M , *J Phys Chem* **1980** *84* 229
Warzinski, R. P Lee Chang-Ha Holder, G D , Supercritical Fluid Solubilization of Catalyst Precursors The Solubility and Phase Behavior of Molybdenum Hexacarbonyl in Supercritical Carbon Dioxide and Application to the Direct Liquefaction of Coal, *J Supercrit Fluids*, **1992**, *5*, 60
Wells P A Chaplin, R. P , Foster N R Solubility of Phenylacetic Acid and Vanillan in Supercritical Carbon Dioxide, *J Supercrit Fluids*, **1990** *3* 8
Weng W L Lee M J Phase Equilibrium Measurements for the Binary Mixtures of 1-Octanol plus CO_2 C_2H_6 and C_2H_4 *Fluid Phase Eqilibria* **1992**, *73*, 117
Yan, J -S Tsai F -N Solubilities of 1-Hexadecanol and 1-Octadecanol in Subcritical and Supercritical Carbon Dioxide, *J Chem Eng Data* **1992**, *37*, (3), 285
Yan, J -S Tsai, F -N , Solubility of Carbon Dioxide in Phenol and in Catehol, *J Chem Eng Data* **1992**, *37*, (2), 141
Yun J S L Liong K. K., Gurdial G S Foster N R Solubility of Cholesterol in Supercritical Carbon Dioxide, *Ind. Eng Chem Res* **1991**, *30*, 2476

Natex Prozesstechnologie GesmbH

Basic-Course

of

Supercritical Fluid Extraction Process

Metal Industries Research & Development Center

Kaohsiung, Taiwan, ROC

Mr TZU-CHEN KUO

THERMODYNAMIC
PROPERTIES
PHASE EQUILIBRIA

EQUATIONS OF STATE

CONTENT

MODELING PHASE EQUILIBRIA

1 CUBIC EQUATIONS OF STATE

1 1 PURE FLUIDS

1 2 EXTENSION OF CUBIC EQUATIONS OF STATE TO MIXTURES

2 NON CUBIC EQUATIONS OF STATE

3 SOLUBILITY IN SUPERCRITICAL FLUIDS

4 INFLUENCE OF THE EQUATION OF STATE

5 INFLUENCE OF MIXING RULES

6 INFLUENCE OF SUBLIMATION PRESSURE

7 REFERENCES

MODELING PHASE EQUILIBRIA

The goals of the modeling are both to correlate the existing data and to attempt prediction of phase equilibria in regions where experimental results are not available An ideal model would use easily measured physical properties to predict phase equilibria at all conditions and it would be theoretically based Unfortunately no such model exists, and any single model cannot treat all situations

Existing correlations of phase equilibria data contain many regressed parameters they are often semi-empirical and they may succeed in fitting the data in portions of the phase diagram even with high accuracy As far as prediction is concerned, models developed for that purpose attempt to justify theoretically a link between the model parameters and real physical phenomena. Often the distinction between these two methods is lost, since theoretically based models are forced to fit the data better by the introduction of additional adjustable parameters (Ekart et al , (1991))

The critical review of existing approaches for modeling supercritical mixtures is presented by Johnston, (1989) The general conclusion is that modeling is still case specific As the critical point is approached predictions and even correlations of critical curves and solubilities are extremely difficult because of the nonclassical behavior in this region Another problem in prediction concerns the effect of cosolvents on solubilities since the strength of various interactions between the cosolvent and solute must be taken into account

The models introduced in predicting equilibria in the supercritical region can be mainly divided in the following groups (Ekart et al , (1991))

equation of state approach
- cubic equation of state
- perturbation equation of state
  lattice gas equation of state
  association models

- expanded liquid treatment
  computer simulations

The most widely used method for analyzing supercritical fluid equilibria data are cubic equations of state They are quite simple, they can correlate supercritical fluid phase behavior, cubic equations can be rapidly solved analitically, they can be also easily extended to multicomponent systems Due to the approximated and somewhat empirical basis of the equation, mixing rules are crucial in the determining the quality of the model

1 CUBIC EQUATIONS OF STATE

1 1 PURE FLUIDS

The earliest cubic equation of state is the van der Waals equation

$$P = \frac{RT}{v-b} - \frac{a}{v^2} \qquad (1)$$

In this equation the constant b is the excluded volume that is that part of the molar volume which is not available to a molecule due to the presence of others This contribution increases the pressure above that for an ideal gas at the same density and

temperature The second term on the right which van der Waals took to be independent of temperature is due to attractive forces and decreases the pressure We can define an accessible or free volume v_f as the difference between the total volume and the excluded volume, that is, $v_f = v - b$

There remain the questions of how to determine the parameters in this (and other) equation of state There are two alternatives The first is to choose the parameters to fit vapor pressure and liquid or vapor density With the van der Waals equation, in which the parameters are constants, this can be done only at one temperature, for the equations we discuss below with parameters that are a function of temperature, this is done over a range of temperatures The second way is too fit the parameters to the critical point using the critical point conditions

A very large number of other more accurate cubic equations of state have been suggested

An important modification was made by Redlich and Kwong (1949) who introduced a temperature dependence and a slightly different volume dependence in the attractive term

$$P = \frac{RT}{v-b} - \frac{a}{\sqrt{T}v(v+b)} \tag{2}$$

This equation gives a somewhat better critical compressibility (Z_c = 0 333 instead of 0 375 given by vdW equation) but is still not very accurate for the phase bondary (vapor pressure) and the liquid density

Wilson (1964) changed the temperature dependence of the attractive parameter in Redlich-Kwong equation by writing

$$P = \frac{RT}{v-b} - \frac{a_c\alpha}{v(v+b)} \tag{3}$$

with

$$\alpha = T_r\left[1 + (1\ 57 + 1\ 62\omega)(\frac{1}{T_r} - 1)\right] \tag{4}$$

where ω is the acentric factor (Pitzer 1955, 1977) defined as

$$\omega = -\log\frac{P(T_r = 0\ 7)}{P_c} - 1\ 0$$

However, it was Soave's modification (1972) for the α parameter

$$\alpha(T_r) = \left[1 + (0\ 48 + 1.57\omega - 0\ 176\omega^2)\left(1 - \sqrt{T_r}\right)\right]^2 \tag{5}$$

resulting in accurate vapor pressure predictions (especially above 1 bar) for light hydrocarbons, which led cubic equations of state becoming an important tool for the prediction of vapor-liquid equilibria at moderate and high pressures for non polar fluids Peng and Robinson (1976) used a different volume dependence to give slightly improved liquid volumes (that is Zc = 0 307)) and changed the temperature dependence of α to give accurate vapor pressure predictions for hydrocarbons in the 6 to 10 carbon number range as follows

$$P = \frac{RT}{v-b} - \frac{a_c \alpha}{v^2 + 2bv - b^2} \qquad (6)$$

with

$$\alpha = \left[1 + (0.37464 + 1\ 54226\omega - 0\ 2699\omega^2)(1 - T_r^{0.5}\right]^2$$

Many other α functions have been proposed and a representative sample is given in Table 1

Table 1 Temperature Dependence of α Function.

$\alpha = 1 + c_1(1 - T) + c\left(\frac{1}{T} - 1\right)$	Soave (1984)
$\alpha = 1 + c_1(1 - \sqrt{T}) + c(1 - T)$	Carrier et al (1985)
$\alpha = \left[1 + c_1(1 - \sqrt{T}) + c\left(\frac{1}{T} - 1\right)\right]$	Harmens and Knapp (1980)
$\alpha = [1 + c_1 \ln(T) + c(\ln T)]$ $(T > 1)$	Harmens and Knapp (1980)
$\alpha = [1 + c_1(1 - \sqrt{T}) + c(1 - T)(0\ 7 - T)]$	Mathias (1983)
$\alpha = [1 + c_1\tau + c\tau^2 + c_3\tau^3]$ where $\tau = 1 - \sqrt{T}$	Mathias and Copeman (1983)
$\alpha = [1 + c_1\tau + c\tau^2 + c_3\tau^3]$ where $\tau = 1 - T^{0.5}$	Androulakis et al (1989)
$\alpha = T^{c(c-1)} \exp[c_1(1 - T^{c\,c})]$	Twu et al (1991)
$\alpha = \exp[c_1(1 - T)]$	Heyen (1980)
$\alpha = 10^{[c(1-T)]}$	Adachi and Lu (1984)
$\alpha = 10^{[c(\ln \alpha T \quad T)]}$	Yu and Lu (1987)
$\alpha = \exp[c_1(1 - T) + c(1 - \sqrt{T})]$	Melhem et al (1989)

The Peng-Robinson (PR) and SRK equations are widely used since they require little input information (only critical properties and acentric factor for the generalized

parameters) little computer time These equations have also some important shortcomings In particular liquid densities are not well predicted the generalized parameters are not accurate for nonhydrocarbons (especially polar and associating fluids), and these equations do not lead to accurate predictions for long-chain molecules On top of this these equations are not accurate in the critical region and vapor pressure predictions are not very accurate below 10 torr

A clever method of improving the saturated liquid molar volume predictions of a cubic equation of state was introduced by Peneloux et al (1982) by translating the calculating volumes without changing the predicted phase equilibrium The volume translation $v \rightarrow c + c$ and $b \rightarrow b + c$ applied to the RKS EOS leads to

$$P = \frac{RT}{v-b} - \frac{a_c \alpha}{(v+c)(v+b+2c)} \tag{8}$$

where the volume translation parameter c is chosen to give the correct liquid saturation volume at some temperature usually at a reduced temperature $T_r = T/T_c = 0\ 7$ which is near the normal boiling point Making c a function of temperature it is possible to improve further the densities

So far the discussion has centered on the general behavior of cubic equations of state The region around the critical point of a fluid or mixture is one where cubic equations of state are inherently inaccurate Among their shortcomings is the failure to obey the following (and other) scaling laws approaching the critical point

- Along the saturation curve
  $\lim_{T \rightarrow Tc} (v^g - v_c) \sim (T - T_c)^\beta$ and
  $\lim_{T \rightarrow Tc} (v^l - v_c) \sim (T - T_c)^\beta$ with $\beta = 0\ 32 \pm 0\ 01$
  where the subscripts g and l indicate the vapor and liquid phases respectively
- Along the critical isotherm,
  $\lim_{v \rightarrow vc} |P - P_c| \sim (v - v_c)^\delta$ with $\delta = 4\ 8 \pm 0\ 2$

These laws have been derived from theory and verified by experiment In contrast all classical equations of state give $\beta = 0\ 25$ and $\delta = 3\ 0$ independent of the values of the parameters in the equation. As a consequence we can conclude that is the functional form of the equations which is incorrect in the critical region Also real fluids exhibit a diverging specific heat near their critical point which is not predicted from a cubic equation of state

1 2 EXTENSION OF CUBIC EQUATIONS OF STATE TO MIXTURES

The greatest utility of cubic equations of state is for phase equilibrium calculations involving mixtures The assumption inherent in such calculations is that the same equation of state used for pure fluid can be used for mixtures if we have a satisfactory way of obtaining the mixtures parameters This is most commonly done using the van der Waals one-fluid mixing rules,

$$a = \sum_i \sum_j a_{ij} z_i z_j \tag{9}$$

$$b = \sum\sum b_{ij} z_i z_j$$

In addition, combining rules are needed for the parameters a_{ij} and b The usual combining rules are

$$a_{ij} = \sqrt{a_{ii} a_{jj}}\left(1 - k_{ij}\right)$$

and

$$b_{ij} = \frac{(b_{ii} + b_{jj})}{2}(1 - l_{ij}) \qquad (10)$$

where k_{ij} and l_{ij} are the binary interaction parameters obtained by fitting equation of state predictions to experimental vapor-liquid equilibrium (VLE) data for k_{ij} or VLE and density data for k_{ij} and l_{ij} Generally, l_{ij} is set equal to zero, in which case we have $b = \Sigma x_i b_{ii}$

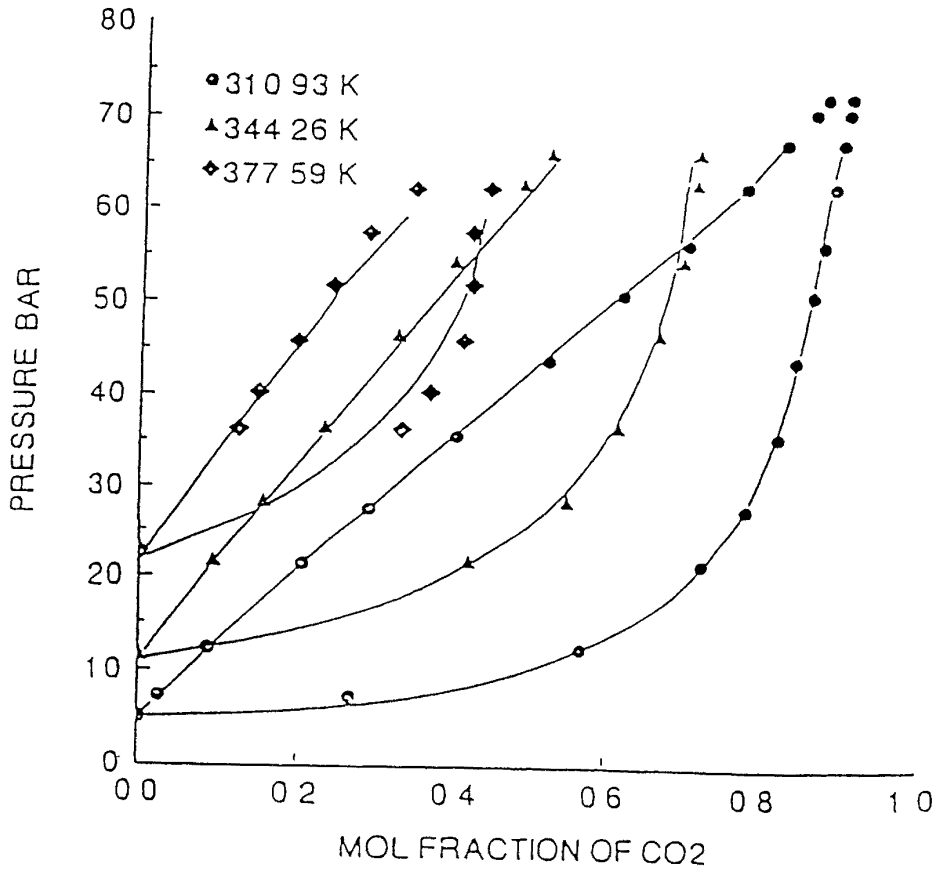

Figure 1 Correlation of VLE data of CO_2 Isobutane system with PR EOS

The justification for the combining rule for the a parameter is that it is related to the attractive forces, and from intermolecular potential theory the attractive parameter in the intermolecular potential for a mixed interaction is given by a relation like the first of Equation (10) Similarly, the excluded volume or repulsive parameter b would be given by the second of Equations (10) if molecules were hard spheres Since most molecule are nonspherical and do not have only hard interactions and there is not a one to-one relation between the attractive part of the intermolecular potential and a parameter in an equation of state consequently these combining rules do not have a rigorous basis and other has been proposed

In Figure 1 some results obtained correlating high pressure vapor liquid equilibrium data for the carbon dioxide - isobutane system using Peng Robinson equation of state and classical vdW mixing rules are reported In this case only a single binary parameter was fitted to the experimental data

In Figure 2 similar results are reported for the system nitrogen - n butane always with Peng Robinson equation of state

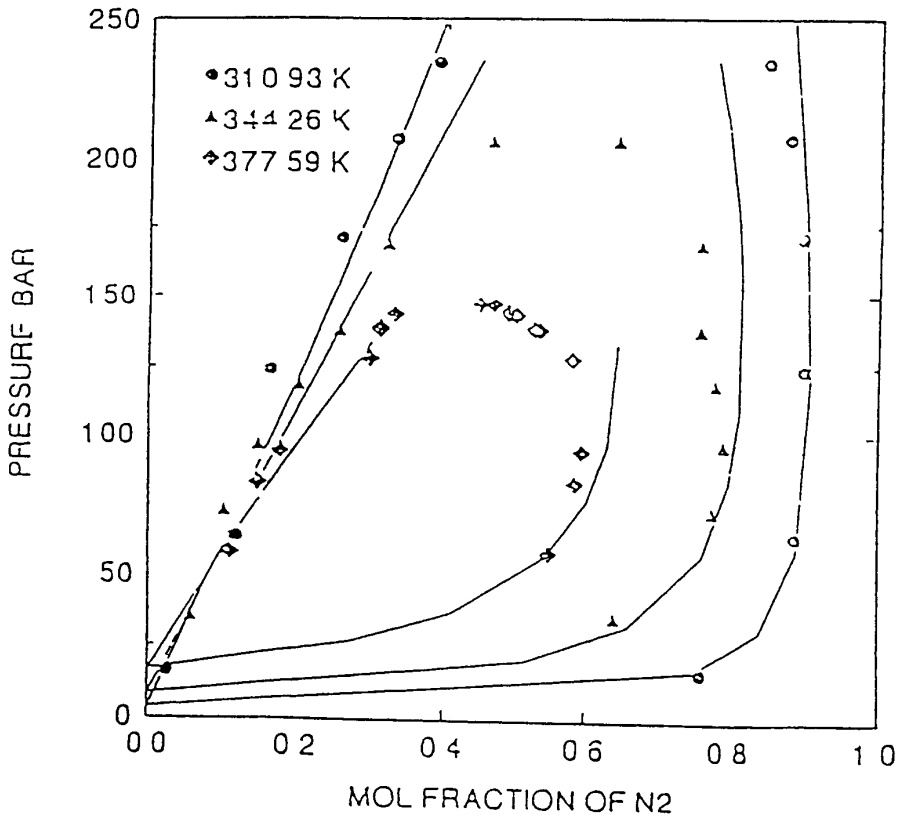

Figure 2 Correlation of VLE data for the system nitrogen - n.butane using PR EOS and classical mixing rules

A shortcoming of the vdW one-fluid (or classical) mixing rules is that they are applicable only to mixtures of relatively moderate solution (in contrast with PvT) non-ideality Starting from the following relation between the excess Gibbs free energy of mixing, G^{ex}, and fugacity coefficients calculated from an equation of state

$$G^{ex} = RT\left(\ln \phi - \sum x_i \ln \phi_i\right) \tag{11}$$

where ϕ and ϕ_i are the fugacity coefficients of the solution and of the pure component i calculated from

$$\ln \phi = \frac{1}{RT}\int_{\infty}^{v}\left(\frac{RT}{v} - P\right) dv - \ln Z + (Z - 1) \tag{12}$$

it is possible to show that for a binary mixture, using vdW EOS, we can obtain

$$\frac{G}{RT} = \ln\left(\frac{P}{RT}\prod_{i=1} \frac{v_{f_i}}{v_{f_i}}\right) - \frac{x_1 x_2}{RT(x_1 b_{11} - x_2 b_{22})}\left(\sqrt{\frac{b_{11}}{b_{22}}} - \sqrt{\frac{a_{22} b_{11}}{b_{22}}}\right) + \frac{2\sqrt{a_{11}a_{22}}(1 - k_{12})}{x_1 b_{11} - x_2 b_{22}} \tag{13}$$

The excess Gibbs free energy computed using the vdW cubic equation of state and the vdW one-fluid mixing rules contain three contributions The first, which is the Flory free-volume term, arises from the hard-core or free volume terms is completely entropic in nature The second term is very similar to the excess Gibbs free energy in regular solution theory The third term is similar in form to aterm, which appears in augmented regular solution theory The conclusion, then, is that the combination of a cubic equation of state with one fluid mixing rules can only reperesent mixtures which have approximately the same moderate degree of solution nonideality as can be described by regular solution theory

Since many mixtures of interest in the chemical industry exhibit much greater degrees of nonideality and have traditionally been described by activity coefficient (free energy) models Huron and Vidal (1979) dictated which solution model they wanted an equation of state/mixing rule combination to represent and then used Equation (11) to develop the mixing rules that produce this result They asume that G^{ex} is independent of pressure (which is an incorrect assumption) and then equating the excess free energy and equation of state results at infinite pressure thereby ensuring that a liquid root of the equation of state was being used However since

$$G^{ex} = A^{ex} + P\,V^{ex} \tag{14}$$

for G^{ex} to remain finite at infinite pressure V^{ex} must be zero which requires that vdW mixing rules of Equation (9) for the b parameter be used The mixing rule for the a parameter then is

$$a = b\left[\sum x_i\left(\frac{a}{b}\right) - \sigma G^{ex}\right] \tag{15}$$

where σ is a numerical constant which depends on the particular equation of state used

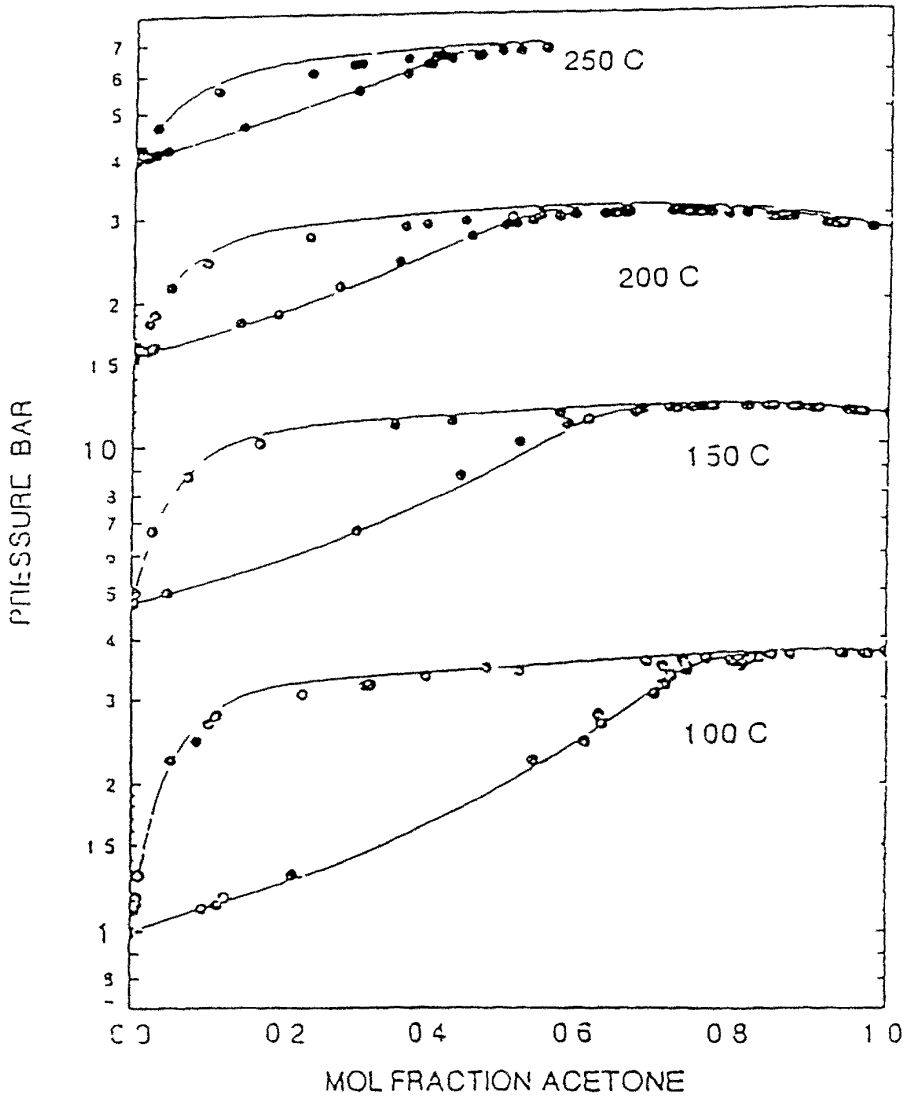

Figure 3 Correlation of VLE data for the acetone - water system using PR EOS and Huron and Vidal mixing rules

This mixing rule when combined with the Wilson or NRTL models gives excellent results for describing some highly nonideal systems

Figure 3 reports some results obtained with Peng Robinson EOS and Huron and Vidal approach (NRTL model for excess free energy) It is necessary to point out that the results reported in the Figure 3 were obtained by fitting individually each isotherm and consequently obtaining three parameters per each isotherm.

However the Huron-Vidal mixing rule has some theoretical and computational difficulties The mixing rule may not be successful in describing non polar hydrocarbon mixtures and this is a problem when a multicomponent mixture contains both polar and nonpolar components since all species must be represented by the same mixing rule Another theoretical deficiency of the Huron-Vidal mixing rule is that it does not satisfy the quadratic composition dependence required of the second virial coefficient Further it is necessary to remind that the numerical values of parameters of the excess free energy model used in the mixing rules are not the same as those obtained whn correlating data directly with the activity coefficient model

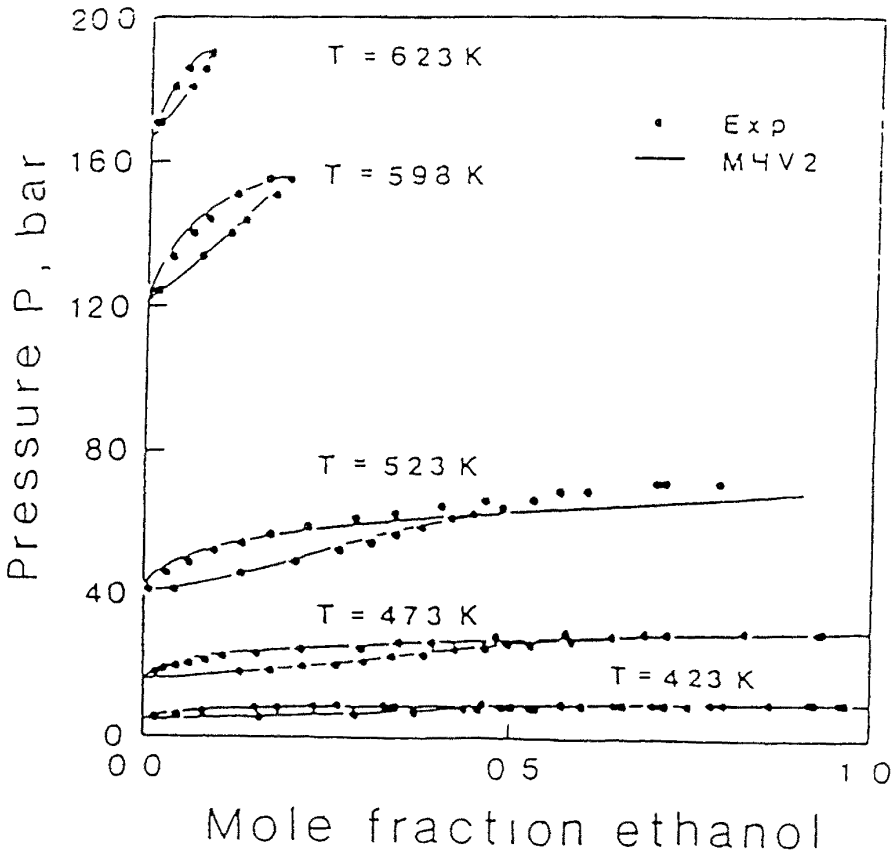

Figure 4 Pxy diagram for ethanol water using Modified UNIFAC with the MHV2 mixing rule

Some effort has ben directed toward relaxing the infinite pressure limit in the Huron-Vidal mode' (Michelsen 1990a, 1990b) the most successful of these is the modified UNIFAC group contribution method to make predictions in absence of experimental data (MHV2 model)

The model uses the SRW equation of state and the Huron-Vidal approach but with the equation of state and excess Gibbs free energy models matched at liquid density and zero pressure at the temperature of interest One difficulty in removing the infinite pressure (and v = b)) assumption is that then volume appears in Equation (11) through the fugacity coeffcient expression this can lead to computational difficulties that require empirical extrapolations

Figure 4 and 5 report as an example some results obtained by the MHV2 model applied to ethanol-water and acetone water mixtures

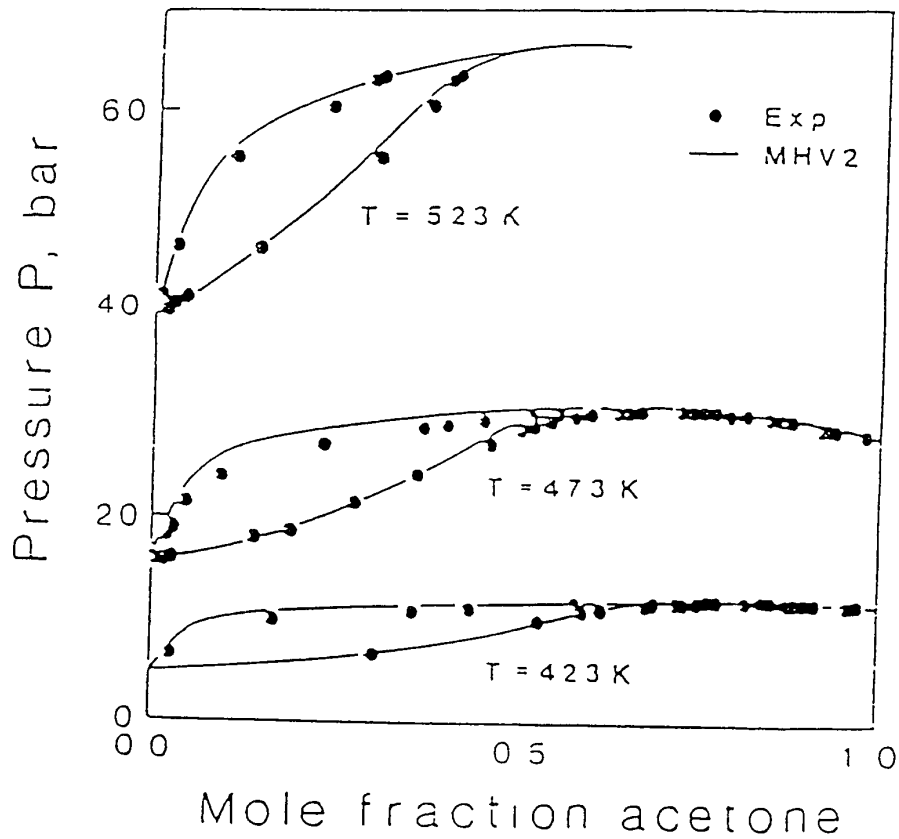

Figure 5 Pxy diagram for acetone - water using modified UNIFAC with the MHV2 mixing rule

Recently Soave and al (1994) have investigated the use of infinite dilution activity coefficients to define parameters of the Redlich-Kwong equation of state with the Huron-Vidal mixing rules the model using a gruoup contribution expression of the UNIFAC type is able to predict vapor-liquid equilibria for a number of significant systems including strongly polar components

Wong and Sandler (1992) have recently developed a promising new mixing rule which produces the desired EOS behavior at both low and high densities without being density dependent uses existing G^{ex} parameter tables This new mixing rule is based on the following observations The first is that in order to ensure the proper composition dependence of the second virial coefficient the following condition constitutes a constraint for a and b

$$b(x, T) = \sum_i \sum_j x_i x_j B_{ij}(T) = \sum_i \sum_j x_i x_j \left(b_{ij} - \frac{a_{ij}}{RT}\right) = b - \frac{a}{RT} \qquad (16)$$

together with the combining rule

$$b_{ij} - \frac{a_{ij}}{RT} = \frac{1}{2}\left[\left(\frac{b_{ii} - a_{ii}}{RT}\right) + \left(b_{jj} - \frac{a_{jj}}{RT}\right)\right](1 - k_{ij}) \qquad (17)$$

which introduces a second virial coefficient binary interaction parameter k_{ij}

A second observation is that the excess Helmholtz free energy of mixing is much less pressure dependent than the excess Gibbs free energy, this is shown in Figure 6 for the system methanol-benzene at 373 K.

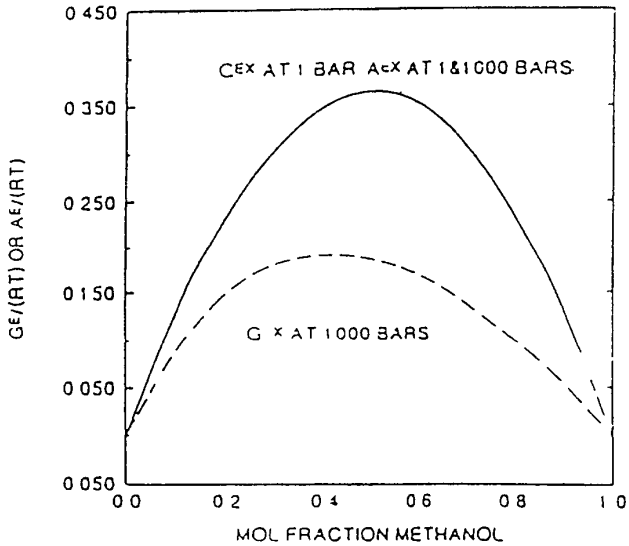

Figure 6 Excess Gibbs and Helmholtz free energies of mixing for the methanol benzene system at 1 bar and 1000 bar calculated with PR EOS and Wong-Sandler mixing rules

From this result it is possible to argue that

$$G^{ex}(T, P = 1\ \text{bar}, x) = A(T, P = 1\ \text{bar}, x) = A(T, \text{high pressure}, x) \quad (18)$$

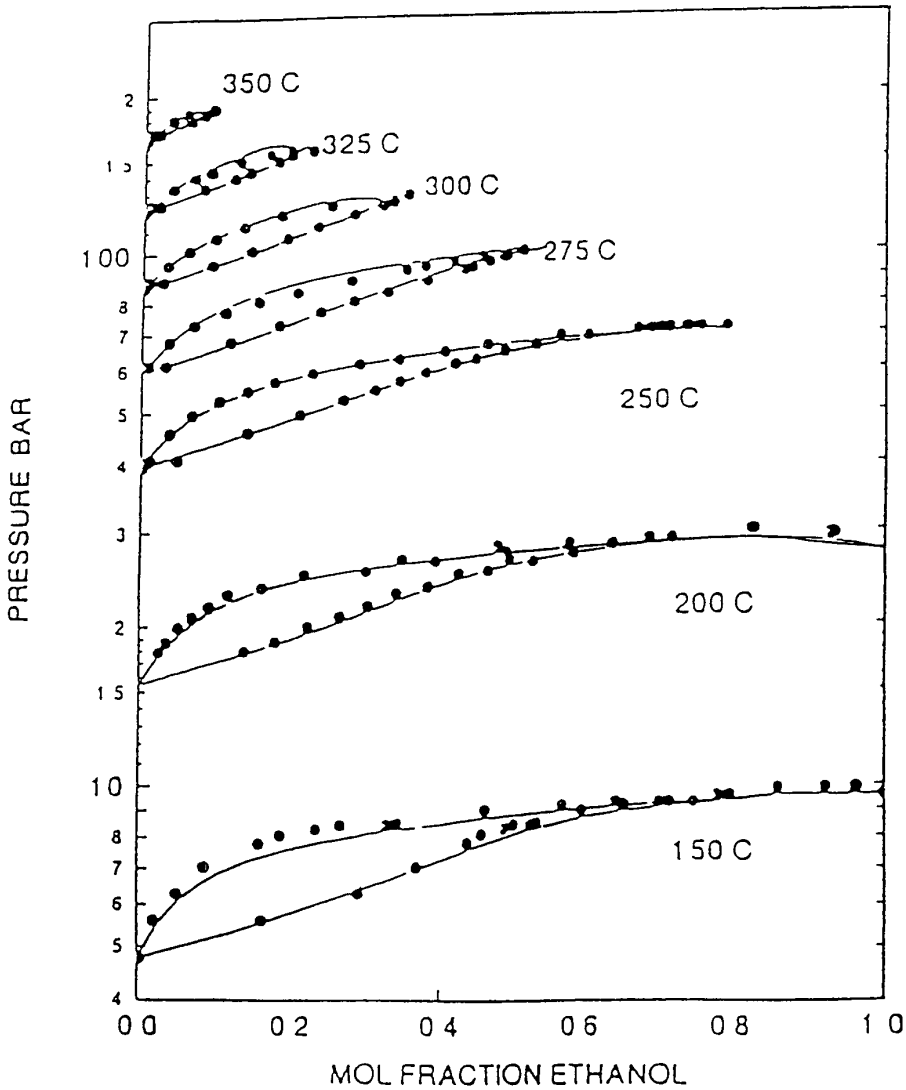

Figure 7 Prediction of the vapor liquid equilibrium for ethanol - water system using PR EOS and the Wong-Sandler mixing rule with temperature

The first of these equalities follows from the fact that $G^{ex} = A^{ex} + Pv^{ex}$ and that the Pv^{ex} term is very small at low pressures The second of the equalities is a result of the essential

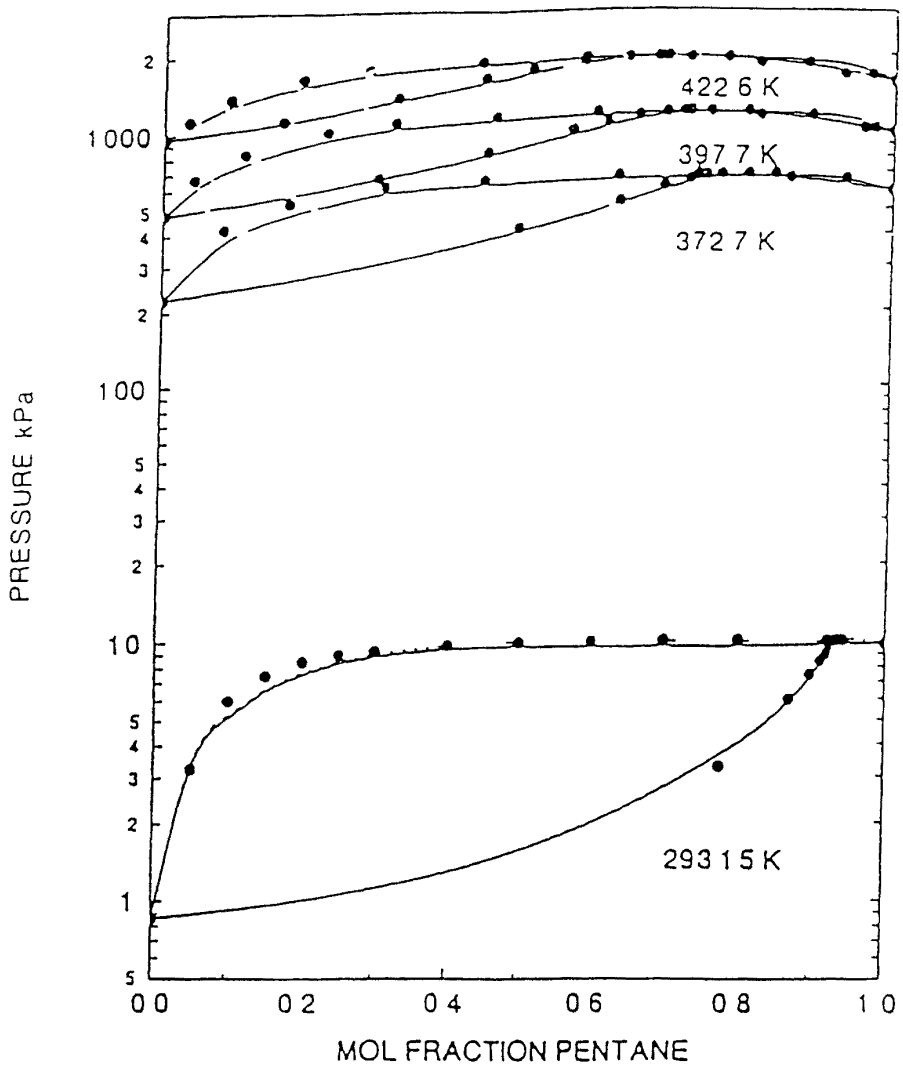

Figure 8 Prediction of the vapor - liquid equilibria for the n. pentane - ethanol system using PR EOS and the Wong-Sandler mixing rule with parameters obtained from UNIFAC model.

pressure (or density) independence of A^{ex} The second equation for the parameters of the equation of state then comes from the condition that

$$\begin{aligned} A_{EOS}(T\ P = \infty\ x) &= A\ (T\ P = \infty\ ) \\ &= A\ (T\ \text{low}\ P\ x) \\ &= G\ (T\ \text{low}\ P\ x) \end{aligned} \tag{19}$$

Here the subscript EOS refers to the Helmholtz free energy derived from an equation of state while A^{ex} and G^{ex} without subscript indicate a free energy or activity coefficient model Combining these equations gives the following mixing rules

$$\frac{a}{RT} = Q\frac{D}{1-D} \qquad b_m = \frac{Q}{1-D} \tag{20}$$

where

$$Q = \sum\sum x\,x\left(b - \frac{a}{RT}\right)_{ij}$$
$$D = \sum x\frac{a}{bRT} + \frac{G^{ex}(x)}{\sigma RT} \tag{21}$$

Here σ is a constant which depend on the equation of state ($\sigma = (\ln(\sqrt{2}\ 1))\sqrt{2}$ for the PR EOS), and any excess free energy model may be used for G^{ex}

The results (as it possible to observe from the data reported in Figures 7 and 8) are very promising due to the flexibility of the model obtained with an appropriate choice of the excess free energy model and with the use of parameters obtained by fitting low pressure equilibrium data.

In this way the new mixing and combining rules allow cubic equations of state to be used for accurate calculations and predictions but still it remains the problem of the accurate representation of the critical and near-critical regions of pure fluids and mixtures

Among these uses problems arising in using cubic equations of state are discussed by Soave et al (1993) and Soave et al (1995) with particular emphasis to the evaluation of pure component parameters and by Bertucco et al (1995) with reference to the estimation of chemical equilibria in high pressure gaseous systems

2 NON CUBIC EQUATIONS OF STATE

The statistical mechanics and computer simulation have contributed to the development of new generations of equations of state in contrast with those discussed until now that are mainly based on empiricism.

The original van der Waals idea was that pressure in a fluid was the result of both repulsive forces or excluded volume effects which increase as the molar volume decreases and attractive forces which reduce the pressure Since the molecules have a finite size, there would be a limiting molar volume, b, which could be achieved only at infinite pressure At large separations, London dispersion theory establishes that attractive forces increase as r^{-6} where r is the intermolecular separation distance Since volume is proportional to r^3, this provides some explanation also for the second term in the van der Waals equation of state

These arguments provide a plausible explanation for the form of the van der Waals equation but the modern statistical mechanics has shown that neither the repulsive nor the attraction term in the equation is correct For a fluid of hard spheres (without attractive forces) the accurate equation of state is given by the Carnahan-Starling expression

$$Z = Z(\eta) = \frac{1 + \eta + \eta - \eta}{(1 - \eta)^3} \qquad (22)$$

where $\eta = \pi \rho \sigma^3 / 6$ with σ being the hard-sphere diameter and ρ the density
Based on molecular dynamics computer simulation of square-well molecules Alder et al (1972) found that to describe the attractive part of the equation of state accurately they needed the double power series expansion in reduced temperature and pressure shown below

$$p^{attr} = -\sum_n \sum_m A_{nm} \left(\frac{\varepsilon}{kT}\right)^n (\rho\sigma^3)^m \qquad (23)$$

where σ is the hard core diameter and ε is the well depth.

As a consequence Carnahan Starling repulsion term and the Alder expression can be used together for obtaining a perturbed hard-sphere equation of state Due to the mathematical difficulties (the resulting equation is not more cubic) different authors have mixed the Carnahan repulsive term with different expressions for the attractive part like the Van der Waals one or the Redlich-Kwong The different equations know as perturbed equations of state are reported in Table 2

In these equations of state the van der Waals repulsive term v/(v-b) is substituted with the expression for systems of hard spheres $(1+\xi + \xi^2 - \xi^3)/(1-\xi)^3$ where ξ =b/v In the Carnahan-Starling-Van-der-Waals (CSVDW) equation of state the interaction energy, parameter a_{12}, was adjustable and found to be only slightly temperature dependent
The Carnahan-Starling-Redlich-Kwong (CSRK) equation incorporates both the better repulsive and attractive terms and gave improved results as well The Augmented van der Waals (AVDW) equation of state contains the improved Carnahan-Starling repulsive term and uses the molecular dynamics square well results to include second-order perturbation effects and improve the attractive term. The Hard-sphere-van-der-Waals (HSVDW) equation incorporates an accurate repulsive expression for the hard-sphere mixture with the standard van der Waals attractive term.

These models based on perturbed hard chain theory seem particularly promising In fact it is well known that, normal cubic equations of state give poor results in reproducing, with the same set of parameters volumetric and equilibrium properties On the other hand, one of the main advantages of non cubic equations of state is represented by their capacity of reproducing, at the same time, equilibrium and volumetric properties thus indicating their more solid theoretical base

Table 2 Perturbation Equations of State

Name	Equation	Parameters
CSVDW	$P = RT\frac{\xi}{b_0}\frac{\left(1-\xi+\xi^2-\xi^3\right)}{(1-\xi)^3} - \frac{a}{V^2}$	$\xi = b/V$
CSRK	$P = RT\frac{\xi}{b_0}\frac{\left(1-\xi+\xi^2-\xi^3\right)}{(1-\xi)^3} - \frac{a}{T^{1/2}V(V+b)}$	
AVDW	$P = RT\frac{\xi}{b_0}\frac{\left(1-\xi+\xi^2-\xi^3\right)}{(1-\xi)^3} - \frac{1}{b}\sum_{m-1}^{6} mA_{1m}\xi^{m+1}\varepsilon + \frac{\beta}{RTb\beta^{max}}\sum_{m-1}^{9} mA_{2m}\xi^{m+1}\varepsilon^2$	A_{nm}=Alder const ε=energy term β=-(1/V)(∂V/∂P) β^{max}=maximum β at given temperature
HSVDW	$P = RT\frac{\xi}{b_0}\frac{\left[\left(1-\xi+\xi^2-\xi^3\right)-3\xi(y_1+y_2\xi)-\xi^3 y_3\right]}{(1-\xi)^3} - \frac{a}{V^2}$	$\xi, y_1\ y_2\ y_3 = f$ (hard-sphere diameters and mole fractions)

The perturbed hard chain theory equation of state derived by Cotterman et al (1986) is based on the generalized van der Waals theory The model has been developed in terms of the Helmholtz function by considering an attractive and a repulsive contribution

$$a^r = a^{ref} + a^{pert} \tag{24}$$

where a^r is the residual Helmholtz function, a^{ref} is the reference or the repulsive term and a^{pert} is the perturbation or attractive term.

These terms are introduced for describing the high density and the low density region the latter is based on a generalized form of the Carnahan Starling equation.

Dispersion and polar contributions to the free energy are considered in each part of the attractive term as well as dipole and quadrupole contributions These values could be set to zero if no experimental data are available An interpolation function between the two limiting cases of dense fluid and zero density fluid, is included in the model based on empirical non adjustable parameters

In this model each pure substance is characterized by three molecular parameters v^* T^* and c The soft core volume is defined as

$$v^* = \frac{r\sigma^3 N}{\sqrt{2}} \tag{25}$$

where r is the number of segments, σ is the soft core diameter of one segment and N is Avogadro s number The constant T^* is defined as

$$T^* = \varepsilon q / ck \tag{26}$$

where $\varepsilon q/k$ is the potential energy per molecule, ε is the potential energy per unit surface area, q is surface area of the molecules and k is Boltzmann s constant The parameter c is the number of external degrees of freedom, i e a measure of flexibility and asymmetry of the molecule

Gregorowicz et al (1991) reported the expression for the pure component parameters of the equation of state The extension to mixture of the equation of state requires the definition of combining and mixing rules

Table 3 Pure component calculations for different equations of state

Substance	SRK	PR	PHCT	N VLE	N PVT
Argon	3 8	5 4	0 91	20	60
nitrogen	4 1	5 8	0 65	20	40
methane	4 1	5 8	0 92	20	50
ethylene	5 3	5 2	1 11	20	42
ethane	5 4	4 2	1 14	19	40
propane	6 2	3 2	1 56	20	40
n butane	7 7	3 6	1 61	18	35
benzene	9 5	4 6	0 93	13	25
carbon dioxide	7 5	2 7	1 24	20	60
hydrogen sulfide	6 8	4 9	1 48	15	48
methyl chloride	10 9	3 2	1 69	18	48
trifluoromethane	14 1	6 0	1 72	15	40
ammonia	18 6	10 0	2 10	20	60
acetone	25 0	13 6	1 25	6	10
methanol	32 4	22 3	2.77	26	
ethanol	21 6	12 0	2 01	25	
n heptadecane			2 88	25	
diphenyl			2 01	20	
naphthalene			1 12	20	

To summarize the model includes at most three binary interaction parameters one of them (the second virial term) becomes relevant only at very low pressure and therefore will not be considered for high pressure calculations
Excellent results are obtained both for pure components properties and for mixtures (Kikic et al 1990 Gregorowicz et al 1991 Fermeglia and Kikic 1993) as it is shown in Tables 3 4 and 5

Π comp	T [K]	DP/P	Dy	DV/V'	DV/V"	k_{ij}
propane	277 344	9 2	020	2.6	14 0	0
		1 1	007	1 8	3 1	0.0
n heptane	310-394	12 1	010	3 0	34 0	0
		1 8	003	3 0	5 4	039
n octane	313-383	7 0	008	22.0	25 0	0
		5 0	002	4 0	10 0	0.1
n decane	344-377	15 0	015	1.5	41 0	0
		2.0	006	1.2	9 1	041
n hexadecane	463-663	12.0	030			0
		1 0	007			052

Table 4 **Binary VLE calculations for systems containing carbon dioxide**

Π comp	T [K]	DP/P	Dy	DV/V'	DV/V"	k_{ij}
n pentane	310—1	5 0	030	3 8	7 0	0
		2.0	010	3 3	2 7	015
n hexane	310	17 0	006	1 3	26 0	0
		1 0	003	8	2.8	03-1
hyd sulfide	277	16 7	045	4 0	28 0	0
		2 9	020	2.6	6 0	037

Table 5 **Binary VLE calculations for systems containing methane**

3 SOLUBILITY IN SUPERCRITICAL FLUIDS

Solubility in supercritical fluids can be evaluated with the same equation of state models previously described Very few researchers have tried to apply activity coefficient models for the description of a supercritical phase
However thermodynamic description of supercritical systems requires particular care due to the fact that normal equations of state have some difficulties around the critical point For that reason non cubic equations of state are mainly used for the correlation of supercritical systems without solid phases
In the case of the evaluation of solubility of solid compounds in supercritical fluids there are two main problems

- the difficulties connected with critical properties evaluation for the heavy component
- the evaluation of the sublimation pressure for the heavy component

The critical properties, specially needed for cubic equations of state, can be estimated with group contribution methods, it results very often that a range of values can be obtained depending of the evaluation method used The absolute value it is not so important since the data and the process is not volving close to the critical point of the solute but instead close to the critical conditions of the supercritical fluid Nevertheless different sets of critical properties used in solubility calculations can give completely different values of the solubility in the supercritical fluid
Experimental values of sublimation pressures are very scarces and on the other hand are quite difficult to measure since normal values are normally around the limits of the experimental techniques
Gangadhara Rao and Mukhopadhyay, (1990) proposed a model for predicting solid solubilities in supercritical fluids, avoiding the use of critical properties and acentric factors They proposed the use of van der Waals volume and the heat of sublimation of the solid These properties are predicted using the molecular structure and the Bondi's group contribution method The disadvantage of this model is that it was developed from a small group of solutes and consequently it can be used only for these substances or only for the very similar ones
Neau et al, (1990) proposed the prediction of solubility in carbon dioxide from low pressure equilibrium data. The method is illustrated with the hard-sphere equation of state, but the main feature is the use of the low-pressure, low-temperature solubility data for determining the binary interaction parameters General correlations developed by Gregorowicz et al. (1991) can be also very useful in this case
For detailed explanation the reader is referred to Johnston et al (1989), Brennecke and Eckert, (1989), Ekart et al, (1991)
Since supercritical fluid phase can be also treated as an expanded liquid, the integration through the critical region is not necessary But difficulties arise, because instead of ϕ, as in the equation of state approach, the knowledge of two thermodynamic properties activity coefficient, γ and partial molar volume for the solute, is necessary
The appearance of highly efficient computers has enabled new possibilities in the study of supercritical fluid solutions Because of nonanalytic nature of the results and still time-intensive computer use they are not yet a good tool for modeling supercritical fluid phase

equilibria. On the other hand computer simulations might provide insight on molecular level which will form the basis for improved mathematical models
The article by Battersby et al, (1993) focuses on the use of a neural network to predict analyte solubility in supercritical carbon dioxide Recent developments in computer technology are leading to dramatic increases in the use of computational chemistry for modeling optimization and artificial intelligence
As stated before, there is still deficiency in widely applicable models for predicting behavior in the supercritical fluid region Nevertheless, a suitable model can be found to solve certain problems e g at the densities in the near critical region, where the fluid is highly compressible perturbed hard sphere models with higher order terms or lattice models are required to treat clustering, which increases the attractive interactions When applying a certain model one should be aware of its drawbacks for an example in the case of models based on the ideal gas reference state the limitation is based on the lack of vapor pressure data.

In the following a discussion will be presented on the influence of the use of different cubic equation of state, different mixing rules and different group contribution methods (for the estimation of pure component properties) on the correlation of the solubility in supercritical fluids The EOS energy parameters were determined by using classical mixing rules or UNIFAC method
In any cases, the critical parameters T_c and P_c, and acentric factor ω are unknown and should be estimated by G C methods Different approaches are available in literature and have been applied for the calculation of the solubility Four G C approaches for the evaluation of T_c P_c and ω have been used for characterising steroids and non steroidal drugs In particular, the Ambrose approach (Reid et al (1987)) was used by calculating the normal boiling point T_b with Constantinou and Gani approach (method 1) and with the Lydersen method modified by Joback (Reid et al (1987)) (method 2), the method 3 is the Lydersen approach modified by Joback, the method 4 is the Constantinou and Gani approach (Constantinou and Gani (1994), Constantinou et al (1995)) The results obtained with the different methods using the PR EOS (Peng and Robinson (1976)) and fitting the parameter k_{12} of the classical Van der Waals mixing rules are reported in Table 3 For these calculations the sublimation pressure P^{sub} and solid volume v^s_2 were taken from the literature
By comparing the different deviations dY% on the solubility of the solid in the supercritical phase, some remarks can be made steroid compound solubilities are generally better correlated by method 1, while method 4 seems more suitable for the other compounds This can be explained by considering the values of the critical pressures for steroid compounds The Constantinou and Gani approach (method 4) is underestimating P_c (for example, for cholesterol P_c/bar = 11 9 with method 4, and 17 7 with method 1) with close values of T_c This behaviour can be due to the particular structure of steroids which mainly contain naphthenic carbons for which few experimental data of P_c are available in the literature On the contrary, for the other molecules having many different functional groups (esters aromatics, heterocycles) the more detailed Constantinou and Gani method leads to more realistic critical pressures (for example for nitrendipine, with similar T_c, method 4 gives 12 2 bars while method 1

gives 45 1 bars) Methods 2 and 3 give intermediate results Also the Somayajulu method (Somayajulu (1989)) was applied and led to deviations comparable to method 2 and 3

In further calculations we focused on steroid compounds and only method 1 was used for the estimation of the pure solid properties

Table 6 Choice of critical properties for the calulation of solubility (y) of solids in CO_2 using the PR equation (1 - Ambrose with T_b Constantinou Gani 2 - Ambrose with T_b Lydersen modified by Joback 3 Lydersen modified by Joback 4 - Constantinou and Gani)

Compounds	T/K	1	2	3	4	Authors
		Dy%	Dy%	Dy%	Dy%	
Cholesterol	308 15	32 48	70 17	86 10	86 10	Wong and
	318 15	66 18	69 11	69 21	69 21	Johnston
	328 15	66 54	59 47	63 37	63 27	(1986)
Cholesterol	328 15	18 40	38 19	83 56	59 43	Kosal and al
	333 15	33 00	41 81	82 81	58 81	(1992)
Cholesterol	313 15	20 38	73 49	96 87	85 59	Yun and al
	323 15	18 08	73 98	90 08	87 37	(1991)
	333 15	23 28	66 70	86 27	73 73	
Progesterone	308 15	17 75	58 82	84 58	53 80	Kosal and al
	313 15	18 67	52 56	73 96	51 04	(1992)
	318 15	17 03	44 63	71 64	43 90	
	328 15	35 01	66 72	80 46	67 09	
Progesterone	313 15	27 46	12 06	41 40	11 93	Valli
	333 15	19 43	13 79	44 13	13 44	(1995)
Testosterone	308 15	14 26	43 79	68 36	56 92	Kosal and al
	313 15	21 78	49 45	66 88	61 22	(1992)
	318 15	32 11	57 49	77 61	70 51	
	328 15	21 72	32 33	45 10	40 34	
Stigmasterol	308 15	45 07	85 07	87 74	87 23	Wong and
	323 15	50 84	80 42	84 95	80 38	Johnston
	333 15	70 31	81 25	83 80	85 81	(1986)
Ketoprofene	312 50	17 18	21 33	20 90	15 13	Mosca
	331 50	26 58	33 63	28 02	20 92	(1995)
Piroxicam	312 50	29 33	13 74	25 34	15 57	Mosca
	331 50	25 15	12 04	20 17	14 90	(1995)
Nimesulide	313 15	28 11	20 84	10 27	9 52	Schuchardt
	333 15	48 24	39 03	16 73	24 61	(1995)
Nitrendipine	333 15	53 42	44 07	29 73	12 08	Knez and al
	350 15	57 37	46 10	40 60	23 24	(1995)
	373 15	65 85	51 75	21 18	21 23	
Nifedipine	333 15	55 01	47 39	24 73	16 24	Knez and al
	353 15	52 04	44 48	19 60	19 75	(1995)
	373 15	61 87	47 20	24 21	20 40	

Influence of the equation of state

The original Peng Robinson EOS (Table 6) is compared in Table 7 with
the PR EOS with the volume correction of Peneloux (PR_{corr}) (Peneloux et al, (1982)),
the Soave Redlich-Kwong EOS (SRK) (Soave (1972))
- and the PR EOS with a modification of the volume function in the attractive part (PR_{mod}) where the assumption of the one fluid model is not more valid (Trassy and Neau, (1995))

Table 7 Fitting of k_{12} using different EOS (PR with volume correction (Pr_{corr}) SRK, PR with modified volume function (Pr_{mod})) and pure prediction using UNIFAC model with scaling factor

Compounds	T/K	PR_{corr}	RKS	PR_{mod}	UNIFAC	Authors
Cholesterol	308 15	27 02	38 93	22 45	64 26	Wong and Johnston
	318 15	64 42	68 70	71 36	59 72	(1986)
	328 15	64 21	69 92	75 76	65 35	
	global	51 88	59 18	56 52	63 11	
Cholesterol	328 15	17 66	20 63	25 36	53 83	Kosal and al
	333 15	31 33	35 62	35 06	66 49	(1992)
	global	21 76	25 12	28 13	57 64	
Cholesterol	313 15	20 52	21 34	4 28	17 03	Yun and al
	323 15	16 12	19 44	4 43	18 77	(1991)
	333 15	22 26	24 57	11 06	22 97	
	global	19 48	21 62	6 33	19 39	
Progesterone	308 15	18 01	18 61	9 32	28 93	Kosal and al
	313 15	16 18	21 48	7 17	23 53	(1992)
	318 15	16 13	18 28	16 29	26 86	
	328 15	34 66	36 84	27 76	35 19	
	global	21 24	23 80	15 14	28 63	
Progesterone	313 15	28 69	25 91	35 38	93 33	Valli
	333 15	19 28	22 82	40 45	88 69	(1995)
	global	24 41	24 51	37 68	91 22	
Testosterone	308 15	15 22	13 75	14 80	72 54	Kosal and al
	313 15	20 27	23 64	17 46	64 71	(1992)
	318 15	30 92	34 25	23 52	64 93	
	328 15	19 89	24 85	38 95	66 66	
	global	21 61	24 13	23 84	67 27	
Stigmasterol	308 15	40 28	49 46	36 12	>100	Wong and Johnston
	323 15	48 59	54 65	46 17	>100	(1986)
	333 15	66 43	74 97	75 63	>100	
	global	51 16	59 16	51 77	>100	

For all the calculations the parameter k_{12} of the classical van der Waals mixing rules was fitted It can be seen from Table 7 that the volume correction does not give a significant

improvement slightly worst results are obtained with SRK EOS while the Pr_{mod} shows a clear improvement at lower temperatures (as in the case of Cholesterol Progesterone)

Influence of mixing rules

The UNIFAC model was introduced in the attractive parameters of the EOS using a scaling factor L_{12} according to Garduza (Garduza (1993)) and Garnier (Garnier, (1995)) this approach is similar to the method proposed by Wong and Sandler (Wong and Sandler (1992))

Table 8 Influence of sublimation pressure (P^{sub}) on the calculation of the solubility (for PR and UNIFAC models, k_{12} and L_{12} were fitted respectively together with the parameters of the sublimation pressure)

Compounds	T/K	PR		UNIFAC		Authors
		P^{sub}	dY%	P^{sub}	dY%	
Cholesterol	308 15	$1\ 10\ 10^{10}$	16 47	$1\ 18\ 10^{10}$	16 86	Wong and Johnston (1986)
	318 15	$9\ 27\ 10^{10}$	46 35	$1\ 09\ 10^{-09}$	46 34	
	328 15	$6\ 81\ 10^{-09}$	33 49	$8\ 75\ 10^{-09}$	32 77	
	global		32 10		31 99	
Cholesterol	328 15	$7\ 37\ 10^{-08}$	13 09	$4\ 33\ 10^{-08}$	13 23	Kosal and al (1992)
	333 15	$1\ 44\ 10^{-07}$	33 42	$1\ 56\ 10^{-07}$	33 36	
	global		19 19		19 27	
Cholesterol	313 15	$6\ 01\ 10^{10}$	5 38	$5\ 31\ 10^{10}$	5 25	Yun and al (1991)
	323 15	$2\ 12\ 10^{-09}$	7 33	$2\ 09\ 10^{-09}$	7 50	
	333 15	$6\ 98\ 10^{-09}$	5 93	$7\ 56\ 10^{-09}$	7 05	
	global		6 23		6 57	
Progesterone	308 15	$6\ 71\ 10^{11}$	7 91	$7\ 45\ 10^{11}$	7 81	Kosal and al (1992)
	313 15	$1\ 35\ 10^{10}$	6 22	$1\ 51\ 10^{10}$	6 01	
	318 15	$2\ 67\ 10^{10}$	14 73	$2\ 98\ 10^{10}$	14 59	
	328 15	$1\ 02\ 10^{-09}$	20 84	$1\ 10\ 10^{-09}$	22 00	
	global		12 43		12 60	
Progesterone	313 15	$6\ 70\ 10^{-09}$	10 45	$6\ 66\ 10^{-09}$	10 36	Valli (1995)
	333 15	$5\ 36\ 10^{-08}$	13 79	$5\ 32\ 10^{-08}$	14 31	
	global		11 97		12 16	
Testosterone	308 15	$1\ 60\ 10^{10}$	14 02	$1\ 97\ 10^{10}$	13 95	Kosal and al (1992)
	313 15	$3\ 41\ 10^{10}$	15 53	$4\ 19\ 10^{10}$	15 87	
	318 15	$7\ 12\ 10^{10}$	24 02	$8\ 68\ 10^{10}$	25 07	
	328 15	$2\ 89\ 10^{10}$	22 04	$3\ 49\ 10^{-09}$	21 49	
	global		18 99		19 18	
Stigmasterol	308 15	$2\ 18\ 10^{12}$	15 71	$1\ 94\ 10^{12}$	15 62	Wong and Johnston (1986)
	323 15	$2\ 90\ 10^{11}$	13 43	$3\ 00\ 10^{11}$	13 76	
	333 15	$1\ 43\ 10^{10}$	21 15	$1\ 63\ 10^{10}$	20 46	
	global		16 71		16 56	

The calculations performed with the original UNIFAC parameters (Holderbaum and Gmehling ('991), Gmehling et al. (1993) Fischer and Gmehling (1995)) do not give satisfactory results This probably is due to the use of the reported interaction parameters a_{mn} between CO_2 and the functional groups present in paraffins instead of those characteristic of cyclic paraffins which are present in the steroidal structure Fitting the solubility data new parameters a_{mn} and a_{nm}, setting b_{mn} and c_{mn} equal to zero were obtained these parameters with a single scaling factor L_{12} were used for the pure prediction of solubility data presented in Table 7 The deviations are sometimes in the same order as with classical mixing rules fitting one k_{12} parameter and as it was expected in other cases the prediction is very poor

Influence of sublimation pressure

As Chen (Chen et al (1993) pointed it out the calculation of solubility data requires a proper estimation of sublimation pressures The data were correlated using the PR EOS with classical mixing rules and the UNIFAC model with previously determined a_{mn} parameters n each cases two parameters for correlating the sublimation pressure were fitted together with the k_{12} (classical mixing rules) or L_{12} (UNIFAC scaling factor) parameter Results of the calculations are reported in Table 8
In both cases there is a clear improvement of the estimation of the solubility when using a proper evaluation of the sublimation pressure Similar conclusions were drawn by Chen (Chen et al. (1993)), but using a higher number of parameters Furthermore, the order of magnitude of the P^{sub} obtained in both cases is realistic It must be underlined that the values of the solubility y_2 and the sublimation pressure are close even if the two approaches are different

REFERFNCES

Adachi Y Lu B C-Y Simplest equation of state for vapor-liquid equilibrium calculations - A modification of the van der Waals equation, *AIChE Journal*, **1984**, 30, 991

Alder B J Young D A, Mark M A Studies in molecular dynamics X Corrections to the augmented van der Waals theory for the squar-well fluid, *J Chem Phys* **1972**, 56 3013

Battersby, P Dean, J R. Hitchen, S M Tomlinson, W R Myers P Neural Networks A Method for Predicting Solubility in Supercritical Fluid Extraction, *LC GC INT* **1993** *6* (7) 428

Bertucco, A, Barolo, M, Soave, Estimation of Chemical Equilibria in High-Pressure Gaseous Systems by a Modified Redlich-Kwong-Soave Equation of State, *Ind Eng Chem Res* **1995** 34 3159

Brennecke, J F Eckert C A, Phase Equilibria for Supercritical Process Design, *AIChE Journal* **1989**, *35* (9), 1409

Carrier B Rogalski, M, Peneloux, A Correlation and prediction of physical properties of hydrocarbons with the modified Peng-Robinson equation of state, *Ind Eng Chem Res* **1988**, 27, 1714

Chen, P C, Chen, Y P, Wong, D S H, *Fl Ph Eq*, **1993**, 83, 175

Constantinou, L and Gani R., *AIChE*, **1994** 40,1697

Constantinou, L, Gani, R. and J P O'Connell, *Fl Ph Eq*, **1995**, 103, 11

Cotterman, R.L Prausnitz, J M, Molecular Thermodynamics for Fluids at Low and High Densities, Part II Phase Equilibria for Mixtures Containing Components with Large Differences in Molecular Size or Potential Energy, *AIChE Journal* **1986b** *32* (11), 1799

Cotterman, R.L, Schwarz, B J, Prausnitz, J M, Molecular Thermodynamics for Fluids at Low and High Densities, Part I Pure Fluids Containing Small or Large Molecules, *AIChE Journal* **1986a**, *32* (11), 1787

Ekart M P, Eckert C A, Proc 2nd Int Symposium on Supercritical Fluids Boston, Massachusetts, May 20-22, **1991**, p 63

Fermeglia, M, Kikic, I, The perturbed hard chain theory for the prediction of supercritical fluid extraction binary mixtures, *Chem Eng Sci*, **1993** 48 3889

Fischer, K., Gmehling, J, *Fl Ph. Eq* **1995**, 112 1

Gangadhara Rao V S Mukhopadhyay M Solid Solubilities in Supercritical Fluids from Group Contributions, *J Supercritical Fluids* **1990**, *3*, (2), 66

Garnier, S Master of science report 1995 Aix-Marseille III France

Gmelhing, J, Jiding, L, Schiller, M, *Ind Eng Chem Res*, **1993**, 32, 178

Gregorowicz, J Fermeglia, M, Soave G, Kikic, I, The Perturbed Hard Chain Theory for the Prediction of Supercritical Fluid Extraction Pure Component Properties *Chem Eng Sci* **1991**, *46*, 1427

Harmens A, Knapp, H, Three parameter cubic equation of state for normal substances *Ind Eng Chem Fund* **1980**, 19 291

Hernandez Garduza, O Thesis, **1993** Aix Marseille III France

Heyen, G Liquid and Vapor properties from a cubic equation of state in *Proceedings of the 2nd International Conference on Phase Equilibria and Fluid Properties in the*

Chemical Industry (H Knapp and S I Sandler eds) DECHEMA, Frankfurt/Main, **1980**, 9

Holderbaum, T Gmehling, J , *Fl Ph. Eq* **1991** 70 251

Huron, M -J , Vidal, J , New mixing rules in simple equations of state for representing vapor-liquid equilibria of strongly nonideal mixtures *Fluid Phase Equilibria*, **1979**, 3, 255

Johnston, K P Peck D G Kim S , Modelling Supercritical Mixtures How Predictive Is It? *Ind. Eng Chem Res* **1989**, *28* (8), 1115

Johnston, K P , Zieger D H , Eckert C A Solubilities of Hydrocarbon Solids in Supercritical Fluids The Augmented van der Waals Treatment, *Ind Eng Chem Fundam* **1982** *21* (3) 191

Kikic I , Alessi P Fermeglia, M , Gregorowicz, J High Pressure phase equilibria calculations by means of a non cubic equation of state , *Proc 2nd High Pressure Chemical Engineering Symposium*, Erlangen, 1990 353

Mathias P M , A versatile phase equilibrium equation of state, *Ind. Eng Chem Process Design Dev* , **1983**, 22 385

Mathias, P M Copeman, T W Extension of the Peng-Robinson equation of state to polar fluids and fluid mixtures, *Fluid Phase Equilibria*, **1983**, 13, 91

Melhem, G A , Saini, R., Goodwin, B M , A modified Peng-Robinson equation of state, *Fluid Phase Equilibria*, **1989**, 47, 189

Michelsen, M L A method for incorporating excess Gibbs free energy models in equations of state, *Fluid Phase Equilibria*, **1990a**, 60, 47

Michelsen, M L A modified Huron-Vidal mixing rules from excess Gibbs free energy models, *Fluid Phase Equilibria*, **1990b**, 60, 213

Mosca, T , Thesis, 1995, DICAMP, University of Trieste Italy

Neau, E Alessi, P , Fermeglia, M Kikic I Low-Pressure Equilibrium Data for the Prediction of Solubility in Carbon Dioxide, *Chem Eng Sci* **1990**, *45*, (4), 795

Peng, D Y , Robinson, D B , A new two-constant equation of state, *Ind. Eng Chem Fund* , **1976** 15 59

Peneloux, A , Rauzy, E , Freze, R., A consistent correction for Redlich-Kwong-Soave volumes, *Fluid. Phase Equilib* , **1982**, 8, 7

Redlich, O , Kwong, J N S , On thermodynamics of solutions V An equation of state Fugacities of gaseous solutions, *Chem Rev* **1949** 44, 233

R C Reid, J M Prausnitz and B E Poling, *Properties of gases and liquids*, Mc Graw Hill, New-York, **1987**

Robinson, D B , Peng, D Y , The characterization of the heptanes and heavier fractions for the GPA Peng-Robinson Programs, *GPA Res Rep 28* **1978**

Schuchardt, A., Thesis, 1995 DICAMP University of Trieste, Italy

Somayajulu, G R., *J Chem Eng Data* , 1989 34, 106

Soave G , Equilibrium constants from a modified Redlich-Kwong equation of state *Chem Eng Sc* 1972, 27 1197
Soave, G Improvements of the van der Waals equations of state, *Chem. Eng Sci* 1984 27 1197
Soave G Bertucco A , Vecchiato L Equation of State Group Contributions from Infinite-Dilution Activity Coefficients *Ind Eng Chem Res* 1994, 33, 975
Soave G , Barolo, M , Bertucco, A Estimation of High-Pressure Fugacity Coefficients of Pure Gaseous Fluids by a Modified SRK Equation of State *Fluid Phase Equilibria* 1993 91 87
Soave, G , Bertucco, A , Sponchiado M , Avoiding the Use of Critical Constants in Cubic Equations of State, *AIChE Journal* 1995 41, 1964
Trassy L , Neau, E , Personal Communication, 1995 Pau, France
Valli M Thesis, 1994 DICAMP University of Trieste Italy
Wilson, G M , Vapor-liquid equilibria correlated by means of a modified Redlich-Kwong equation of state, *Adv Cryogen Eng* 1964 9 168
Wong, J M Johnston, K.P , *Biotech Progress*, 1986, 2 29
Wong, D S H Sandler, S I A theoretically correct mixing rule for cubic equations of state, *AIChE Journal*, 1992, 38 671
Yu, J M Lu, B C -Y , A three parameter cubic equation of state for asymmetric mixture density calculations, *Fluid Phase Equilibria*, 1987, 34, 1
Yun J S L Liong K. K. Gurdial G S Foster N R., Solubility of Cholesterol in Supercritical Carbon Dioxide, *Ind Eng Chem Res* 1991, *30*, 2476

Natex Prozesstechnologie GesmbH

Basic-Course

of

Supercritical Fluid Extraction Process

Metal Industries Research & Development Center

Kaohsiung, Taiwan, ROC

Mr TZU-CHEN KUO

THERMODYNAMIC
PROPERTIES
PHASE EQUILIBRIA

COMPUTER PROGRAMS

CONTENT

PROGRAM VLEEOS

1 INTRODUCTION

2 PURPOSE

3 USE OF THE PROGRAM

4 RESULTS

5 SAMPLE INPUT

6 SAMPLE OUTPUT

PROGRAM EOSKIJ

1 INTRODUCTION

2 PURPOSE

3 USE OF THE PROGRAM

4 RESULTS

5 SAMPLE INPUT

6 SAMPLE OUTPUT

PROGRAM VLEEOS

1 Introduction

The program has been written in FORTRAN 77, version 3 31, and should run on all IBM PC XT, AT and any other compatible computer system. There are five files concerning this program

1 VLEEOS FOR contains the source program
2 VLEEOS EXE contains the executable file
3 VLEEOS HLP contains all necessary information about the program
4 VLE DAT contains data for an example
5 VLE RES contains the results for the example

2 Purpose

This program performs Bubble Point Pressure (BP P) calculations using cubic Equations of State (EoS) The available EoS are

1 SRK-GD (Graboski Daubert)
2 SRK-78 (Soave, 1978)
3 PR (Peng & Robinson)
4 t-PR
5 t-VdW
6 VdW-711

Details on the above EoS are given in Tassios (1993) and also reported at the end of the Appendix D and e as Appendix E1

For a given temperature (T in K) and liquid phase composition (x) VLE calculates the pressure of the mixture (P in bar) and the composition (y) of the vapour phase, which is in equilibrium with the liquid phase at this temperature

Near-critical points, where convergence difficulties may occur, receive a special treatment

The program has been developed for binary mixtures, but it can be easily modified to perform calculations for multicomponent mixtures Modifications include alteration of the data input statements and extention of the program arrays

3 Use of the program

To use the program simply construct an input file to include the input data. This can be done using any appropriate editor Then run the executable file VLEEOS EXE The output of the program will be contained in a specified output file The filenames of both the input and the output files are asked by the program and supplied by the user during execution.

The data required are the critical temperature (Tc,K), pressure (Pc,bar) and the acentric factor (ω), the interaction coefficient of the mixture components and for each data point the temperature the liquid phase composition and initial estimates for the pressure and the vapor phase composition (the experimental values for example if available)

The input file should be constructed according to the following pattern

line 1	TEXT			
line 2	Tc(1)	Pc(1)	w(1)	
line 3	Tc(2)	Pc(2)	w(2)	
line 4	K12			
(subsequent lines)	T	Pexp	x(1)exp	y(1)exp

where

- TEXT is a character variable (80 chars wide) containing any relevant information about the system.
- Tc(i), Pc(i), w(i) are the critical temperature (K), critical pressure (bar) and the acentric factor for component i (i=1 2)
- K12 is the interaction coefficient between the two components If its value is unknown, a value of 0 should be input
- T (in K) and x(1)exp, are the desired temperature and liquid phase composition, Pexp (in bar) and y(1)exp are estimate (starting) values, or experimental values if available (the index 1 refers to component 1)
  Up to 99 such data points can be input

4 Results

The output file contains the relevant input information and the following tabulated VLE results

- the temperature (T) and the estimated (or experimental) pressure (Pexp)
- the calculated pressure, Pcalc
- the percent error in P err%(P)
- the input liquid phase composition, X1exp
- the estimated (or experimental) vapor phase composition, Y1exp
- the calculated vapour phase composition, Y1calc
- the deviation in Y, DY1

The average absolute percent error in P and deviation in the vapor phase composition Y are also reported (These of course are meaningful only when the corresponding experimental values are the real ones, not estimated)
Other output information includes the number of the rejected points and the names of the files used by the program.
The integer variable IERR, which is reported for each run, indicates the result of convergence as following

IERR=0	convergence was accomplished without any problem
IERR=1	the compressibility factor cubic polynomial had less than three real roots
IERR=2	Zv or Zl was less than zero
IERR=3	P was less than zero
IERR=4	maximum number of iterations was exceeded (The program uses internally a max number of iterations = 1000)

5 Sample Input

As an example an input file named VLE DAT is constructed containing the following data, for a CO2 nC4 mixture

```
System CO2-nC4  Experimental data  Knapp et all  VLE for mixtures  (VOL VI)
304 19          73 815             0 2276
425 18          37 969             0 1931
0 0
310 93          4 137              0 006          0 132
310 93          5 516              0 022          0 332
310 93          6 895              0 036          0 454
310 93          8 618              0 056          0 556
310 93          10 342             0 076          0 628
310 93          12 066             0 095          0 679
310 93          13 789             0 115          0 714
310 93          17 237             0 155          0 765
310 93          20 684             0 196          0 798
310 93          24 131             0 239          0 822
310 93          27 579             0 284          0 840
310 93          31 026             0 330          0 855
310 93          34 473             0 378          0 867
310 93          41 368             0 478          0 886
310 93          55 158             0 689          0 910
310 93          62 052             0 786          0 925
310 93          68 947             0 871          0 944
310 93          72 394             0 908          0 949
310 93          75 497             0 940          0 940
```

6 Sample Output

The results for these data, are shown on screen and stored in a disk file named VLE RES They should look like the following

*** PROGRAM VLEEOS OUTPUT ***

System CO2-nC4, experimental data Knapp et al , VLE for mixtures (VOL VI)

EOS SELECTED t-PR

Tc(1)	304 19	Tc(2)	425 18	[K]
Pc(1)	73 8150	Pc(2)	37 969	[bar]
w(1)	22760	w(2)	19310	
K12	0000			

N	T [K]	Pexp [bar]	Pcalc [bar]	err%(P)	X1exp	Y1exp	Y1calc	DY1	IERR
1	310 93	4 1370	3 8513	-6 91	0060	1320	0737	- 0583	0
2	310 93	5 5160	4 6375	-15 93	0220	3320	2266	- 1054	0
3	310 93	6 8950	5 3312	-22 68	0360	4540	3248	- 1292	0
4	310 93	8 6180	6 3319	-26 53	0560	5560	4293	- 1267	0
5	310 93	10 342	7 3442	-28 99	0760	6280	5065	- 1215	0
6	310 93	12 066	8 3168	-31 07	0950	6790	5632	- 1158	0
7	310 93	13 789	9 3525	-32 17	1150	7140	6108	- 1032	0
8	310 93	17 237	11 462	-33 50	1550	7650	6816	- 0834	0
9	310 93	20 684	13 679	-33 86	1960	7980	7327	- 0653	0
10	310 93	24 131	16 069	-33 41	2390	8220	7723	- 0497	0
11	310 93	27 579	18 644	-32 40	2840	8400	8038	- 0362	0
12	310 93	31 026	21 362	-31 15	3300	8550	8290	- 0260	0
13	310 93	34 473	24 298	-29 52	3780	8670	8500	- 0170	0
14	310 93	41 368	30 783	-25 59	4780	8860	8829	- 0031	0
15	310 93	48 263	38 310	-20 62	5840	9000	9080	0 0080	0
16	310 93	55 158	46 625	-15 47	6890	9100	9274	0 0174	0
17	310 93	62 052	55 355	-10 79	7860	9250	9430	0 0180	0
18	310 93	68 947	64 251	-6 81	8710	9440	9564	0 0124	0
19	310 93	72 394	68 677	-5 13	9080	9490	9627	0 0137	0
20	310 93	75 497	72 902	-3 44	9400	9400	9683	0 0283	0

AVERAGE ABSOLUTE ERROR IN PRESSURE	22 30 %
AVERAGE ABSOLUTE DEVIATION IN Y1	05694
NUMBER OF REJECTED POINTS	0

NAME OF DATA FILE	vle dat
NAME OF OUTPUT FILE	vle res

End of Output

PROGRAM FOSKIJ

1 Introduction

This program has been written in FORTRAN 77 version 3 31 and should run on all IBM PC XT AT and any other compatible computer system. There are five files concerning this program

1 EOSKIJ FOR contains the source program
2 EOSKIJ EXE contains the executable file
3 EOSKIJ HLP contains all necessary information about the program
4 KIJ DAT contains data for an example
5 KIJ RES contains the results for the example

2 Purpose

This program determines the value of the interaction coefficient K12 that best describes a given set of binary VLE data with a cubic equation of state (EoS) The program uses ZXSSQ subroutine which is found in ZERXTD LIB of IMSL Math Library This subroutine varies the parameter(s) of a function in order to minimise an objective function (here the relative error in pressure) The parameter in this case is the K12 coefficient and the objective function is the sum of squares of the relative error in pressure
Near-critical points, where convergence difficulties may occur, have a special treatment
The program has been developed for binary mixtures, but it can be easily modified for multicomponent mixtures Modifications include change of the data input statements and extension of the program arrays

3 Use of the program

To use the program construct an input file to include the input data, using any appropriate editor Then simply 'run' the executable file EOSKIJ EXE The output of the program will be displayed on the screen and stored in a disk file Both files (input and output) are specified by the user during execution.
The input data required are the critical temperature (Tc,K), critical pressure (Pc,bar), the acentric factor (à) of the mixture components and for each data point the temperature, pressure and the liquid phase composition An initial estimate for the interaction coefficient of the mixture components and for each point an initial estimate of the vapour phase composition (experimental value, for example if available) are also required The format of the input file is shown below

line 1	TEXT			
line 2	Tc(1)	Pc(1)	w(1)	
line 3	Tc(2)	Pc(2)	w(2)	
line 4	K12			
(subsequent lines)	T	P	x(1)	y(1)

where

- TEXT is a character variable containing any important information about the system in no more than 80 characters

- Tc(i) Pc(i) w(i) are the critical temperature (K), critical pressure (bar) and the acentric factor for each component i (i=1 2)
- K12 is an initial estimate for the interaction coefficient between components 1 and 2 (use 0 if no other better guess is available)
- T P x(1) and y(1) are the systems temperature (K), pressure (bar) and liquid phase composition, while y(1) is the experimental (or initial estimate) for the composition of the vapor phase The program can read up to 99 such data points

The user can select one of the following EoS to use

1 SRK GD (Graboski-Daubert)
2 SRK-78 (Soave, 1978)
3 PR(Peng & Robinson)
4 t-PR
5 t-vdW
6 vdW 711

4 Results

The output of the program includes the relevant input information and the following results

- the optimum value of K12
- tabulated values of the results for all data points
- the percent errors in the pressure values
- the average absolute percent error in pressure
- the deviation between experimental and calculated y(1) values
- the average absolute deviation in y(1)
- an integer index IERR, which is related to the convergence of the optimisation routine used as follows

IERR=0 convergence was accomplished without any problem
IERR=1 the compressibility factor cubic polynomial had less than three real root
IERR=2 Zv or Zl was less than zero
IERR=3 P was less than zero
IERR=4 maximum number of iterations (1000) was exceeded

Note The deviation in Y is only meaningful when the experimental Y values are real not estimates

The program displays on screen the intermediate values of the objective function, for each iteration cycle

5 Sample Input

As an example an input file, named KIJ DAT was constructed, containing thefollowing data for a CO2 nC4 mixture

```
System CO2 nC4, Experimental data Knapp et all VLE for mixtures Vol VI
304 19     73 815     0 2276
425 18     37 969     0 1931
0 0
310 93     4 137      0 0060     0 1320
310 93     5 516      0 0220     0 3320
310 93     6 895      0 0360     0 4540
310 93     8 618      0 0560     0 5560
310 93     10 342     0 0760     0 6280
310 93     12 066     0 0950     0 6790
310 93     13 789     0 1150     0 7140
310 93     17 237     0 1550     0 7650
310 93     20 684     0 1960     0 7980
310 93     24 131     0 2390     0 8220
310 93     27 579     0 2840     0 8400
310 93     31 026     0 3300     0 8550
310 93     34 473     0 3780     0 8670
310 93     41 368     0 4780     0 8860
310 93     48 263     0 5840     0 9000
310 93     55 158     0 6890     0 9100
310 93     62 052     0 7860     0 9250
310 93     68 947     0 8710     0 9440
310 93     72 394     0 9080     0 9490
310 93     75 497     0 9400     0 9400
```

6 Sample Output

The output of the program, based on the previous input data, is stored in file KIJ RES and should look like the following

*** PROGRAM EOSKIJ OUTPUT ***

System CO2 nC4 experimental data Knapp et al , VLE for mixtures ,(Vol VI)

EOS SELECTED SRK-78 (Soave 1978)

Tc(1)	304 19	Tc(2)	425 18	[K]
Pc(1)	73 815	Pc(2)	37 969	[bar]
w(1)	22760	w(2)	19310	

OPTIMUM K12 1398

N	T [K]	Pexp [bar]	Pcalc [bar]	err%(P)	X1exp	Y1exp	Y1calc	DY1	IERR
1	310 93	4 1370	4 1485	+0 28	0060	1320	1195	- 0125	0
2	310 93	5 5160	5 5521	+0 66	0220	3320	3301	- 0019	0
3	310 93	6 8950	6 7774	-1 71	0360	4540	4442	- 0098	0
4	310 93	8 6180	8 5225	-1 11	0560	5560	5511	- 0049	0
5	310 93	10 342	10 260	-0 79	0760	6280	6218	- 0062	0
6	310 93	12 066	11 905	-1 33	0950	6790	6700	- 0090	0
7	310 93	13 789	13 627	-1 17	1150	7140	7080	- 0060	0
8	310 93	17 237	17 042	-1 13	1550	7650	7608	- 0042	0
9	310 93	20 684	20 496	-0 91	1960	7980	7963	- 0017	0
10	310 93	24 131	24 059	-0 30	2390	8220	8222	0 0002	0
11	310 93	27 579	27 711	+0 48	2840	8400	8418	0 0018	0
12	310 93	31 026	31 352	+1 05	3300	8550	8566	0 0016	0
13	310 93	34 473	35 041	+1 65	3780	8670	8685	0 0015	0
14	310 93	41 368	42 319	+2 30	4780	8860	8857	- 0003	0
15	310 93	48 263	49 414	+2 39	5840	9000	8978	- 0022	0
16	310 93	55 158	55 973	+1 48	6890	9100	9069	- 0031	0
17	310 93	62 052	62 111	+0 10	7860	9250	9153	- 0097	0
18	310 93	68 947	68 319	- 91	8710	9440	9250	- 0190	0
19	310 93	72 394	71 405	-1 36	9080	9490	9293	- 0197	0
20	310 93	75 497	0000	00	9400	9400	0000	0 0000	3

AVERAGE PERCENT ERROR IN PRESSURE 1 11
AVERAGE ABSOLUTE DEVIATION IN Y1 0061
NUMBER OF REJECTED POINTS 1

NAME OF INPUT FILE kij dat
NAME OF OUTPUT FILE kij res

End of Output

In the following table 1 the basic equations for SRK, PR, vdW 711 models used in the programs are reported

Table 1 **Basic equations for SRK, PR and vdW-711 equations of state**

$$SRK \qquad P = \frac{RT}{V-b} - \frac{a}{V(V+b)}$$

$$PR \qquad P = \frac{RT}{V-b} - \frac{a}{V(V+b)+b(V-b)}$$

$$vdW\text{-}711 \qquad P = \frac{RT}{V+t-b} - \frac{a}{(V+t)^2}$$

$$a = \alpha a_c \qquad a_c = a_0 \frac{(RT_c)^2}{P_c}$$

$$\alpha = [1+m(1-T_r^{0.5})]^2$$

$$m = d_0 + d_1\omega + d_2\omega^2$$

$$b = b_0 \frac{RT_c}{P_c}$$

	SRK[1]	PR	vdW-711
a_0	0 42748	0 45724	27/64
b_0	0 08664	0 07780	1/8
d_0	0 48508	0 37464	0 48553
d_1	1 55171	1 54226	1 62400
d_2	-0 15613	-0 26992	0 21884

$$t = t_0 + (t_c - t_0)\exp[\beta|(1-T_r)|]$$

$$t_0 = \frac{RT_c}{P_c}(0\ 0348 + 0\ 0937\,\omega - 0\ 1661\,\omega^2 + 0\ 1250\,\omega^3)$$

$$t_c = \frac{RT_c}{P_c}\left(\frac{3}{8} - z_c\right)$$

$$z_c = 0\ 2890 - 0\ 0701\,\omega - 0\ 0207\,\omega^2$$

$$\beta = -7\ 35 - 24\ 52\,\omega + 9\ 20\,\omega^2$$

It was proposed, in order to extend the good predictions of saturated liquid volumes of vdW-711 EOS to high molecular weight hydrocarbons to modify some equations reported in Table B1 for t following the equations reported below together with the numerical values of the parameters

$$t = t_0 + (t_c - t_0)\exp(\beta|1-T_r|)$$

$$t_0 = \frac{RT_c}{P_c}(k_0 + k_1\omega + k_2\omega^2 + k_3\omega^3 + k_4\omega^4)$$

$$\beta = l_0 + l_1\omega$$

$$t_c = \frac{RT_c}{P_c}(z_c' - z_c)$$

$$m = d_0 + d_1\omega + d_2\omega^2 + d_3\omega^3$$

$$m = d_0 + d_1\omega + d_2\omega^2 + d_3\omega^3 + d_4\omega^4$$

	SRK(1)	PR(2)	t-vdW(3)	t-PR(3)
d_0	0 47979	0 379642	0 483798	0 384401
d_1	1 57600	1 485030	1 643232	1 522760
d_2	-0 19250	-0 164423	-0 288718	-0 213808
d_3	0 02500	0 016666	0 066013	0 034616
d_4	---	---	0 0	-0 001976
k_0	---	---	0 036722	-0 014471
k_1	---	---	0 063541	0 067498
k_2	---	---	-0 076221	-0 084852
k_3	---	---	0 060362	0 067298
k_4	---	---	-0 015772	-0 017366
l_0	---	---	7 099630	-10 244700
l_1	---	---	21 156900	-28 631200

(1) Soave (1979)

(2) Robinson and Peng (1978) for $\omega > 0\ 5$ for $\omega \leq 0\ 5$ see Table 8 3

(3) Magoulas (1990)

NB The programs are used with the authorization of Prof D Tassios (University of Athens)

Cubic Equations of State for Mixtures

$$P = \frac{RT}{v - b_m} - \frac{a_m}{v^2 + ub_m v + wb_m^2}$$

mixing parameter a_m

$$a_m = \sum_i \sum_j x_i x_j a_{ij}$$

with $a_{ij} = \sqrt{a_{ii} a_{jj}}(1 - k_{ij})$

interaction parameter

binary system

$$a_m = x_1^2 a_{11} + 2\, x_1 x_2 a_{12} + x_2^2 a_{22}$$

k_{12} needed

experimental data

ternary system

$$a_m = x_1^2 a_{11} + x_2^2 a_{22} + x_3^2 a_{33} + 2x_1x_2a_{12} + 2x_1x_3a_{13} + 2x_2x_3a_{23}$$

k_{12}, k_{13} and k_{23} needed

mixing parameter b_m

1. linear mixing rule $b_m = \sum x_i b_i$

   binary system $b_m = x_1 b_1 + x_2 b_2$

   ternary system $b_m = x_1 b_1 + x_2 b_2 + x_3 b_3$

2. quadratic mixing rule
   (較精確,但複雜)

$$b_m = \sum_i \sum_j x_i x_j b_{ij}$$

$$b_{ij} = \frac{b_{ii} + b_{jj}}{2}(1 - l_{ij})$$

interaction parameter

Fugacity coefficient φ from cubic equations of state

$$\boxed{\ln \varphi_i = \frac{b_i}{b}(z-1) - \ln(z - B^*) + \frac{A^*}{B^*\sqrt{u^2-4w}}\left(\frac{b_i}{b} - \delta_i\right)\ln\frac{2z + B^*(u+\sqrt{u^2-4w})}{2z + B^*(u-\sqrt{u^2-4w})}}$$

with

$$\frac{b_i}{b} = \frac{T_{ci}/P_{ci}}{\sum_j y_j T_{cj}/P_{cj}}$$

$$\delta_i = \frac{2a_j^{0.5}}{a}\sum_j x_j a_j^{0.5}(1-k_{ij})$$

$$A^* = \frac{a_m P}{R^2T^2} \qquad B^* = \frac{b_m P}{RT}$$

u, w depending which equation of state is used

Program "EVE"

"OHGFOR" for vapour-liquid equilibria

Data file
In directory "Data" first a file with experimental data has to be created, filename consists normally of the two codenumbers of the compounds (102-6 is for CO2-hexane)

Input in data file

First line	'Title, authors, reference all marked with ' at the beginning and end, showing the program that this is a text'
Second line	codenumber of component 1"
	"codenumber of component 2"
	"1 = x,p and y are used, 2 = only x and p are used"
	"number of experimental points in this data set"
	"1 = use this data set, 2 = do not use this data set"
Third line	"Temperature in K"
	"saturation pressure of comp 1, can be set 0 "
	"saturation pressure of comp 2, can be set 0 "
	"conversion of pressure 1 if p is given in bar
	10 if p is given in MPa
	1E-2 if p is given in kPa
	1 01325 if p is given in atm
	6894 76E-5 if p is given in psi
Following lines "X CO2" P" "Y CO2"	

$x_i \, P_i^L = y_i \, P_i^V$

The inputs have to be separated by a blank

Directory "eve_new"

X_{CO_2} molar fraction of liquid phase
Y_{CO_2} vapor phase

File "HP D"
Includes the data of the pure compounds The codenumber related to a compound is fixed by this file and has to correspond in all other files
For input of new compounds you have to take care not to use the same codenumber as already used because the program used the first be found in the list Normally the ranging is not important, because the program will run through the whole list and start again at the beginning for searching the codenumber

First line	"codenumber" "name
Second line	"molecular weight" "TC in K" PC in bar' "omega" 'ZC
Third line	"Class" "M1" M2" "Tb boiling temperature" can all be set 0
Fourth line	"aAntoine" "bAntoine" "cAntoine" "Tmin" "Tmax'
	Antoine constants if available, otherwise set 0

File "indic"

In this file you decide what you want to do 0 _ CALCUL →

Option	1 adjustment of parameters k_{ij}, l_{ij},
	2 calculation with given parameters up to critical point
iajust	method how to calculate, normally 2
n	2 calculated binaries
	3 calculate ternaries
nsyst	how many systems from your file "comp" will be calculated
imp	normally 0
testbul	1 E-07 accuracy of calculation
model	for cubic EOS
	8 linear mixing rule for b
	9 quadratic mixing rule for b
ieqs	not used for EOS and model 8,9
lamda0	not used for EOS and model 8,9
iunifac	not used for EOS and model 8,9
iamn	not used for EOS and model 8,9
ibmn	not used for EOS and model 8,9
maj,naj	not used for EOS and model 8,9
chmodel1	not used for EOS and model 8 9
puis	not used for EOS and model 8,9
iorder2	not used for EOS and model 8,9
ieos	decides which EOS will be used
	2 Peng Robinson
	1 Redlich Kwong
	0 Van der Waals
irks	which function a(T) will be used
	0 Soave original normally used
	1 Soave general
	2 Carrier
isoav	0 m(omega) original normally used
	1 m(omega) general P R
	2 m(omega) Tassios
icrit	0 covolume and a(Teb)
	1 critical specifications normally used
Icorv	correction of the calculated volume v
	1 correct the volume
	2 do not correct the volume, normally used

File "kij eqs"

In this file you give the starting values for calculating the mixing parameter **b linear** (model 8 in "indic") or you can enter your calculated parameters if you want to run "dessin" in indic

First line	"codenumber comp 1"
	"codenumber comp 2"
	"start value for $k_{ij}0$"
	"start value for $k_{ij}T$"

the k_{ij}-value results $k_{ij} = k_{ij}0 + k_{ij}T\ (298\ 15/T - 1)$

If you enter 0 for a value always put a after (0)

File "klij eqs"
For calculating mixing parameter **b quadratic** (model 9 in "indic")
First line "codenumber comp 1"
"codenumber comp 2"
"start value for kij0"
"start value for kijT"
"start value for lij0"
"start value for lijT"
Take care that even you put 0 for lij0 and lijT you have a different mixing rule than using b linear!

File "comp"
"name comp 1"
"name com 2"
"name of file in directory data"
"number of isothermal sets"
"number of isobaric sets"
"number of excess enthalpies"
"number of log gammai'
"number of liquid-liquid"
"number of Henry constants"
"which set has to be taken"
example '102' '6' '102-6' 12 0 0 0 0 0 1
means that the system CO2 – hexane has to be calculated, the file in directory data is 102-6 including 12 isothermal sets

Take care, that always the first set will be calculated, so you have to put your system in the first row!!

If all the inputs are okay type calc
numbers to be adjusted
0 calculation with given data in kij eqs or klij eqs depending on the model you have chosen in indic
1 2 3 or 4 how many parameters will be fitted
enter
which parameters have to be fitted
1 kij0
2 kijT
3 lij0 } for b quadratic
4 lijT
if you want to fit more than one parameter you have to put enter between the numbers

The results are given in the file "res" and can easily be transformed into Excel

The data of "dessin" are given in "eqlv des"

Phase Equilibria Data CO2 - Methanol

273 15 K					$k_{ij}0$ = 0 0565 $k_{ij}1$ = 0 1361			
			k_{ij} = 0 0635		k_{ij} = 0 044		k_{ij} = 0 069 l_{ij} = 0 0168	
X CO2	P [bar]	Y CO2	Pcal/bar	Ycal	Pcal/bar	Ycal	Pcal/bar	Ycal
0	0	0	0 0351	0 0000	0 0351	0	0 0351	0
0 0828	6 895	0 9942	9 1287	0 9956	7 5291	0 9948	7 732	0 995
0 1692	13 789	0 9970	16 8314	0 9973	14 0777	0 9969	14 8674	0 9971
0 2210	17 237	0 9974	20 5388	0 9976	17 3597	0 9974	18 5775	0 9975
0 2710	20 684	0 9979	23 4691	0 9978	20 0685	0 9977	21 6884	0 9978
0 4163	27 579	0 9984	28 6522	0 9980	25 5277	0 998	27 8676	0 9981
0 5394	30 820	0 9985	30 0633	0 9981	27 8421	0 9981	30 0129	0 9982
0 7680	33 026	0 9985	33 1274	0 7680	29 5395	0 9983	35 5025	0 768
0 8160	33 233	0 9985	30 2912	0 9981	29 9579	0 9983	30 4713	0 9982
0 8754	33 371	0 9986	30 8949	0 9982	30 7558	0 9985	30 9984	0 9983
			DP/P %	DY	DP/P %	DY	DP/P %	DY
			12 22	0 026	6 7	0 0002	6 58	0 0259

313 15 K					k_{ij} = 0 063			
X CO2	P [bar]	Y CO2	Pcal/bar	Ycal	Pcal/bar	Ycal	Pcal/bar	Ycal
0	0	0	0 3488	0 0000	0 3488	0 0000	0 3488	0
0 0682	13 2	0 9646	13 3600	0 9646	13 3141	0 9693	11 7768	0 9663
0 0911	16 7	0 9727	17 5081	0 9727	17 4482	0 9753	15 5464	0 9734
0 1159	20 3	0 9815	21 8650	0 9815	21 7906	0 9791	19 575	0 9778
0 1372	24 7	0 9843	25 4893	0 9843	25 4033	0 9812	22 9824	0 9803
0 1773	31 3	0 9849	32 0009	0 9849	31 8949	0 9835	29 2391	0 9832
0 2006	36 1	0 9857	35 5876	0 9857	35 4713	0 9844	32 764	0 9842
0 2318	39 6	0 9867	40 1510	0 9867	40 0225	0 9851	37 3355	0 9852
0 2733	45 6	0 9876	45 7742	0 9876	45 6323	0 9857	43 1142	0 986
0 3464	55	0 9881	54 3502	0 9881	54 1938	0 9859	52 2892	0 9865
0 3838	59 1	0 9879	58 0437	0 9879	57 8850	0 9857	56 4048	0 9864
0 4128	62	0 9882	60 5725	0 9882	60 4143	0 9855	59 2932	0 9863
0 4658	66	0 9871	64 4301	0 9871	64 2787	0 9850	63 8359	0 9858
0 5138	69	0 9865	67 0877	0 9865	66 9488	0 9846	67 0855	0 9853
0 5467	70 6	0 9867	68 4775	0 9867	68 3502	0 9842	68 8318	0 9849
0 5907	73 9	0 9864	69 8475	0 9864	69 7387	0 9839	70 5812	0 9845
0 6816	76 9	0 9842	71 3734	0 9842	71 3074	0 9834	72 4498	0 9839
0 8783	80 3	0 9677	74 6872	0 9677	74 6827	0 9829	75 1025	0 9833
			DP/P %	DY	DP/P %	DY	DP/P %	DY
			3 26	0 003	3 24	0 003	5 55	0 0026

330 K					k_{ij} = 0 0696			
X CO2	P [bar]	Y CO2	Pcal/bar	Ycal	Pcal/bar	Ycal	Pcal/bar	Ycal
0	0	0	0 7517	0 0000	0 7517	0	0 7517	0 0000
0 02449	6 895	0 8791	6 3510	0 8741	6 6057	0 8785	5 6751	0 8606
0 05582	13 789	0 9403	13 3616	0 9355	13 9299	0 9377	11 9551	0 9295
0 08742	20 684	0 9572	20 2464	0 9540	21 1158	0 9554	18 2502	0 9507
0 11830	27 579	0 9668	26 7797	0 9625	27 9277	0 9635	24 3439	0 9606
0 18500	41 368	0 9746	40 1679	0 9704	41 8584	0 9709	37 2108	0 9700
0 25970	55 157	0 9772	53 8336	0 9733	56 022	0 9733	50 9085	0 9738
0 34480	68 947	0 9773	67 4198	0 9732	70 0077	0 9728	65 1666	0 9744
0 44150	82 737	0 9735	79 9012	0 9707	82 6809	0 9694	78 9565	0 9723
0 58300	96 526	0 9621	91 7744	0 9633	94 1999	0 9598	92 9543	0 9641
0 71270	103 421	0 9347	96 3043	0 9557	97 6449	0 9507	98 3742	0 9527
0 74750	104 800	0 9203	96 8483	0 9542	97 8411	0 9498	98 8264	0 9506
			DP/P %	DY	DP/P %	DY	DP/P %	DY
			4 21	0 008	2 51	0 0066	8 78	0 0095
			DP/P %	DY	DP/P %	DY	DP/P %	DY
			5 72	0 0101	3 86	0 0034	6 76	0 0103

CO_2 - Methanol at 330 K

		kij = 0		kij = 0 02		kij = 0 05		kij = 0 07		kij = 0 1		kij = 0 0713	
Xliq	Pexp/bar	Pcal/bar	Ycal	Pcal/bar	Ycal	Pcal/bar	Ycal	Pcal/bar	Ycal	Pcal/bar	Ycal	Pcal/bar	Ycal
0	0	0 7517	0 0000	0 7517	0 0000	0 7517	0 0000	0 7517	0 0000	0 7517	0 0000	0 7517	0 0000
0 0245	6 895	4 3053	0 8192	4 8510	0 8383	5 8343	0 8638	6 6213	0 8788	8 0449	0 8985	6 6752	0 8797
0 0558	13 789	8 8214	0 9080	10 0299	0 9177	12 2115	0 9304	13 9646	0 9378	17 1603	0 9474	14 0850	0 9382
0 0874	20 684	13 3384	0 9365	15 1729	0 9427	18 4909	0 9508	21 1690	0 9555	26 0927	0 9615	21 3535	0 9558
0 1183	27 579	17 7110	0 9501	20 1138	0 9545	24 4679	0 9602	27 9980	0 9635	34 5491	0 9677	28 2418	0 9637
0 1850	41 368	26 9950	0 9640	30 4675	0 9664	36 7850	0 9693	41 9623	0 9709	51 8092	0 9726	42 3225	0 9710
0 2597	55 157	37 0806	0 9708	41 4713	0 9719	49 4925	0 9730	56 1570	0 9733	69 3281	0 9725	56 6255	0 9733
0 3448	68 947	48 0755	0 9743	53 1131	0 9744	62 3515	0 9739	70 1682	0 9728	86 7665	0 9670	70 7262	0 9727
0 4415	82 737	59 7803	0 9758	64 9907	0 9749	74 5621	0 9726	82 8549	0 9693	107 4858	0 8924	83 4619	0 9690
0 5830	96 526	75 0262	0 9753	79 3752	0 9731	87 2862	0 9679	94 3555	0 9595	165 7794	0 7229	94 9026	0 9585
0 7127	103 421	86 6903	0 9723	89 2746	0 9691	93 8086	0 9618	97 7313	0 9503	168 3208	0 7127	98 0361	0 9487
0 7475	104 800	89 4325	0 9710	91 4586	0 9675	94 9607	0 9600	97 9043	0 9495	158 3560	0 7475	98 1259	0 9482
		dP/P %	DY	dP/P %	DY	dP/P %	DY	dP/P %	DY	dP/P %	DY	dP/P %	DY
		29 41	0 023	22 76	0 0182	10 71	0 0113	2 6	0 0065	34 99	0 0694	2 97	0 0063

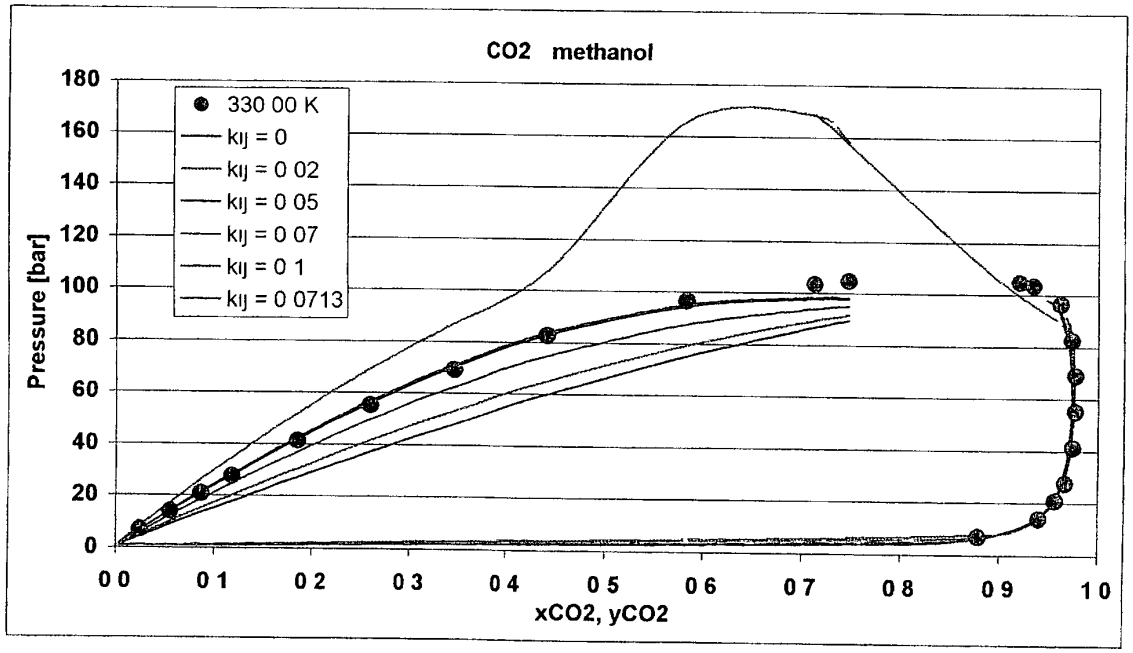

CO_2 - Methanol at 330 K

Xliq	Pexp/bar	kij = 0 0713 Pcal/bar	Ycal	kij0 = 3 0893 kij1 = 31 2713 Pcal/bar	Ycal	kij = 0 076 lij = 0 0063 Pcal/bar	Ycal	kij0 = 0 0884 kij1 = -0 0021 lij0 = 1 8334 lij1 = 18 8221 Pcal/bar	Ycal
0	0	0 7517	0 0000	0 7517	0 0000	0 7517	0 0000	0 7517	0 0000
0 0245	6 895	6 6752	0 8797	6 6684	0 8796	6 5040	0 8769	6 4177	0 8756
0 0558	13 789	14 0850	0 9382	14 0699	0 9382	13 7469	0 9371	13 6261	0 9369
0 0874	20 684	21 3535	0 9558	21 3303	0 9557	20 9030	0 9552	20 8295	0 9554
0 1183	27 579	28 2418	0 9637	28 2112	0 9637	27 7326	0 9635	27 7796	0 9638
0 1850	41 368	42 3225	0 9710	42 2772	0 9710	41 8416	0 9711	42 3733	0 9716
0 2597	55 157	56 6255	0 9733	56 5665	0 9733	56 3878	0 9736	57 7628	0 9741
0 3448	68 947	70 7262	0 9727	70 6559	0 9727	70 9618	0 9730	73 5663	0 9731
0 4415	82 737	83 4619	0 9690	83 3852	0 9691	84 3610	0 9691	88 5402	0 9675
0 5830	96 526	94 9026	0 9585	94 8331	0 9586	96 6443	0 9557	106 6780	0 8614
0 7127	103 421	98 0361	0 9487	97 9972	0 9489	102 4278	0 7746	122 7935	0 7138
0 7475	104 800	98 1259	0 9482	98 0977	0 9483	102 8871	0 7475	121 5667	0 7475
		dP/P %	**DY**	**dP/P %**	**DY**	**dP/P %**	**DY**	**dP/P %**	**DY**
		2 97	**0 0063**	**2 92**	**0 0063**	**1 71**	**0 0332**	**6 88**	**0 0475**

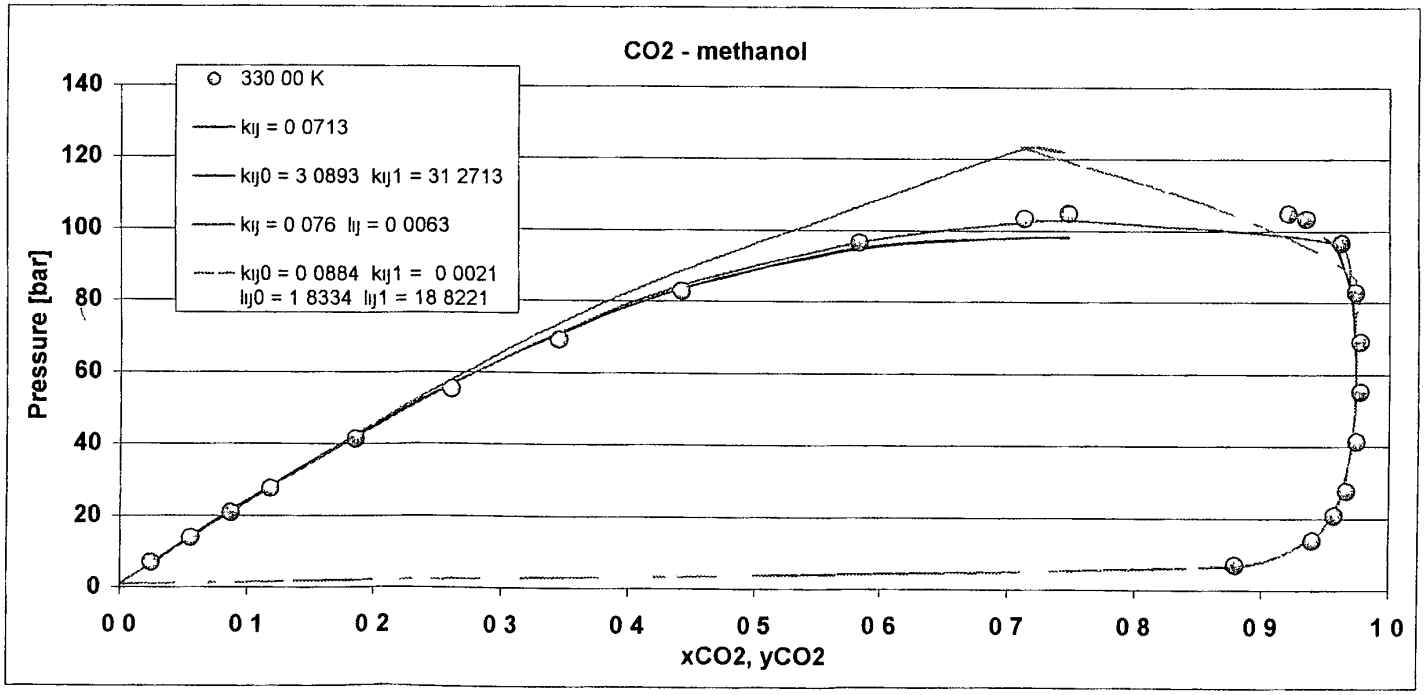

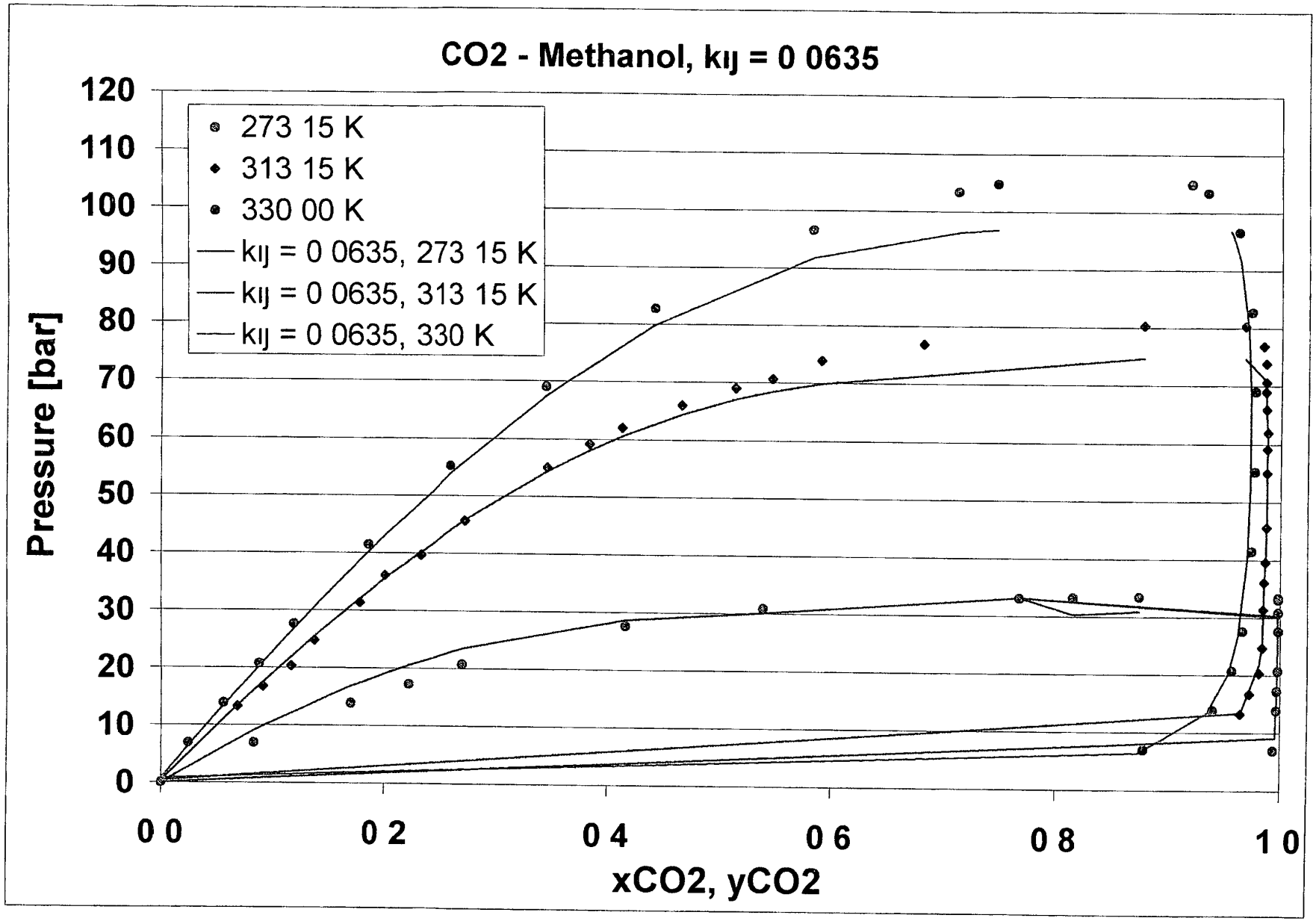
CO2 - Methanol, kij = 0 0635
273 15 K
313 15 K
330 00 K
kij = 0 0635, 273 15 K
kij = 0 0635, 313 15 K
kij = 0 0635, 330 K
Pressure [bar]
120
110
100
90
80
70
60
50
40
30
20
10
0
0 0
0 2
0 4
0 6
0 8
1 0
xCO2, yCO2

61-a

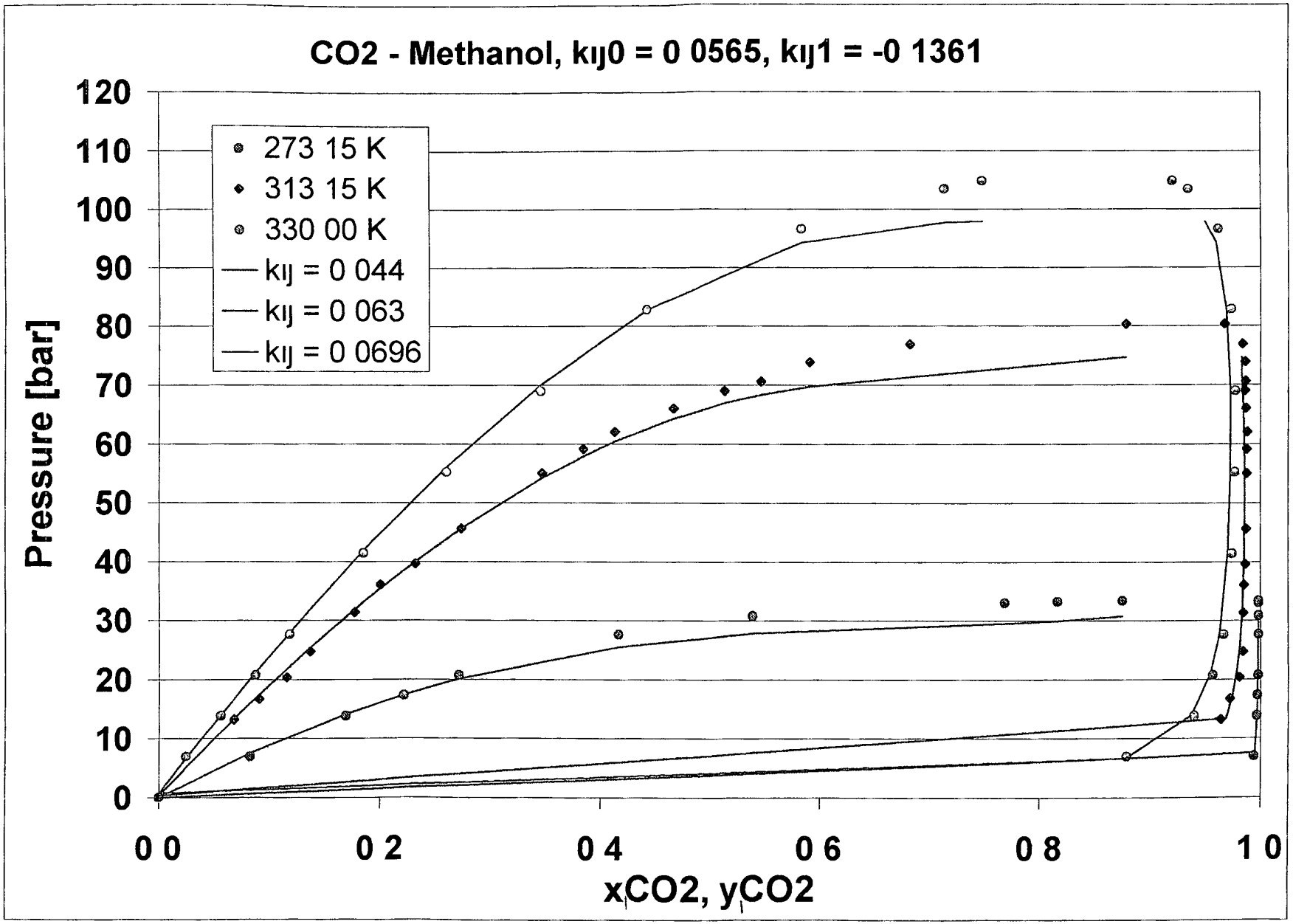
CO2 - Methanol, kij0 = 0 0565, kij1 = -0 1361
273 15 K
313 15 K
330 00 K
kij = 0 044
kij = 0 063
kij = 0 0696
Pressure [bar]
120
110
100
90
80
70
60
50
40
30
20
10
0
0 0
0 2
0 4
0 6
0 8
1 0
xCO2, yCO2

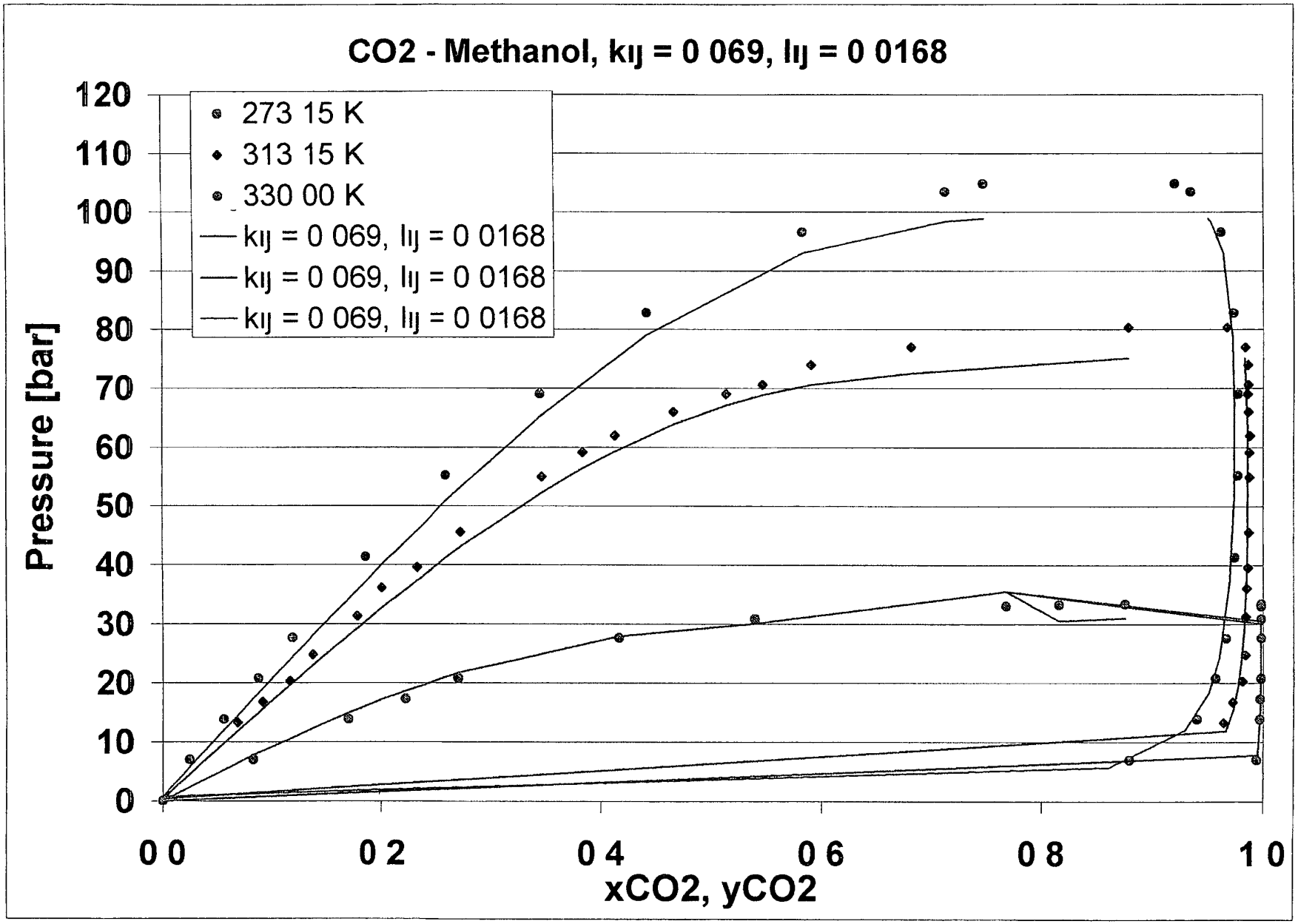
CO2 - Methanol, kij = 0 069, lij = 0 0168
273 15 K
313 15 K
330 00 K
kij = 0 069, lij = 0 0168
kij = 0 069, lij = 0 0168
kij = 0 069, lij = 0 0168
Pressure [bar]
120
110
100
90
80
70
60
50
40
30
20
10
0
0 0
0 2
0 4
0 6
0 8
1 0
xCO2, yCO2

K-9

Solubility calculation of substances in compressed gases

Robin et al

$$\log \underline{c} = A + B\rho$$

concentration gram/l CO_2

Stahl et al

$$\ln c = m \ln \rho + konst$$

Mitra et al

$$\ln y = A\rho + BT + C$$

Chrastil

$$c = \rho^k \exp(a/T + b)$$

gram/l

only for binary sys

Adachi et al

$$c = \rho^k \exp(a/T + b)$$

$$k = e_1 + e_2\rho + e_3\rho^2$$

Solubilities in supercritical CO_2

high solubility	organic oxygen compounds with low molecular weight, e g ketones, esters, alcohols, aldehydes
good solubility	most of the non polar organic substances with low molecular weight, e g alkanes, alkines and terpenes
low solubility	polar organic substances with high molecular weight

* within a homologous series the solubility decreases with increasing molecular weight

* the presence of a polar group lowers the solublity of the compound

* alcaloids are often insoluble in liquid carbon dioxide but some are soluble in supercritical CO_2

Furfural - CO_2

Daten gemäß der vorliegenden Arbeit

Chrastil-Gleichung	$c = \rho^{k} \exp(a/T + b)$
Parameter fur Furfural - CO_2	
	k = 7 485
	a = 2116 29
	b = -52 41
Gultigkeitsbereich	25°C - 60°C
	80 bar - 330 bar

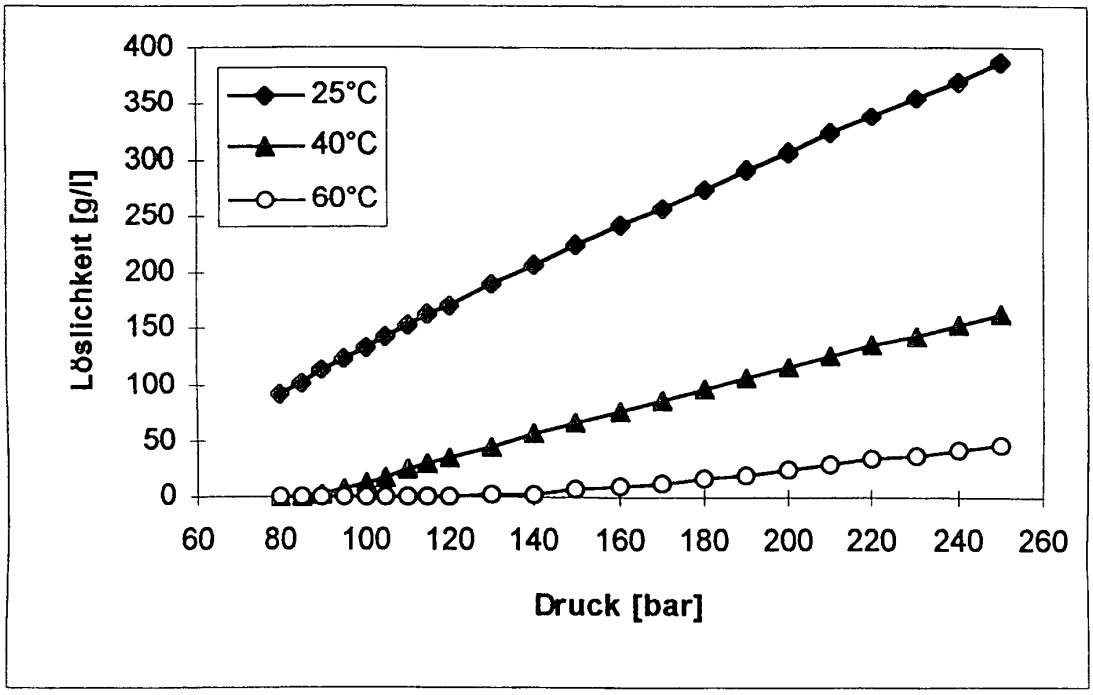

Tripalmitin - CO_2

Chrastil-Gleichung	$c = \rho^k \exp(a/T + b)$
Parameter fur Tripalmitin - CO_2	
	k = 2 98 a = -2387 8 b = -12 15
Gultigkeitsbereich	25°C - 60°C 80 bar - 250 bar

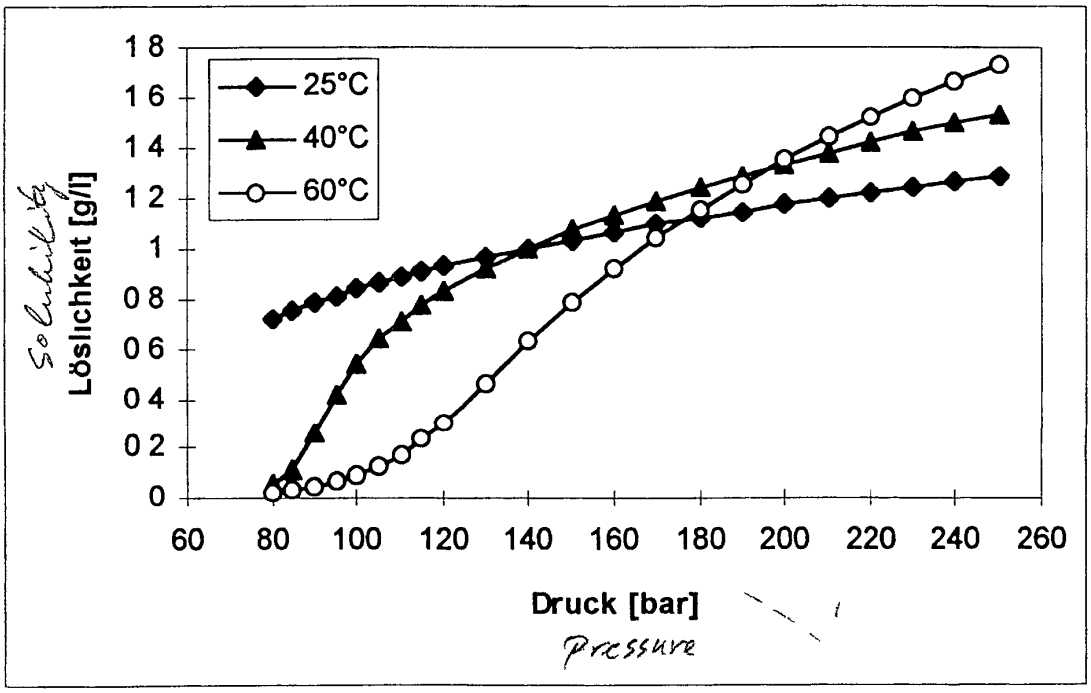

HIGH PRESSURE PHASE EQUILIBRIA

Ass Prof Dipl -Ing Dr techn Thomas Gamse

Institute of Thermal Process and Environmental Engineering
University of Technology Graz
Inffeldgasse 25, A-8010 Graz
Tel ++43 316 873 7477
Fax ++43 316 873 7472
email Gamse@tvtut tu-graz ac at
homepage www tvtut tu-graz ac at
personal homepage http //communities msn de/ThomasGamse

E

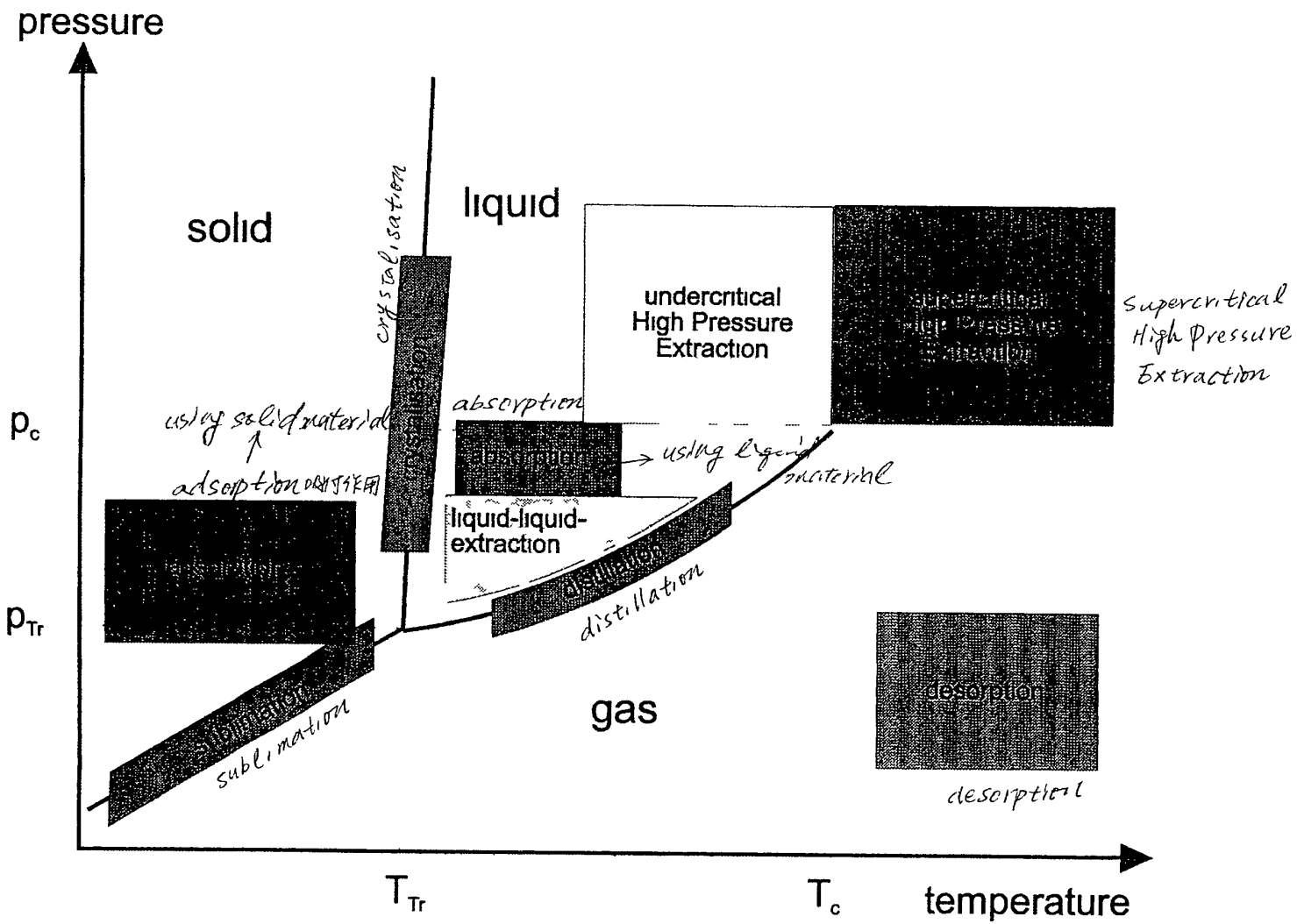
pressure
solid
liquid
gas
undercritical
High Pressure
Extraction
liquid-liquid-
extraction
desorption
sublimation
distillation
crystallisation
absorption
adsorption
using solid material
using liquid material
Supercritical
High Pressure
Extraction
desorption
p_c
p_{Tr}
T_{Tr}
T_c
temperature

E-1

Physical-chemical data of different gases suitable for extraction of natural substances

	T_C [°C]	p_C [bar]
ethene	9 9	50 5
triflouromethan	25 9	46 9
carbon dioxide	**31 0**	**72 9**
ethane	32 2	48 2
dinitrogen monoxide	36 5	71 7
sulfur hexaflouride	45 6	37 7
propene	91 9	45 4
propane	96 8	42 4

higher solubility than CO_2

E-2

Physical properties at different state of aggregation

	gas	supercritical fluid	liquid
density [kg/dm^3]	10^{-3}	0 3 - 0 9	1
diffusions coefficient [cm^2/s]	10^{-1}	10^{-3} - 10^{-4}	10^{-5}
viscosity [g/cm s]	10^{-4}	10^{4} - 10^{-3}	10^{-2}

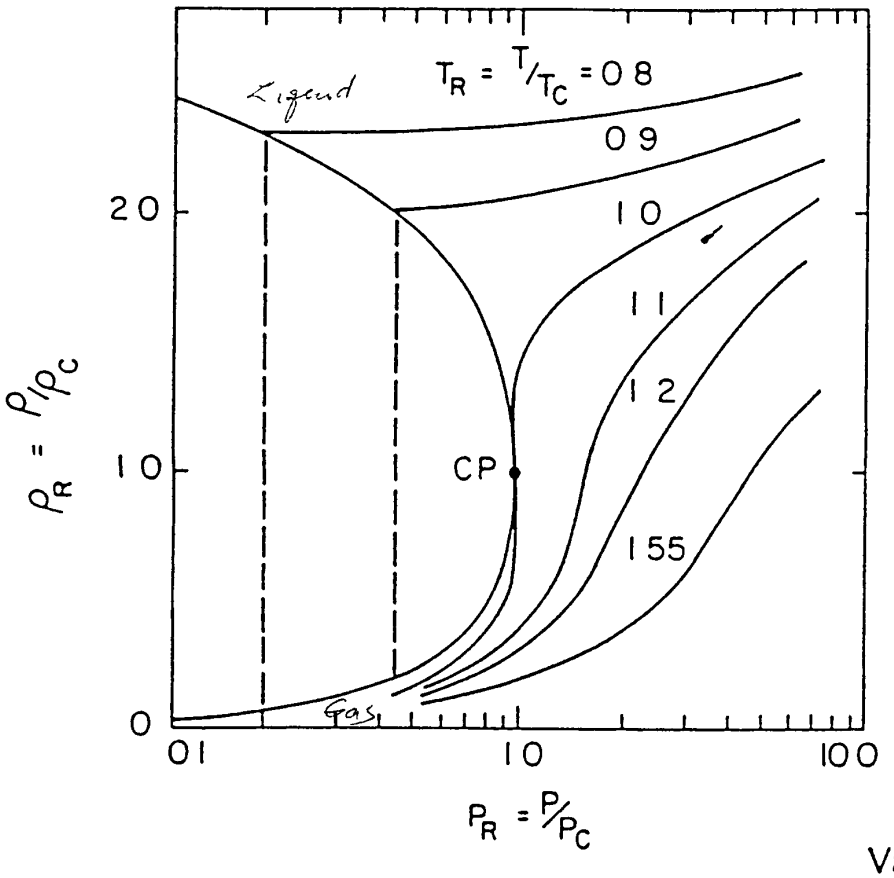

Variation of the reduced density (ρ_R) of a pure component in the vicinity of its critical point

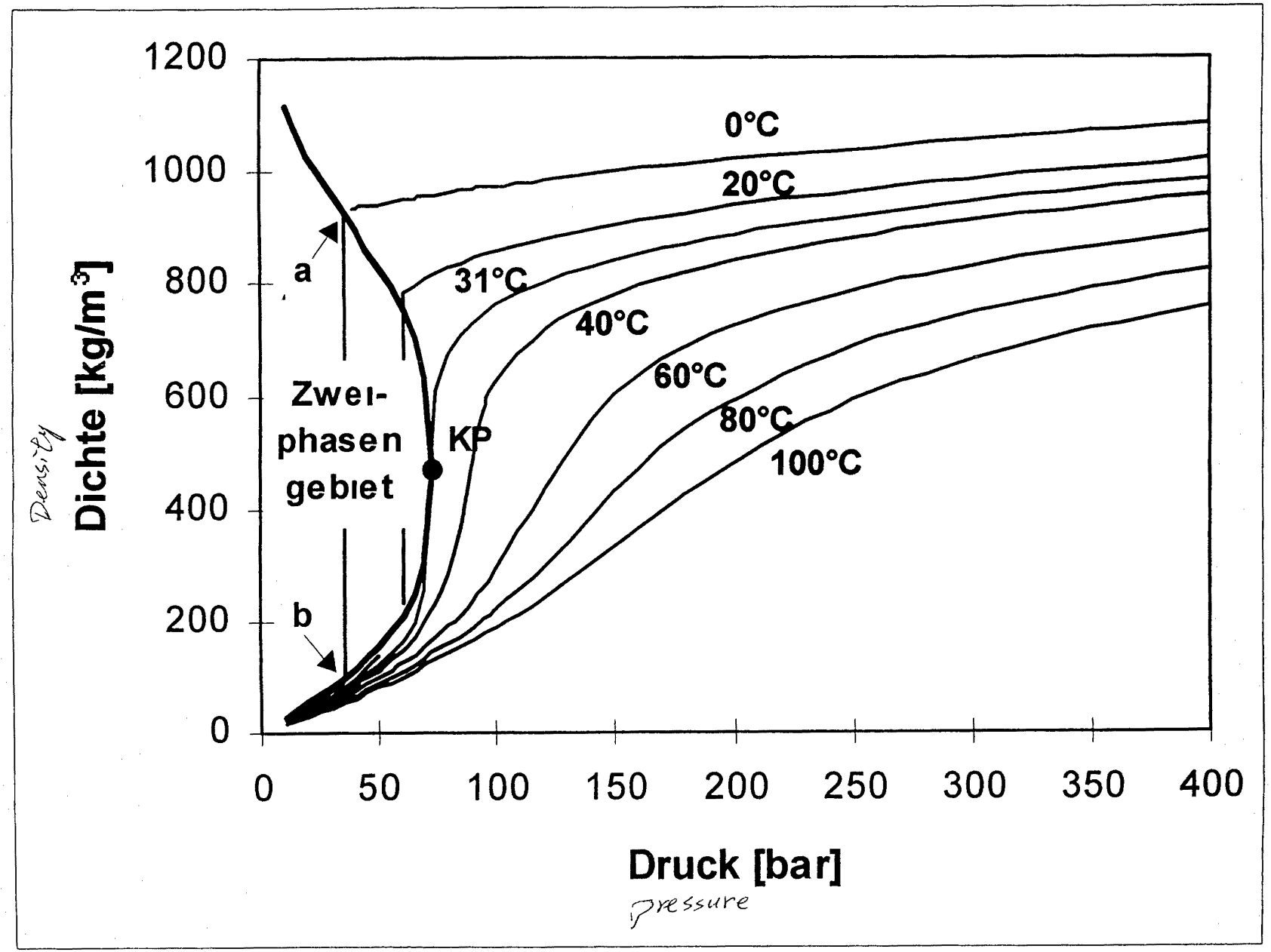
1200
1000
800
600
400
200
0
Dichte [kg/m³]
Density
0
50
100
150
200
250
300
350
400
Druck [bar]
pressure
0°C
20°C
31°C
40°C
60°C
80°C
100°C
a
b
Zwei-
phasen
gebiet
KP

5-3

Temperatur-Entropie (T,s)-Diagramm ür Kohlensaure (CO_2)

NATÜRLICHE CARBO® KOHLENSÄURE

CARBO Kohlensäurewerke GmbH & Co KG
Sprudelstr 53557 Bad Honningen
Telefon 0 26 35/7 89 0
Telefax 0 26 35/7 89 10

Kohlensäurewerk Hannover eG
Meineckestr 12 14 30880 Laatzen
Telefon 0 51 02/9 19 20
Telefax 0 51 02/40 89

CARBO-CO_2-Tech
Problemlösungen mit türlicher Kohl säure.

CARBO ÖKOTECH
Eine Initiative zum Schutz unserer Umwelt.

CARBO BIOTECH
Qualitätsförderung mit natürlicher Kohl nsä re.

Einheiten

T s Diagramm

Druck p in bar
spezifische Enthalpie h in kJ / kg
spezifisches Volumen v in m³ / kg

Bezugsgrößen

Die Enthalpie des idealen Gases wurde festgelegt bei
T_0 = 298 15 K h_0 (298 15 K) = 0 kJ / kg

Die Entropie des idealen Gases wurde festgelegt bei
T_0 = 298 15 K und p_0 = 1 atm = 1 01325 bar
s_0 (298 15 K 1 01325 bar) = 0 kJ / (kgK)

© Copyright CARBO Kohlensäurewerke GmbH & Co KG Bad Hönningen
Die Datenangaben sind ohne Gewähr

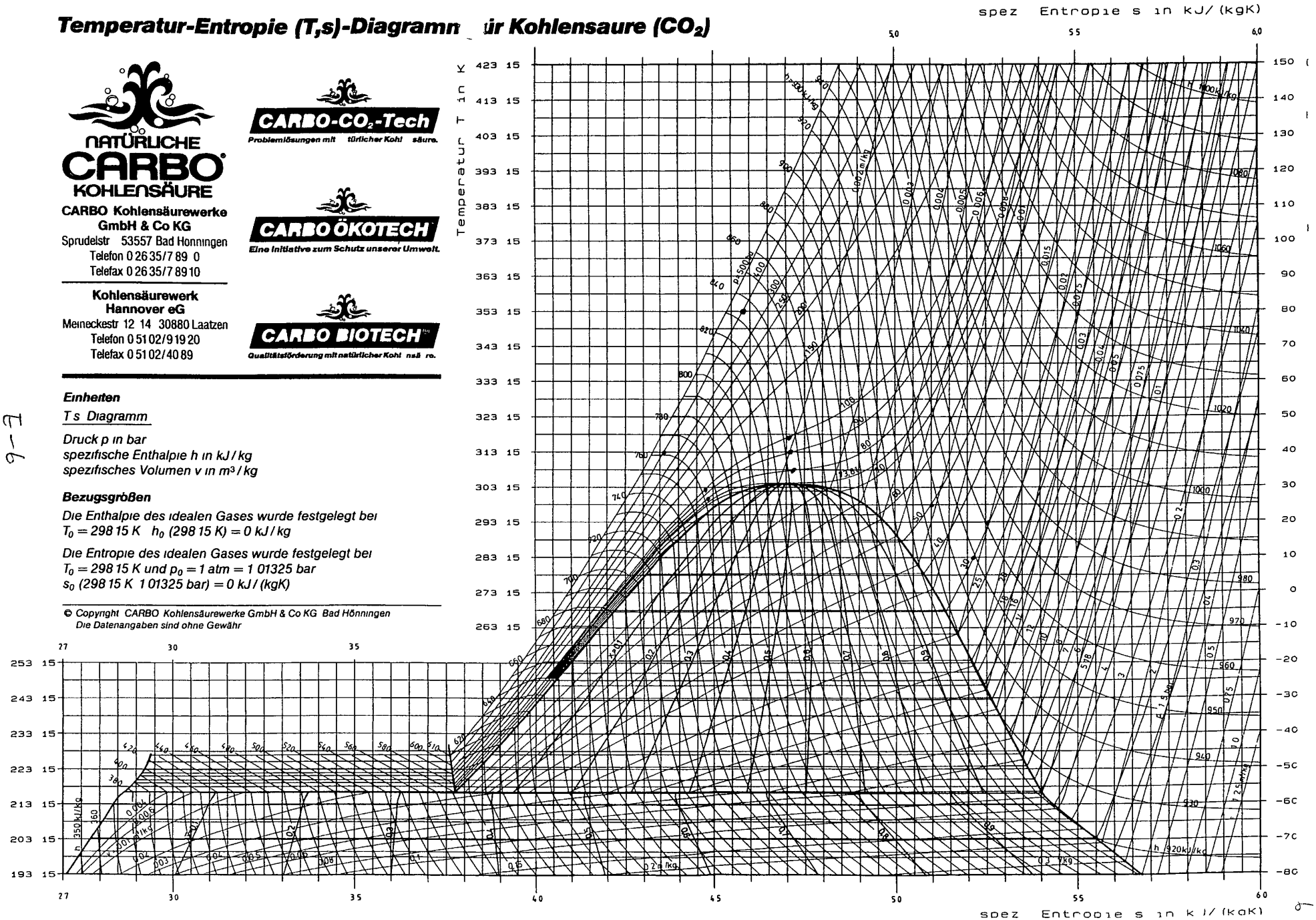

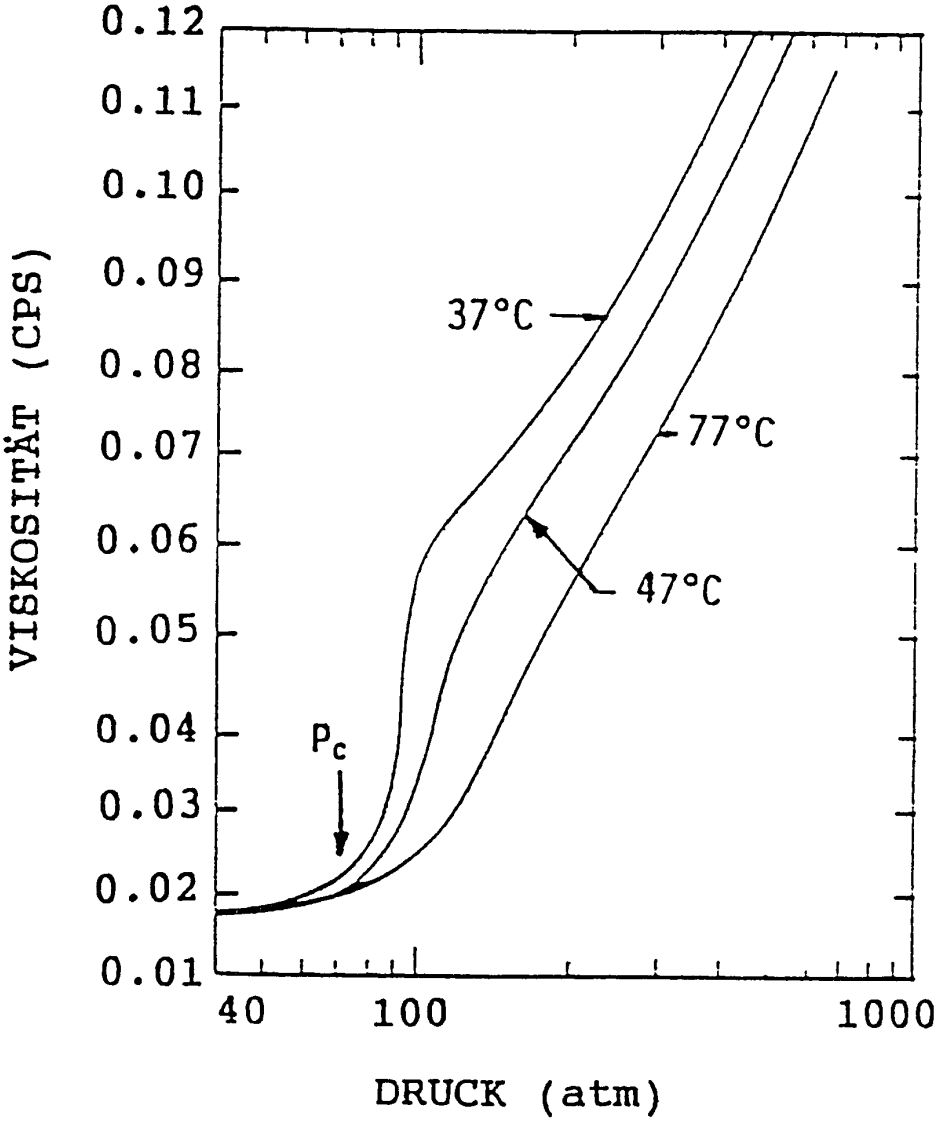
0.12
0.11
0.10
0.09
0.08
0.07
0.06
0.05
0.04
0.03
0.02
0.01
VISKOSITÄT (CPS)
37°C
77°C
47°C
P_c
40
100
1000
DRUCK (atm)

E-7

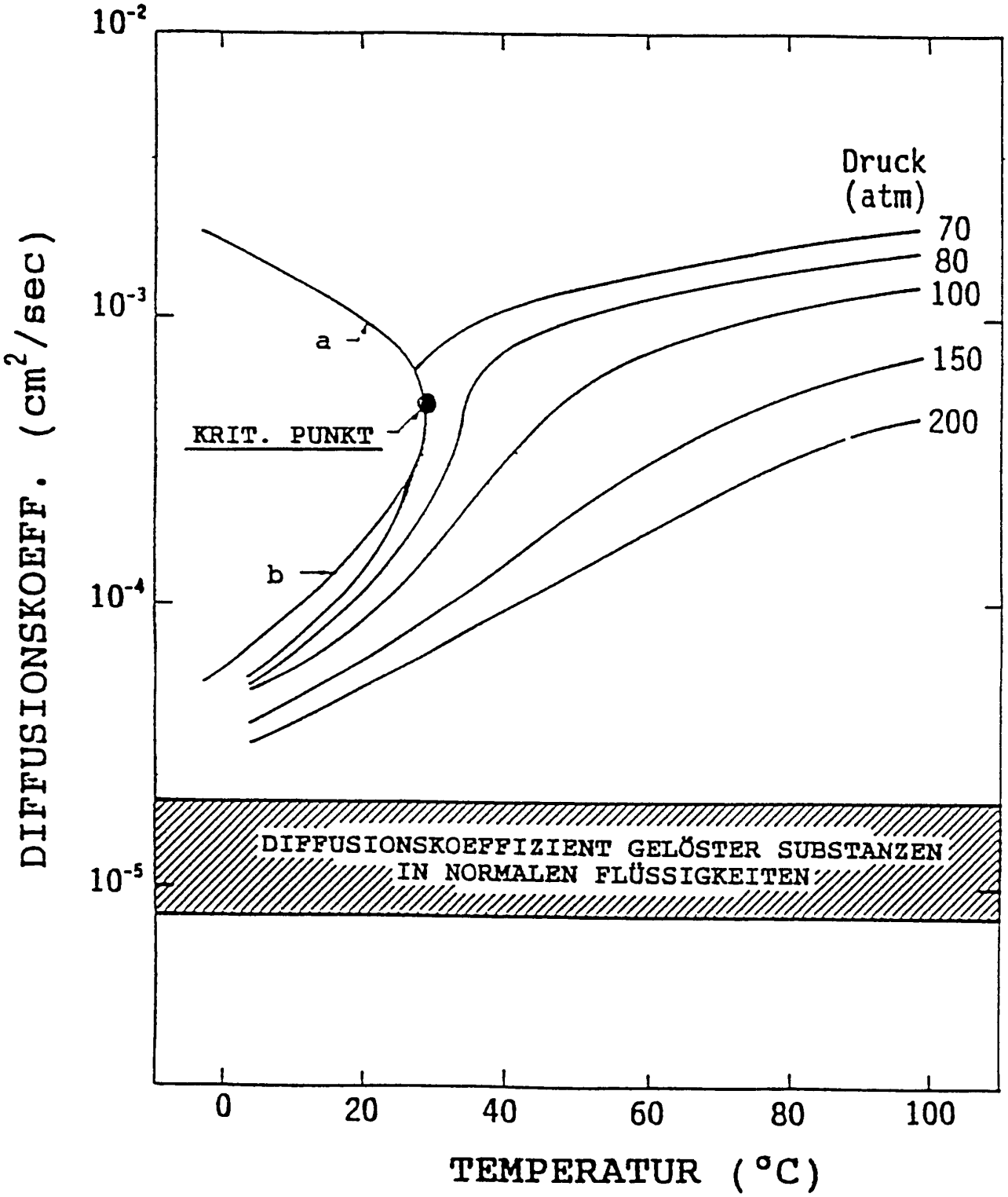

Diffusivity behavior of carbon dioxide

EXTRACTION TREND LINES

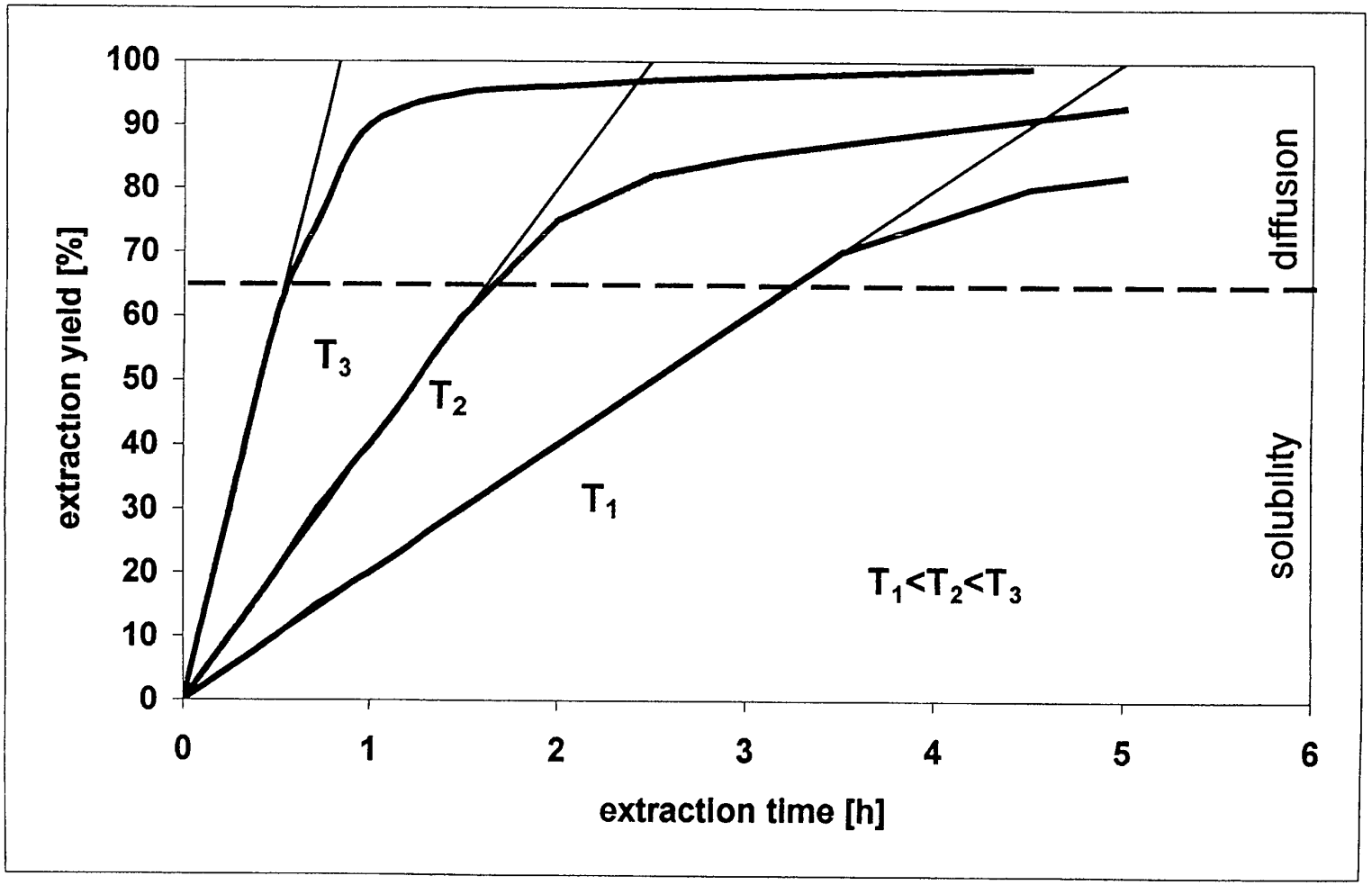

E-9

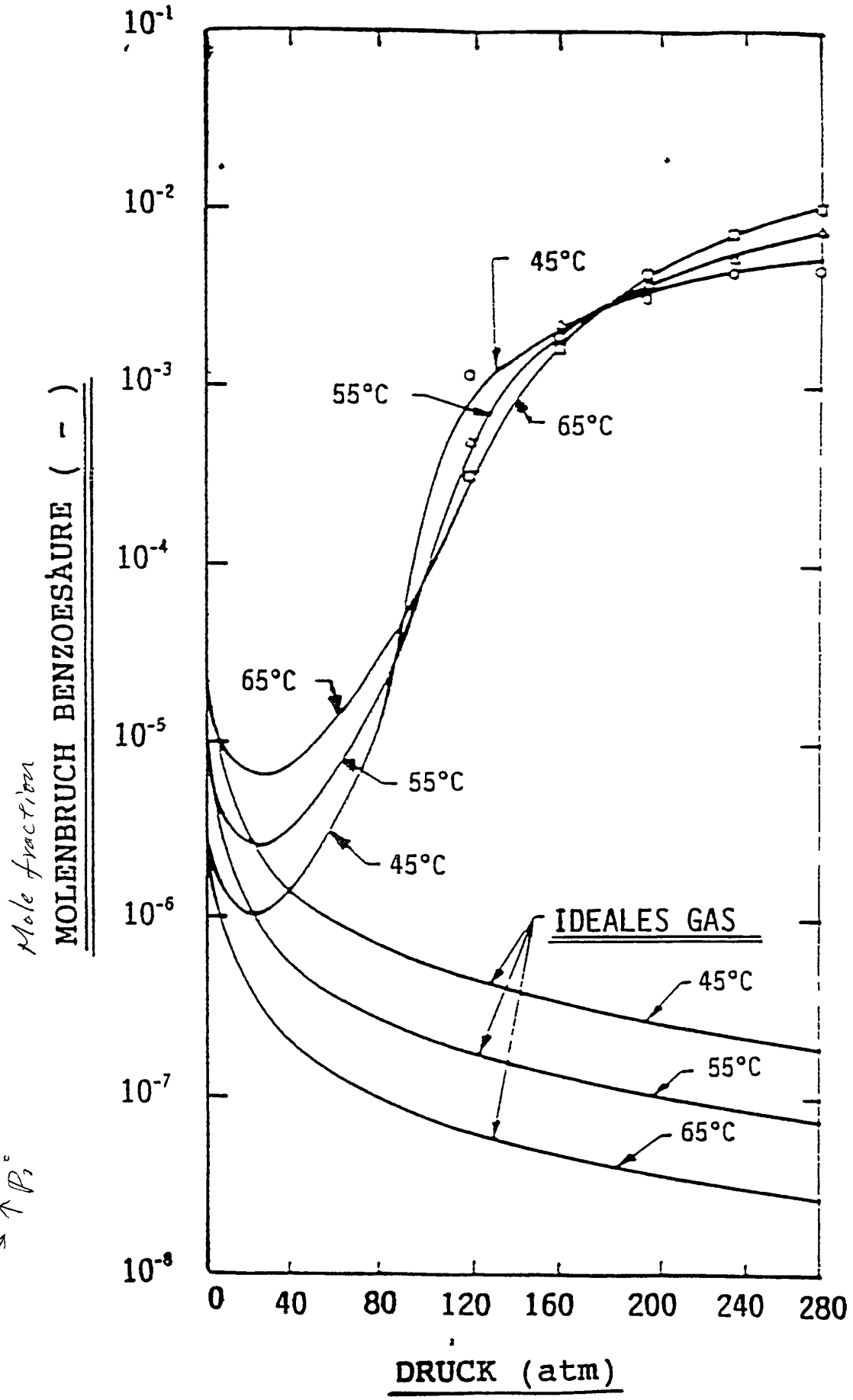

熱的因子 T → ↓P
↑P_2°

E-10

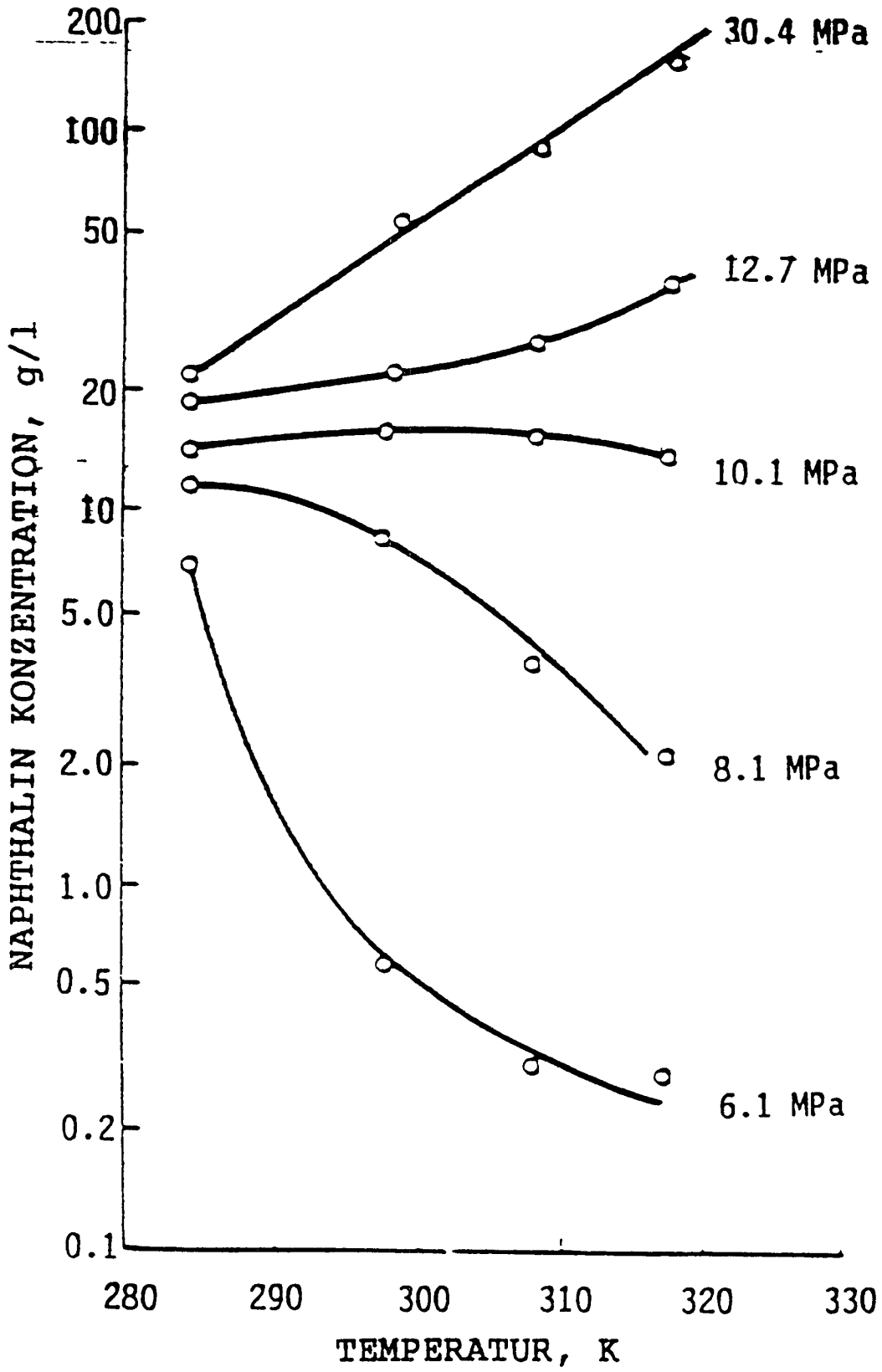

ig. 5 Solubility of naphthalene in supercritical ethylene as a inction of temperature at different pressures (Ethylene Tc = 282 K, Pc = 5 MPa)

E-11

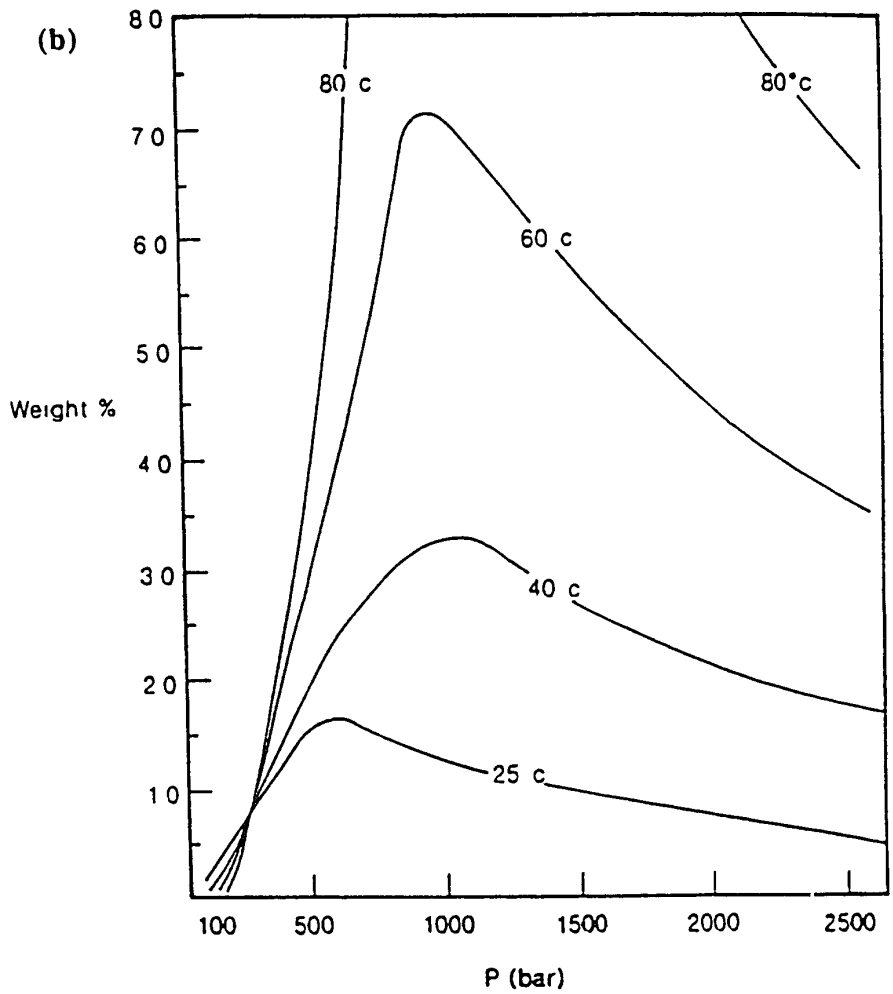

Figure 1 15 (a) Solubility of soybean oil in near-critical carbon dioxide as function of pressi and temperature (Data of Quirin [68]) (b) Solubility of soybean oil in compressed carbon dioxi over extended pressure range (data of Stahl and Quirin [78])

PHASE EQUILIBRIA

GIBBS ENTHALPY

$G = H - TS$ $\quad$ H = enthalpy

S = entropy

$dG = -S\,dT + V\,dP + \sum \mu_i\, dn_i$ $\quad$ μ_i = chemical potential

$G = G(T, P, \mu_i)$

Phase equilibrium in heterogeneous systems

$U = U^\alpha + U^\beta + \ldots + U^\pi$ = minimum $\quad$ U internal energy

$S = S^\alpha + S^\beta + \ldots + S^\pi$ = constant

$V = V^\alpha + V^\beta + \quad + V^\pi$ = constant $\quad$ volume

$n_i = n_i^\alpha + n_i^\beta + \quad + n_i^\pi$ = constant $\quad$ $i = 1, \ldots n$

for each phase φ the Gibbs fundamental equation is valid

$$dU^\varphi = T^\varphi\, dS^\varphi - P^\varphi\, dV^\varphi + \sum \mu_i^\varphi\, dn_i^\varphi$$

→ for equilibrium

$$T^\alpha = T^\beta = \quad = T^\varphi = \quad T^\pi$$

$$P^\alpha = P^\beta = \quad = P^\varphi = \quad P^\pi$$

$$\mu_i^\alpha = \mu_i^\beta = \quad = \mu_i^\varphi = \quad \mu_i^\pi$$

PHASE EQUILIBRIA

Compressibility factor z

ideal gas $P\,v = R\,T$

or $P\,V = n_T\,R\,T$

n_T = total mole amount

R = universal gas constant

R = 8,31433 J / mole K

compressibility factor z $z = \frac{P\,v}{R\,T}$

for ideal gas $z = 1$

for real fluids $z \neq 1$

all fluids behave like ideal gas if the pressure P is lowered to 0

↓ interactive force ≐ 0

$\rightarrow \lim_{P \rightarrow 0} z = 1$

PHASE EQUILIBRIA

FUGACITY, FUGACITY COEFFICIENT

for ideal gas and T = constant

$$dg^{id} = \frac{RT}{P}dp = RT\,d\ln P$$

for real fluids introduction of fugacity f

$$dg = RT\,d\ln f$$

for P → 0 real fluids must behave the same as ideal gas

$$\rightarrow \lim_{P\to 0}\frac{f}{P} = 1 \qquad f = P$$

this means that the fugacity is a corrected pressure, for a pure ideal gas the pressure and the fugacity are the same

fugacity coefficient φ

$$\boxed{\varphi = \frac{f}{P}}$$

for ideal gas $\varphi = 1$

for real gases $g^{id}(T,P) = g^{id}(T,P^o) + RT\ln\frac{P}{P^o}$

$$g(T,P) = g(T,P^o) + RT\ln\frac{f}{f^o}$$

for $P^o \rightarrow 0$ is $\frac{f^o}{P^o} = 1$ and therefore $(g - g^{id}) \rightarrow 0$

$$\boxed{(g-g^{id})_{T,P} = RT\ln\frac{f}{P} = RT\ln\varphi}$$

PHASE EQUILIBRIA

REAL PART

is the difference of thermodynamic properties of a real fluid and of an ideal gas at same temperature and pressure

$$(\underline{m} - \underline{m}^{id})_{T,P}$$

m 可為 Gibbs' energy entnalpy, entropy etc

for Gibbs enthalpy $G = H - TS$

$$(g - g^{id})_{T,P} = (h - h^{id})_{T,P} - T\,(s - s^{id})_{T,P}$$

with

$$(h - h^{id})_{T,P} = \int_0^P \left[v - T\left(\frac{\partial v}{\partial T}\right)_P \right] dP$$

$$(s - s^{id})_{T,P} = \int_0^P \left[-\left(\frac{\partial v}{\partial T}\right)_P + \frac{R}{P} \right] dP$$

$$\rightarrow \quad (g - g^{id})_{T,P} = \int_0^P \left[v - T\left(\frac{\partial v}{\partial T}\right)_P + T\left(\frac{\partial v}{\partial T}\right)_P - \frac{RT}{P} \right] dP$$

$$\rightarrow \quad \boxed{(g - g^{id})_{T,P} = RT \ln \varphi = \int_0^P \left[v - \frac{RT}{P} \right] dP}$$

or

$$\boxed{(g - g^{id})_{T,P} = RT \ln \varphi = RT(z - 1 - \ln z) + \int_\infty^V \left[\frac{RT}{V} - P \right] dv}$$

Phase equilibria calculations

Equilibria conditions:

$$T^L = T^V,\ P^L = P^V,\ f_i^L = f_i^V$$

Fugacity calculation

Activity Coeff.

Saturation

Variant 1 $\quad y_i\, \varphi_i^V P = x_i\, \gamma_i\, \varphi_i^s P_i^s\, \underline{Poy_i}$

Variant 2: $\quad y_i\, \varphi_i^V = x_i\, \varphi_i^L$

Poynting factor

Calculation of fugacity coefficient

$$\ln \varphi = Z - 1 - \ln Z + \frac{1}{RT}\int_{\infty}^{v}\left(\frac{RT}{v} - P\right)dv$$

Equations of state for pvT-behaviour

1) Ideal gas law

$$\boxed{pv = RT} \qquad \boxed{Z = \frac{pv}{RT}}$$

2) Viral-equation

Berlin-form $$\boxed{z = 1 + B'(T)p + C'(T)p^2 +} \qquad \boxed{B' = \frac{B}{RT}}$$

Leiden-form $$\boxed{z = 1 + B(T)\rho + C(T)\rho^2 +}$$

$\rho < 0{,}5\ \rho_{\underline{krit}}$ if cutting after 2nd term

Critical

3) Empirical equations of state

Benedict-Web-Rubin (BWR)

$$\boxed{p = RT\rho + (B_0RT - A_0 - \frac{C_0}{T^2})\rho^2 + (bRT - a)\rho^3 + a\alpha\rho^6 + \frac{c\rho^3(1+\gamma\rho^2)\exp(-\gamma\rho^2)}{T^2}}$$

Starling-Han

$$\boxed{p = RT\rho + (B_0RT - A_0 - \frac{C_0}{T^2} + \frac{D_0}{T^3} - \frac{E_0}{T^4})\rho^2 + (bRT - a - \frac{d}{T})\rho^3 + \alpha(a + \frac{d}{T})\rho^6 + \frac{c\rho^3(1+\gamma\rho^2)\exp(-\gamma\rho^2)}{T^2}}$$

Bender: (可作CO_2密度之计算很準 其餘不行)
S H etc

$$\boxed{p = RT\rho + B\rho^2 + C\rho^3 + D\rho^4 + E\rho^5 + F\rho^6 + \\ +(G + H\rho^2)\rho^3 \exp(-a20\,\rho^2)}$$

with

$$B = a_1 T - a_2 - \frac{a_3}{T} - \frac{a_4}{T^2} - \frac{a_5}{T^3}$$

$$C = a_5 T + a_7 + \frac{a_8}{T}$$

$$D = a_9 T + a_{10}$$

$$E = a_{11} T + a_{12}$$

$$F = a_{13}$$

$$G = \frac{a_{14}}{T^2} + \frac{a_{15}}{T^3} + \frac{a_{16}}{T^4}$$

$$H = \frac{a_{17}}{T^2} + \frac{a_{18}}{T^3} + \frac{a_{19}}{T^4}$$

Parameters for Bender equation for CO_2

R	=	0,188918		$J\ g^{-1}\ K^{-1}$
a_1	=	0,22488558		$J\ cm^3\ g^{-2}\ K^{-1}$
a_2	=	0,13717965	10^3	$J\ cm^3\ g^{-2}$
a_3	=	0,14430214	10^5	$J\ cm^3\ g^{-2}$
a_4	=	0,29630491	10^7	$J\ K^2\ cm^3\ g^{-2}$
a_5	=	0,20606039	10^9	$J\ K^3\ cm^3\ g^{-2}$
a_6	=	0,45554393	10^{-1}	$J\ cm^6\ g^{-3}\ K^{-1}$
a_7	=	0,77042840	10^2	$J\ cm^6\ g^{-3}$
a_8	=	0,40602371	10^5	$J\ K\ cm^6\ g^{-3}$
a_9	=	0,40029509		$J\ cm^9\ g^{-4}\ K^{-1}$
a_{10}	=	-0,39436077	10^3	$J\ cm^9\ g^{-4}$
a_{11}	=	0,12115286		$J\ cm^{12}\ g^{-5}\ K^{-1}$
a_{12}	=	0,10783386	10^3	$J\ cm^{12}\ g^{-5}$
a_{13}	=	0,43962336	10^2	$J\ cm^{15}\ g^{-6}$
a_{14}	=	-0,36505545	10^8	$J\ K^2\ cm^6\ g^{-3}$
a_{15}	=	0,19490511	10^{11}	$J\ K^3\ cm^6\ g^{-3}$
a_{16}	=	-0,29186718	10^{13}	$J\ K^4\ cm^6\ g^{-3}$
a_{17}	=	0,24358627	10^8	$J\ K^2\ cm^{12}\ g^{-5}$
a_{18}	=	-0,37546530	10^{11}	$J\ K^3\ cm^{12}\ g^{-5}$
a_{19}	=	0,11898141	10^{14}	$J\ K^4\ cm^{12}\ g^{-5}$
a_{20}	=	5,00000000		$cm^6\ g^{-2}$

CO_2 Density calculated by equation of Bender

Pressure [bar]	Temperature [°C] 0	10	20	30	40	50	60	70	80	90	100
10	20 85	19 94	19 11	18 36	17 68	17 05	16 47	15 93	15 43	14 97	14 53
20	45 65	43 04	40 81	38 87	37 15	35 62	34 24	32 98	31 83	30 77	29 79
30	77 33	71 06	66 20	62 25	58 93	56 06	53 55	51 32	49 31	47 50	45 84
35	97 96	88 03	80 90	75 38	70 90	67 13	63 88	61 04	58 51	56 24	54 18
40	933 32	108 32	97 51	89 78	83 77	78 87	74 73	71 17	68 04	65 26	62 76
45	937 51	134 54	116 86	105 80	97 73	91 39	86 17	81 75	77 93	74 57	71 57
50	941 52	870 49	140 53	124 00	113 02	104 81	98 26	92 83	88 20	84 18	80 63
55	945 36	877 09	172 51	145 30	130 00	119 30	111 10	104 46	98 90	94 13	89 96
60	949 06	883 20	784 97	171 49	149 20	135 10	124 79	116 69	110 04	104 42	99 56
65	952 62	888 91	798 59	206 86	171 48	152 50	139 48	129 61	121 68	115 09	109 46
70	956 07	894 28	810 02	268 98	198 31	171 92	155 34	143 29	133 86	126 15	119 65
75	959 40	899 35	819 96	657 91	232 63	193 98	172 58	157 83	146 63	137 65	130 17
80	962 63	904 15	828 80	699 94	281 33	219 58	191 48	173 34	160 04	149 59	141 03
85	965 76	908 73	836 79	725 12	363 10	250 10	212 39	189 96	174 15	162 02	152 24
90	968 81	913 10	844 10	743 73	484 08	287 53	235 73	207 83	189 02	174 96	163 81
95	971 76	917 28	850 86	758 74	571 93	334 15	262 00	227 11	204 73	188 45	175 77
100	974 64	921 30	857 16	771 41	622 64	389 91	291 66	247 96	221 32	202 52	188 13
120	985 46	935 98	878 87	809 22	716 14	581 08	437 40	348 06	297 37	264 85	241 69
140	995 35	948 90	896 75	836 24	762 81	670 16	560 10	458 66	385 34	335 95	301 44
160	1004 50	960 49	912 09	857 66	794 91	721 16	636 10	547 86	470 18	409 69	364 65
180	1013 00	971 05	925 60	875 60	819 75	756 74	686 37	620 00	539 88	477 26	426 31
200	1020 90	980 76	937 72	891 13	840 19	784 23	723 19	658 61	594 16	534 28	482 02
220	1028 40	989 77	948 77	904 88	857 67	806 75	752 14	694 79	636 81	581 08	530 15
240	1035 50	998 20	958 90	917 27	873 01	825 90	776 03	724 03	671 26	619 64	571 09
260	1042 30	1006 10	968 31	928 57	886 71	842 61	796 39	748 51	699 91	651 92	605 98
280	1048 70	1013 60	977 10	938 98	899 12	857 48	814 16	769 54	724 32	679 44	636 00
300	1054 80	1020 70	985 35	948 65	910 50	870 90	829 97	788 00	745 54	703 31	662 13
320	1060 70	1027 50	993 14	957 68	921 01	883 15	844 21	804 46	764 31	724 33	685 17
340	1066 40	1033 90	1000 50	966 17	930 80	894 44	857 20	819 32	781 13	743 08	705 71
360	1071 80	1040 10	1007 60	974 18	939 96	904 91	869 15	832 87	796 37	760 00	724 21
380	1077 10	1046 00	1014 30	981 78	948 58	914 69	880 23	845 35	810 30	775 40	741 01
400	1082 10	1051 70	1020 70	989 01	956 73	923 88	890 55	856 90	823 15	789 54	756 40

4) Cubic equations of state

general

$$\boxed{z = z^{an} + z^{ab}}$$

$$\boxed{p = \frac{RT}{v-b} - \frac{a}{v^2 + u\,b\,v + w\,b^2}}$$

Van der Waals (u = 0, w = 0)

$$\boxed{z = \frac{v}{v-b} - \frac{a}{v+b}\frac{1}{RT^{3/2}}}$$

$$\boxed{p = \frac{RT}{v-b} - \frac{a}{v^2}}$$

$$a = \frac{27}{64}\frac{R^2 T_c^2}{p_c} \qquad b = \frac{RT_c}{8p_c}$$

Redlich - Kwong (RK) (u = 1, w = 0)

$$\boxed{z = \frac{v}{v-b} - \frac{a}{v+b}\frac{1}{RT^{3/2}}}$$

$$\boxed{p = \frac{RT}{v-b} - \frac{a}{v^2 + b\,v}}$$

$$a = \frac{0\ 42748\ R^2 T_c^{2\ 5}}{p_c} \qquad b = \frac{0\ 08664\ RT_c}{p_c}$$

Soave - Redlich - Kwong (SRK) (u = 1, w = 0)

$$\boxed{z = \frac{v}{v-b} - \frac{a(T)}{RT(v+b)}}$$

$$\boxed{p = \frac{RT}{v-b} - \frac{a}{v^2 + b\,v}}$$

$$a = \frac{0\ 42748\ R^2 T_c^2}{p_c}\left(1 + f\,\omega\left(1 - T_r^{0\ 5}\right)\right)^2 \qquad b = \frac{0\ 08664\ RT_c}{p_c}$$

$f(T)$

$$f\omega = 0\ 48 + 1\ 574\,\omega - 0\ 176\,\omega^2$$

Peng - Robinson (PR) (u = 2, w = -1)

$$\boxed{z = \frac{v}{v-b} - \frac{a(T)\,v}{RT\left[v(v+b)+b(v-b)\right]}}$$

$$\boxed{p = \frac{RT}{v-b} - \frac{a}{v^2+2b\,v-b^2}}$$

$$a = \frac{0\ 45724\ R^2 T_c^2}{p_c}\underbrace{\left(1+f\,\omega\left(1-T_r^{0\,5}\right)\right)^2}_{f(T)} \qquad b = \frac{0\ 0778\,RT_c}{p_c}$$

$$f\,\omega = 0\ 37464 + 1\ 54226\,\omega - 0\ 26992\,\omega^2$$

Calculation of acentric factor ω

$$\boxed{\omega = -1{,}000 - \log \underbrace{p_{r}^{o}}_{\text{reduced vapor pressure}}\left(T_r = 0{,}7\right)} \qquad T_r = \frac{T}{T_c}$$

or

$$\boxed{\omega = \frac{3}{7}\,\frac{\Theta}{1-\Theta}\log p_c - 1} \qquad \Theta = \frac{T_s}{T_c}$$

boiling temp at 1 atm

or

$$\boxed{\omega = \frac{\alpha}{\beta}}$$

with $\alpha = -\ln p_c - 5{,}97214 + 6{,}09648\,\Theta^{-1} + 1{,}28862\ln\Theta - 0{,}169347\,\Theta^6$

$\beta = 15{,}2518 - 15{,}5875\,\Theta^{-1} - 13{,}4721\ln\Theta + 0{,}43577\,\Theta^6$

Berechnung kritischer Daten:

for calculation of T_c, p_c, V_c

Ambrose - Gleichung:

$$T_c = T_s\left[1+\left(1{,}242+\sum\Delta T\right)^{-1}\right]$$

$$p_c = M\left(0{,}339+\sum\Delta p\right)^{-2} \qquad V_c = 40+\sum\Delta V$$

Joback-Modifikation der Lydersen -Methode

$$T_c = T_s\left[0{,}584+0{,}965\sum\Delta T-\left(\sum\Delta T\right)^2\right]^{-1}$$

$$p_c = \left(0{,}113+0{,}0032 n_A-\sum\Delta p\right)^{-2}$$

$$V_c = 17{,}5+\sum\Delta V \qquad T_s = 198+\sum\Delta b$$

Fedors - Methode

$$T_c = 535\log\sum\Delta T$$

Klincewicz - Methode

$$T_c = 50{,}2-0{,}16M+1{,}41T_s$$

Natex Prozesstechnologie GesmbH

Basic-Course

of

Supercritical Fluid Extraction Process

Metal Industries Research & Development Center

Kaohsiung, Taiwan, ROC

Mr TZU-CHEN KUO

High-PressureTechnology

Numerical data descriptions of methods or equipment and other information presented in this book have been carefully checked for accuracy Nevertheless authors and publishers do not assume any liability for misprints faulty statements or other kinds of errors Persons intending to handle chemicals or to work according to information derived from this book are advised to consult the original sources as well as relevant regulations in order to avoid possible hazards

Production Director Maximilian Montkowski
Production Manager Myriam Nothacker

Library of Congress Card No 84 25 829

Deutsche Bibliothek Cataloguing in Publication Data

Ullmann's encyclopedia of industrial chemistry / executive ed Wolfgang Gerhartz Senior ed Y Stephen Yamamoto Ed Lydia Kaudy [Ed advisory board Hans Jurgen Arpe] — Weinheim New York NY VCH
Teilw mit d Erscheinungsorten Weinheim Deerfield Beach Fl
Bis 4 Aufl u d T Ullmanns Enzyklopadie der technischen Chemie

NE Gerhartz Wolfgang [Hrsg] Encyclopedia of industrial chemistry

Vol A Alphabetically arranged articles
9 Dithiocarbamic acid to ethanol — 5 completely rev ed — 1987

ISBN 3 527 20109 2 (Weinheim)
ISBN 0 89573 159 2 (New York)

© VCH Verlagsgesellschaft mbH D 6940 Weinheim (Federal Republic of Germany) 1987

Distribution
VCH Verlagsgesellschaft P O Box 12 60/12 80 D 6940 Weinheim (Federal Republic of Germany)
Switzerland VCH Verlags AG P O Box CH 4020 Basel (Switzerland)
Great Britain and Ireland VCH Publishers (UK) Ltd 8 Wellington Court Wellington Street Cambridge CB1 1HW (Great Britain)
USA and Canada VCH Publishers Suite 909 220 East 23rd Street New York NY 10010 4606 (USA)

All rights reserved (including those of translation into other languages) No part of this book may be reproduced in any form — by photoprint microfilm or any other means — transmitted or translated into a machine language without written permission from the publishers
Authorization to photocopy items for internal or personal use or the internal or personal use of specific clients is granted for libraries and other users registered with the Copyright Clearance Center (CCC) Transactional Reporting Service provided that the base fee of $ 1 00 per copy plus $ 0 25 per page is paid directly to CCC 27 Congress Street Salem MA 01970 0740 9451/85 $ 1 00 + 0 25
Registered names trademarks etc used in this book and not specifically marked as such are not to be considered unprotected

Cover design Wolfgang Schmidt
Composition printing and bookbinding Graphischer Betrieb Konrad Triltsch D 8700 Wurzburg
Printed in the Federal Republic of Germany

High-Pressure Technology

GERHARD VETTER Universitat Erlangen Nurnberg Federal Republic of Germany (Chaps 1 and 3)
ERICH KARL BASF Aktiengesellschaft Ludwigshafen Federal Republic of Germany (Chaps 2 and 4)

1	**Applications of High Pressures**	587
2	**Pressure Vessels**	588
2 1	**Solid-Wall Vessels**	588
2 2	**Multiwall Vessels**	588
2 2 1	Designs with a Purely Mechanical Joint	588
2 2 2	Welded Designs (Layered Wall Vessels)	589
2 3	**Strength Calculations**	590
2 3 1	Cylindrical Wall	590
2 3 1 1	Stresses Due to Internal Pressure	590
2 3 1 2	Initial Stresses in Shrink Joints	591
2 3 1 3	Residual Stresses Due to Auto frettage	591
2 3 1 4	Thermal Stresses	592
2 3 1 5	Avoiding Brittle Fracture	592
2 3 2	Cylindrical Wall with Radial Bore	592
2 3 3	End Pieces	593
2 4	**Corrosion in High Pressure Plant**	593
2 5	**Material Selection**	594
2 6	**Design Details**	594
2 6 1	Corrosion Protection	594
2 6 2	Covers and Their Attachment	596
2 6 3	Cover Seals	596
2 6 4	Seals for Piping	596
2 7	**Example of the Design of Pressure Vessels**	597
3	**High Pressure Machinery for Chemical Plants**	598
3 1	**Special Features of High Pressure Machines**	598
3 2	**Creation of Pressure by Pumps and Compressors**	598
3 3	**Pumps**	600
3 3 1	Reciprocating Displacement Pumps	603
3 3 1 1	Metering Pumps	603
3 3 1 2	Transfer Pumps	606
3 3 2	Rotary Displacement Pumps	607
3 3 3	Centrifugal Pumps	607
3 3 3 1	Multistage Centrifugal Pumps	608
3 3 3 2	High Speed Centrifugal Pumps	608
3 3 3 3	Hermetic Centrifugal Pumps	610
3 4	**Compressors**	611
3 4 1	Piston Compressors	611
3 4 2	Diaphragm Compressors Laboratory High Pressure Compressors	614
3 4 3	Turbo Compressors	614
3 5	**Other High-Pressure Machines**	616
3 6	**Special Problems Involving High-Pressure Machines**	616
3 6 1	Strength of the Components	616
3 6 2	Seals	618
3 6 3	Wear and Vibration	621
4	**Piping and Fittings**	621
5	**References**	623

1 Applications of High-Pressures

Internal combustion engines thermal power plants hydraulic power transmission the arms industry the process industries and the manufacturing industries commonly use high pressures Process and manufacturing plants use pressures in the range 100–4000 bar In research pressures up to 10000 bar may be employed High pressures are used to improve the efficiency of an operation in some way [1 1]

In chemical reaction engineering high pressure may create a favorable reaction environment or determine the reaction phases Pressure may decisively affect the reaction rate state of equilibrium yield and products High pressure is particularly advantageous for reactions in which a reduction in volume takes place [1 2]

Typical industrial high pressure chemical reactions are hydrogenation amination polymerization carbonylation oxo synthesis oligomerization oxidation and cracking (Table 1) Some well known products of high pressure processes are methanol ammonia urea propionic acetic and terephthalic acids butyraldehyde (oxo synthesis) butanediol and polyethylene In many

Table 1 High pressure processes

Polyethylene	< 3000 bar
Acetic acid	< 700 bar
Methanol ammonia urea oxo synthesis butanol coal and heavy oil hydrogenation hydrocracking steam cracking heavy water	< 300 bar
Fischer–Tropsch synthesis aluminum alkyls (Ziegler) alcohols (Alfol) gas treating	< 200 bar
Ore digestion (bauxite) coal pressure gasification	< 150 bar
Supercritical extraction	< 300 bar
Reverse osmosis	< 100 bar
Spray drying	< 300 bar

Table 2 Pressure as a form of energy

Autofrettage	< 12000 bar
Isostatic molding	< 5000 bar
Water jet cutting	< 4000 bar
High pressure cleaning	< 1500 bar
Homogenizing mixing extrusion cell cracking tobacco impregnation	< 500 bar
Petroleum and natural gas recovery	< 400 bar
Spinning pumps polymer melt pumping and filtration	< 500 bar
HPLC	< 1000 bar
Water and oil hydraulic systems	< 500 bar
Slurry conveying	< 200 bar

processes e g extraction of ores, high pressure ensures that reaction takes place in the liquid phase

Some separation processes e g supercritical gas extraction [1 3] become more effective at high pressure because of favorable changes in the solubilities Other separation processes—reverse osmosis ultrafiltration and spray drying—require high pressures for hydromechanical reasons

The number of manufacturing processes that use high pressure as a tool or as a reservoir of potential energy (Table 2) appears to be expanding [1 4] The pressure is used not only statically e g in isostatic molding but also dynamically as stream flow kinetic energy e g in water jet cutting and homogenizing In many cases high pressure merely serves to overcome hydraulic resistances

2 Pressure Vessels

Pressure vessels are chiefly used as reactors scrubbers heat exchangers buffer vessels or pulsation dampers The cylindrical wall of thick walled pressures vessels (i e those with an outer to inner diameter ratio $d/d > 1\ 2$) can either be produced as one solid piece (solid wall vessels) or be constructed from several layers (multiwall vessels)

2 1 Solid-Wall Vessels

The term solid wall vessel is applied to all designs in which the cylindrical wall consists of a single layer Solid wall vessels are suitable for all types of pressure vessels in particular for high temperatures

Thermal stresses arising during heating or cooling are smaller than with multilayer vessels because of the good thermal conduction through the wall Solid wall vessels are therefore good for batch processing

Production Solid wall vessels can be produced by the following methods

1) A one piece hollow body is forged without welding seams
2) Forged rings are joined to form the vessel by circular seams
3) Thick sheets are bent around and welded into sections by one or more longitudinal seams The sections are then joined by circular seams to form the vessel
4) Pressure vessels are also produced by submerged arc welding The vessel wall is constructed together with flange and bottom by deposit welding onto a thinner tube Vessels of any shape can be produced in this way

2 2 Multiwall Vessels

Multiwall vessels are suitable for all types of pressure vessels in particular those with large diameters lengths and wall thicknesses Thermal conduction through the wall is lower than that for solid wall vessels so that heating and cooling rates must be taken into account The type of joint between the wall elements is used as the distinguishing feature

2 2 1 Designs with a Purely Mechanical Joint

Multiwall vessels can be produced by shrinking one or more seamlessly forged cylinders onto a core shell The difference required between the outer diameter of the smaller cylinder and the inner diameter of the larger cylinder must be precalculated Before being shrunk the larger cylinder is heated and the smaller may be cooled

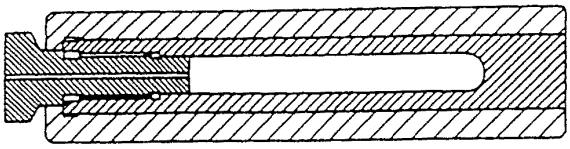

Figure 1 Two layer shrunk autoclave for 10 000 bar

During the shrinking on process initial compressive stresses are produced in the smaller cylinder and initial tensile stresses in the larger cylinder both in the circumferential and longitudinal directions

Nowadays this process is applied only in special cases for example for compressor cylinders or for vessels used in batch processing at pressures exceeding 2000 bar Figure 1 shows an example

Figure 2 shows a pressure vessel produced by the BASF Schierenbeck strip-winding process In this process a profiled steel strip is heated to 650–950 °C and helically wound onto a core tube The strip is cooled and annealed by blowing on air and shrinks at high tension onto the underlying strip layers The strip layers are joined to one another and to the core tube by profiled grooves so that apart from the circumferential stresses they are also able to absorb longitudinal stresses produced by the internal pressure The end pieces are produced from forging ingots and are joined to the cylindrical shell by overwinding The flanges are wound from the same profiled strip and the threaded bores for the cover bolts can then be drilled directly into the wound flange

2 2 2 Welded Designs (Layered-Wall Vessels)

Welded designs consist of sheets which are welded together to form a shell Figure 3 shows widely used manufacturing processes for layered wall vessels

Multiwall Design Tubes having different precalculated diameters are produced from 25–50 mm thick sheets welded with longitudinal seams These tubes are shrunk on top of one another without prior machining to produce individual shell sections These are joined to one another and to the forged end pieces and flanges by circular seams

Multilayer Design Half shells formed from 6–22 mm thick sheets are applied to the core tube which is seamless or welded by a longitudinal seam The shells are joined to one another and to the underlying layer by two longitudinal seams (three sheet seams) The half shells are tangentially prestressed by the welding contraction Uniform distribution of the welds around the circumference is achieved by offsetting the longitudinal seams from layer to layer When

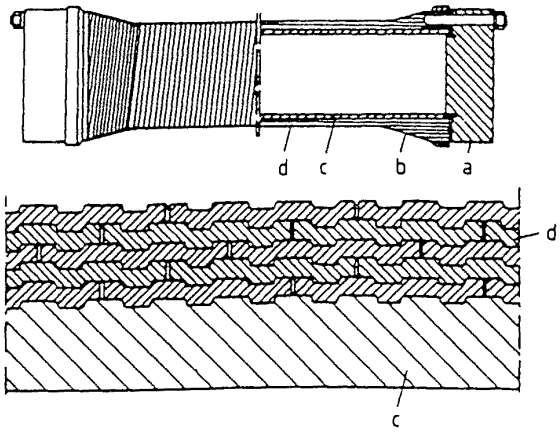

Figure 2 Pressure vessel produced by the BASF strip winding process showing a sectional view of the wound wall
a) Cover b) Strip-wound flange c) Core tube d) Strip wound vessel wall

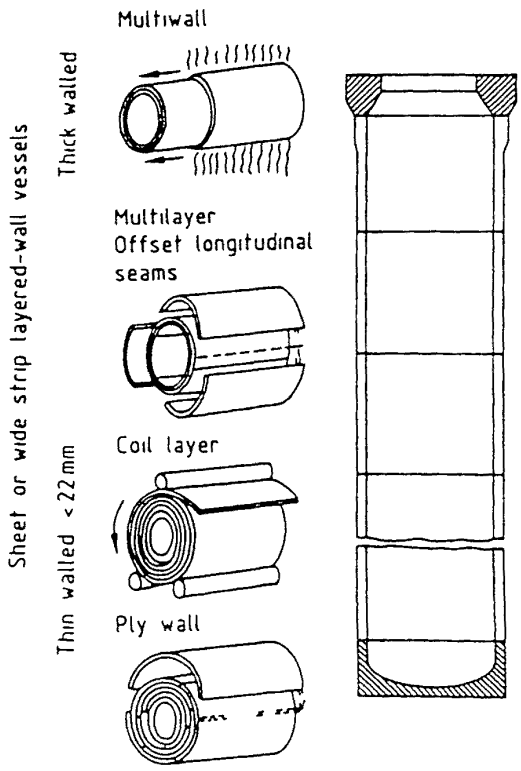

Figure 3 Various designs of layered wall vessels [2 6]

larger diameters are required three or four sheet segments are arranged on the circumference instead of half shells The individual sections are joined to one another by circular seams

Coil Layer Design The shell is produced by spirally winding a 3–5 mm thick sheet strip onto the core tube The outer shell is applied after completion of the winding The beginning and end of the winding require wedges Longitudinal seam welds are made at the beginning and end or whenever a sufficiently long strip is not available

Plate Wall Design This design is a combination of the coil layer and multilayer designs the spiral construction of the shell section is combined with three sheet longitudinal weld seams

2 3 Strength Calculations

2 3 1 Cylindrical Wall

2 3 1 1 Stresses Due to Internal Pressure

The stresses generated by internal pressure in a cylindrical body with the outer to inner diameter ratio $u = d_o/d_i$ are listed in Table 3

Figure 4 shows the stresses produced by internal pressure in a cylinder with $u = 2$ The stress is substantially higher on the inner than on the outer wall The differences between the inside and outside increase with the square of the diameter ratio This means that with thick walled vessels the material is only partly exploited if a safety margin of for example 1 5 with respect to the tensile yield strength is maintained on the inside of the wall The unfavorable stress distribution over the wall thickness can be improved by appropriate design methods (shrink joints) it can be altered by using an increased test pressure (autofrettage) or it can be ignored by selecting a different computational method (complete plastic yielding)

Selection of the operating pressure depends on the safety margin with respect to the pressure at which the vessel is deformed to an impermissible degree or bursts When pressure is increased in a thick walled vessel the wall expands elastically in a uniform manner until the stress at the inside of the wall is equal to the tensile yield strength of the material With further pressure increase the outside of the wall continues to expand elastically whereas the inside the wall is increasingly deformed plastically Once the plastic deformation has reached the outside of the wall as well so called complete plastic yielding occurs

In the computation according to the GE hypothesis (v Mises) plastic deformation begins on the inside of the wall if

$$p_{el} = \sigma_{0\,2}\,\frac{u^2 - 1}{u^2\sqrt{3}} \qquad (1)$$

Table 3 Stresses and loads due to internal pressure p (N/mm²) in a closed hollow cylinder*

Property		Inside	Outside
Tangential stress	σ_t	$= p\,\frac{u^2+1}{u^2-1}$	$p\,\frac{2}{u^2-1}$
Longitudinal stress	σ_l	$= p\,\frac{1}{u^2-1}$	$p\,\frac{1}{u^2-1}$
Radial stress	σ	$= -p$	0
Stress according to the GE hypothesis	σ	$= p\,\frac{u^2\sqrt{3}}{u^2-1}$	$p\,\frac{\sqrt{3}}{u^2-1}$
Stress according to the shear stress hypothesis	σ_d	$= p\,\frac{2u^2}{u^2-1}$	$p\,\frac{2}{u^2-1}$

p = internal pressure in N/mm² u = diameter ratio d_o/d_i

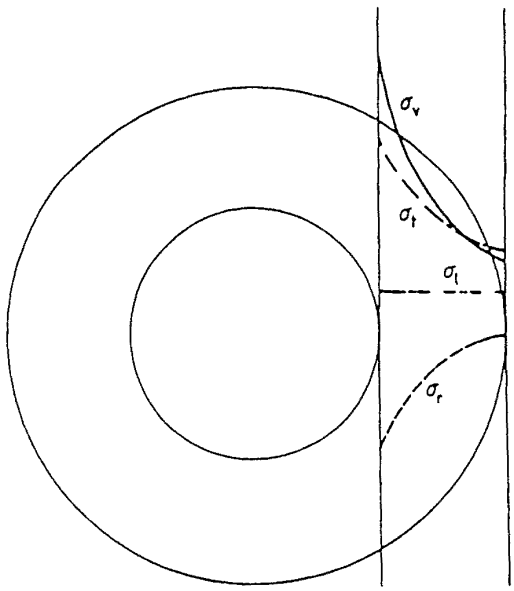

Figure 4 Stress components in a thick walled hollow cylinder under internal pressure
σ_t = tangential stress σ = radial stress σ_l = longitudinal stress σ = stress intensity

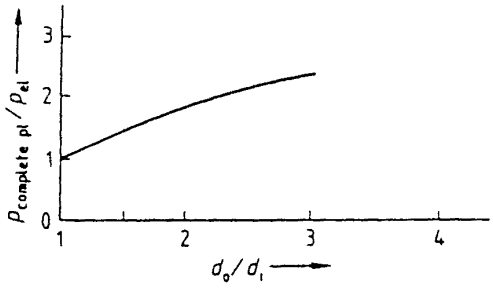

Figure 5 Ratio of complete plastic yielding to plastic deformation as a function of the diameter ratio

and complete plastic yielding is reached when

$$p_{complete\ pl} = d_{0\,2}\frac{2}{\sqrt{3}}\ln u \qquad (2)$$

where $\sigma_{0\,2}$ is the 0 2% proof strength

Figure 5 shows the ratio $p_{complete\ pl}/p_{el}$ as a function of the diameter ratio u Thus the material of thick walled vessels is more fully exploited if complete plastic yielding is used as the design limit

An ASME (American Society of Mechanical Engineers) committee is preparing a new code for calculating high pressure vessels (Sect VIII Div 3) It uses the type of calculation presented above and selects a safety factor of $S = 2$ relative to complete plastic yielding according to the GE hypothesis or $S = 1\ 732$ with respect to complete plastic yielding according to the shear stress hypothesis The permissible internal pressure is thus

$$p = \sigma_{0\,2}\frac{1}{1\ 732}\ln u \qquad (3)$$

The following points must also be considered

1) The stress must not exceed the tensile yield strength at any point
2) The fatigue strength must be taken into account
3) Brittle fracture must not occur

Initial stresses for example caused by shrinking or autofrettage may also be considered in these calculations

2 3 1 2 Initial Stresses in Shrink Joints

The unfavorably high tangential stresses on the inside of the wall can be substantially reduced if two or more cylinders are shrunk onto one another Shrink joints are generally produced by heating the outer cylinder prior to joining However it is also possible to press conical cylinders onto one another In order to calculate the initial stresses generated by shrinking it is important to make an exact measurement of the diameter at the joint surface before shrinking takes place

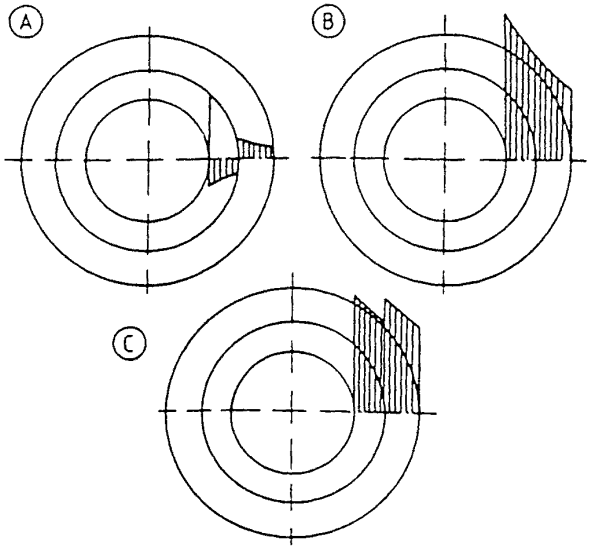

Figure 6 Tangential stress in two layer shrink vessels A) After shrinking B) Due to internal pressure alone C) Tangential stress resulting from shrinkage and internal pressure

The shrinkage should be selected such that at operating pressure the inner and outer cylinders have the same safety margin with respect to the tensile yield strength or the fatigue strength

Figure 6 shows the tangential stresses after shrinking and due to the internal pressure

2 3 1 3 Residual Stresses Due to Autofrettage

Autofrettage can be used to generate a favorable stress distribution in the vessel wall A higher internal pressure causes the material on the inside of a thick walled vessel to flow while the outside is only elastically expanded The pressure is released after part of the wall or even the entire wall has been plastically deformed The material in the vicinity of the inside of the wall is strongly plastically deformed in the autofrettage process and tends to remain deformed The material near the outside of the wall is least deformed or may not be deformed at all and therefore tends to return to its original shape As

a result tangential residual stresses are produced as compressive stress on the inside of the wall and as tensile stress on the outside they vary nonuniformly over the wall thickness The residual compressive stresses on the inside of the wall later counteract the tangential stresses produced by the internal pressure The result is that with pulsating pressure there is a reduction in the mean stress which increases service life

The risk of brittle fracture is also reduced by autofrettage since the stress intensity factor at a crack tip or a cracklike inclusion is lowered This slows down crack growth and increases the critical crack depth

The residual stresses obtained by autofrettage can be computed according to ASME Section VIII/3 three methods are used

1) Measurement of the mean tangential expansion at the outside of the wall at the maximum autofrettage pressure
2) Measurement of the mean residual expansion at the inside of the wall

When calculating the load the initial stresses can be superimposed on the other stresses The first step is thus to add together the individual stresses in each of the three main axes from which the load can then be calculated

Autofrettage pressure is often selected so that ca 30% of the wall thickness is plastically deformed Figure 7 shows the tangential stress occurring in a pipe after autofrettage and the stress resulting from autofrettage and internal pressure

2 3 1 4 Thermal Stresses

When pressure vessels are operated at constant temperature thermal stresses do not generally need to be taken into account If however the vessel is heated or cooled under internal pressure the stress on the vessel wall can increase considerably Thermal stress must be taken into account when heating occurs from outside through the wall or when the vessel wall is cooled by the contents

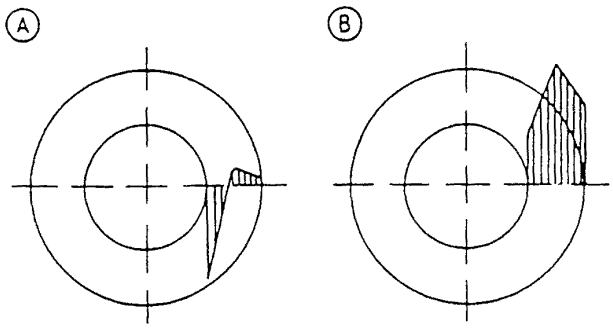

Figure 7 Tangential stress in vessels treated by autofrettage
A) After autofrettage B) Tangential stress resulting from autofrettage and internal pressure

2 3 1 5 Avoiding Brittle Fracture

Brittle fracture is a type of failure in which a crack present in a part subjected to tensile stresses spreads suddenly and without plastic deformation and thus destroys the component

The tendency to brittle fracture is increased by

1) High tensile strength of the material and thus low toughness
2) Low temperature and thus low toughness
3) Large tensile stresses
4) Large wall thickness
5) Unfavorable design (peak stresses)
6) Corrosion

The calculation of the critical crack length in vessels under internal pressure is difficult since steep stress gradients are present at the risk sites and high internal pressure at the crack tip has a substantial influence on brittle fracture behavior In the case of the steels that are usually used this calculation is generally only necessary for large vessels in which the operating pressure exceeds 1000 bar

2 3 2 Cylindrical Wall with Radial Bore

Radial bores are used for thermal measurements and pipe connections

Stresses Due to Internal Pressure In the region where the bore penetrates the inside of the cylinder the internal pressure produces a stress which is approximately three times that on the intact cylinder wall This site is therefore often the starting point for fatigue cracks The risk of cracks can be reduced by rounding off and polishing the edges

Residual Stresses as a Result of Test Pressure or Autofrettage Even at relatively low pressure the tensile yield strength is exceeded at the point of penetration As a result an autofrettage effect can often be achieved in this region during pressure testing As an example a residual compressive stress of 0 5 times the tensile yield strength is generated for a diameter ratio u of 2 25 at the

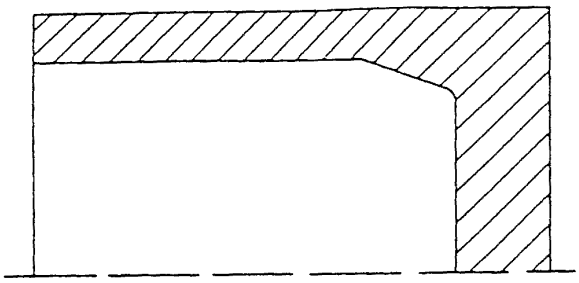

Figure 8 Favorably shaped conical transition from cylinder to end plate

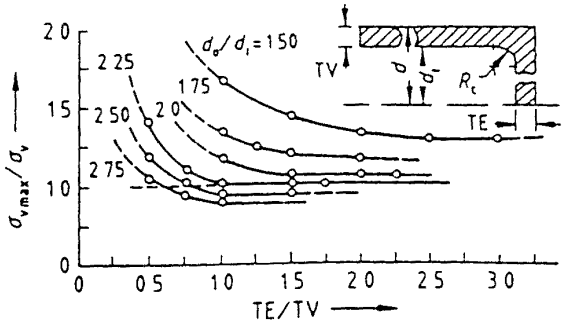

Figure 9 Ratio σ_m/σ at the radius of transition from cylinder to end plate according to [2.2] (only if $R_c/TV = 0.25$)

point of penetration if the inside of the wall of the intact cylinder has been loaded up to the tensile yield strength during pressure testing

2.3.3 End Pieces

As a rule end pieces that are forged or welded on are constructed either as hemispherical or flat plates *Hemispherical end plates* require a wall thickness of approximately 60% of the cylinder wall They ensure good distribution of stress at the transition from the hemisphere to the cylinder A *flat end plate* is frequently chosen for production engineering reasons High stresses which are strongly influenced by the form of the transition from cylinder to end plate are produced at the transition from the flat plate to the cylinder wall In the case of a favorably shaped conical transition (Fig 8) the load is only slightly higher than in the cylindrical wall

The shape factor σ_{max}/σ is shown in Figure 9 for a wall thickness ratio $d_o/d_i > 1.5$ and applies only if the transition radius is one quarter of the wall thickness ($R_c/TV = 0.25$) The stress can be reduced only slightly by using a larger radius

2.4 Corrosion in High-Pressure Plant

Only those types of corrosion which are influenced by high pressure are dealt with in this chapter

Hydrogen Attack at Elevated Temperatures (→ Corrosion B1 pp 8.37–8-39) The action of molecular hydrogen at high pressure on steels must be considered in a number of high-pressure processes e g hydrogenation and ammonia production At elevated temperatures (> 200 °C)

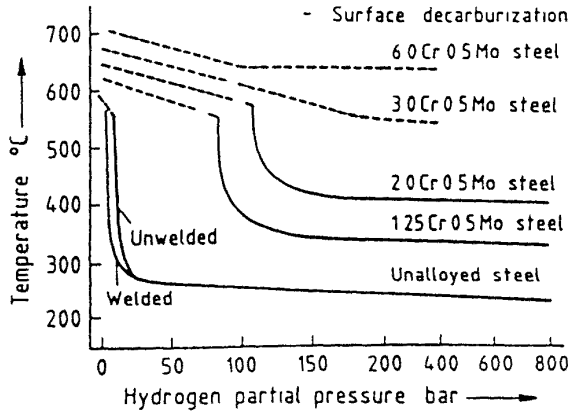

Figure 10 Resistance limits for the attack of pressurized hydrogen on steels (Nelson diagram)

and under pressure hydrogen tends to decarburize carbon steels which causes embrittlement and deterioration of the mechanical properties Hydrogen attack can be prevented by using carbon binding alloying elements such as chromium molybdenum vanadium, and tungsten The hydrogen-resistant steels used nowadays contain 2–6% Cr 0.2–0.6% Mo and a few types are additionally alloyed with up to 0.86% V and 0.45% W Figure 10 shows the resistance limits for different steels

Corrosion by Carbon Monoxide (→ Corrosion B1 pp 8-47–8-49) Carbon monoxide under pressure attacks unalloyed and low alloy steels at 130–140 °C with formation of iron pentacarbonyl Attack virtually ceases above 350 C With high alloy chromium and chromium–nickel steels the damage is significantly less Chromium steels with 30% Cr and austenitic steels with 25% Cr and 20% Ni are completely resistant If the iron pentacarbonyl is entrained

in a synthesis cycle it may decompose exothermically at a higher temperature with the formation of active pyrophoric iron

Nitriding by Ammonia (→ Corrosion B 1 pp 8-47–8 49) At temperatures above 250 °C ammonia forms a nitride layer on steels and embrittles the underlying material Welding is then difficult owing to the nitrogen enrichment and these parts are often irreparable after lengthy operating times Apart from Armco iron austenitic steels are the least subject to attack Although a nitride layer does form with austenitic steels above 350 °C no loss of material occurs because this layer does not flake off This layer must be ground off before repair welding but the welding properties of the base material are not affected

2 5 Material Selection

Low alloy steels (as specified in e g DIN 17200) are generally used for the load-bearing wall of pressure vessels In the case of relatively thick walls good annealing characteristics and good toughness are important Wall temperatures exceeding 350 °C may produce temperature embrittlement which can be reduced by limiting the content of impurities (S P Zn As) Hydrogen resistant materials are necessary at temperatures above 200 °C with hydrogen containing media It is generally necessary to use high strength steels at operating pressures above 2000 bar Since elongation at rupture and toughness decrease with increasing strength good toughness is particularly important with these steels Fracture mechanical investigations are advisable if these steels are used for wall thicknesses exceeding 150 mm

Some typical steels for high pressure vessels and piping are listed in Table 4

Table 4 Steels used for high pressure applications

Type of steel	Material no	Uses
10 CrMo910	1 7380	for forgings and pipes to prevent hydrogen attack above 200 C
12 CrMo910		for forgings and pipes to prevent hydrogen attack above 200 C
24 CrMo5	1 7258	for covers flanges bolts
21 CrMoV57	1 7709	for forgings at high temperatures not hydrogen resistant
30 CrNiMo8	1 6580	pipes forgings at pressures above 1000 bar
24 CrMo10	1 7273	forgings to prevent hydrogen attack above 200 C
20 CrMoV135	1 7779	pipes forgings to prevent hydrogen attack above 200 C
X20 CrMoV121	1 4922	pipes and forgings to prevent hydrogen attack above 450 C

2 6 Design Details

2 6 1 Corrosion Protection

The types of corrosion that are specifically intensified by high pressure are described in Section 2 4 Apart from these there are other types of corrosive attack that are independent of pressure

Vessel Walls Made from Corrosion-Resistant Material This is the simplest corrosion protection method but it is only possible in a few cases because of cost reasons In the case of hydrogen attack the wall can be protected by using the alloying elements Mo Cr Ni and V Multilayer vessels are advantageous since they require hydrogen resistant steel only for the inner layer The other layers need not be hydrogen resistant if design (e g , venting channels) ensures that hydrogen diffusing through the inner layer is drawn off

Cladding Abrasion can be prevented by roll-bonding cladding or weld overlay cladding However this type of protection is often not possible with the steels and wall thicknesses used for high pressure vessels An advantage of this method is that the cladding materials (e g austenitic steel) often have a different thermal expansion than the vessel wall This leads to thermal stresses in the cladding during heating and cooling If the cladding is joined solidly to the vessel wall the expansion of the base material is imposed on every part of the cladding The thermal stresses are therefore equal in all parts of the cladding

Disadvantages of this method include

1) The base material is attacked if the cladding is damaged at any point and the damage often cannot be detected in time

2) In weld overlay cladding the solidifying melt forms columnar crystals perpendicular to the wall surface Along the grain boundary of these crystals the corrosion resistance is lower than in the rolled material In the case of heavy corrosion at least a two layer weld overlay cladding should therefore be selected
3) Cladding does not protect against hydrogen attack since hydrogen diffuses through the cladding to the base material

Lining With loose linings the tightness can be monitored during operation For this purpose the space between the lining and the pressure bearing wall is monitored by means of venting holes The lining must be attached to the pressure bearing wall in such a way that different thermal expansion cannot produce a displacement between the lining and the vessel wall

An advantage over cladding is that the lining can be checked for leaks at any time Disadvantages of this method compared to cladding include

1) Given large differences in thermal expansion or an unsuitable attachment to the pressure-bearing wall the expansions can be concentrated on the weakest point and cause damage there
2) The joining of a nozzle lining to the lining of the vessel can be a weak spot

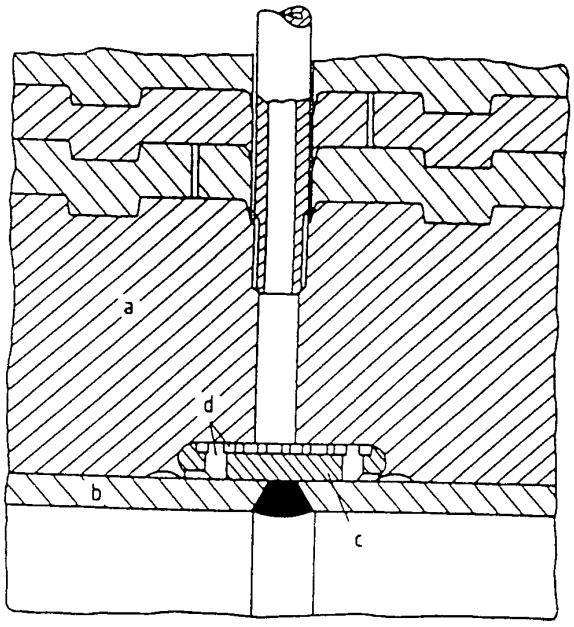

Figure 11 Titanium lining in a pressure vessel attached in the axial direction by mortised titanium strips
a) Core tube of a multilayer vessel or vessel wall b) Titanium sheet c) Titanium strip with grooves d) Bores for blanketing gas and leakage monitoring

Figure 11 shows the attachment of a loose titanium lining by means of mortised titanium strips The venting hole through the vessel wall is used to introduce the protective gas

Floating Bladders The floating bladder principle is used under extreme corrosion conditions The balloon is made from an alloy that is resistant to the extremely aggressive medium and is surrounded by pressurized water so that the internal pressure of the balloon and the pressure of the water surrounding it are virtually identical (see Fig 12)

An advantage of this method is that the high pressure shell and the high pressure seals are not

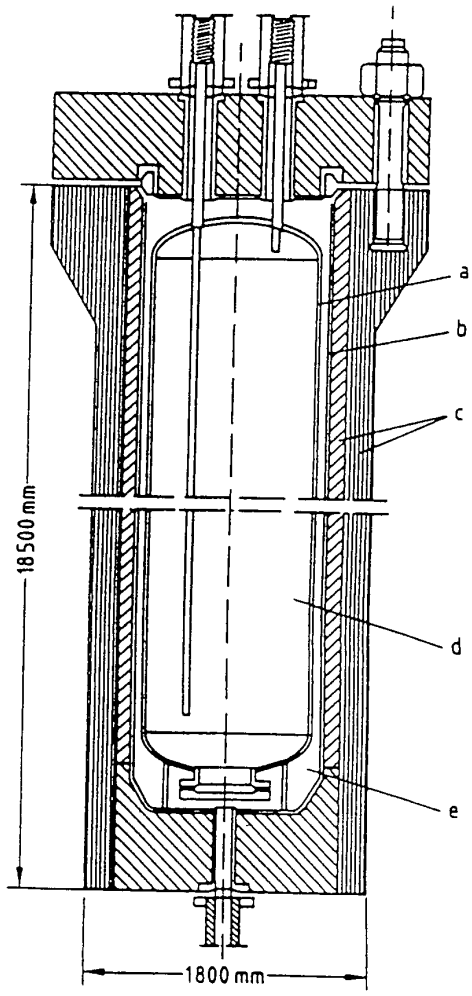

Figure 12. Pressure vessel with internal bladder of highly corrosion resistant material
a) Internal bladder of highly corrosion resistant material
b) Austenitic steel lining c) BASF Schierenbeck multilayer vessel (low alloy steel) d) Highly corrosive medium (pressure p) e) Water (pressure p_w monitored by chemical analysis) $p_w = p + 2$ bar

directly exposed to the aggressive medium Leaks in the bladder can be detected by chemical monitoring of the pressurized water A disadvantage of this method is that the required pressure equalization between the balloon and the pressurized water space necessitates additional outlay on piping measuring instruments and balancing tanks

2 6 2 Covers and Their Attachment

The most commonly used types of closure are shown in Figure 13

The *cover seals* (Fig 13 A–E) are attached by means of threaded bolts and are used for all diameters and pressure ranges The bolts are generally tightened hydraulically or pneumatically It is however also possible to prestress the bolts longitudinally and then to tighten the nuts

In the *Bredtschneider seal* (Fig 13 F) the force acting on the cover due to the internal pressure is led via the sealing ring (a) onto the split ring (b) which is supported in the groove of the shell This design requires only small bolts which bring the cover and sealing ring together in the pressureless state

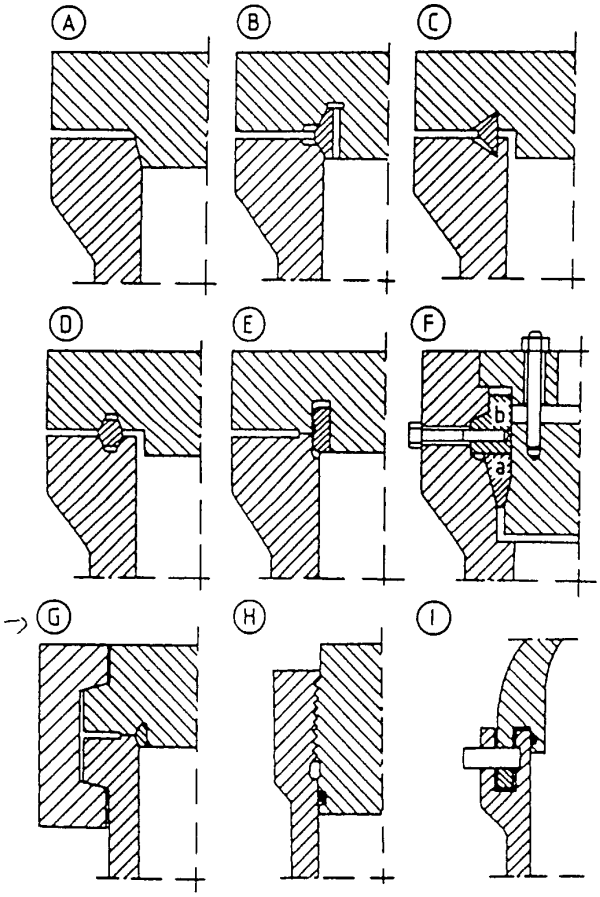

Figure 13 Forms of cover and forms of seals (see text for explanation)

The *clamp seal* (Fig 13 G) permits rapid opening and closing of the pressure vessel The two or three part clamp is pushed over the collar on the cover and vessel and fixed The elastic seal is pressed onto the sealing surface by the internal pressure It is easy to automate the closing process which is why this joint is frequently used for batch processing e g in extraction with supercritical gases

Screwed in covers (Fig 13 H) are used for smaller inner diameters The Hahn and Clay *finger pin seal* (Fig 13 I) is suitable for large diameters An elastomeric seal is necessary Opening and closing can easily be automated

2 6 3 Cover Seals

Metal seals are usually necessary as cover seals in chemical high pressure plants The single cone (Fig 13 A) with a conical slope of 10° is chiefly used for cover openings of up to 800 mm diameter and pressures up to 400 bar The double cone ring (Fig 13 B) with a conical slope of 30° is more complicated than the single cone and is used for cover openings larger than 500 mm and pressures up to 700 bar The delta ring (Fig 13 C) and the RTJ ring (Fig 13 D) can be regarded as smaller versions of the double cone ring The wave ring seal (Fig 13 E) is pressed by the internal pressure against the cylinder sealing surfaces and is plastically deformed in the process This is a special seal for stirred tank polyethylene reactors where they are used up to 300 °C and 2500 bar Flat sealing rings and metallic O rings are seldom used in chemical plants

2 6 4 Seals for Piping

These seals are used for substantially smaller diameters than the cover seals For cost reasons the aim is to have simple shapes which can also be replaced easily Larger tightening forces during assembly are then acceptable

Figure 14 shows the most common designs for piping seals The lens ring seal (Fig 14 A) is used in Europe for pressures up to 4000 bar The conical ring seal (Fig 14 B) is the most widely used in the United States for pressures from 1000

to 2000 bar The Grey lock seal (Fig 14C) is used in the United States predominantly for pressures up to 2000 bar The ring joint seal (Fig 14D) can be used for pressures up to 200 bar and temperatures up to 700 °C The conical seal with cap nut (Fig 14E) can be used for small nominal pipe sizes and pressures of up to 6000 bar Flat seals (Fig 14F) are rarely used in high pressure plants

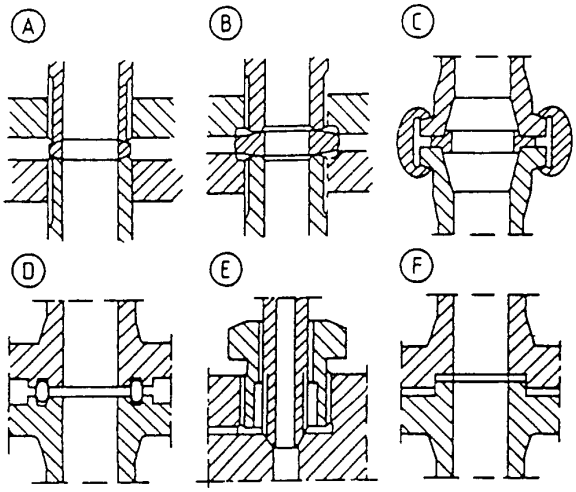

Figure 14 Seals for high pressure piping (see text for explanation)

2 7 Example of the Design of Pressure Vessels

Figure 15 shows the upper part of a reactor having internal cooling tubes a central high pressure connection and an inserted temperature measuring tube The reactor is lined inside with stainless steel and the cover is sealed to the vessel wall by means of a double cone seal The cooling liquid is led through the lateral branches (nominal diameter 125 mm) into the distribution chamber above the cover The liquid flows through the dip pipes to the lower end of the cooling tubes which are closed at the bottom and returns to the top around the dip pipes

Figure 16 shows the dimensions of the reactors used in ammonia plants since 1910 Even larger pressure vessels are built as hydrocrackers and desulfurization reactors which have inner diameters of 4 1 m a wall thickness of 280 mm and a total weight of 1100 t The material employed has largely been ASTM A 336 F 22 with special purity requirements These reactors generally have a stainless steel weld cladding

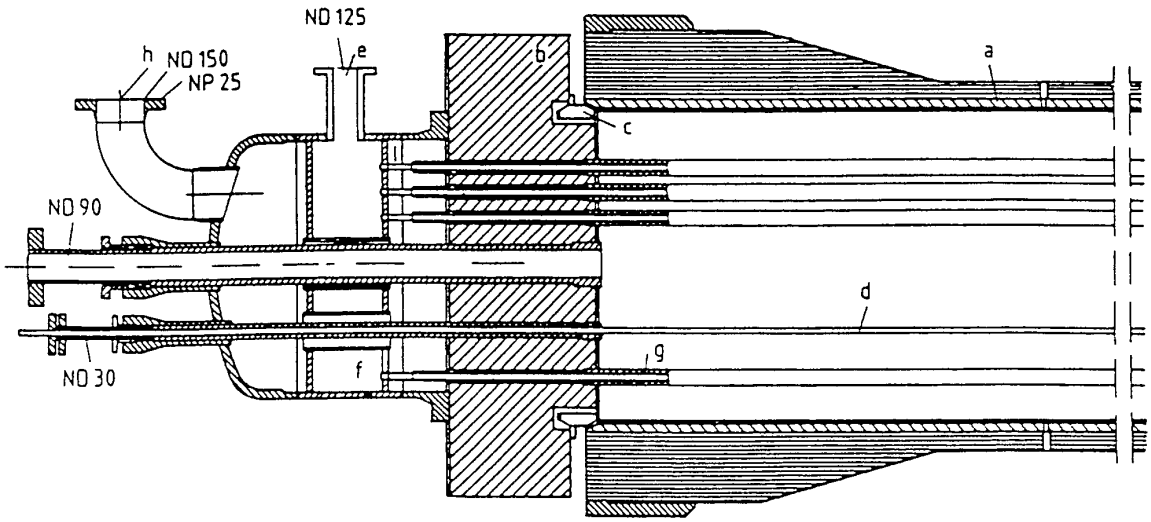

Figure 15 Reactor with internal cooling tubes
a) High pressure vessel b) Flat cover c) Double cone sealing ring d) Thermowell e) Inlet nozzle for cooling fluid f) Distribution chamber g) Field tubing for cooling h) Outlet nozzle for cooling fluid
ND = nominal diameter in millimeters NP = nominal pressure in bar

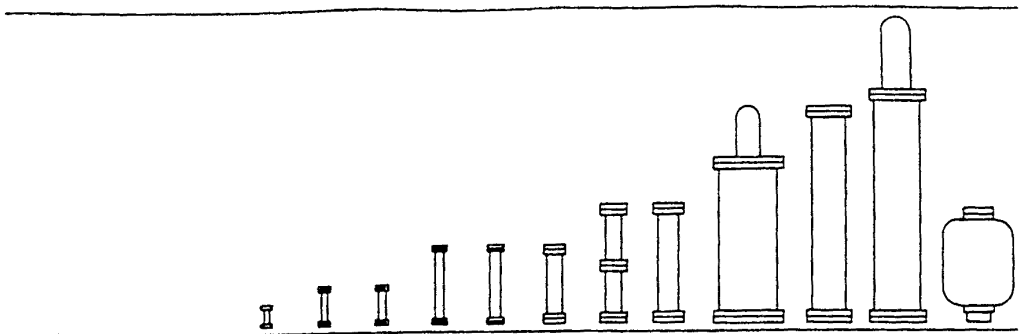

Year of fabrication	1910	1911	1912	1913	1913	1914	1915	1956	1963	1969	1972*	1982**
Inner diameter mm	90	90	160	200	300	500	800	1200	2900	2000	2400	3350
Height m	1 8	4	4	8	8	8	12	12	22	22	34	9
Weight t					3 5		65	105	270	386		190
Volume of catalyst m^3					0 09		1 1	4 85	64	36	56	53
Operating pressure bar					200		300	300	150	350	210	210
Capacity t/d					3 6-4 8		85	195	910	1200	1580	1800

*Horizontal **2 Reactors

Figure 16 Development of the dimensions of ammonia reactors since 1910 [2 16]

3 High-Pressure Machinery for Chemical Plants

Because of severe stresses it is necessary to design and fabricate high-pressure machines very carefully Experience has shown that in high-pressure processes the high pressure pumps and compressors present the greatest problems as regards lifetime and maintenance In process and production engineering high pressure is generally understood as 100–4000 bar Most important applications also fall within this range [3 1] (see Tables 1 and 2)

3 1 Special Features of High-Pressure Machines

High pressure machines are expensive to develop, produce, supply with energy and maintain Since the components are subject to high stress careful stress analysis is necessary For dynamic stresses a design with few notches and with excellent surface quality is required At points that are especially prone to risk local material properties must be improved and stress peaks must be reduced

The solution of sealing problems especially under dynamic stress, requires a great deal of experience The piston seals of reciprocating displacement pumps present special problems since these pumps overcome very high pressure differences (up to several thousand bar) in a single stage The sealing of problem fluids such as suspensions and materials with low viscosity and poor lubricating action requires special measures

In selecting materials for high pressure components special attention should be paid to high strength good isotropy homgeneity toughness and quality Apart from high strength ferritic tempering steels fabricated with special purity soft martensitic semiaustenitic, and precipitation hardened chromium–nickel steels are increasingly being used to meet corrosion resistance requirements Homogeneity is achieved by the smelting method and isotropy is achieved by forging the slugs as much as possible from all sides

For dynamic seals, all capabilities of modern materials development for plastics bronzes sintered metal carbides and layers of hard material are utilized The special material properties of fluids at high pressures e g compressibility viscosity changes density and solidification temperature must be taken into account

3 2 Creation of Pressure by Pumps and Compressors

The approximately isentropic change of state during a pressure increase (Fig 17) causes a temperature rise which is small in liquids but large in

gases This temperature rise limits the pressure ratio which can be produced by one stage in compressors The required work is generally determined by the difference of the total enthalpies For gas compressors efficiency data refer either to isothermal or isentropic changes of state which leads to considerable differences

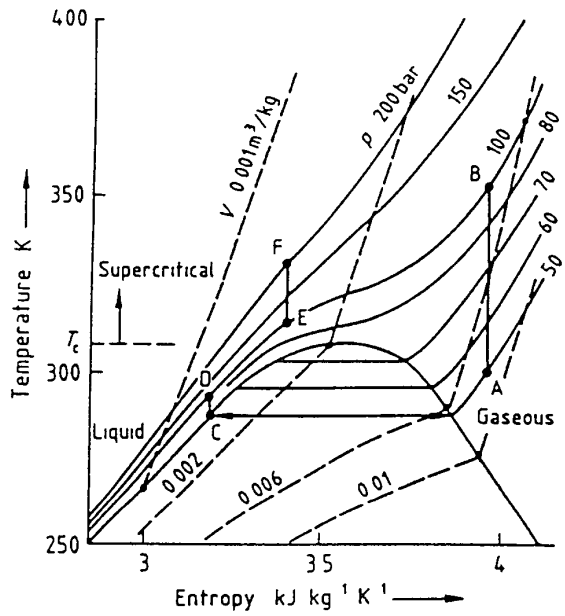

Figure 17 Isentropic change of state of carbon dioxide A–B gases C–D liquids E–F supercritical fluids

For *reciprocating piston machines* the clearance volume fluid compressibility and working space elasticity determine the volumetric efficiency (also known as the transfer or discharge level) which is a measure for the utilization of the structurally determined swept volume High pressure piston compressors require a multistage arrangement with intermediate cooling to approximate the energetically favorable isothermal change of state for economical operation The pressure ratios produced by one stage amount to 2–5 in the case of process gas compressors (Fig 18 left) By contrast piston pumps for liquids overcome very high pressure differences in a single stage because liquids are much less compressible (Fig 18 right) The fatigue of the pump component with a cyclical interior pressure [3 2] [3 3] and the lifetime of the piston seals are limiting factors

With *rotary displacement machines* e g gear pumps, interior leakage losses determine the volumetric efficiency For high pressure applications such pumps are suitable only for highly viscous fluids

When pressure is generated hydrodynamically, as in *turbomachines* (Fig 19) the circumferential velocity u of the commonly used radial impellers is very important for the pressure increase per stage $\Delta p_t = \psi \varrho u^2/2$ (where ψ is the coefficient of pressure ϱ is the fluid density) The

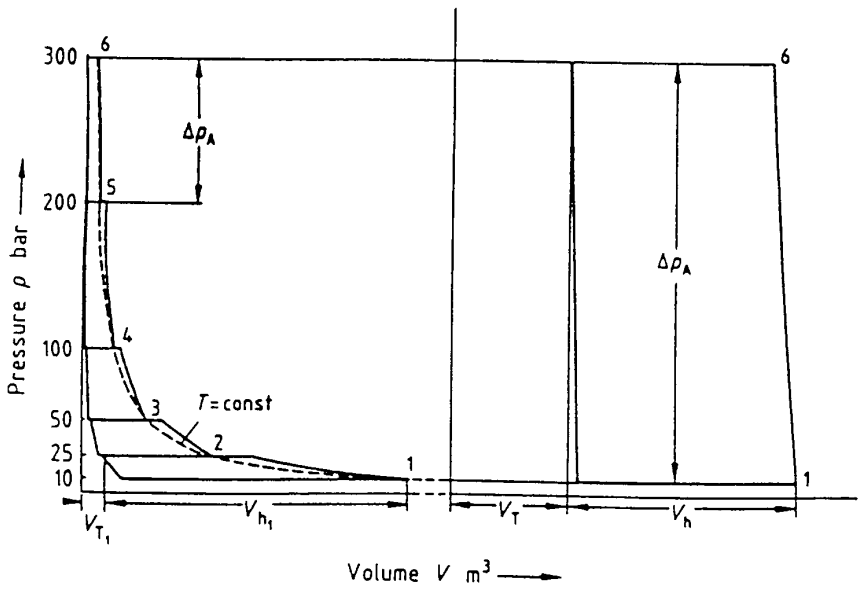

Figure 18 Gas and liquid compressor (pump) The $p-V$ diagram for a Left five stage gas compression Right single stage liquid compression
V_h = stroke volume V_T = clearance volume Δp_A = pressure increase per stage

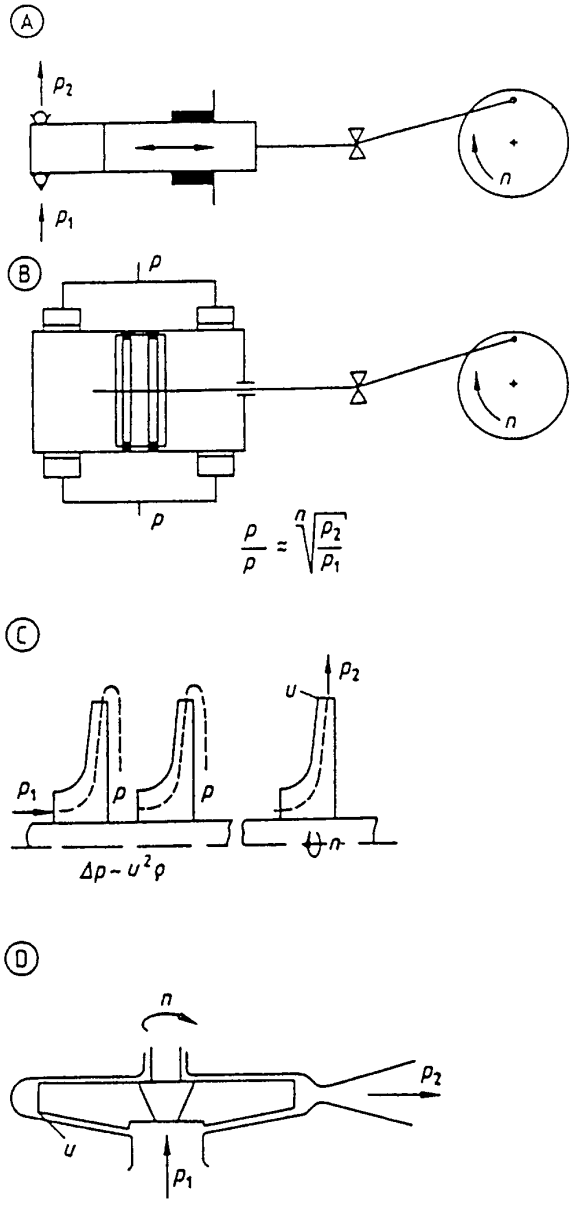

Figure 19 Principles of pressure generation
A) Single stage piston pump B) Piston compressor stage (double action) C) Multistage centrifugal pump (or turbo compressor) D) High speed (partial emission) single stage centrifugal pump

rotor stress limits the circumferential velocity for pumps to about 100–200 m/s For turbo compressors the speed of sound (ca 300–400 m/s) is the limit generally Mach numbers < 0 7 are used

Nevertheless pressure increases of 50–250 bar per stage can be achieved for liquids, depending on the power For gas compression more stages are needed than for liquid pumps because of the lower fluid density and intermediate cooling is required

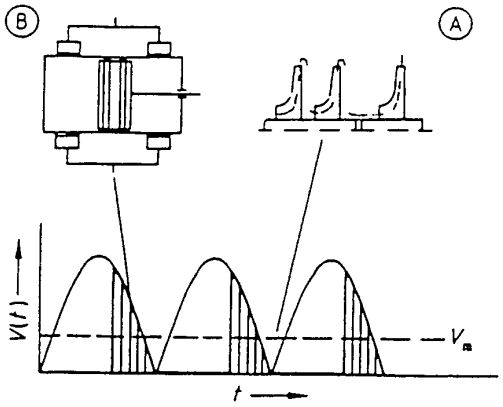

Figure 20 Time behavior of the fluid flow
a) Hydrodynamic pump or compressor b) Hydrostatic (double action) piston machine
V_m = average volume flow V (t) = time volume flow

Compared to hydrodynamic turbomachines hydrostatic displacement machines exhibit pulsation of the flow rate (Fig 20) Generally displacement machines are more efficient for comparable power, but turbomachines have the advantage of being smaller in size thus requiring less space and running quieter

3 3 Pumps

In high-pressure systems pumps are used for volumetric metering, transfer circulation and pressure maintenance Volume flow rates range from ca 1 cm^3/h to > 10^3 m^3/h The pressure range generally extends up to 300–1000 bar more rarely into the range of 1000–4000 (10000) bar (Fig 21)

The characteristic curves of pump construction types differ mainly in their pressure stiffness (the influence of pressure on flow rate) (Fig 22A) Because of their pressure elastic curve centrifugal pumps can also be regulated by throttling (Fig 22A the operating point shifts from A to B) Regulation of the rotational speed is more favorable energetically (Fig 22A the operating point shifts from A to B) Bypass regulation in which part of the pump s flow rate is recycled to suction through a regulation valve is also customary for large machines and low energy costs Displacement machines have pressure stiff characteristic curves they thus impress their flow rate on the pumping system (Fig 22A lines d and e) As a rule the flow rate depends approximately linearly on the regulated variables (rotational speed n, stroke length h)

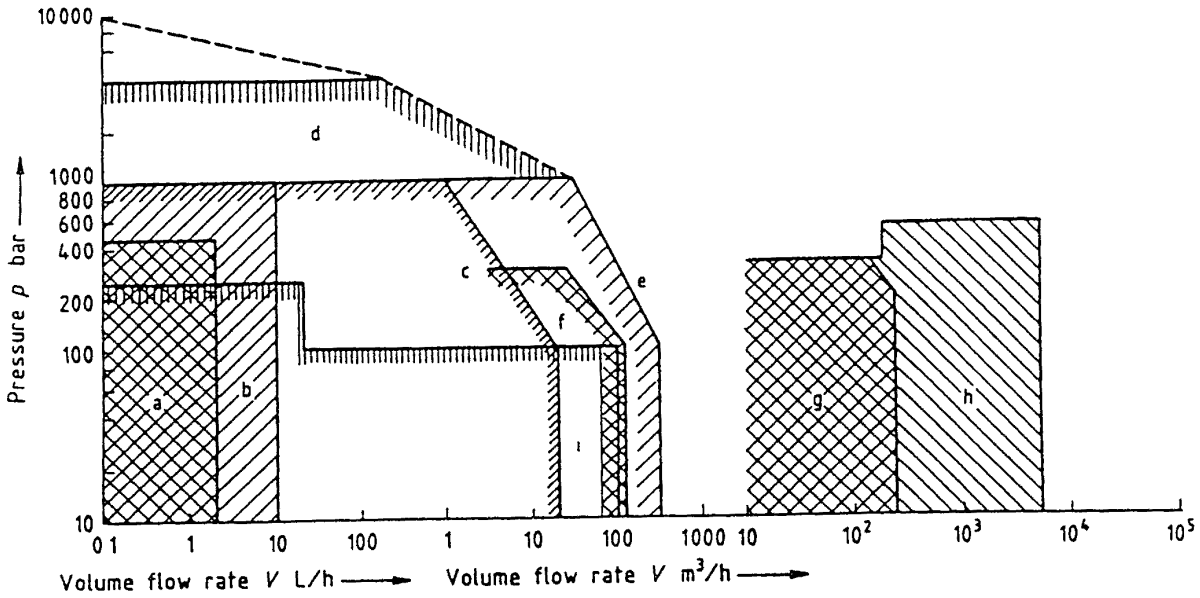

Figure 21 Power range of various types of high pressure pumps
a) Micrometering pumps (piston diaphragm gear spinning pumps) b) Metering pumps for laboratory and pilot systems (piston diaphragm/hydraulic) c) Metering pumps (piston diaphragm/hydraulic) d) Ultrahigh pressure piston pump e) Multicylinder piston pump f) Multicylinder diaphragm pump g) Centrifugal pumps (high speed single /two stage) h) Centrifugal pumps (multistage) i) Rotating displacement pumps (gear spindle)

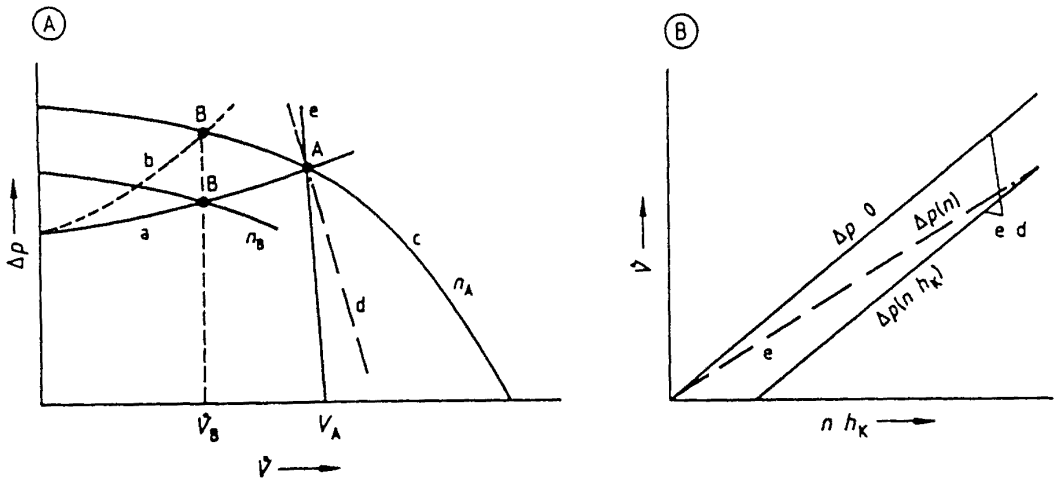

Figure 22 Characteristic curves for various types of pumps
A) Pump in the system throttle/rpm regulation of centrifugal pumps B) Regulation characteristics of displacement pumps
a) b) Characteristic curve for the system c) centrifugal pumps d) rotating displacement pumps e) reciprocating displacement pumps
V = fluid flow Δp = pressure difference n = rpm h_K = stroke length A B B = operating points

carrera

(Fig 22 B) With reciprocating displacement pumps the high differential pressure shifts the characteristic curve from the origin due to elasticity effects of the working space and the fluid [3 4] The same applies to rotary displacement pumps at higher pressure differences due to interior clearance leakages With rotational speed n_0 (e g gear pump) and stroke length h_0 (e g reciprocating metering pump) the flow rate is 0 Only in the case of reciprocating displacement pumps is there proportionality between the flow rate V and the regulated variable n because the interior leakage currents tend to vanish (Fig 26 B)

desaparece

Designation		Functional principle	Displacer kinematics	Adjustment	Displacer system
Spindle drive one- and two-cylinder electro-mechanical hydraulic	a	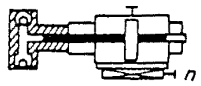	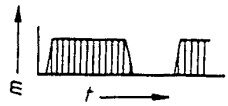	$n(h)$ $n < 30\ \mathrm{min}^{-1}$	P DH
	b	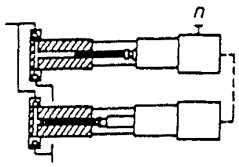			
Cam with pulsating angular velocity	c	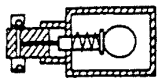 $\omega = f(t)$	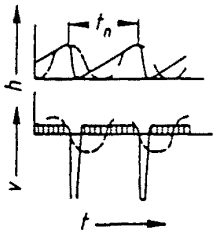	n $n < 60\ \mathrm{min}^{-1}$	P DH
Superposition drive two cylinder with cams	d	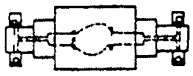	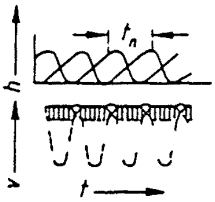	n $n < 100\ \mathrm{min}^{-1}$	P DH
Linear drive single-cylinder magnetic	e	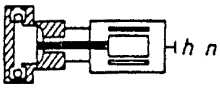	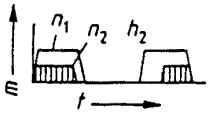	$h\ n$ $n < 100\ \mathrm{min}^{-1}$	P DH
Stroke-adjustable quasi-harmonic drive single and multi-cylinder	f	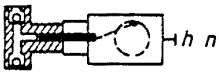	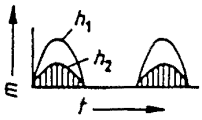	$h(n)$ $n < 350\ \mathrm{min}^{-1}$	P DH
	g		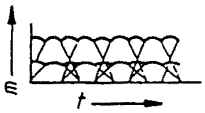		
Stroke-adjustable drive with lost motion drive	h	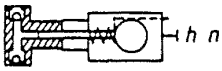	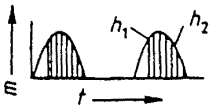	$h(n)$ $n < 150\ \mathrm{min}^{-1}$	P DH
Linear drive super- position two-cylinder hydraulic	i		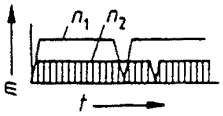	n $n < 100\ \mathrm{min}^{-1}$	P DH

Figure 23 Types of reciprocating metering pumps
P = piston pump head DH = diaphragm pump head (hydraulic)

3 3 1 Reciprocating Displacement Pumps

In high-pressure engineering reciprocating piston and diaphragm pumps are used in many variants up to pressures of 10 000 bar They may have electrical hydraulic or pneumatic linear or mechanical crank or eccentric drives and their stroke or speed may be adjustable The following sections refer to metering and transfer pumps and are oriented in terms of important applications

3 3 1 1 Metering Pumps

For very small pulsation free metering flows (e g $10-10^3$ cm^3/h) hydraulic and mechanical (spindle) linear drives are used for pressures up to several thousand bar By operating two systems in parallel these can also be operated without interruption (Fig 23a and b) [3 4] By superposing two displacement pistons or by controlling the angular velocity ω with a special cam drive small metering flows with low pulsation are achieved up to a pressure range of about 700 bar This can even be done with leak-free hydraulic diaphragm pump heads (Fig 23c and d) Such pumps are also used in HPLC analysis [3 5] [3 6] If high frequency metering flow pulsations do not interfere with the process as is the case in most applications reciprocating piston or diaphragm metering pumps with adjustable stroke and speed are used

Magnetic linear drives (Fig 23e) are distinguished by their ease of operation and their small construction size They are suitable for flow rates <1 L/h and pressures up to 500 bar with diaphragm pump heads For larger metering flows reciprocating metering pumps with an adjustable stroke and with mechanical transmissions have proved suitable These pumps can be designed with several cylinders for metering several components or to smooth out pulsations (Figs 23f and g) [3 7] The automated systems are activated by stroke actuators or by drives with variable speed

Diaphragm metering pumps with a hydraulic diaphragm drive are suitable for very high pressures Up to about 500 bar their diaphragm consists of polytetrafluoroethylene (PTFE) beyond this up to about 3000 bar it consists of metal

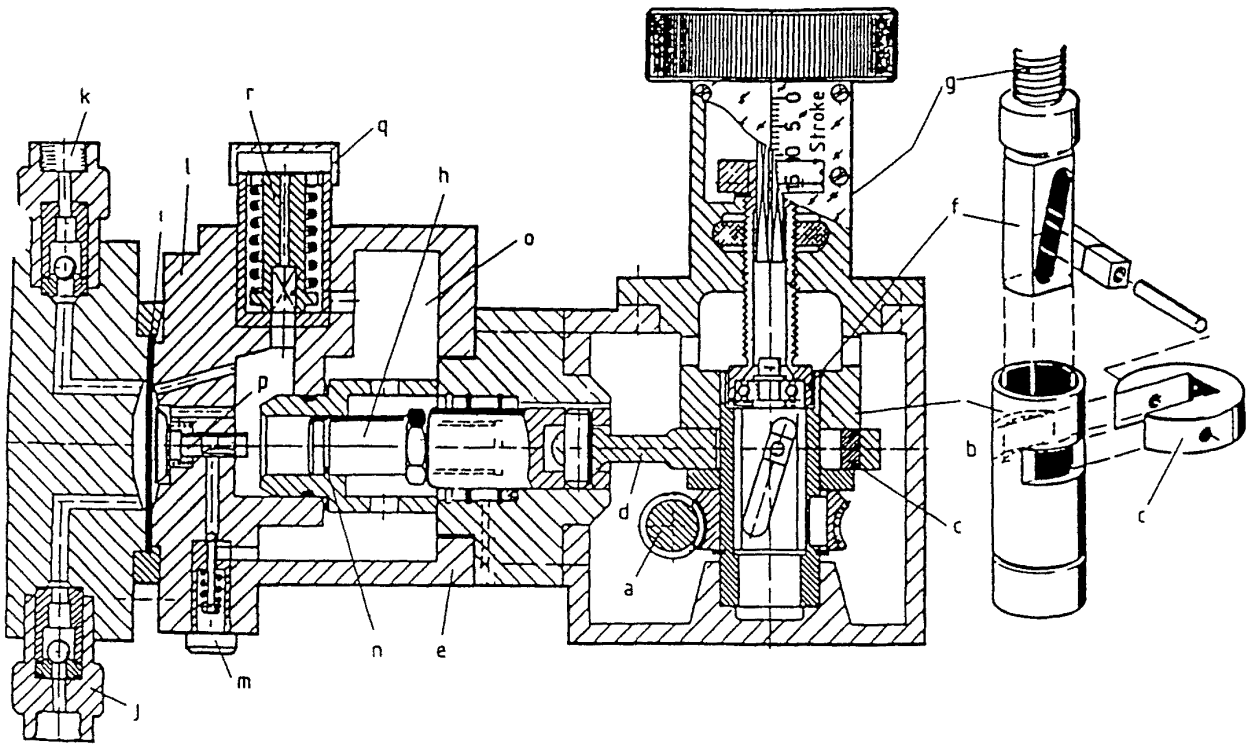

Figure 24 Diaphragm metering pump with stroke adjustment through an eccentric adjustment system (Lewa)
a) Eccentric adjustment drive h) Piston i) Diaphragm j) k) Pump valves l) Pump cylinder m) Replenishing valve n) Piston seal o) Hydraulic supply vessel p) Sliding gate q) Overflow valve r) Venting valve

(e g chromium–nickel steel) [3 7] [3 8] The leak free design operates reliably is easy to maintain presents no problems with hazardous fluids and circumvents piston sealing problems

With smaller metering flows spring loaded cam drive systems predominate because they make it possible to adjust the stroke without backlash (Fig 23h) For larger metering flows (hydraulic power up to 50 kW per metering element) all types of drive designs with adjustable stroke are in use All of these are based on the familiar conventional crank mechanism (Fig 24)

The lifetime of PTFE diaphragms which are primarily used up to 500 bar far exceeds 10000 h Diaphragm rupture can be signalled by sandwich diaphragms [3 9] [3 10], which consist of two diaphragms the space in between being connected to a pressure sensor via a check valve If one of the diaphragms ruptures the discharge pressure operates a pressure switch In normal operation the two diaphragms are connected by an adhesive intermediate fluid during suction and by direct mechanical support on one another during discharge

For very high pressures (>1500 bar) diaphragm pumps with metal diaphragms are used only for laboratory and pilot systems because they are quite sensitive to surface damage by dust particles which reduces the fatigue limit in this pressure range

The trend in the development of reciprocating high-pressure metering pumps is therefore towards diaphragm technology Exceptions are the above mentioned piston designs for HPLC analysis where extremely favorable operating conditions prevail

For process and production engineering piston metering pumps with a low frequency long stroke linear drive (Fig 25) also known as pressure converters are suitable for very high pressures (1500–4000 bar) (Fig 23i) The uni-

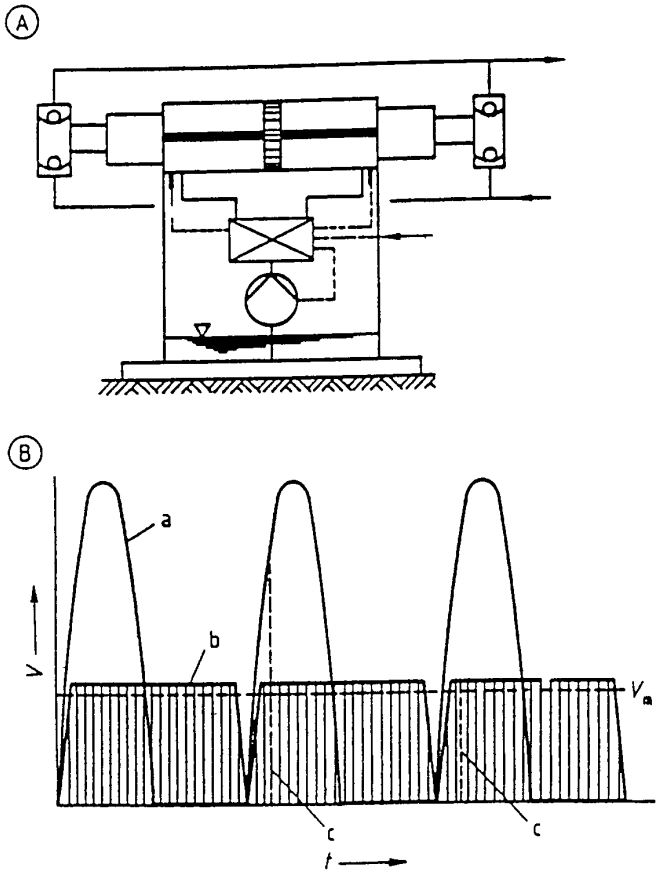

Figure 25 Superposition system with hydraulic linear drive (Uhde)
A) Principle arrangement B) Pulsation of the fluid flow
a) Single-cylinder piston pump b) Two-cylinder linear drive (as in Fig 25 A) c) Basic effect of reduced volumetric efficiency due to elasticity
V_m = average flow rate of fluid t = time

form slow piston motion leads to an operationally reliable piston seal and when two pump heads are superposed, to low pulsation of the flow rate [3 11]

For pressures of several thousand bar such as those required for metering in polyolefin production or for water jet cutting the piston heads are designed with coaxial pump valves to avoid the notch effect (see Fig 28 and Chap 3 6 1) Hydraulic pressure converter pumps can also be easily controlled at high powers for automation purposes

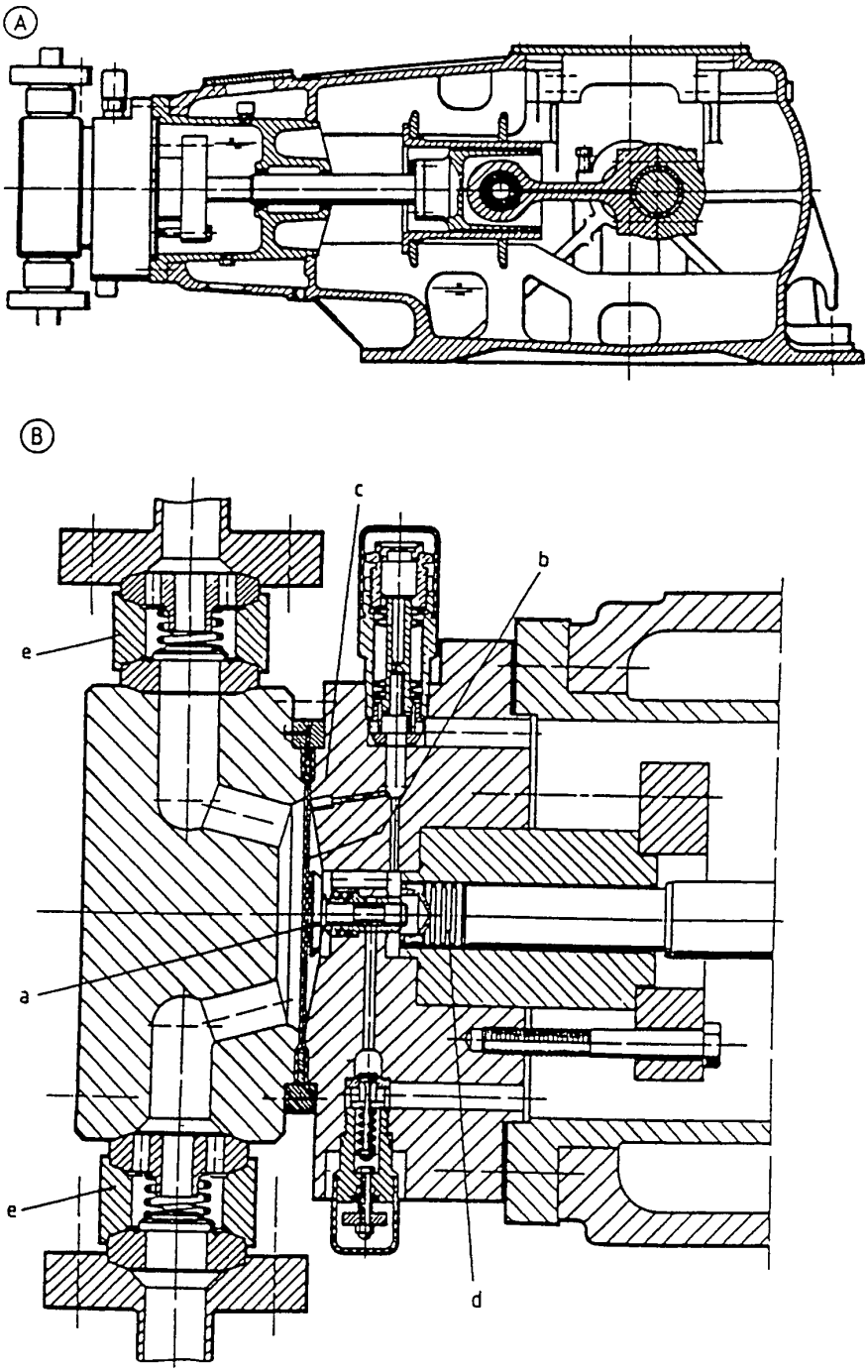

Figure 26 Process diaphragm pump for high pressure (Lewa)
A) Propulsion system with straight thrust crank drive for multihead arrangement B) Diaphragm pump head for the pressure range up to 500 bar
a) Sliding gate for controlling the position of the diaphragm b) Diaphragm (PTFE sandwich form) c) Hydraulic cylinder d) Piston with seal e) Pump valves

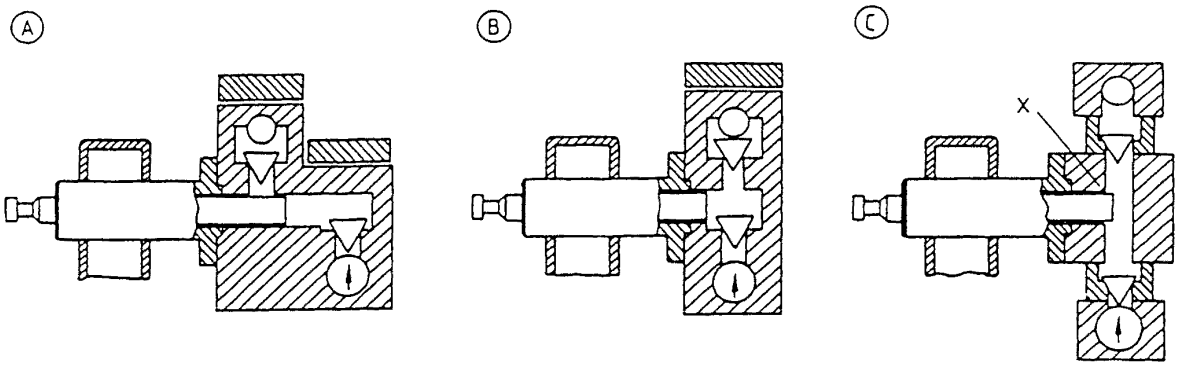

Figure 27 Monoblock and component mode of construction (URACA)
A) Monoblock valves displaced B) Monoblock valves flush C) Component mode of construction

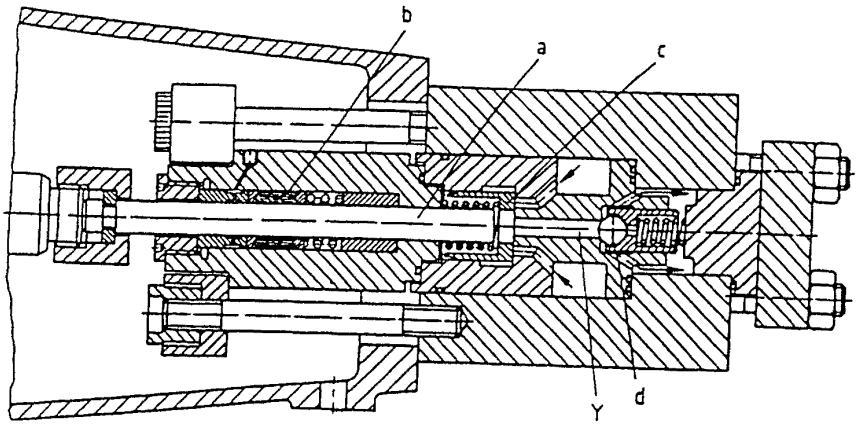

Figure 28 Coaxial arrangement of the pump valves
a) Piston b) Piston seal c) Suction valve d) Pressure valve

3 3 1 2 Transfer Pumps

In contrast to metering pumps, which generally have a single cylinder and an adjustable stroke transfer pumps are always designed with several cylinders (e g , triplex) in a multihead structure in order to smooth out pulsations in the flow rate (Fig 23 g) Powers over 1 MW are achieved in a vertical or horizontal mode of construction Piston pump heads currently still predominate Drives for multihead piston and diaphragm pumps are very similar (Fig 26 a) At high pressure and when using corrosion resistant high-strength steels the mono-block mode of construction (Fig 27 A B) is replaced by a component mode of construction (Fig 27 C) The advantage is that the parts which are most subject to fatigue can be replaced more easily Above 100–300 bar, a coaxial valve arrangement (Fig 28) is suitable because in this way the notch stresses can be reduced by at least a factor of two compared to the customary T intersection of the pump head bores (see Chap 3 6 1) Such designs can deal with differential pressures up to ca 1500 bar with long-term operational reliability Such pressures are presently required for example in high-pressure cleaning technology

Diaphragm transfer pumps in a multihead structure with powers up to about 1 MW have recently also been built for the pressure range up to 1000 bar (Fig 26 B) [3 9] [3 12] The avoidance of piston seals with fluid contact and leakages leads to remarkable operational reliability For this reason multihead diaphragm pumps are economical for hazardous fluids at high pressures as compared to multihead piston pumps despite the higher investment costs

With the development of pipeline transport of coal or ores the chemical refining of ore and coal hydrogenation high-pressure pumps are

currently being used for suspensions that are loaded with solids There are various methods to keep abrasive particles away from the piston seal e g hydraulic isolating lines sedimentation spaces and flushing systems [3 13] For predominantly aqueous abrasive slurries with a high concentration of solids multicylinder diaphragm pumps are suitable up to a pressure of 200 bar and for powers of ca 1 5 MW They generally have a four cylinder arrangement and elastomer diaphragms [3 14]

A new branch of high pressure engineering is the conveyance of materials with high consistency e g mortar concrete sludge slurries over long distances for which pressures of up to 200 bar may be necessary This can be carried out with slow hydraulic long-stroke piston displacement elements if the inlet opening of the two-cylinder arrangement is controlled with sliding switches which operate as valves [3 15]

3 3 2 Rotary Displacement Pumps

At high differential pressures rotary displacement pumps are suitable only for viscous fluids As the viscosity increases the internal sealing clearances seal better and the pump efficiency and the attainable pressure difference reach satisfactory values Gear and screw pumps are suitable for process engineering applications up to 300 bar with fluid viscosities > ca 100 mPa s Typical applications for gear pumps are the injection conveyance filtration and spinning of polymer melts (viscosities $> 10^6$ mPa s) Delivery pressures up to 450 bar occur in these applications In the case of hot and direct spinning processes the heated high-pressure gear pump with a large inlet cross section takes the polymer melt from a reactor which may be under vacuum and presses it through filters towards the gear spinning pumps whose flow rate is especially uniform and does not depend greatly on the delivery pressure Gear pumps (Fig 29) are used behind compounding extruders to increase the pressure (e g from 100 to 300 bar) and to smooth out fluctuations in the extruder output [3 16]–[3 20]

3 3 3 Centrifugal Pumps

Centrifugal pumps require high circumferential speeds and several or many stages at high

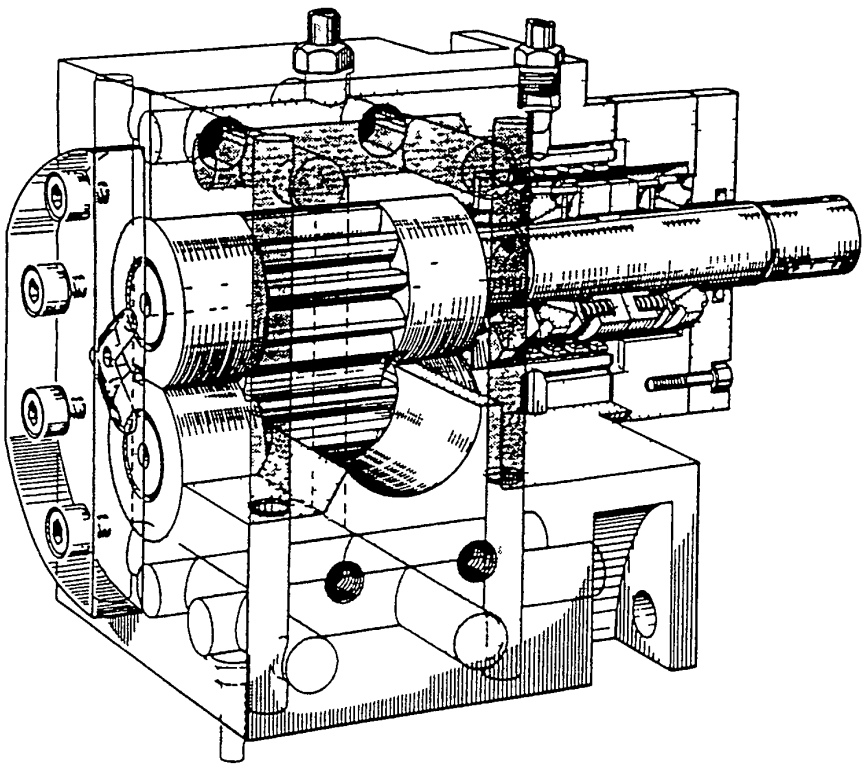

Figure 29 High pressure gear pump (heated) for polymer melts (Maag) [3 20]

pressure differences Economic application of centrifugal pumps depends on the specific speed of the single stage (at least 10–20 rpm) and thus on the magnitude of the flow rate and the hydraulic power

3 3 3 1 Multistage Centrifugal Pumps

High pressure centrifugal pumps have long been used as feed pumps for steam boilers [3 21], [3 22] power extends to beyond 30 MW and pressures up to 400 bar The design of high pressure centrifugal pumps for process engineering varies depending on the pressure level the temperature conditions (including those during starting) and the operational requirements as well as the directives of the international regulations

For high pressure process engineering centrifugal pumps with vertically-split barrel construction have become established for powers above ca 1 MW in petrochemistry as well as in petroleum and natural gas exploration especially as injection pumps [3 23], [3 24] Injection pumps for surface water and seawater impose much more stringent requirements as regards corrosion and erosion resistance of their components (power up to ca 20 MW pressure up to 300 bar) The entire running gear can be withdrawn without disassembling the housing which facilitates repairs (Fig 30) For pressures below 250 bar and lower powers multistage centrifugal pumps are also used with staged housings and modular construction They generally require lower investment costs For the pressure range up to 150 bar a longitudinally divided (horizontally split) housing design (pipeline pump) is suitable for many applications including boiler feeding and transferring liquids into chemical processes

3 3 3 2 High-Speed Centrifugal Pumps

In recent years high speed single stage and two stage centrifugal pumps have been introduced (Fig 31) They now represent a significant alternative to multistage centrifugal pumps in the range up to 100 m^3/h The required high circumferential speed (max 200 m/s) is effected by high rotor speed by using gears (up to ca 30000 rpm) so that pressure increases per stage up to about 200 bar are possible Although the efficiency is then generally poorer than in the case of multistage pressure increase high-speed centrifugal pumps have a compact construction [3 25]

Two-stage gear-centrifugal pumps (Fig 31 B) achieve higher pressures than single stage pumps (Fig 31 A) However the shaft seal of the second stage is exposed to higher pressure, the slow-running booster stage that is shown in Figure 31 B is

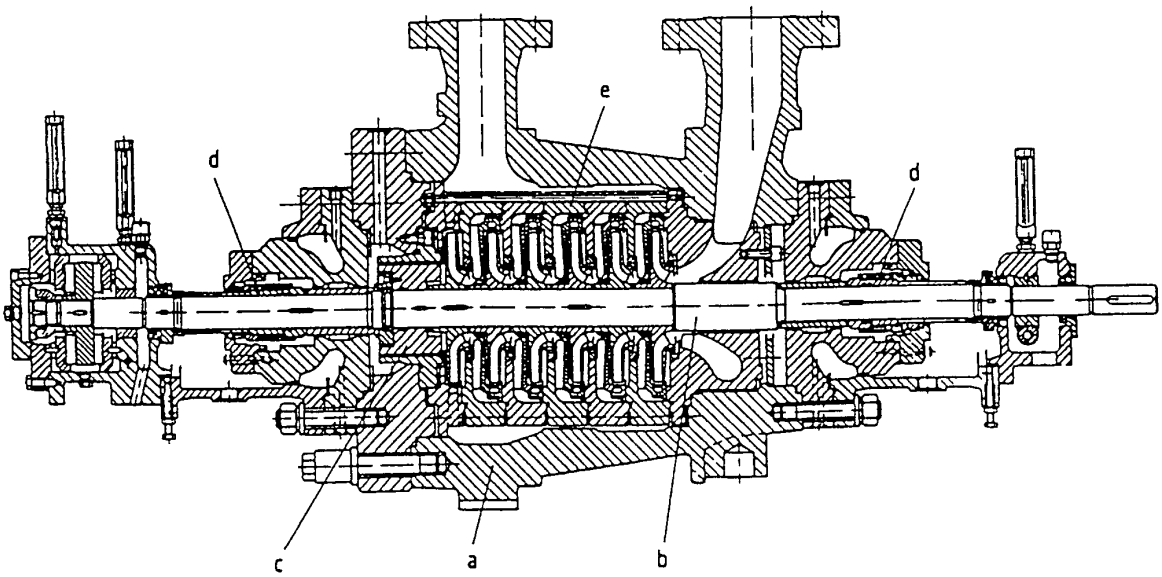

Figure 30 Six stage vertically split barrel housing centrifugal pump (Sulzer)
a) Barrel housing b) Shaft c) Axial thrust compensation d) Shaft seal e) Six internal pump stages

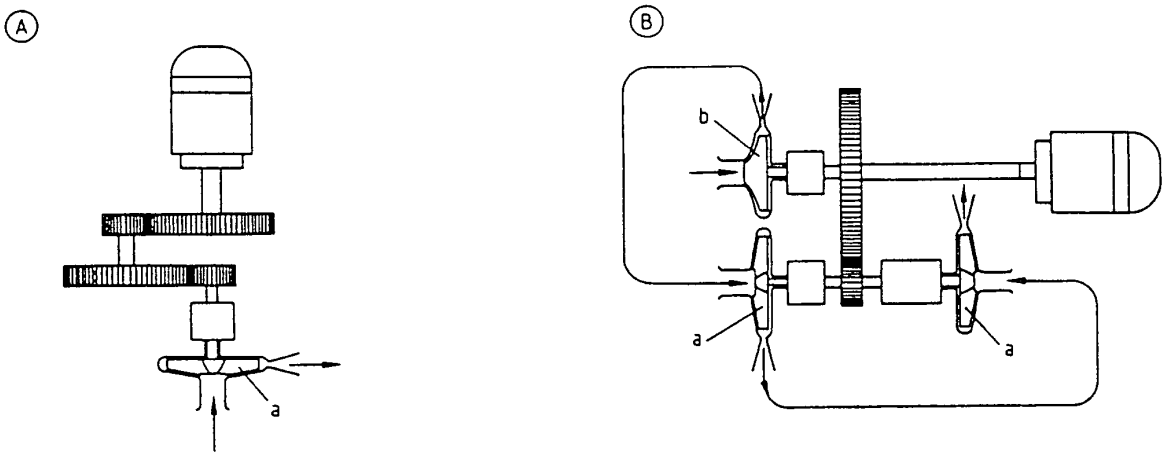

Figure 31 High speed gear centrifugal pumps (Sunstrand)
A) Single stage B) Two stage with booster stage for improving the NPSH
a) Stages b) Booster stage

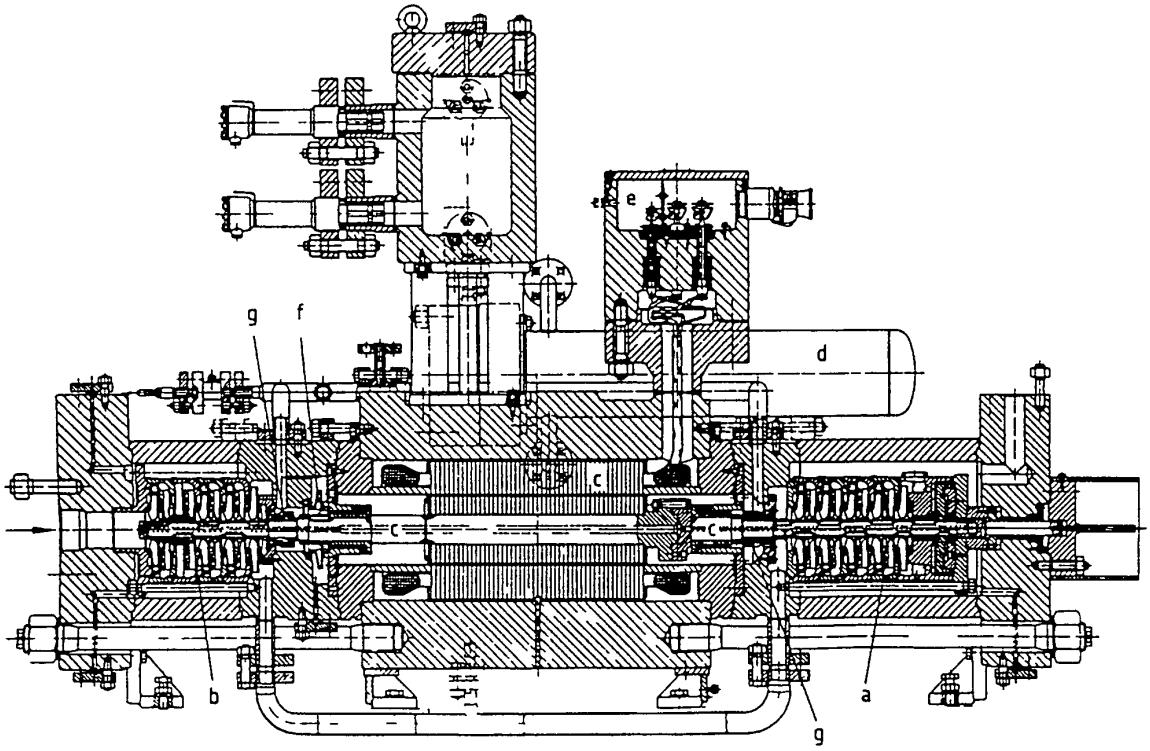

Figure 32 Ten stage canned motor centrifugal pump in tandem arrangement for carbon dioxide circulation (HERMETIC)
a) b) Tandem rotor c) Canned motor d) Cooler e) Terminal box f) Cooling circuit impeller g) Mechanical shaft seals

used to increase the suction pressure or the head above vapor pressure to avoid cavitation

For hydraulic powers below 1 MW (pressures from 100 to 300 bar) only a detailed cost benefit calculation will generally indicate the most favorable choice between multistage centrifugal pumps high speed one or two stage centrifugal pumps or reciprocating multi head piston or diaphragm pumps The energy consumption and expenses for investment and maintenance determine the optimal solution

3 3 3 3 Hermetic Centrifugal Pumps

With centrifugal pumps there is also a trend towards avoiding leakages and problems with shaft seals by means of a leak free design Normally the shaft seals of centrifugal pumps are exposed only to intake pressure and thus can be dealt with relatively easily With higher intake pressures or system pressures it is recommended that centrifugal pumps with a canned motor drive be used especially in the power range below 500 kW and if the fluids are toxic or hazardous [3 26] [3 27] Experience is available up to system pressures of 1000 bar the support of the thin walled containment shells of austenitic steel in the grooved stator against the high pressure is especially important The rotor bearings lubricated by the delivery fluid are now frequently made of silicon carbide

Figure 32 shows a multistage canned motor centrifugal pump with a separate water cooling circuit for the motor such as is used for example to circulate carbon dioxide at 300 bar system pressure The pump rotor is mounted in the motor area the tandem pump stages and the cooling circuit impeller operate over mounted on both sides of the bearings The entire internal cooling flow passes the canned motor The cooling circuit is separated from the liquid circuit by mechanical shaft seals (semi hermetic design)

Permanent magnet drives for pumps and stirrers are increasingly being used in high pressure technology [3 26] [3 28] [3 29] The containment shell of the magnet drive in contrast to canned motors must take up the full pressure difference and must have appropriately thick walls

If larger flows of nonproblematic fluids must be circulated at high pressure (e g carbon diox

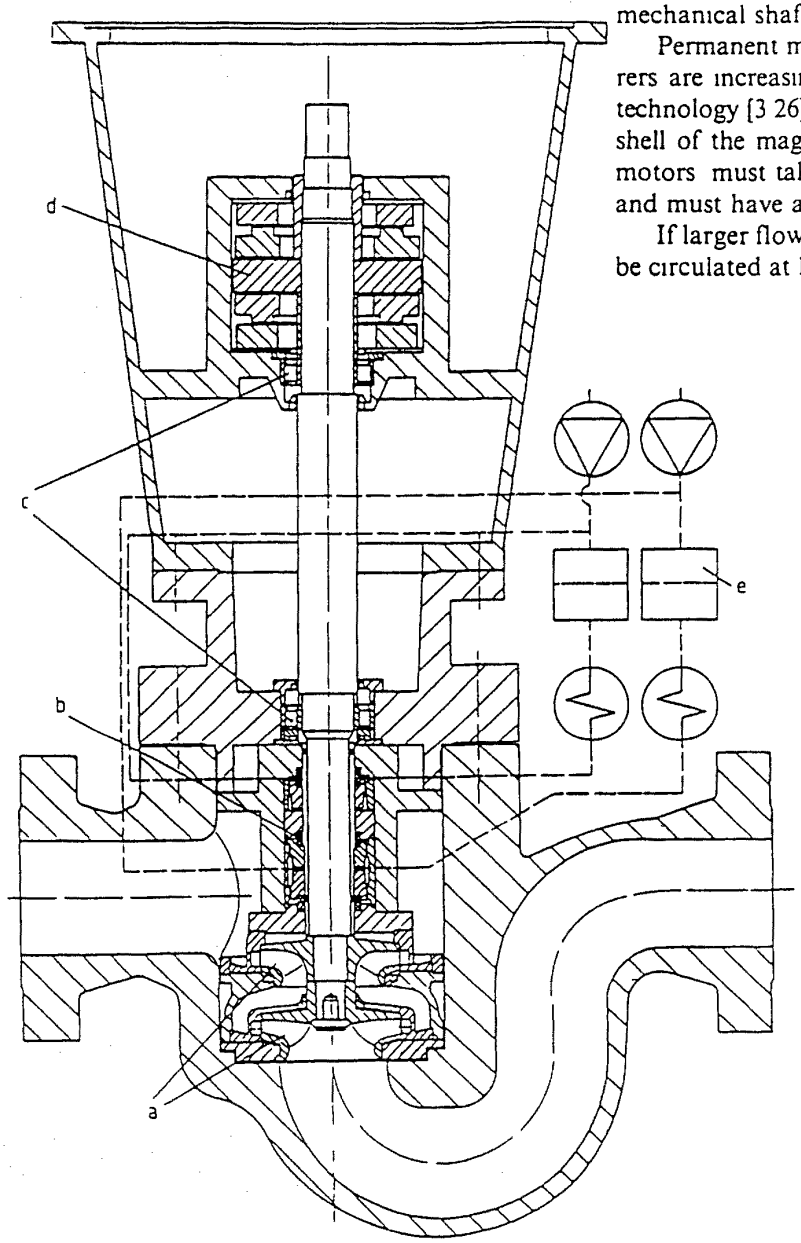

Figure 33 Two stage high pressure centrifugal pump for circulating carbon dioxide at a system pressure of 300–400 bar (Grassel)
a) Pump stages b) Sealed high pressure mechanical seal (two stage) c) Radial bearing d) Axial bearing e) High pressure

ide at 400 bar) two stage mechanical seals with pressure blockage are sometimes used The axial thrust is taken up for example by a segment bearing (Fig 33) Hydrodynamic mechanical seals make it possible to control system pressures up to 300 bar even in a single stage [3 30]

3 4 Compressors

Optimal compressor types for the various power ranges have been developed Figure 34 which shows power ranges for various compres sors was calculated on the basis of 1 bar intake pressure and an isothermal efficiency of 64% [3 31] It can give only approximate reference points for the most favorable area of application which varies depending on the manufacturer If the intake pressure is greater than 1 bar as is the rule it is necessary to recalculate (For example Compression of ethylene at a flow rate of 6400 kg/h ≈ 51 130 m^3/h (STP) from 231 to 2151 bar corresponds to a real intake volume flow rate at 231 bar of 161 m^3/h and a power consumption of 8200 kW)

The application boundary between piston and radial turbo compressors lies approximately at 10^4 m^3/h intake volume flow rate (pow er > 1–5 MW) In individual cases the most economical solution must be determined in the boundary region Development of piston com pressors has partially stagnated in recent years Rotating screw type compressors and radial tur bo machines have taken over certain areas For large multistage horizontal process gas piston compressors built up to powers in excess of 10 MW development has been largely conclud ed The trend toward radial turbo compressors dominates for economic reasons Their advan tages are that they operate with little vibration and pulsation are more easily sealed and re quire less space

3 4 1 Piston Compressors

At lower powers (<2 MW) there is much development of piston compressors in the direc tion of a higher stroke frequency a more com pact modular construction with a horizontal vertical or V shaped arrangement (Fig 35) dry running compression sparing lubrication and simpler maintenance [3 32]–[3 35] The dry-run ning range for continuous operation extends up to about 300 bar depending on the type of gas Labyrinth and piston ring compressors have characteristic fields of application The com pletely encapsulated labyrinth compressor with a pressureproof housing is suitable for gases of higher density (Fig 36) Dry-running piston ring

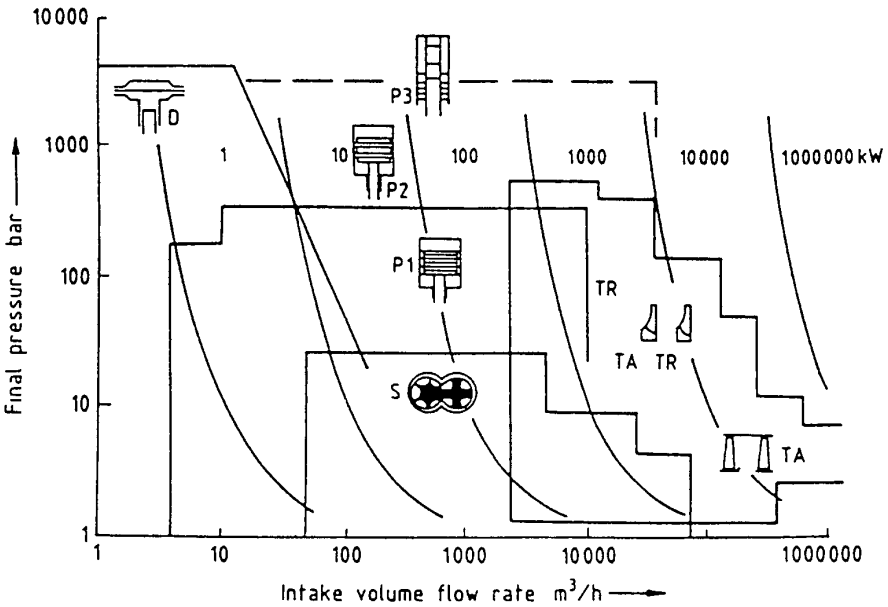

Figure 34 Power range of various compressor types for high pressures [3 31]
D = diaphragm compressor P1 = piston compressor dry running (piston ring labyrinth) P2 = piston compressor lubri cated (piston ring) P3 = ultrahigh pressure compressor lubricated (plunger piston) TR = radial turbo compressor TA = axial turbo compressor S = screw compressor

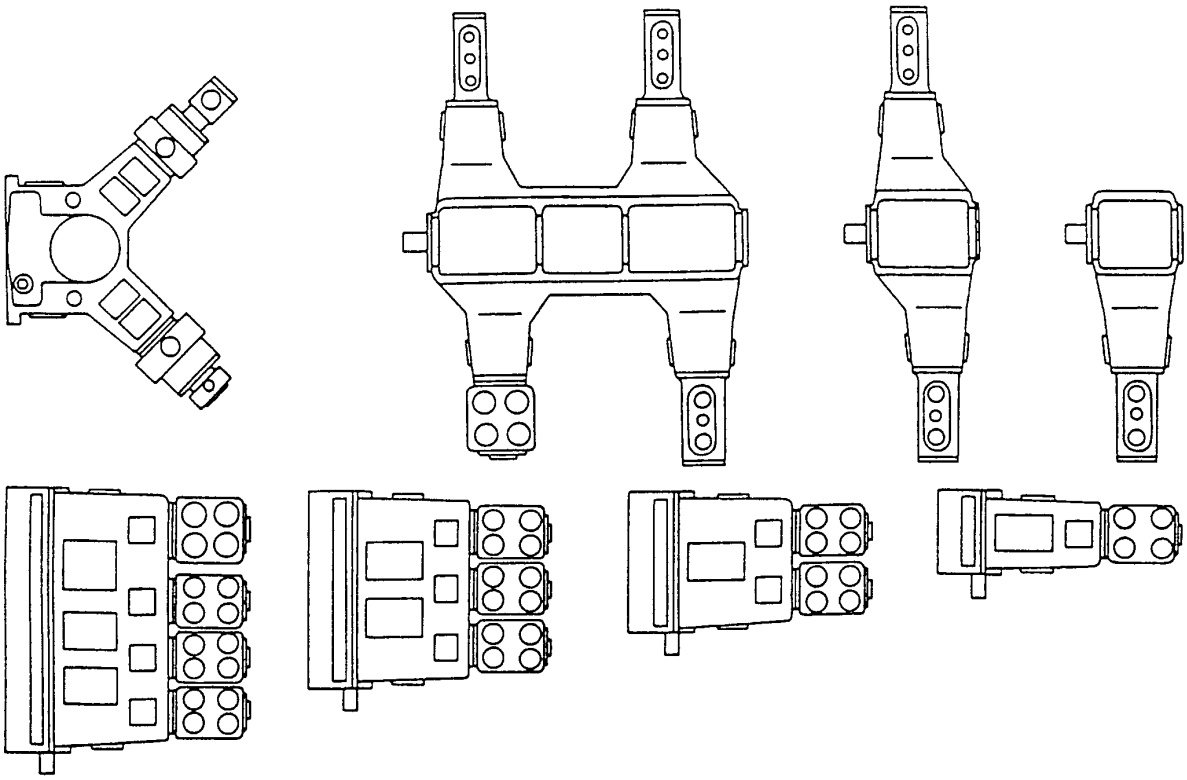

Figure 35 Piston compressor in modular construction (Neuman & Esser)

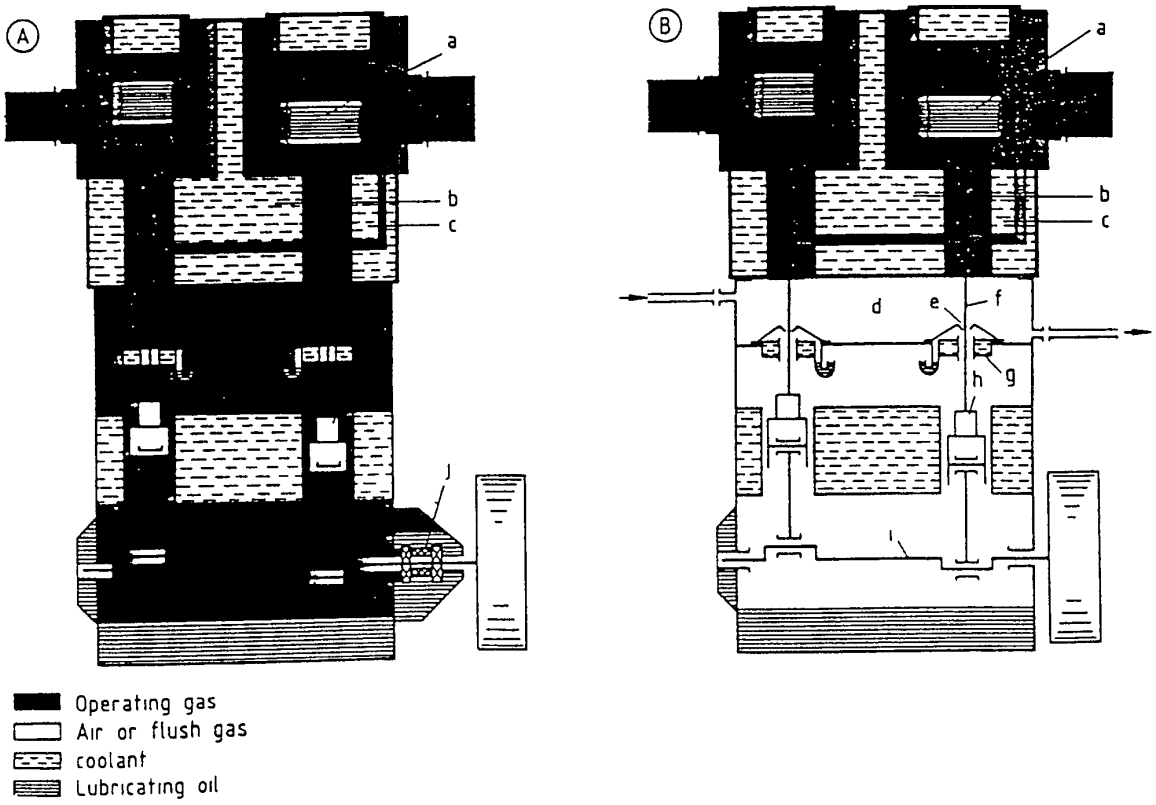

Figure 36 Sealing concepts for labyrinth compressor [3 34]
A) Pressureproof housing B) Spacer
a) Labyrinth piston b) Cylinder c) Labyrinth piston rod seal d) Spacer e) Oil wiper f) Piston rod g) Guide bearing h) Cross head i) Crank shaft j) Mechanical seal

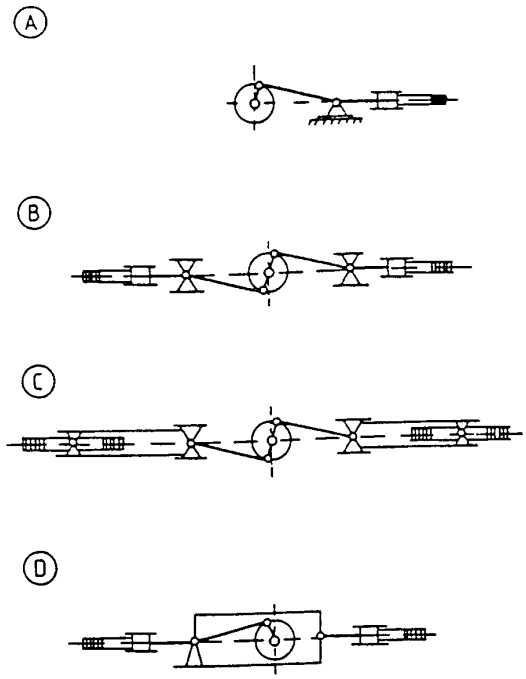

Figure 37 Designs of propulsion systems for high pressure piston compressors
A) Vertical crank B) Horizontal crank C) Horizontal crank (double action) D) Horizontal sliding block

compressors can be used universally as far as gas density is concerned to achieve satisfactory running times (> 10 000 h) modern design and material concepts must be implemented for the piston rings The so called sparing lubrication also plays a role here in reducing the lubricant contamination of the gas However most high pressure piston compressors are designed to be lubricated so that trouble free running times above 10 000 h are the rule

Ethylene secondary compressors are a special case These compress typically from ca 200–300 bar to 2000–3500 bar in two stages and are built for powers of up to ca 10 MW [3 36]–[3 38] In contrast to crank compressors their drives are designed with an interior robust cross head guide (Fig 37 D) and pairwise opposite cylinders The most important principle is to keep any transverse forces away from the piston seal For components subject to cyclical pressure notches are avoided (Fig 38) Valve bodies with cone valves are used here at large capacities several valves are arranged in parallel Superpressure compressors mainly work with stationary piston sealing elements this is a fundamental

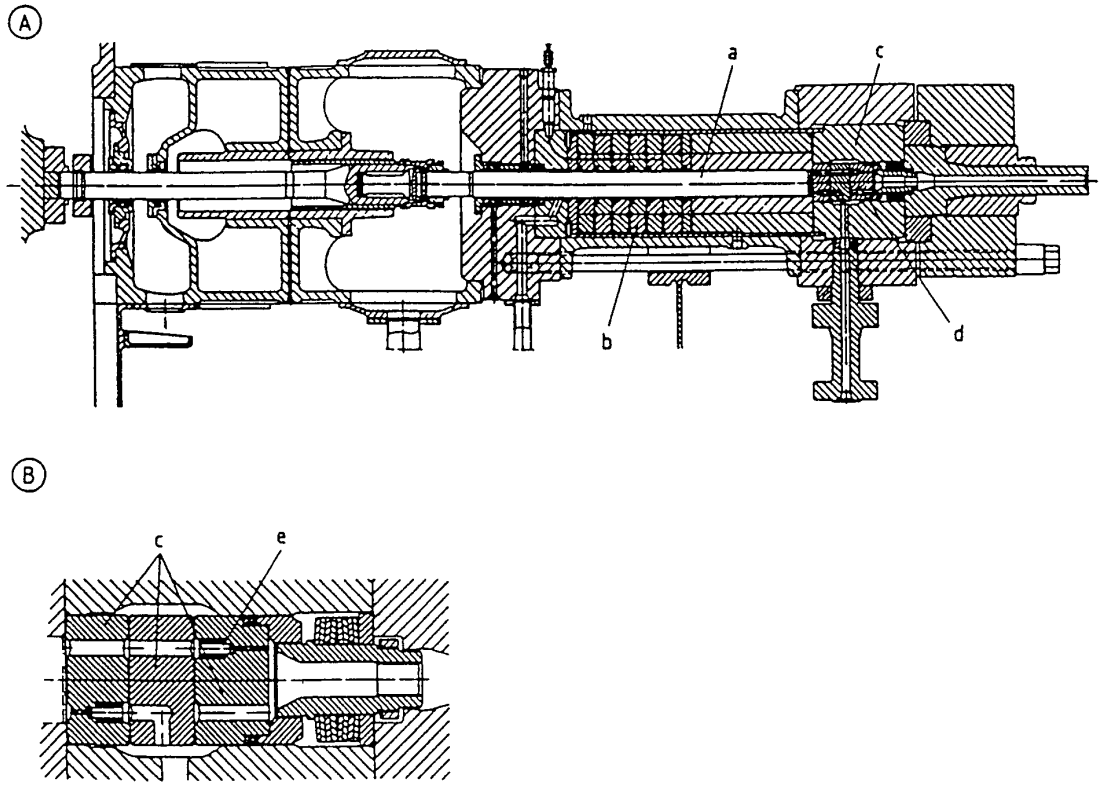

Figure 38 Final stage of an ultrahigh pressure secondary compressor (Sulzer Burkardt) [3 36]
A) Overall arrangement B) Valve block
a) Plunger piston b) Stationary sealing elements c) Valve housing d) Compressor valve arrangement e) Plug valve

difference from standard piston compressors with mobile piston rings Only with a stationary sealing arrangement does one achieve the required effective high pressure lubrication which furthermore requires extremely hard smooth and precisely machined plunger pistons

3 4 2 Diaphragm Compressors, Laboratory High-Pressure Compressors

The diaphragm compressor (Fig 39) one of the oldest leak free machines is limited to lower powers (< 100 kW) because of its sensitive metal diaphragms which must be used because of the high compression temperatures Its applications include laboratories pilot installations and special production facilities An attractive feature is their very high pressure ratio (up to 20) produced by a single stage as a result of the small clearance volume and good cooling At every stroke the diaphragm is pressed against the upper contact surface by a hydraulic fluid (smallest clearance volume) [3 39] However for this reason it is sensitive to particles coatings liquid droplets and surface defects so that its lifetime is generally less than 5000 h It is possible to signal diaphragm rupture by means of sandwich diaphragms [3 40] Diaphragm characteristics and rupture control are similar to diaphragm pumps (see Section 3 3 1 1)

Diaphragm compressors are built for pressures up to 4000 bar at least for short term operation They are economical when leak free operation with no gas contamination is required at low volume flow rates and at high pressure

For very small delivery quantities (0 1 – 1 m^3/h) and pressures up to 2000 bar air driven piston and diaphragm compressors (Fig 40) are suitable for transferring and compressing gases Because of their compact construction their explosion protection and their ease of regulation such machines are attractive for short term operation in research facilities especially for booster and filling applications

3 4 3 Turbo Compressors

For large volume flow rates (2×10^3–10^5 m^3/h), radial turbo compressors have now largely displaced process-gas piston compres-

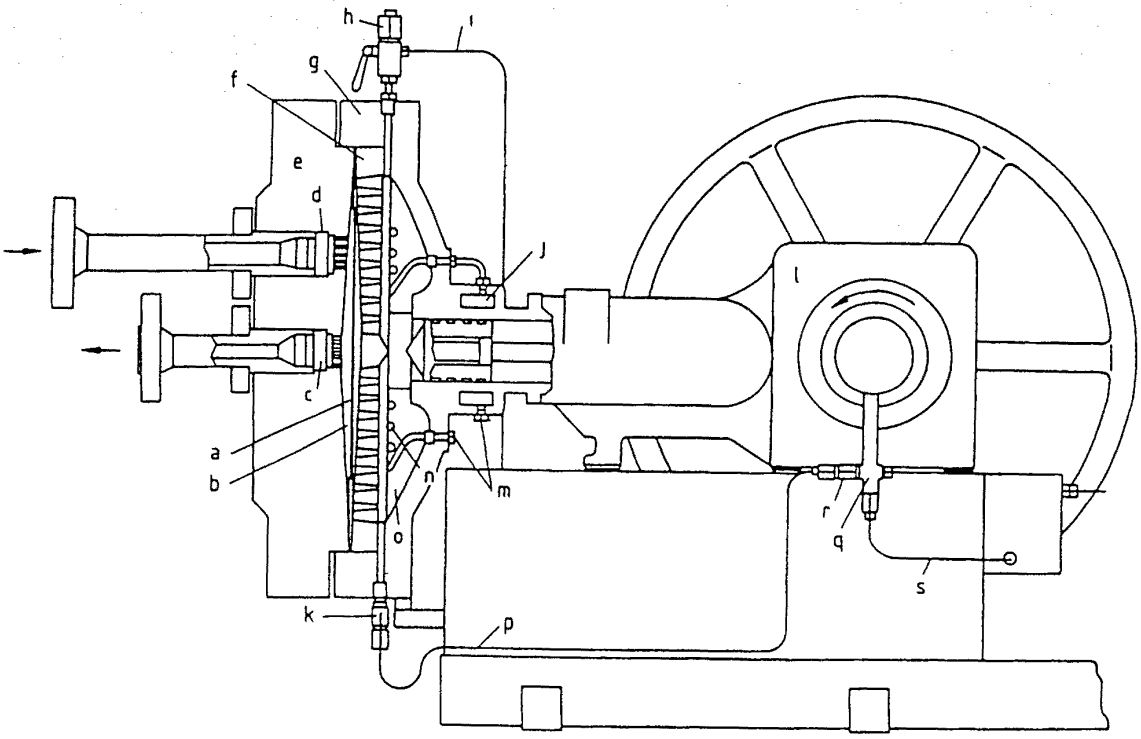

Figure 39 Diaphragm compressor (Hofer) [3 39]
a) Diaphragm b) Gas space c) Pressure valve d) Suction valve e) Diaphragm cover f) Perforated plate g) Hydraulic cylinder h) Oil overflow valve i) Oil return j) Cylinder cooling k) Check valve l) Crank drive m) Cooling water in/out n) Oil cooling coil o) Oil chamber p) Oil injection (leakage compensation) q) Compensation pump r) Check valve s) Oil supply

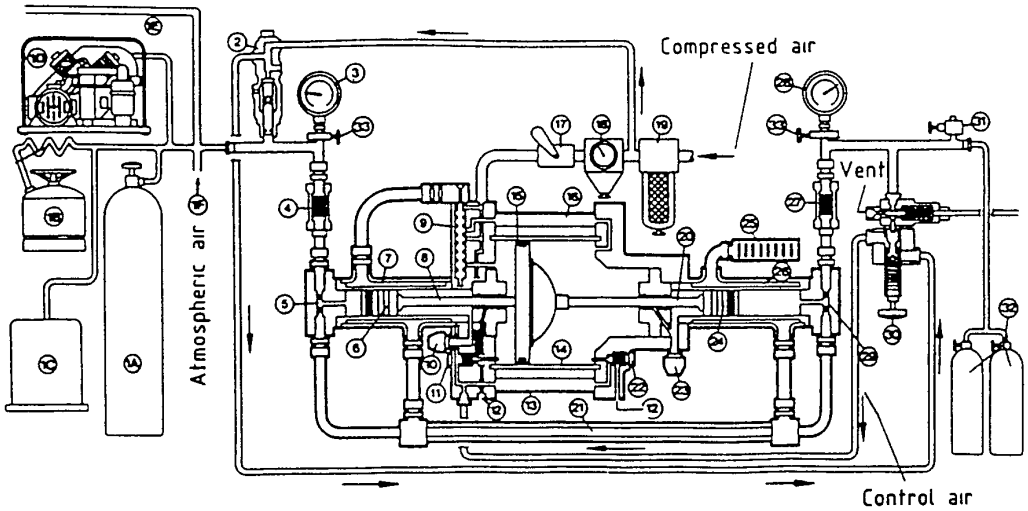

Figure 40 Two stage filling compressor with pneumatic linear drive (Haskel)

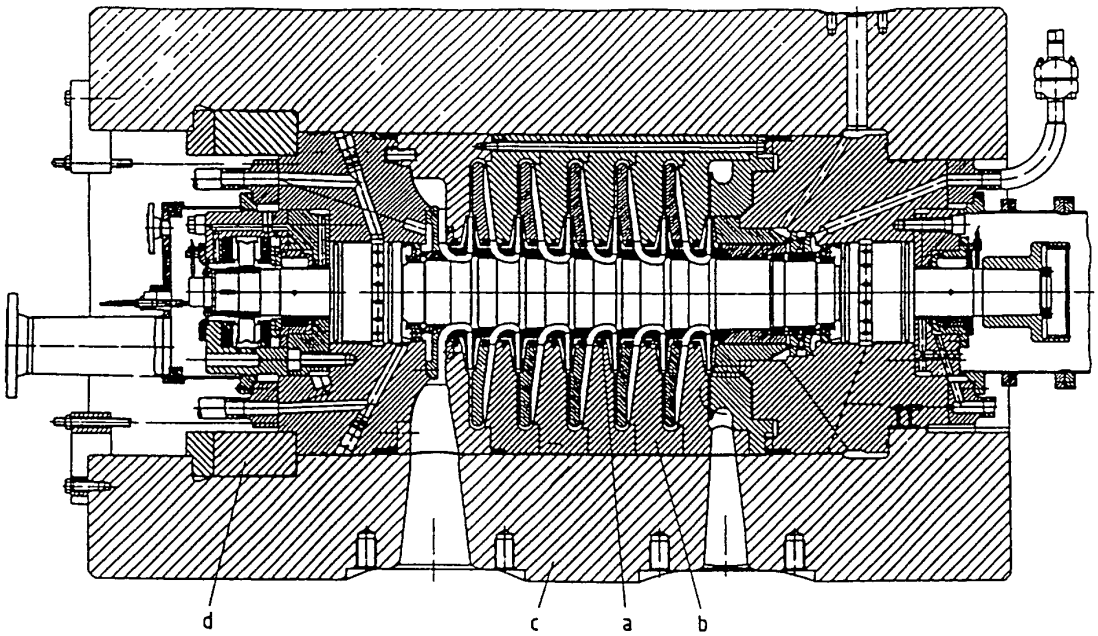

Figure 41 Six stage radial compressor with final stage 350–800 bar (Mannesmann Demag)
a) Rotor with compressor stages b) Stage housing c) Vertically split barrel housing d) Seal for vertically split barrel housing

sors even in the range above 150 bar Typical applications in urea ammonia and methanol plants for compressing synthesis natural and refinery gas as well as for transporting and injecting gas extend up to the pressure range of 400 bar [3 41]

For high pressure technology radial compressors are designed similar to high pressure centrifugal pumps in vertically split barrel con struction For hazardous gases this design is also used for pressures beginning at about 80 bar on account of the more favorable seal There are good possibilities for compensating the axial thrust by an appropriate arrangement of impeller stages with intermediate cooling

Multistage gear–radial turbo compressors are suitable as preliminary stages for high-pres sure stages for pressure ratios up to about 50 bar [3 42] [3 43] For pipeline gas transport single stage and two stage vertically split barrel designs have been produced for final pressures up to 80 bar and for powers above 20 MW These de signs are easy to install and maintain

A series of prototypes were developed to expand the range of application of turbo compressors By way of example Figure 41 shows a six stage high pressure stage (350–800 bar) The impellers are machined smooth and are made up of two disks (e g by soldering) an exit gap of a few millimeters can be achieved here Nevertheless the shaft seals here must seal against the suction side pressure level (350 bar) they work with pressurized oil blockage [3 44]

3 5 Other High-Pressure Machines

The problem of sealing rotating shafts is also encountered with high pressure stirrers and high-pressure extruders which greatly resemble rotating pumps [3 16]–[3 20] [3 28] [3 29] High pressure sluices for bulk goods present special sealing problems [3 45] A new type of high-pressure machine has arisen in the area of high-pressure extractors with automatically opening locks [3 46]

3 6 Special Problems Involving High-Pressure Machines

3 6 1 Strength of the Components

Since high pressure components are generally subject to high loads a precise stress analysis is necessary possibly with the finite element method or with photoelastic testing This is especially true for impellers that have a high circumferential velocity and also for the vibrational analysis of rotor shafts

In general there is no special problem about dealing with stresses in statically loaded pressure housings especially since a suitable stress flux can achieve a favorable strain (e g vertically split barrel design) By contrast it is much more difficult to dimension components that are stressed in cyclical fashion by internal pressure The largest cyclical internal pressure stresses occur with reciprocating liquid pumps The permissible dynamic material stress lies below the yield point of the material The maximum stresses occur at notch points

Compared to the smooth thick-walled pipe the usual notch points (Fig 42) have notch factors from 1 5 to 3 5 [3 3] [3 47] The notch factor characterizes the local stress sizing effect Thus in the T-intersection crossbore (Fig 27) at point X the tangential and radial stresses superimpose whereas the smooth pipe section (Fig 28 point Y), is loaded only by the stress of the corresponding single bore Studies on ferritic tempering steels and recently also on soft martensitic, semiaustenitic and precipitation-hardened high alloy chromium–nickel steels make it possible to design dynamically loaded thick walled components [3 2] [3 3], [3 48]–[3 56] With tough high alloy chromium–nickel

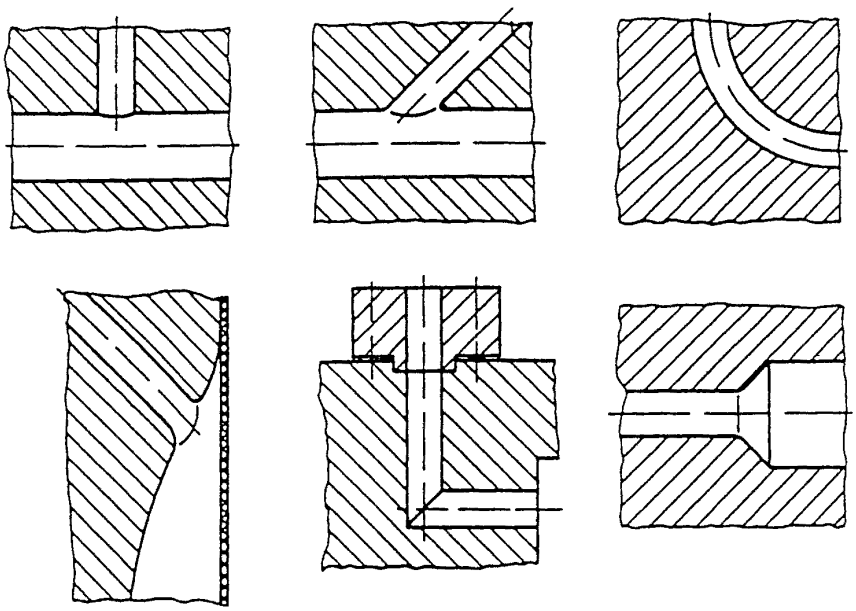

Figure 42 Typical notch points in thick walled high pressure components

steels an increase of their dynamic loadability by autogeneous dynamic autofrettage (see Section 2 3 1 3) has been observed which explains the favorable behavior of these steels in practice Studies show that thick walled forgings can exhibit anisotropy and that the surface quality has a perceptible influence Furthermore the mechanical properties of the material depend on its purity With components subject to very high stress the use of high purity steel grades smelted under inert gas or in vacuum are therefore always recommended All-round forging promotes isotropy

At very high pressures for parts made of brittle steels that are subject to cyclical stresses a clear discrepancy exists between the mechanical properties of the material for uniaxial and thick-walled samples [3 52] Various studies have shown that the penetration of pressures into the microcracks (e g slag inclusions) which are always present in the material creates a noticeable additional stress However with high-alloy chromium–nickel steels these stresses appear to be reduced by local plastification

For thick-walled components the following design measures help to deal with cyclical pressures

1) Avoiding notches for example by a coaxial arrangement of the pump valves (see Section 3 3 1 2 Fig 28) If this cannot be achieved then the point that is subject to the greatest stress must be rendered safe by giving it a Y shape (rounded) instead of a T shape (Fig 43) A tangential layout of the intersecting bores can also yield advantages [3 56]
2) Application of compressive prestresses in the limiting case up to pure cyclic compressive stress by autofrettage cold working shrinkage or local shot peening
3) The use of pure isotropic materials that are as tough as possible and the avoidance of corrosion which lowers fatigue strength [3 57] Reliable data on the fatigue strength of thick walled components have recently become available for modern high-strength soft-martensitic semiaustenitic and precipitation-hardened steels [3 58]

In general, the design of components that are subject to cyclic pressure requires great experience In compressor construction the problems

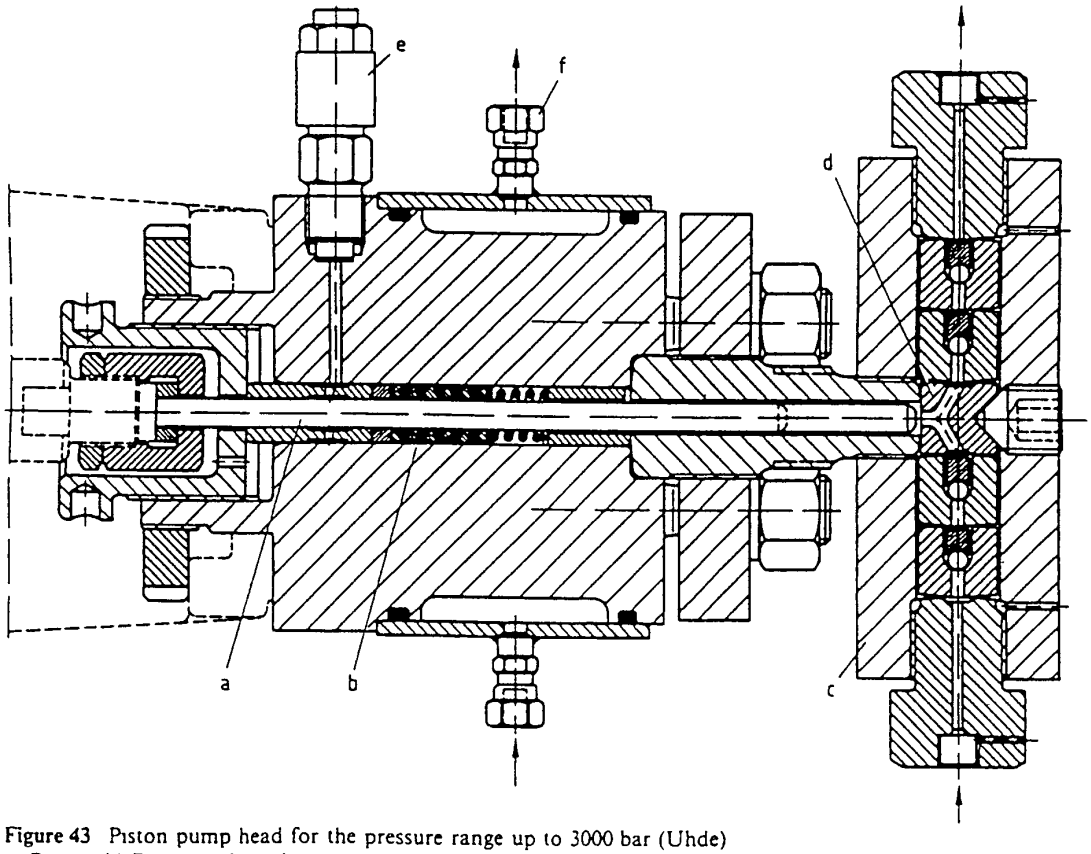

Figure 43 Piston pump head for the pressure range up to 3000 bar (Uhde)
a) Piston b) Piston sealing elements c) Valve head d) Y intersection e) Lubrication f) Cooling

are generally easier to solve because of the smaller pressure amplitudes

3 6 2 Seals

In high pressure technology metallic seals—lenses ring joints cuts—are used as *static seals* Self sealing elastomer sealing rings e g O rings have also proved suitable for easily loosened connections as long as the pressure temperature, and fluid permit their use

Where such seals are unfavorable for example with horizontally split compressor housing structural measures e g vertically split barrel housings are used to guarantee a reliable seal The clamping and sealing of diaphragms for diaphragm pumps and compressors [3 9] require special static seals

The problem points in high-pressure machines are the *dynamic shaft* and *piston seals* Seals create special problems when they slide rapidly under high pressure and if the fluid being sealed does not have any lubricating action Cyclic stress additionally creates fatigue problems in the seal *Noncontact seals* with defined narrow clearances such as labyrinth seals (Fig 44 A) are less problematic due to the generally low differential pressures (< 50 bar) however the fluid should not have an erosive effect Differential pressures up to several hundred bar occur at the axial thrust compensation pistons of centrifugal pumps and compressors but these are distributed over the many labyrinth stages Labyrinth seals on reciprocating pistons require very precise alignment and are limited to gases that do not have too low a molecular mass as well as to pressure differences $\Delta p < 150$ bar (Fig 44 B)

The leakage flow of noncontact gap and labyrinth seals is considerable and must be recycled internally With the *floating ring seal* a typical shaft seal for high pressure turbo compressors, the high-pressure sealing oil system maintains a slight overpressure compared to the gas pressure at the floating ring so that the sealing problem is reduced to the gap seal for the oil [3 44]

Conventional mechanical seals for liquids are limited to pressures below 100 bar [3 59] The limits are determined by the product of the sliding speed v and the differential pressure Δp with the rule of thumb $\Delta p \cdot v < 2000$–5000 bar m s^{-1} This value is based on the friction power arising in the gap With pressures above 100 bar sealing pressure blocking systems are used to reduce the differential pressure to

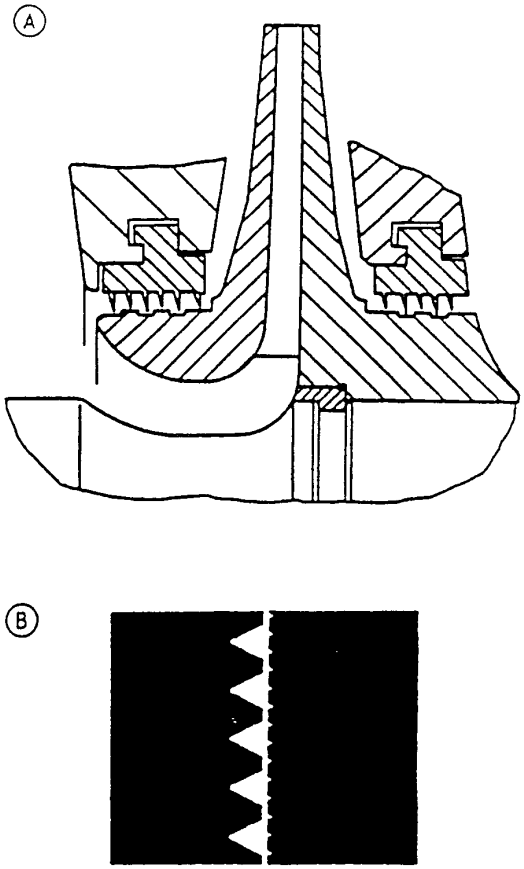

Figure 44 Labyrinth seals
A) Radial impeller B) Labyrinth piston

avoid evaporation to improve lubrication and to provide cooling [3 30] High-pressure mechanical seals are needed for centrifugal pumps only if the system pressure or vapor pressure is high For lower powers leak-free canned motor pumps are generally used

It is especially difficult to seal pistons with reciprocating motion Piston rings are suitable as piston seals in piston compressors up to ca 1500 bar, above 200 bar, lubrication is generally required With dry running or sparsely lubricated piston compressors the use of piston rings made of PTFE composites (Fig 45) has proven effective as an alternative to noncontact labyrinth seals At high pressure the captive piston ring is especially interesting (Fig 45 stage 3) It is supported after a run in process and thus makes contact at low compression [3 60] For lubricated high pressure stages up to 700 bar metallic piston rings are used Generally these are made of perlitic gray cast iron At still higher pressures (up to 1500 bar) piston rings made of forged bronze have also proven suitable

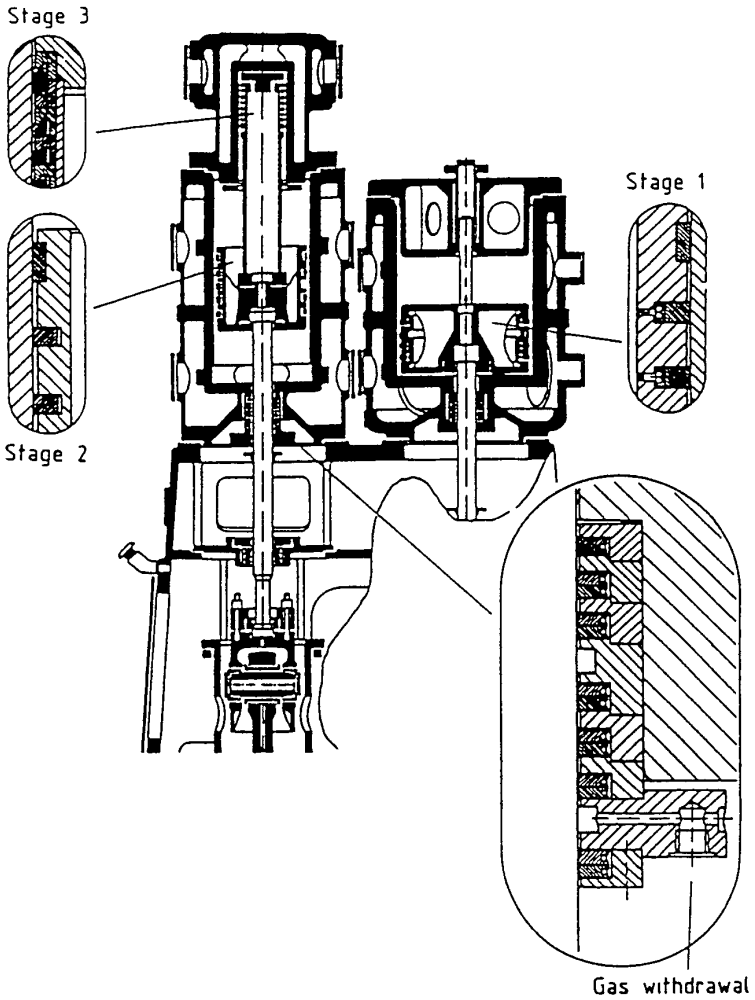

Figure 45 Various designs of piston and rod seals for piston compressors (Neuman & Esser)

Piston seals of ethylene secondary compressors for polethylene production are a special case (Fig 46) Supercritical ethylene is compressed from 300–350 bar in two stages to 3000–3500 bar (specific volume at 4500 bar 1 5 dm^3/kg) Stationary bronze seals which run against hard metal pistons have proven suitable The sealing elements consist of a sequence of radially and tangentially slotted rings generally preceded by a throttle ring Lubricating fluid is injected between the individual sealing elements against the high pressure produced by the compressor [3 61] Similar sealing elements are also successfully used for sealing piston rods at pressures up to 500 bar [3 62]

Piston seals for reciprocating displacement pumps must cope with the highest dynamic pressure differences because compression is always performed in a single stage as well as with a wide spectrum of fluid properties (e g toxicity corrosivity abrasiveness, low vapor pressure) Lubrication is often ineffective because the pumped fluid acts as a solvent The seals vary widely in terms of shape and material Solid or braided PTFE composites are often used The piston should be hard smooth, geometrically precise and guided centrally so that it runs in the seal without force The sealing elements should press just hard enough as is required for sealing Dry running must be avoided possibly by lubrication or flushing (for design forms see Figs 28 and 43) Spring tensioned chevrons with lubrication are used successfully up to very high pressures (up to 3000 bar) As the pressure increases the lifetime decreases quite drastically (e g 3000 h at 500 bar 1000 h at 3000 bar) Packing rings with a separately clamped lubricating or flushing chamber have proven to be a robust

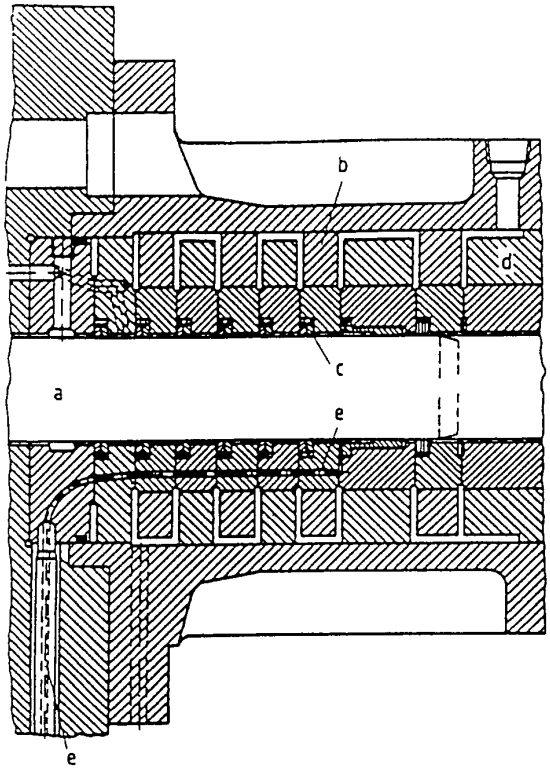

Figure 46 Plunger piston seal of an ethylene ultrahigh pressure compressor for 2000–3000 bar (Nuovo Pignone) a) Plunger piston b) Seal housing c) Sealing rings d) Compressor cylinder e) Oil supply

design for the pressure range from 200 to 300 bar With heterogeneous fluids or with fluids of low lubricity it is advantageous to inject a flushing fluid into the working space (Fig 47)

The maintenance and installation of piston seals requires a great deal of experience the necessary flushing and lubricating systems are sometimes quite complicated Frequently the optimal design (3000–8000 h lifetime) must be determined empirically by systematic troubleshooting At very high pressures (> 1000 bar) special measures are needed pistons and guide bushings of sintered hard metals, extremely precise smooth machining, and seals made of PTFE compounded with carbon graphite ceramic or metal powder To this is added an external lubrication which supports the discharge fluid lubrication as well as sealing elements which operate as automatically as possible under pressure A low piston speed reduces the friction power and increases the lifetime of piston sealing elements In this respect hydraulic linear drives (Fig 25) are more favorable With high pressure piston seals for abrasive suspensions, the particles must be kept away from the seals by injection flushing or by using sedimentation spaces as experience with coal slurry pumps (3000 bar) has shown [3 13]

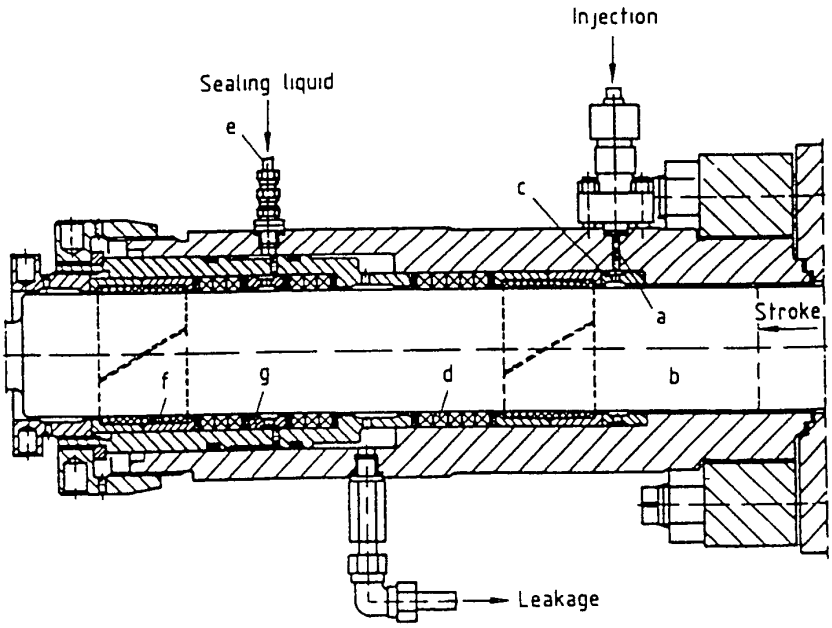

Figure 47 Piston seal with packing rings lubrication and injection flushing (URACA)
a) Injection b) Piston c) Injection bushing d) High pressure seal e) Flushing lubricating f) Guide bushings g) Low pressure seal

Problems with piston or shaft seals can be avoided totally by using hermetic diaphragm or canned motor pumps

3 6 3 Wear and Vibration

The wear of automatic pump valves and the determination of pressure oscillations in reciprocating pumps and compressors at high pressure are dealt with in [3 63]–[3 68]

4 Piping and Fittings

Standard DIN parts are not generally used in the chemical industry for high pressure piping Since the large scale chemical industry used high pressures and temperatures earlier than for example the power engineering sector the development of piping elements took place independently and was concluded as early as 1930 for pressures up to 700 bar The so-called IG Standard developed at that time was used in all German high-pressure plants, and was also common outside Germany it is still used today From 1950 further pressure stages up to 4000 bar were added for polyethylene plants

The following pressure ratings are used for new plants

Nominal pressure	325 bar for nominal bores up to	200
Nominal pressure	700 bar for nominal bores up to	58
Nominal pressure	3600 bar for nominal bores up to	65

The following steels are predominately used

CK 15 and CK 35	for pipes flanges bolts up to	700 bar
20 CrMoV 135	for pipes above 200 C up to	700 bar
30 NiCrMo 8	for pipes flanges bolts up to	3600 bar
18/8 CrNi steels	for corrosion resistant piping up to	700 bar

Pipes are used only in seamless designs Pipe bends are produced from pipes which are bent when cold or hot, or from hollow cylinders which are bent in a forging die Tighter bending radii can be achieved with bending in a die but the reduction in wall thickness arising during bending must be taken into account

Only forged steel is used for valves and fittings (e g T pieces) Pipes and valves are connected by flanged joints with threaded flange and lenticular sealing rings The piping itself can be flanged or welded for use at pressures up to 700 bar Welding is not possible at higher pressures because the steels used here are with very few exceptions not weldable

For ease of production shut off valves are designed predominantly as angle valves

Figures 48 and 49 show angle valves for 325 and 3600 bar A coupling between the upper and lower valve spindles of the 325 bar valve eliminates the need for the spindle to rotate in the seal during opening and closing V-shaped rings of reinforced polytetrafluoroethylene have proved to be good packing materials for the gland at temperatures of up to 250 °C This valve can be operated manually In contrast the large valves for 3600 bar can be operated only hydraulically or by an electric drive

For instrument lines and high pressure laboratories frequent use is made of valves of the form shown in Figure 50 The screwed fitting can be used for pipes with an inner diameter of up to ca 8 mm

Relief valves are constructed as spring-loaded proportional valves or full stroke values Figure 51 shows a full stroke relief valve for 3600 bar A stainless steel ball takes over the function of sealing and assisting the stroke since it is lifted by the back pressure generated during blow-off

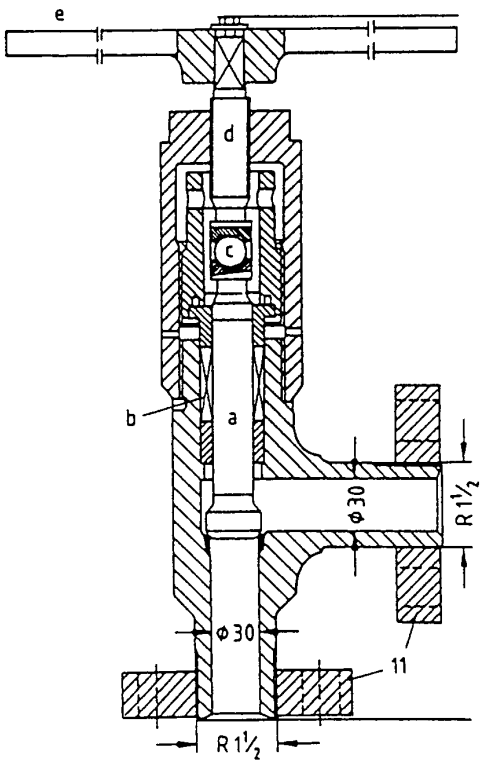

Figure 48 Manually operated angle valve for 325 to 700 bar
a) Lower stem b) Packaging rings c) Coupling between upper and lower stem to prevent rotation of lower stem d) Upper stem e) Handle

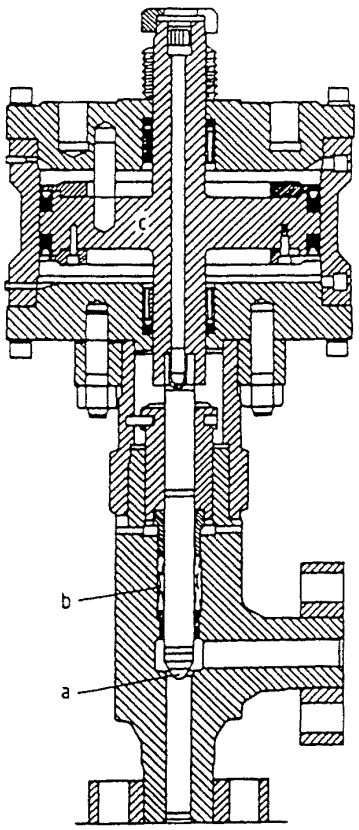

Figure 49 Angle valve with operation by oil plunger for 3600 bar
a) Stem b) Packaging rings c) Hydraulic piston

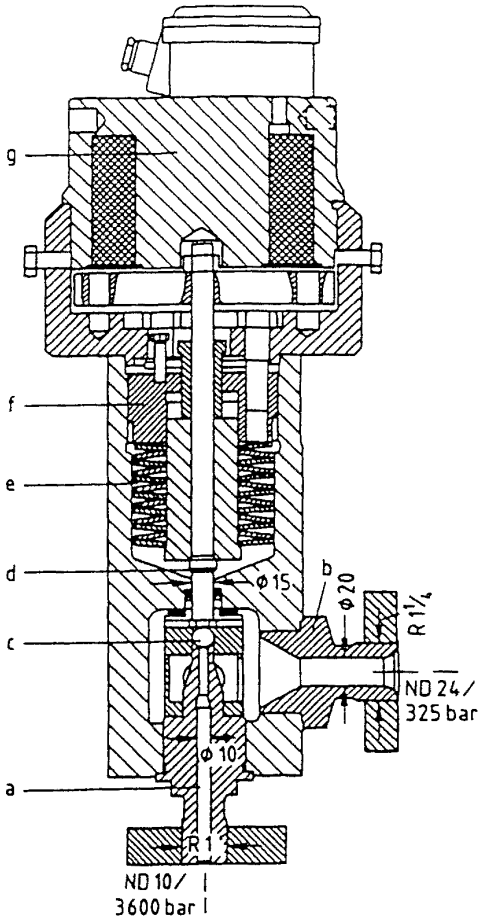

Figure 51 Full stroke relief valve for 3600 bar
a) Inlet nozzle b) Outlet nozzle c) Stainless steel ball d) Stem e) Disk springs f) Adjusting screw for spring load g) Magnetic lifting device

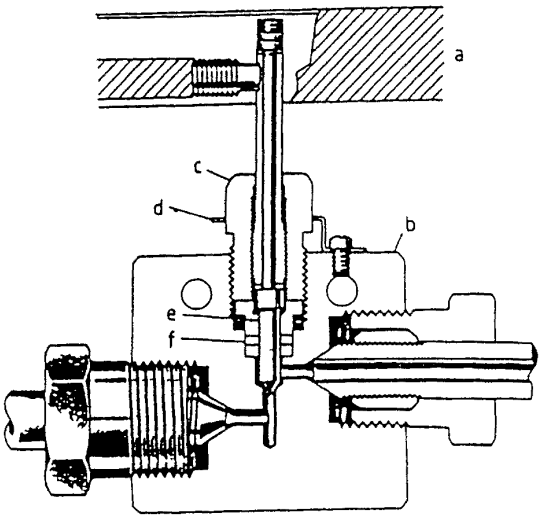

Figure 50 Straight way valve for small nominal sizes
a) Designer handle b) Stainless steel body c) Packing gland d) Loading device e) Nonrotating stem f) Adjustable packing below threads

The disk spring chamber is designed for an internal pressure of 325 bar so that the gas to be discharged can be collected in a pressure vessel The valve can be opened by the lifting magnet even if the internal pressure has not yet risen to the set blow off pressure Rupture disks are also used up to 3000 bar instead of the relief valves

Nonreturn ball valves are manufactured up to nominal width 30 mm spring-loaded plate valves are used for larger nominal sizes The check valves with pear shaped cones that were developed for coal hydrogenation plants are now rarely used Check valves should be installed vertically with the flow direction upwards so that the dead weight of the sealing element supports the closing force of the spring The lengths of the valves and fittings are coordinated with one another so that they can be interchanged e g a pipe bend for a corner valve or T piece

5 References

References for Chapter 1

[1 1] S Maier F J Muller Reaktionstechnik bei industriellen Hochdruckverfahren *CIT* **58** (1986) no 4 287–296

[1 2] K H Schmidt Neuentwicklungen in der homogenen Katalyse *Chem Ind* 37 (1985) 762–765

[1 3] R Eggers Energetische Optimierung der Hochdruckextraction *CIT* 53 (1981) 551–554

[1 4] G Vetter Pumpen und Verdichter für hohe Drucke—Festigkeit Dichtungen Verschleiß *CIT* **58** (1986) 183–185

General References for Chapter 2

[2 1] I Class A F Mayer Bauarten von Hochdruckhohlkorpern in Mehrteil insbesondere Mehrlagenkonstruktion *Chem Ing Techn* **24** (1952) 4–9

[2 2] I Class Entwicklung und besondere Vorteile der zylindrischen Mehrlagenhohlkorper für hohe Innendrucke *Werkst Korros* 7 (1956) 8–11

[2 3] J Schierenbeck Wickelverfahren zur Herstellung von Synthese Hochdruckhohlkorpern *Brennst Chem* **1959** 375–381

[2 4] W Witschakowski Large Pressure Vessel Manufacture *Capital and Process Engineering* **1** (1968) 63–66

[2 5] H C Rauschenplat A F Fino Design Fabrication Inspection and Testing of Multiwall Pressure Vessels *Am Soc Mech Eng Pressure Vessels Piping Div* [*Publ*] 71 PVP 57

[2 6] R Tschirsch Der Mehrlagenbehalter Eigenschaften Versuche und Stand der Anwendung *Stahlbau* **4** (1976) 108–119

[2 7] Nooter Technical Service Plywall Containing High Pressures Economically bulletin no 102 Nooter Corp St Louis Mo 1973

[2 8] J Ehle A Pollanz Grundlagen des Hochdruck Apparatebaues *Chem Ztg* **95** (1971) no 1 28–33

[2 9] E Karl Dichtungen für Hochdruckbehalter *Chem Ing Techn* **43** (1971) 698–704

[2 10] E Karl Strip Wound Pressure Vessels *Chem Eng Prog* **68** (1972) no 11 56–60

[2 11] E Karl Wickel Druckbehalter für Hochdruck Polyathylen Anlagen *CZ Chemie Techn* **2** (1973) no 1 13–17

[2 12] J P Konig H Spahn Korrosion und Korrosionsschutz in der Hochdrucktechnik *Werkst Korros* **24** (1973) 468–477

[2 13] H H Buchter *Apparate und Armaturen der Chemischen Hochdrucktechnik* Springer Verlag Berlin 1967

[2 14] E Karl Seal Design for Pipes and Vessels used in Chemical High Pressure Plants ASME PVP Conference 1981 vol 48 37–51

[2 15] W R D Manning S Labrow *High Pressure Engineering* Leonard Hill London 1971

[2 16] H Spahn Druckgefäße *VGB Kraftwerkstech* **58** (1978) no 7 511–528

[2 17] H Ford E H Watson B Crossland Thoughts on a Code of Practice for Forged High Pressure Vessels of Monobloc Design *Am Soc Mech Eng Pressure Vessels Piping Div* [*Publ*] 78 PVP 62

[2 18] D E Witkin G J Mraz Design Philosophy of Pressure Vessels for Service above 10 KSI (70 MPa) *Am Soc Mech Eng Pressure Vessels Piping Div* [*Publ*] 76 PVP 62

[2 19] J Watanabe et al Temper Embrittlement of 2 Cr–1 Mo Pressure Vessel Steel *ASME 29th Petroleum Mechanical Engineering Conference* Dallas Texas Sept 15–18 1974

[2 20] A Chaaban Static and Fatigue Design of High Pressure Vessels with Blind Ends and Cross Bores Ph D Thesis University of Waterloo Canada 1985

References for Chapter 3

[3 1] H Wendt Apparate und Maschinen der Hochdrucktechnik Achema Berichte *Chem Ing Tech* **57** (1985) no 12 1062–1067

[3 2] G Vetter D Lambrecht G Mischorr The Fatigue of Thickwalled Components with Softmartensitic and Semiaustenitic Chrome Nickel Steels under Pulsating Pressure *2nd Int Symp High Pressure Chemical Eng* Erlangen 1990 Abstrakt Handbook DECHEMA Frankfurt 1990 pp 499 ff

[3 3] G Mischorr Zur Ermudung dickwandiger Rohre aus weichmartensitischen und halbaustenitischen Chrom Nickel Stahlen durch schwellenden Innendruck Dissertation Universitat Erlangen Nurnberg 1990

[3 4] G Vetter Ausführungskriterien und Storeinflusse bei oszillierenden Dosierpumpen in G Vetter (ed) *Jahrbuch Pumpen* Vulkan Verlag Essen 1987 pp 521–529

[3 5] H Funke Eluentenfördersysteme in der HPLC *Labor Praxis* **1984** 18–29

[3 6] H Fritsch Leckfreie Mikro Dosierpumpen in G Vetter (ed) *Leckfreie Pumpen* Vulkan Verlag Essen 1990 pp 97–118

[3 7] G Vetter Oszillierende Dosierpumpen in leckfreier Ausführung in G Vetter (ed) *Leckfreie Pumpen* Vulkan Verlag Essen 1990

[3 8] J Jarosch High Pressure Diaphragm Pumps for High Flow Rates *2nd Int Symp High Pressures Chemical Eng* Erlangen 1990 Abstract Handbook DECHEMA Frankfurt 1990 pp 517 ff

[3 9] G Vetter Reliability and Future Development of High Pressure Diaphragm Pumps for Process Service *Proc of the 5th International Pump Users Symposium* Houston Texas 1988 pp 49 ff

[3 10] R Brauer Leckfreie Dosierpumpen für schwierige Anwendungen *3* [*Drei*] *R Rohre Rohrleitungsbau Rohrleitungstransp* **27** (1988) no 7 pp 494–497

[3 11] J P Korner P S I Crofton Entwicklung und Konstruktion eines Druckubersetzers für den Dauerbetrieb bei Druck uber 3000 bar *Chem Tech (Heidelberg)* 8 (1980) no 11 561–565

[3 12] H Fritsch Prozeßmembranpumpen in G Vetter (ed) *Leckfreie Pumpen* Vulkan Verlag Essen 1990 pp 118–138

[3 13] W Dettinger Eigenschaften von Kohlemaischepumpen für Hydrieranlagen *Chem Ing Tech* **54** (1982) no 5 500–501

[3 14] G H Holthuis P W H Simons The Economics of Positive Displacement Slurry Pumps *5th Int Techn Conf on Slurry Transportation* Las Vegas 1981

[3 15] L Schuster Hydraulically Driven Twocylinder Pistonpumps for Solid Transport with Viscous Materials in Pipelines *1st Int Congr Fluid Handling Systems Abstract Handbook* Essen 1990 p 507 ff

[3 16] W T Rice S Lavin *Thermorex Zahnradpumpen – Anwendung in Verbindung mit Extrudern* Druckschrift Maag Zahnrader Zurich 1981

[3 17] W Branscheid Die Zahnradpumpe als volumetrisches Dosieraggregat für Kunststoffe *VDI Fachtagung Speichern Fordern und Dosieren von Kunststoffen* VDI Dusseldorf 1976

[3 18] J M McKelly V Maire F Haupt How Gear Pumps and Screw Pumps Perform in Polymer Processing Applications in *Fluid Movers* McGraw Hill New York 1979 pp 290–298

[3 19] G Balder H Langhorst Zahnrad Schmelze Pumpen in der Extrusion *Kunststoffe* **1988** no 1 27–33

[3 20] T Bartilla Zahnradpumpen im Extrusionsprozeß *Der Extruder im Extrusionsprozeß – Grundlagen für Qualitat und Wirtschaftlichkeit* VDI Verlag Dusseldorf 1989 pp 201–240

[3 21] G Feldle Neue Baureihe Hochdruck Kreisel pumpen – Einfluß der Gesamtkostenbetrachtung auf die Entwicklung *KSB Technische Berichte* (1986) no 20 50–55

[3 22] H B Matthias Speisepumpen für Dampfkraftwerke und Nuklear Kraftwerke bis 1300 MW Blockleistung *Pumpen und Pumpenanlagen* Lexika Verlag Grafenau 1979

[3 23] G Fussle Betriebserfahrungen mit Injektionspumpen *Techn Rundsch Sulzer* (1985) no 2 12–17

[3 24] P E Huber Seawater Injection Pumps for Secondary Oil Recovery World Pumps 1983 pp 125–127

[3 25] V S Lobanoff R R Ross *Centrifugal Pumps – Design and Application* Gulf Publ Co Houston 1985

[3 26] R Kramer R Neumaier *Centrifugal Pumps and Rotary Positive Displacement Pumps of Hermetic Design* Hermetic Pumpen GmbH Gundelfingen 1988

[3 27] R Kramer R Neumaier Hermetic Drive Systems in High Pressure Circuits *2nd Int Symp High Pressure Chemical Eng* Erlangen 1990 Abstract Handbook pp 507–516

[3 28] M Knorr Stopfbuchslose Kreisel und Verdrangerpumpen mit permanentmagnetischer Synchronkupplung in G Vetter (ed) *Leckfreie Pumpen* Vulkan Verlag Essen 1990

[3 29] J P Korner Developmental Tendencies in the Design and Constructions of High Pressure Vessels especially of Large Scale Stirrer Vessels with Permanent magnet Rotary Stirrer Drives *2nd Int Symp High Pressure Chem Eng* Erlangen 1990 Abstract Handbook pp 489–496

[3 30] K H Victor Kontakt und verschleißfrei arbeitende Elasto Hydrodynamik Gleitringdichtungen für den Hochdruckeinsatz *Pumpentagung* Karlsruhe 1988

[3 31] H R Klay Gasverdichter (Übersicht) in G Vetter (ed) *Verdichter Handbuch* 1st ed Vulkan Verlag Essen 1990 pp 1–5

[3 32] H Gernandt Kolbenkompression für die Verfahrenstechnik in G Vetter (ed) *Verdichter Handbuch* 1st ed Vulkan Verlag Essen 1990 pp 200–206

[3 33] H Gernandt Some Problem Solutions with High Pressure Reciprocating Compresors *2nd Int Symp High Pressure Chem Eng* Erlangen 1990 Abstract Handbook pp 523–529

[3 34] H R Klay Labyrinth Kolben Kompressoren in G Vetter (ed) *Verdichter Handbuch* 1st ed Vulkan Verlag Essen 1990 pp 207–212

[3 35] Industrial Gases Committee (IGC) Kolben Verdichter für Sauerstoff Betrieb IGC Dok 10/81/D

[3 36] C Matile Industrie Hochstdruck Verdichter *Techn Rundsch Sulzer* (1971) no 1 1–8

[3 37] E Giacomelli P Pinzanti S Corsi Autofrettage in Secondary Ethylene Compressors Some Practical Aspects *Quaderni Pignone* **44** (1988) 19–26

[3 38] A Traversari P Beni Approaches to Design of a Safe Secondary Compressor for High Pressure Polyethylene Plants *Saf High Pressure Polyethylene Plants* AICHE **1974**

[3 39] I Meyn Membrankompressoren für hohe Drucke in G Vetter (ed) *Verdichter Handbuch* 1st ed Vulkan Verlag Essen 1990 pp 107–111

[3 40] W Rieß Einsatzgebiete und konstruktive Ausführung von Turbokompressoren – Stand der Technik und Zukunftsperspektiven in VDMA (ed) *Pumpen Vakuumpumpen Kompressoren* 89 Harnisch Verlag Nurnberg 1989 pp 44–50

[3 41] E Rothstein Neue Losungen in der Prozeßindustrie – der Einsatz von sechsstufigen Getriebe Turboverdichtern in G Vetter (ed) *Verdichter Handbuch* 1st ed Vulkan Verlag Essen 1990 pp 213–222

[3 42] I Ispas W Bosen Mehrstufige Getriebe Turboverdichter in G Vetter (ed) *Verdichter Handbuch* 1st ed Vulkan Verlag Essen 1990 pp 128–138

[3 43] J Hutgens F J Mangelmann H O Jeske Gastransport mit einstufigen axial ansaugenden Pipelinekompressoren in G Vetter (ed) *Verdichter Handbuch* 1st ed Vulkan Verlag Essen 1990

[3 44] *Turboverdichter für sehr hohes Druckniveau* Mannesmann Demag Druckschrift MA 25 69 dt/11 81 1981

[3 45] R Reimert Schleusen für Druckreaktoren – Konzepte und Ausführungen *Chem Ing Techn* **53** (1981) 335–344

[3 46] J P Korner New Development in the Design and Construction of Industrial size SCGE Plants *Proced of the Int Symp on Supercritical Fluids* Nice 1988 p 633 ff

[3 47] A Chaaban *Static and Fatigue Design of High Pressure Vessels and Blind Ends and Cross bores* Thesis University Waterloo 1985

[3 48] J L M Morrison B Crossland J S C Parry Strength of Thick Cylinders Subjected to Repeated Internal Pressure *Proc Inst Mech Eng* **14** (1960) 95 ff

[3 49] J S C Parry R W E Shannon Fatigue and Fracture of Thickwalled Pressure Vessels *Proc Int Conf High Pressure Engineering* Brighton 1975 I Mech E 1977 p 267 ff

[3 50] G H Haslam The Fatigue Limit of Cylinders Subjected to Repeated Internal Pressure *High Pressures – High Temperatures* **1** (1969) 705 ff

[3 51] P S J Crofton Optimization of Duplex Cylinders for Fatigue Resistance *ASME Pressure Vessels and Piping Conf* Pittsburgh USA 1988

[3 52] P S J Crofton *The Role of Inclusions in the Initiation and Propagation of Fatigue Cracks in Low Alloy Steels* Doctoral Thesis Imp Coll of Science and Techn London 1980

[3 53] E Karl Fatigue Resistance of Thick Walled Pipes under Pulsating Internal Pressure *Int Symp High Pressure Chem Eng* Erlangen 1984 Abstract Handbook p 41

[3 54] M Nishihara Y Yamaguchi S Hattori Fatigue Design of Thick Walled Cylinders for Very High Pressure *R & D Res Div (Kobe Steel Ltd)* **26** (1978) no 2

[3 55] G Vetter G Mischorr Fatigue of Thick walled Cylinders from High alloyed Corrosion Resistant CrNi Steels under Pulsating Pressure *Proc Int Conf on Fract and Fract Mech* Shanghai 1987 p 721 ff

[3 56] B N Cole G Graggs I Ficinec Strength of Cylinders Containing Radial or Offset Cross Bores *J Mech Eng Sci* **18** (1976) no 6 279–285

[3 57] U Gramberg Beitrag zur Problematik der Auslegung schwingend beanspruchter Bauteile *Chem Ing Tech* **56** (1984) 661–666

[3 58] G Vetter D Lambrecht G Mischorr Fatigue of Thick Walled Pipes from Soft Martensitic and Semi austenitic Chrome Nickel Steels under Pulsating Internal Pressure *Chem Eng Technol* **15** (1992) 1–13

[3 59] E Mayer *Axiale Gleitringdichtungen* VDI Verlag Dusseldorf 1982

[3 60] Neuman & Esser *Process Gas Compressors* Druckschrift 1989

[3 61] K Scheuber Dynamische Druckverteilung in der Zylinderdichtung von Hochstdruckkompressoren *Ölhydraulik und Pneumatik* **25** (1981) 583–586

[3 62] P de Haas BORSIG Druckschrift *Besondere Merkmale von Borsig Kolbenkompressoren* 1989

[3 63] G Vetter U Stork Zum Verschleiß selbsttätiger Pumpenventile oszillierender Verdrängerpumpen durch abrasive Suspensionen *Konstruktion* **41** (1989) 67 ff

[3 64] G Vetter F Schweinfurter Vermeidung storender und gefährlicher Druckschwingungen durch Hochdruckpumpen *VDI Ber* **748** (1989) 21 ff

[3 65] H Fritsch Hydraulische Schwingungen und ihre Dampfung in Rohrleitungen oszillierender Verdrangerpumpen *Chem Tech (Heidelberg)* **13** (1984) no 10 61–74

[3 66] W Nimitz Reciprocating Compressor Performance *Pipeline and Gas Journal* **212** (1985) 12–20

[3 67] H J Brokowski H Kayss T Wierschem Sichere Gestaltung von Arbeitsmaschinen und deren Umfeld *Chem Tech* **15** (1986) 23–26

[3 68] H Lankenau Entstehung von Schwingungen in Kolbenkompressorenanlagen unter Berucksichtigung der Wirkung von Pulsationsdämpfern in G Vetter (ed) *Verdichter Handbuch* 1st ed Vulkan Verlag Essen 1990 pp 165–173

Natex Prozesstechnologie GesmbH

Basic-Course

of

Supercritical Fluid Extraction Process

Metal Industries Research & Development Center

Kaohsiung, Taiwan, ROC

Mr TZU-CHEN KUO

Design and operation
of the
pressure vessels

8 Design and operation of the pressure vessels used in near-critical extraction processes

R EGGERS

8 1 Introduction

Industrial processes proposed for the extraction of natural products with near-critical solvents work in a pressure range between 50 bar and 500 bar, and in some exceptional cases up to 1000 bar Therefore this type of extraction must be regarded as a high pressure process The pressure vessels are very important, since it is in these that the initial extraction takes place and also in which the saturated solvent is separated from the product The design and operation of the pressure vessels have a decisive influence on the successful performance of equipment for extracting natural products with near-critical solvents While the calculation of the necessary wall thicknesses is based on well-established codes of practice for pressure vessels the mechanical design and especially the operation itself are specific to the type of extraction process considered

8 2 Classification of pressure vessels

8 2 1 Influence of process type on pressure vessel requirements

The processes for extracting natural products with near-critical solvents which are of industrial interest at the present time can be divided into four basic types or groups (Table 8 1)

Type A Extraction is from a particulate solid material and separation of the product from the solvent is effected by reduction of pressure (or change of temperature) In addition to the idealised single-stage version shown, in which one pressure vessel is used for extraction and a second one for separation, several different procedures have been developed Fractional extraction for example may be practised with several separators connected in series and working at different pressures, or 'quasi-countercurrent' extraction may be achieved with a battery of switched extractors (see chapter 1) For the basic process, the extraction vessels (Ex) on the loading side have to be charged and discharged respectively before and after each extraction and must therefore be equipped with quick opening and closing mechanisms The same applies to

Table 8 1 Basic types of near critical extraction process and the associated pressure vessels

Process type		Key to pressure vessel requirements
A Extraction of solid material with separation by reduction of pressure	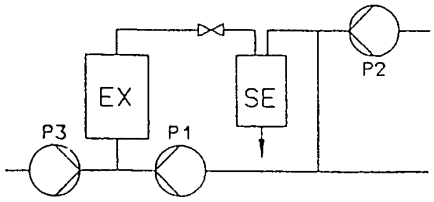	EX Extractors may be solid or multi layer vessels Quick closure system required Special inner baskets may be required SE Separators may be solid or multi layer vessels Quick closure system required Inner heating systems
B Extraction of solid material with separation by adsorption	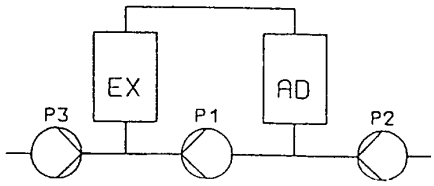	EX As above AD Adsorption vessels (solid or multilayer construction) Quick closure system required Inner baskets
C Extraction of solid material with separation by absorption	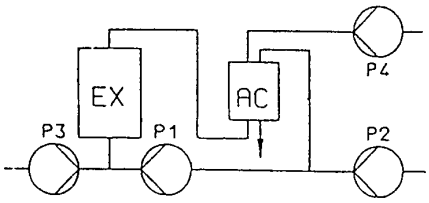	EX As above AC Absorption column Internals may include dispersing systems packings filling materials or operate as spray tower
D Continuous extraction of pumpable materials	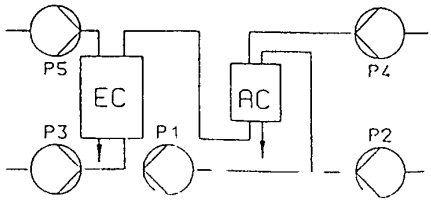	EC Extraction column with dispersing systems and sight glasses Packings filling materials required or operate as spray tower AC As above

the separation stage, if the separated extract is obtained as a solid However, the extract is often mobile so that it can flow continuously out of the pressure

vessel and thus a quick-acting closure mechanism is unnecessary for withdrawing the product

Type B In the basic process the solute is separated from the solvent (and the solvent is 'regenerated') by passing it through a bed of a suitable adsorbent In contrast to the situation with type A processes substantial pressure changes do not take place within the extractor circuit, so the pressure differential across pump P_1 is much reduced This has economic advantages in terms of energy However the associated disadvantage is that the recovery of the extract from the adsorbent is very difficult, if not impossible The separators are simple pressure vessels which can be equipped with baskets to take the adsorbents In this type of process both the extraction vessels and the vessels containing the adsorbent should have quick-acting closure mechanisms Some decaffeination processes are of type B (see chapter 5)

Type C In order to overcome the disadvantage of loss of extract involved in processes of type B, the adsorption stages may be replaced by absorption into a liquid In processes of this type the extract which has been dissolved in the solvent is absorbed by a wash fluid flowing countercurrent to the extract/solvent stream The absorption takes place in high pressure vessels which may either be operated as spray towers or as packed columns Quick-acting closures are not necessary for these vessels

Some processes for decaffeinating coffee and tea are of type C

Type D Extraction is from material which is sufficiently fluid to be pumped and the product is also a fluid In this case extraction takes place in a high pressure column in which the material to be extracted flows countercurrent to the solvent stream Depending on the product the separation takes place by release of pressure or by adsorption in standard pressure vessels or by absorption in a high pressure vessel operated as a column (Table 8 1 D) Examples of type D processes include the refining and fractionation of seed oils and the fractionation of milk fat at pilot plant scale

In addition to the high pressure vessels and columns listed above, any plant for the extraction of natural products with near-critical solvents will require pressure vessels for the supply and recovery of solvents All the pressure vessels will need to be designed manufactured and inspected to conform with national and international codes of practice

8 2 2 Classification of pressure vessels according to method of construction

Figure 8 1 summarises the most important methods of pressure vessel construction [1] In this figure a distinction is first drawn between vessels with solid walls and those with compound (or layered) walls Solid-walled vessels are normally produced as single forgings In this method of construction the

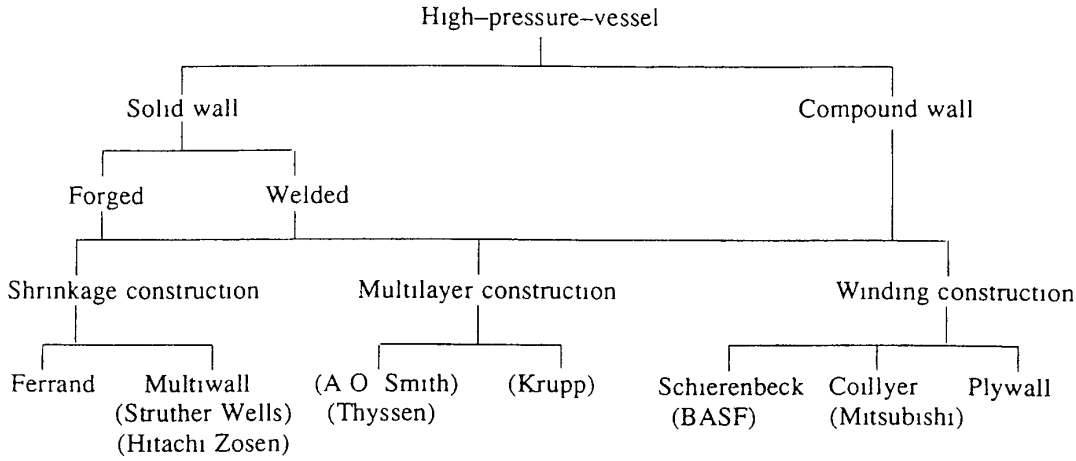

Figure 8 1 Methods of pressure vessel construction

diameter is limited to about 1 m and the wall thickness to about 150 mm Greater heights may be obtained by joining several cylinders by circumferential welding and wall thickness in excess of 200 mm may be achieved by the expedient of producing two half shells in a forging press and joining these by longitudinal welding to give the final cylinder

The technological limitations of weight and size imposed by the above construction methods for solid-walled vessels may be overcome to a large extent by using vessels with laminated walls A number of designs for such vessels are illustrated in Table 8 2 [2]

A common feature of these designs is that the pressure vessel consists of concentric steel layers These are held together by shrinkage and (in many cases) welding The diagram at the top of Table 8 2 shows a vessel consisting of two concentric weldless forged cylinders, the outer one being 'shrunk on' to the inner The diagram beneath it shows the Ferrand system in which seamless rings are 'shrunk on' to a welded central tube Beneath this again is a diagram of a system devised by J Schierenbeck In this system interlocking bands are used in place of the seamless rings used in the Ferrand system These bands are wound on the inner cylinder at temperatures above 900°C Using this procedure vessels have been constructed which can be used at pressures up to 4000 bar, even under fluctuating stress The circumferential and axial stresses are absorbed by the inner cylinder and the winding layers, as a result of the band profile Modifications of this manufacturing procedure have been proposed in which the inner cylinder absorbs all the axial stresses [3]

The remaining diagrams in Table 8 2 show vessels in which welding, as well as shrinkage, is involved A distinction should be made between (1) thick-walled layers with thicknesses above 30 mm, (2) thin-walled layers with wall thicknesses between 3 mm and approx 20 mm

Table 8 2 Alternative ways of constructing laminated high pressure vessels

Compound		Components		System	Shell construction
Mechanical	Defined shrink	Weldless forged shell		—	
		Welded central tube seamless rings		Ferrand	
	Undefined shrink	Welded central tube profiled bands		Schieren beck	
Welded		Layered vessels	Thick wall	Multiwall	
			Thin wall	–A O Smith Multilayer –Krupp	
				Coillayer	
				Plywall	

In the multiwall technique (developed by the Struthers Wells Co) single thick-walled layers are shrunk onto each other and this is followed by longitudinal seam welding The sections produced in this way can be connected by circumferential welding or by welding the forged ends

Laminated pressure vessels with thin-walled layers may be produced by a technique devised by the A O Smith Co of Milwaukee USA and subsequently used by the Struthers Wells Co This and similar techniques (Krupp, Coillayer and Plywall) are illustrated in the bottom three diagrams in Table 8 2 The shell of the multilayer system consists of concentric cylinders, each of which is itself built from three segmented layers with longitudinal seams The segments are staggered and on one side welded to the previous layer by three-plate welding (Figure 8 2)

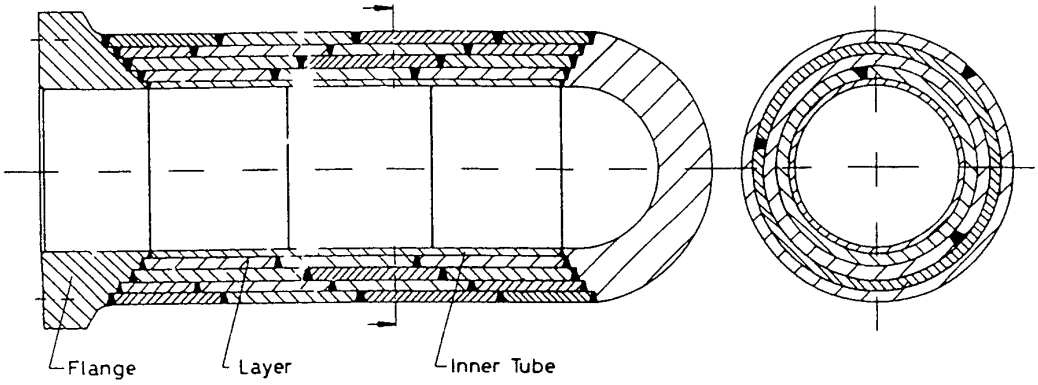

Figure 8 2 Multilayer vessel

The Krupp fabrication technique involves the use of casing cylinders, each of which is closed by a single longitudinal seam These seams are staggered so that they do not form a continous wedge through the wall thickness (Figure 8 2)

The plywall system is a combination of multilayer- and coillayer-construction The shell segments are spirally welded by three-plate welding with the layer below

8 2 3 Relative merits of multilayer and thick solid walled vessels [4]

In welded solid-walled vessels, the wall strength is dependent on the integrity of the longitudinal seam A substantial advantage of the multilayer construction is that this is no longer the case In multilayer technology, due to the way in which the longitudinal seams of the constituent layers are distributed around the vessel circumference (Figure 8 2) the vessel strength is not dependent on a single weld Although the presence of multiple layers is normally beneficial it can produce complications the insertion of a nozzle in a layered wall, for example, requires very careful design

In comparing the two types of vessel, consideration should also be given to properties such as the tensile strength, yield strength ductility homogeneity

and corrosion-resistance of the construction materials used and the way in which these can influence the design in the two cases The elastic constants have much the same importance in the two cases though it is of much greater importance to ensure homogeneity with solid-walled vessels than with multi-layered ones (The latter exhibit the composite principle of crack arrest since a crack in one layer, coil or wire does not propagate to others) The resistance to corrosion is of course of the same importance for both solid and multi-layered-wall pressure vessels Nevertheless, it is much easier to solve a particular corrosion problem with the multilayer vessel, because it is only necessary to select a corrosion resistant material for the inner lining

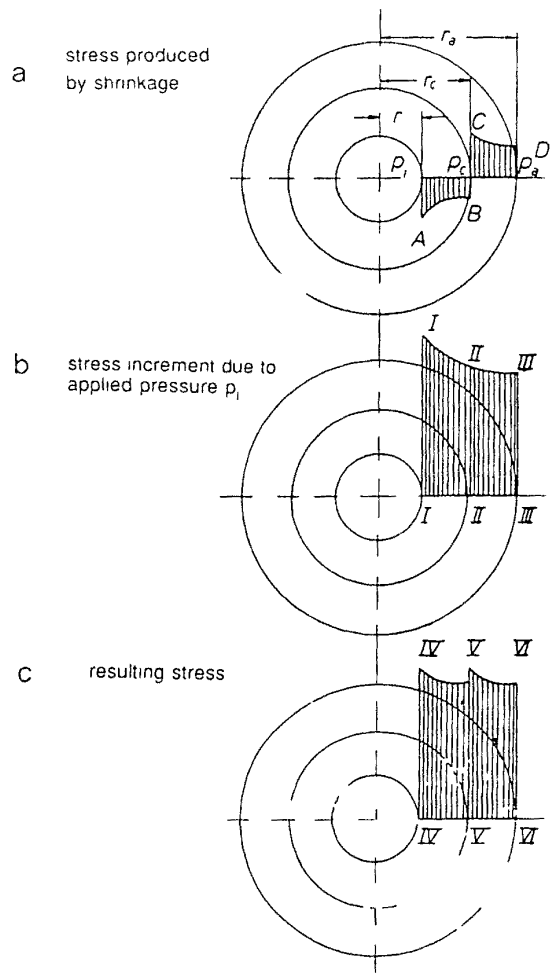

Figure 8 3 Circumferential stresses in a layered wall

Finally mention must be made of some problems which are specific to multilayered technology and which have no parallel in the solid-wall situation

As can be seen from Table 8 2, each element of the multilayer wall consists of a sheet of thin metal which is wound tightly round preceeding sheets after being rounded in a bending machine without the help of bending moulding It

is inevitable therefore that, while zones exist where the contact between the layers is very intensive, there are also other zones where the contact is less intensive or even non-existent because of gaps between the layers This problem is inherent in designs with indeterminate shrinking qualities and in turn determines the manner in which the multilayer wall can be stressed Only under conditions of uniformly intensive contact between layers will there be a similarity to the solid wall Therefore the aim of the fabrication must be to avoid gaps and to obtain a composite wall which is as dense as possible

The initial stress produced by the shrinkage operation is closely related to the subsequent behaviour of the vessel when it is subject to internal pressure A high initial stress favours good contact between the layers and therefore improves the subsequent stress distribution (Figure 8 3)

A further criterion for assessing multilayer vessel design and fabrication is without doubt, the effective thermal conductivity of the vessel wall The transfer of heat through the wall is more or less hindered by the layered cylinder design according to whether contact between the layers is poor or good

In consequence the effective conductivity depends on the pressure within the vessel and the direction of heat flow (both aspects influence the contact between the individual layers) A high pressure improves the effective conductivity as does a heat flow from the inside to the outside (the thermal expansion of the inner layers is then greater than that of the external ones)

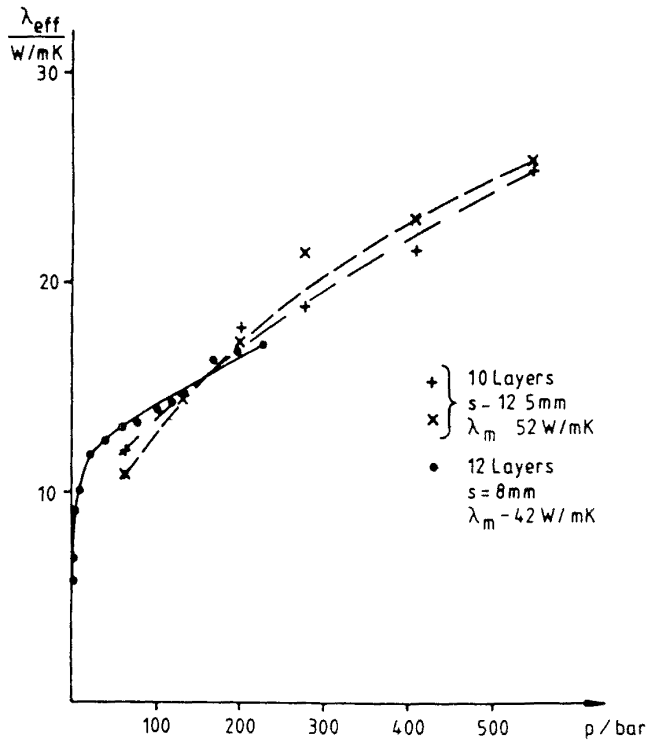

Figure 8 4 Effective thermal conductivity of a layered wall as a function of pressure

On the other hand, external heating of the pressure vessel decreases the thermal conductivity of the layered wall

It is difficult to calculate the effective heat transfer coefficient theoretically because the gap widths are not known exactly, can change with pressure and are not of uniform size Experience shows, however, that the thermal conductivities of laminated walls are typically between $\frac{1}{3}$ and $\frac{1}{4}$ of those for a solid wall made of the same material [5] and they are, as noted above, pressure dependent The pressure dependence is particularly marked at low pressures (Figure 8 4) This fact can be particularly important when thermal calculations are required on batch extraction vessels which require periodic exhaustion and recharging and which consequently undergo substantial pressure changes during the working cycle This situation is of frequent occurrence in plant for extracting natural products with near-critical solvents

8 2 4 Examples of solid-walled and multilayer extraction vessels

Figures 8 5 and 8 6 show two pressure vessels which are used as extractors The solid-walled vessel (Figure 8 5) has an inner volume of 2 m^3 and is used for the extraction of hops A special feature of this extractor is the inner

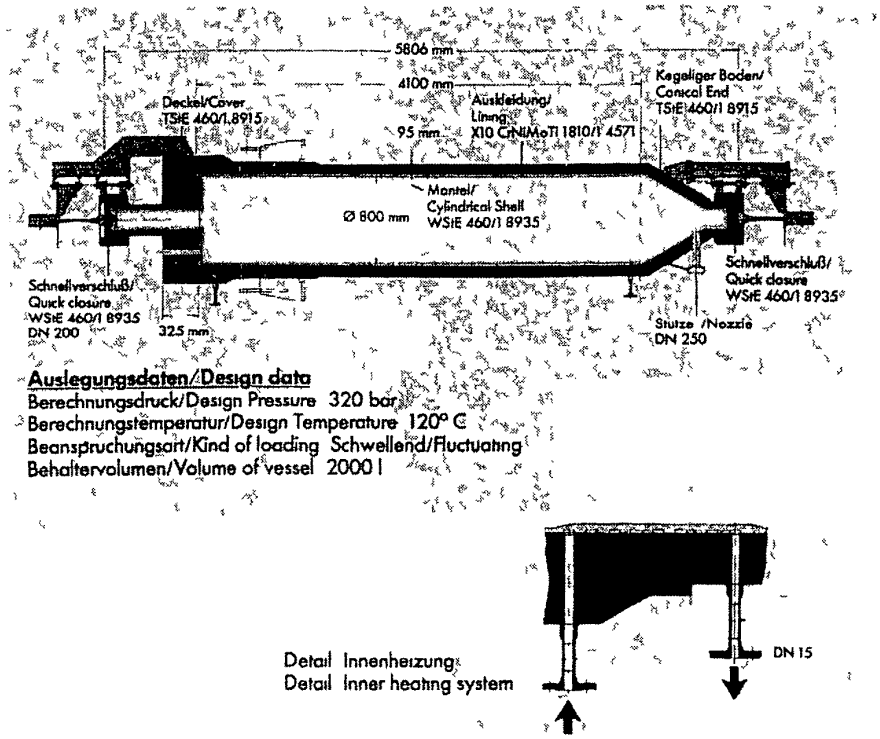

Figure 8 5 Extraction vessel with clamp closure at the bottom Solid walled construction with inner heating (Krupp) Design data pressure = 320 bar temperature = 120°C kind of loading = fluctuating volume of vessel = 2000l

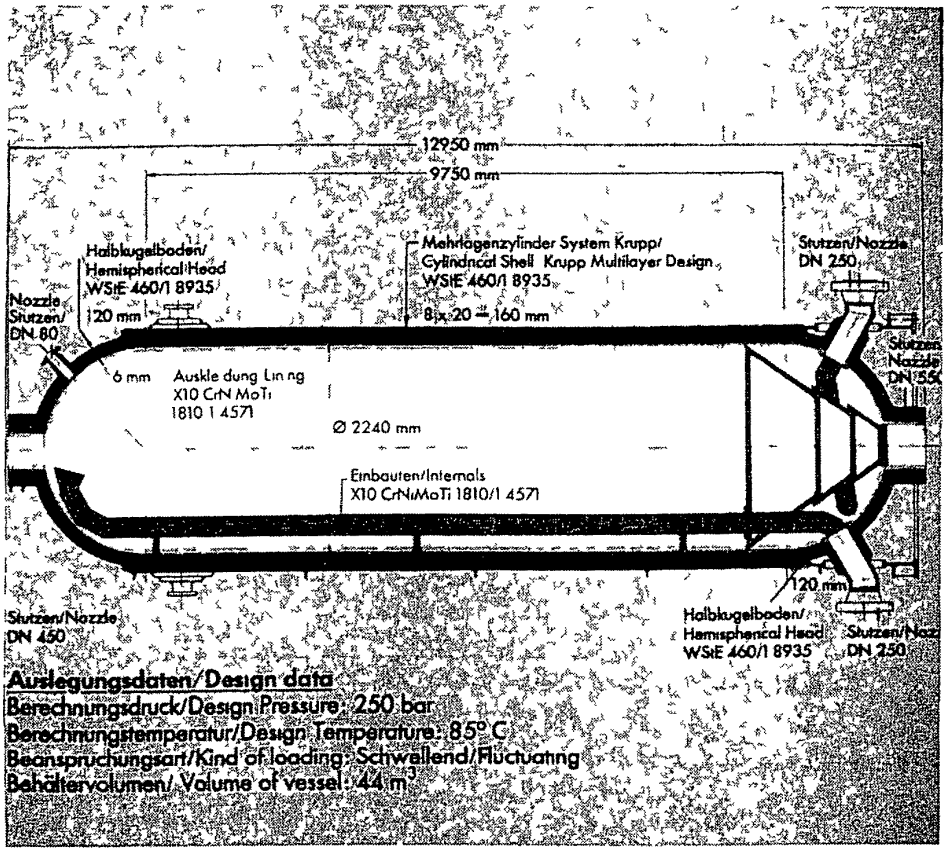

Figure 8 6 Extraction vessel of multilayer construction (Krupp) Design data pressure = 250 bar temperature = 85°C kind of loading = fluctuating volume of vessel = 44 m^3

lining This is provided with ports extending outside the main pressure vessel and protects the pressure bearing walls of the latter from corrosion Its presence also facilitates the installation of an internal heating system as shown in the inset to Figure 8 5 The multilayer vessel (Figure 8 6) is used as an extraction vessel for the decaffeination of raw coffee Its inner volume is 44 m^3 and its layered wall construction consists of 8 layers of 20 mm thickness each

8 3 Vessel design

8 3 1 Process engineering criteria sizing the vessels

The geometry and size of the pressure vessels (A to D in Table 8 1) are determined by both mechanical and process engineering requirements The relevant process variables of importance are listed in Table 8 3 Solubility of hop extract in CO_2 as a function of pressure is shown in Figure 8 7 and rate of extraction of hops with CO_2 in Figure 8 8

In order to illustrate the sizing of a vessel in a typical case it is convenient to take as an example an extractor used for the extraction of hops with

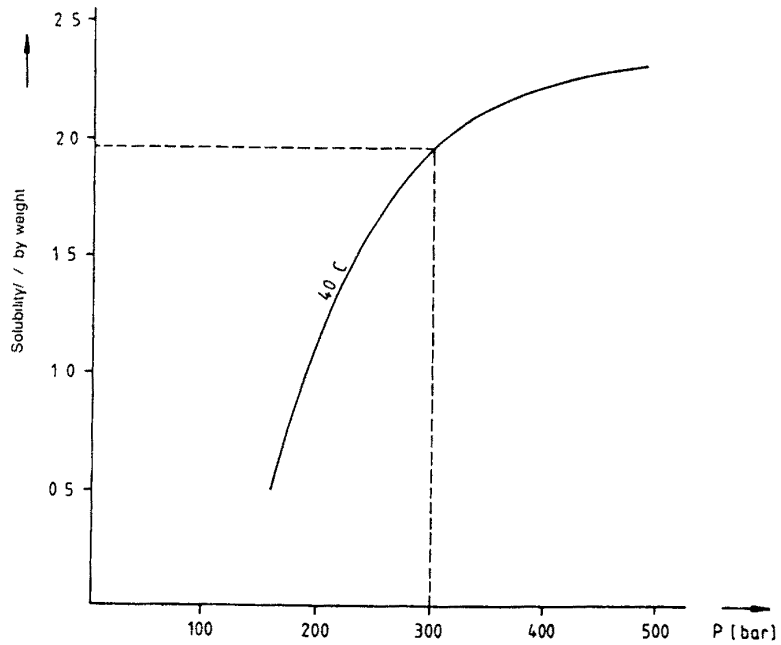

Figure 8 7 Solubility of hop extract in CO_2 as function of pressure at 40°C

supercritical carbon dioxide This batch extractor is typical of those used in type A processes (Hop extraction with liquid carbon dioxide is described in chapter 4) The extractor is to be one of a series each of which will be 'on-line' for a period *t* after which it will be 'off-line' for an equal period during which it is being emptied of exhausted hops, refilled with fresh pellets and brought

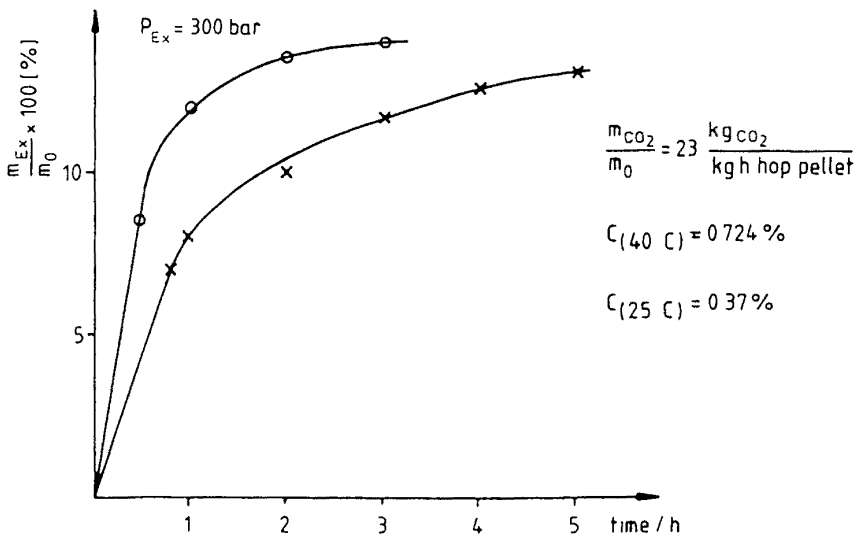

Figure 8 8 Rate of extraction of hops with CO_2 at 300 bar 40°C (data for 25°C shown on lower curve) m_{Ex} = mass of extract collected m_0 = initial mass of hops

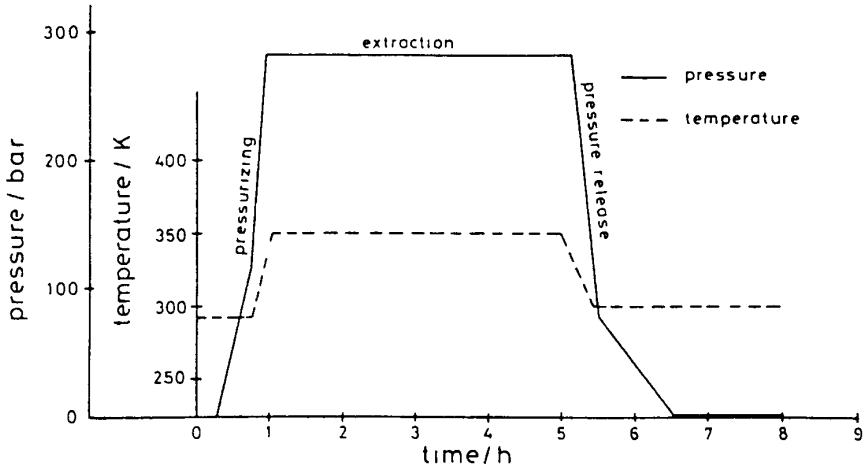

Figure 8 9 Cycle of pressure and temperature changes in a typical batch extractor vessel (see example in section 8 3 1)

back to pressure (see Figure 8 9) According to the above cycle a freshly charged extractor will be inserted every t hours

The calculation of extractor height and volume for the required production capacity and a trial set of process variables is outlined below, together with relevant data from laboratory and pilot plant tests

Required production capacity $M = 1300$ tonnes of hop pellets per annum

Proposed extraction temperature and pressure $\theta = 40°C$, $P = 300$ bar

Table 8 3 Process variables influencing the geometry and size of the pressure vessels used in near critical extraction plant

Extractor (Process types A–C)	Separator (Process type A)	Adsorber (Process type B)	Extraction and absorption columns (Process types C and D)
Productivity	Mass of extract	Mass of extract	Flow regime/ flooding point
Bulk density	Density of extract	Bulk density of adsorbent material	Packing/filling material
Extraction time with charging	Fluidity of extract		Mass transfer/NTU
Process days per year	Particle diameter (If extract is in powder form)	Loading profile	
Process hours per day		Pressure drop	
		Retention of solid material (permissible flow velocity)	
Flow velocity (Residence time of solvent)			
Phase equilibria solvent/extract			
Mass transfer kinetics			

The process types A to D are defined in Table 8 1

Density of CO_2 under extraction conditions	$\rho_{CO_2} = 911\ kg/m^3$
Bulk density of bed of hops	$\rho_B = 400\ kg/m^3$
Bulk porosity	$\varepsilon = 0\ 56$
Working days per year	$n = 300$ d/a
Working hours per day	$z = 24$ h/d
Extraction time excluding charging and discharging (defined above)	$t = 4$ h (see Figure 8 9)
Bed volume within extractor is now calculated from above information	$V = (M\ \ t)/(\rho_B\ \ n\ \ z)$ $= 1\ 8\ m^3$
Mass flow rate of CO_2 per kg of hops in extractor	$(m_{CO_2}/m_0) = 23$ kg CO_2 per hour per kg of hops (trial value)
Mass transfer kinetics at above specific flow rate, concentration C of hop extract in initial 'constant loading' period (see chapter 7) has been determined in small-scale tests	$C =$ (initial gradient of curve for 40°C in Figure 8 8)) $\times (m_0/m_{CO_2})$ $= 0\ 72\%$ at 300 bar, 40°C
(This may be compared with the equilibrium concentration	$C^* = 1\ 9\ \%$ at 300 bar, 40°C (Figure 8 7))

Residence time

$$\tau = \left(\frac{\text{Volume of free space in bed of hops}}{\text{Volume flow rate}}\right)$$

$$= \left(\frac{m_0}{m_{CO_2}}\right) \times \left(\frac{\varepsilon}{\rho_B}\right) \times (\rho_{CO_2}) = 200\ \text{s}$$

Superficial velocity	$W = 10$ mm/s
Required height	$H = (W/\varepsilon) \times \tau = 3\ 6$ m
Bed diameter	$D = 760$ mm

The above values for height and diameter are for the bed of hops within the extractor The actual inner dimensions of the extractor are a little larger so that uniform flow of the solvent can be obtained at the entry and exit points and to allow for various fittings In practice the vessel is as in Figure 8 5 (total volume 2 m^3 inner height 4100 mm inner diameter 800 mm)

8 3 2 Construction

The safe construction of vessels is based on the theory of elasticity and plasticity Rules for the calculation of the required wall thicknesses and associated tests are given in national codes Examples of these are in Germany AD Merkblatter (Arbeitsgemeinschaft Druckbehalter) in Great Britain, appropriate British Standards Specifications (e g BS 5500 for welded vessels) and in

the USA, Boiler and Pressure Vessel Code of the American Society of Mechanical Engineers (ASME)

Although the national codes form the basis for mechanical design and construction, further experimental investigations may be required [6], especially if the vessel geometry is non-standard, to investigate potentially dangerous stress concentrations due to

- nozzles, sectors and their stiffenings,
- tube reactions and their effects on the pressure wall,
- vessel supports,
- installation of fittings,
- deformation of vessel flanges and cover,
- initial stress and relaxation of screws under changing forces and friction,
- temperature distribution in nozzles wall, flanges and supports,
- direct and indirect heat stresses

For a given internal pressure p_i and as long as the elastic limit of the material is not exceeded at any point in the wall, the elastic stress may be represented as three main stresses at right angles to each other These are given by the LAME equations as functions of radius and the ratio of the external to the internal diameters [6, 7, 8]

The relevant equations for cylinders are as follows

For circumferential (or tangential) stress

$$\sigma_t = p_i \frac{(r_a/r)^2 + 1}{(r_a/r_i)^2 - 1} \tag{8 1}$$

For radial stress

$$-\sigma_r = p_i \frac{(r_a/r)^2 - 1}{(r_a/r_i)^2 - 1} \tag{8 2}$$

For axial (or longitudinal) stress

$$\sigma_a = p_i \frac{1}{(r_a/r_i)^2 - 1} \tag{8 3}$$

In the above equations r is the radius r_a and r_i are the external and internal radii

Under an internal pressure the highest tensile stress for a pressure vessel is the circumferential stress at the inner radius ($r = r_i$)

Various theories have been formulated in which the above stresses are used to compute 'worst stresses σ_v within given structures (such as cylindrical shells) These theories have been taken into account in the formulation of the national codes for pressure vessel design, as indicated in Table 8 4 This table lists several relationships for calculating minimum permissible wall thickness for cylindrical shells as a function of internal radius and pressure σ_{code} in these

equations is the maximum design stress allowed by the code in question In general

$$\sigma_{code} \leqslant (K/S) \tag{8 4}$$

K is a specified measure of the strength of the material (e g the ultimate tensile strength or the yield stress) and S is a safety factor usually between 2 and 4 when the UTS is used, or about 1 5 in the case of the yield stress

The use of the following equations, given in the AD Merkblatter code [9] is legally enforced for vessel design in Germany

For $r_a/r_i < 1\ 2$ (thin-walled pressure vessels AD Merkblatter B1)

Table 8 4 Typical design equations for cylindrical pressure vessels with their theoretical background

Theoretical approach	Maximum stress as function of internal pressure and ratio of external to internal radii	Minimum permitted wall thickness (s)	National Code
Expression derived from membrance shell theory (based on maximum tensile strength)	$\sigma_v = p_i \dfrac{1}{r_a/r_i - 1}$	$\dfrac{s}{r_i} = \dfrac{p_i}{\sigma_{code}}$ and also modified formulae	Basics of the the German code (AD Merkblatter)
Expression based on maximum direct stress	$\sigma_v = p_i \dfrac{0\ 6\ (r_a/r_i) + 0\ 4}{(r_a/r_i) - 1}$	$\dfrac{s}{r_i} = \dfrac{1}{(\sigma_{code}/p_i) - 0\ 6}$	
Equation (8 1) taken at maximum stress ($r = r_i$)	$\sigma_v = p_i \dfrac{(r_a/r_i)^2 + 1}{(r_a/r_i)^2 - 1}$	$\dfrac{s}{r_i} = \left(\dfrac{\sigma_{code} + p_i}{\sigma_{code} - p_i}\right)^{1/2} - 1$	ASME Code (US) $r_a/r_i \leqslant 1\ 5$
Maximum shear stress taken as criterion	$\sigma_v = p_i \dfrac{2\ (r_a/r_i)^2}{(r_a/r_i)^2 - 1}$	$\dfrac{s}{r_i} = \dfrac{1}{(1 - 2(p_i/\sigma_{code}))^{1/2}} - 1$	
Theory of von Mises and Maxwell [27 28]	$\sigma_v = p_i \dfrac{\sqrt{3}\ (r_a/r_i)^2}{(r_a/r_i)^2 - 1}$	$\dfrac{s}{r_i} = \dfrac{1}{(1 - \sqrt{3}\,(p_i/\sigma_{code}))^{1/2}} - 1$	

$$s = \frac{p_i\ r_a}{20\ (K/S)\ \nu + p_i} + c_1 + c_2 \qquad [\text{mm}] \tag{8 5}$$

where s = minimum permitted wall thickness r_a = outer radius (mm), r_i = inner radius (mm), p_i = process pressure (bar), S = safety factor, K = elastic limit (N/(mm)^2), ν = attenuation factor c_1 and c_2 are supplementary factors

For the range $1\ 2 < r_a/r_i < 1\ 5$ the following equation (AD Merkblatter B10) must be used

$$s = \frac{2\ p_i\ r_a}{23\ (K/S)\ \nu - p_i} + c_1 + c_2 \qquad [\text{mm}] \tag{8 6}$$

Wall calculations for multilayer vessels (see Figure 8 2) must be carried out using the special VD TUV Merkblatter code [10] which is based on the well-known diaphragm formula Each layer can be considered to be sufficiently thin for a constant average value to be used for the stresses that occur within it

$$s = \frac{2\ p_i\ r_i}{20\ (K/S)\ \nu - p_i} + c_1 + c_2 \qquad [\text{mm}] \qquad (8\ 7)$$

r_i is the inner radius of a multi-layer vessel (mm) and c_1 and c_2 are supplementary factors to the wall thickness

Secondary stresses caused by differences in temperature have to be added to the main stresses

The elastic limit K of the entire wall is calculated as

$$K = \frac{K_i S_i + n k_l s_l}{s_i + n s_l} \qquad (\text{N mm}^{-2}) \qquad (8\ 8)$$

where K_i = elastic limit of the inner tube, K_l = elastic limit of the layer, s_i = wall thickness of the inner tube, s_l = wall thickness of the layer and n = number of layers

An average value for the attenuation factor ν for the entire wall is used with data for the inner tube (i) and the layers (l)

$$\nu = \frac{s_i \nu_i + s_l (n - 1 + \nu_l)}{s_i + n s_l} \qquad (8\ 9)$$

Further equations are required to allow for nozzles and changes in contour

Present high pressure extraction technology involves extracting solid materials (usually these are natural products) discontinuously in high pressure vessels From a mechanical point of view, the charging and discharging process produces a fluctuating pressure loading on the pressure vessel (see Figure 8 9) Because of this the permissible stress σ_{code} must be reduced As an example, the wall thickness of the pressure vessel shown in Figure 8 5 is 95 mm according to AD Merkblatter B10 and S1 for the construction material WSTE 460 1 and fluctuating loading [9] at an assumed loading number $N = 10^4$

It is a requirement of the food laws that areas of the pressure vessel in contact with the product during the extraction of natural substances for human consumption must be made of stainless steel This necessitates the use of austenitic steel As a special feature, the pressure vessel shown in Figure 8 5 is equipped with a lined conical bottom constructed of a special steel which retains its strength at low temperatures This precaution was considered necessary since it is possible to produce very low temperatures when depressurising the vessel at the end of the extraction (see section 8 4 3)

Natex Prozesstechnologie GesmbH

Basic-Course

of

Supercritical Fluid Extraction Process

Metal Industries Research & Development Center

Kaohsiung, Taiwan, ROC

Mr TZU-CHEN KUO

Pumps and Compressors for Supercritical Extraction

9 Pumps and compressors for supercritical extraction design, characteristics and installation

G VETTER

9 1 Introduction

Supercritical extraction processes entail pumping, ducting and metering the flow of fluids over a very wide range of conditions These may range from pressures not far above the vapour pressure of the subcritical fluid in the solvent recovery stage, to pressures upwards of 400 bar for the supercritical fluid in the main extraction unit This range of conditions is almost unique to supercritical extraction processes, although there are on the horizon additional potential applications for supercritical fluids and these will require similar high pressure pumps and compressors [1–5] These potential applications include the use of supercritical reactions and also the production of fine powders and other deposits by controlled expansion of solutions in supercritical solvents (see chapter 3) High pressure machinery such as pumps and compressors, are at the very core of all high pressure plant, and influence the economy, safety and reliability of the plant in a most important manner [6]

The challenge for the high pressure engineer is to cope with the problems of sealing, fatigue, wear, installation and vibration which arise in each specific application The solvents to be pumped in supercritical extraction plants show poor lubrication properties and therefore require special seals The co-solvents which are sometimes used are hydrocarbon-based in many cases, so that leakage must be prevented to avoid pollution and the risk of explosion

Another problem is that, in the near-critical and supercritical region, the solvents must be regarded as somewhat compressible Consequently pulsations can be excited if reciprocating pumps are used

The high pressures – up to 400 or even 600 bar – generate high stresses and strains in the liquid-containing parts combined with cyclic changes This leads to fatigue Special materials and techniques of design and manufacture are required to combat this

The principal solvent is usually CO_2, though various organic entrainers or co-solvents such as C_3H_8 C_4H_{10}, C_2H_4, C_3H_6 and many others [7 8, 9] may also be present

9 2 Process requirements

Supercritical extraction processes show similar requirements with regard to high pressure fluid machinery as do high pressure processes for reactions However, since the principal solvent is usually CO_2 the corrosion and erosion aspects are less demanding than is the case in reaction processing Also the temperature will not usually be high since a limit to the allowable temperature is often set by the properties of the components and the required quality of the products

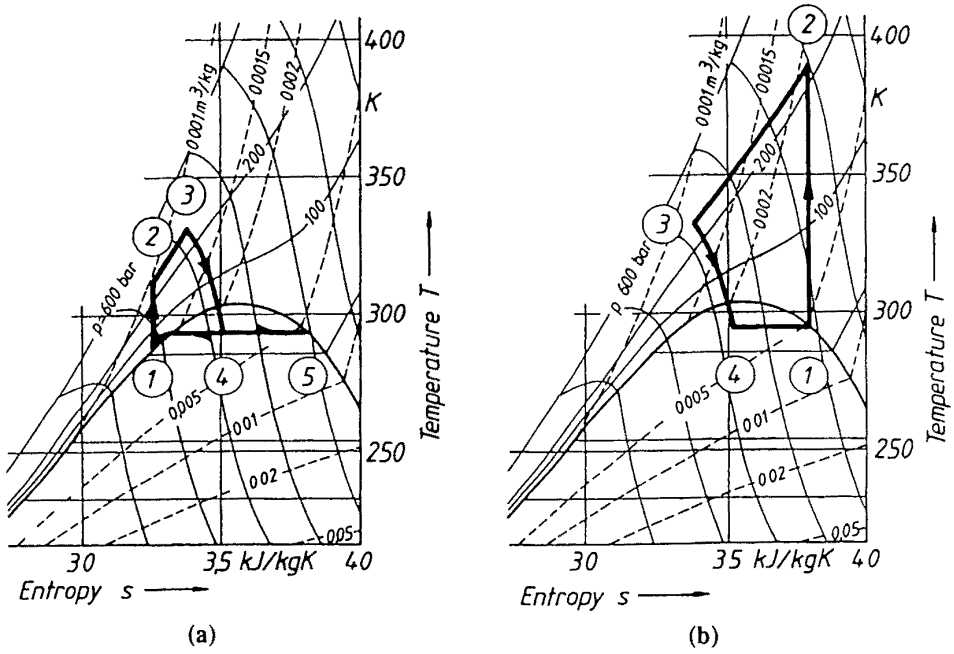

Figure 9 1 State of solvent (here CO_2) during cyclic throttling and recompression shown on a TS diagram (a) with liquid compression and subcritical separation (b) with gas compression

In many (though not all) cases, product recovery and solvent regeneration are effected by passing the stream from the extractor through a throttling valve to the separation unit, where conditions are subcritical The solute is here thrown out of solution and the regenerated solvent is recompressed to the extraction pressure Because of the higher temperatures generated when vapour compression is used and also for economic reasons, the solvent is usually recompressed in the liquid, rather than in the vapour, state The need for this is illustrated in Figures 9 1a and 9 1b which are for liquid and vapour compression respectively The solvent is CO_2 and the desired extraction conditions are shown as point 3 It is seen that in the vapour compression case the temperature rises substantially and that the stream must be cooled before entering the extractor warming is required at this stage in the liquid case When designing the liquid pumping system in the above situation it should be

remembered that there is the danger of pump cavitation when liquid is pumped up from a pressure not greatly exceeding the vapour pressure

Depending on the scale and nature of the extraction problem, it may be necessary to design the extraction process for continuous or discontinuous operation and for single or multistage extraction Furthermore various different separation techniques may be used

9 2 1 Continuous extraction processes

Figure 9 2 shows a continuous process where product recovery is brought about in two stages of pressure reduction The regenerated solvent is finally repressurised by the liquid pump 1 The system is initially charged with solvent by the pumps 2, which also control the solvent mixture and replace any losses The fluid to be extracted is raised to the necessary pressure by pump 3 and, after premixing with solvent in mixer 5, passes to the extraction column 6 The bottom product from this column passes to outlet 9 while the top stream undergoes two stages of pressure reduction at throttling valves 7 After each throttling operation the stream passes through a heat exchanger 8 to adjust the temperature to a suitable value for the separation of the appropriate 'cut' of the top product from the solvent stream The separation takes place in the separators 12, the product outlets being at 10 and 11 After leaving the second separator the solvent is condensed in heat exchanger 13 and returns in the liquid state to vessel 14 for recompression The pump suction temperature may be controlled by heat exchanger 15

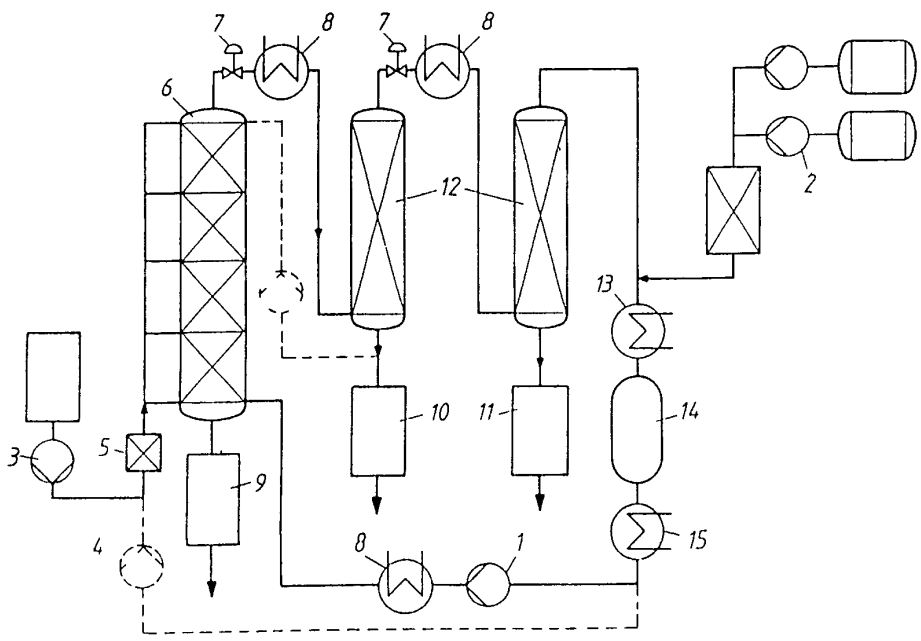

Figure 9 2 Continuous extraction process in which product recovery is by two stage throttling (see text)

9 2 2 *Discontinuous extraction processes*

Bulk solids, such as coffee beans, tea and hops, are normally extracted in a discontinuous manner (see chapters 4, 5 and 6) The material to be extracted is charged into a pressure vessel (or vessels) and compressed solvent is passed through it until the contents have been extracted to a sufficient extent The vessel is then disconnected from the solvent feed and the contents are discharged [10] The exact details of the process depend largely on the properties of the material being extracted A group of automatically accessible extractors operated in semi-continuous mode is normally used One of the extractors in the group is off-line' (being depressurised, discharged of extracted material and recharged) while the solvent stream passes in series through the remaining ones

The extraction vessels are usually interchanged in a sequence which gives pseudo countercurrent flow of the solids with respect to the solvent stream A generalised diagram illustrating the mode of operation is given in Figure 9 3 Solvent regeneration and product recovery in the case shown is by single stage throttling, though other methods are often used In some decaffeination plant, for example, the carbon dioxide solvent is regenerated by washing with water or by passing through a bed of activated carbon at much the same pressure as that in the extractor (see Figures 6 1 and 6 2) Throttling expansion is not used in these cases and the pumping requirements are less demanding

The solvent in Figure 9 3 is circulated continuously by the circulation pump 1 and the amount of solvent in the system is maintained by the filling pump 2 Pump 3 can be used to add water or co-solvent The series of 'on-line

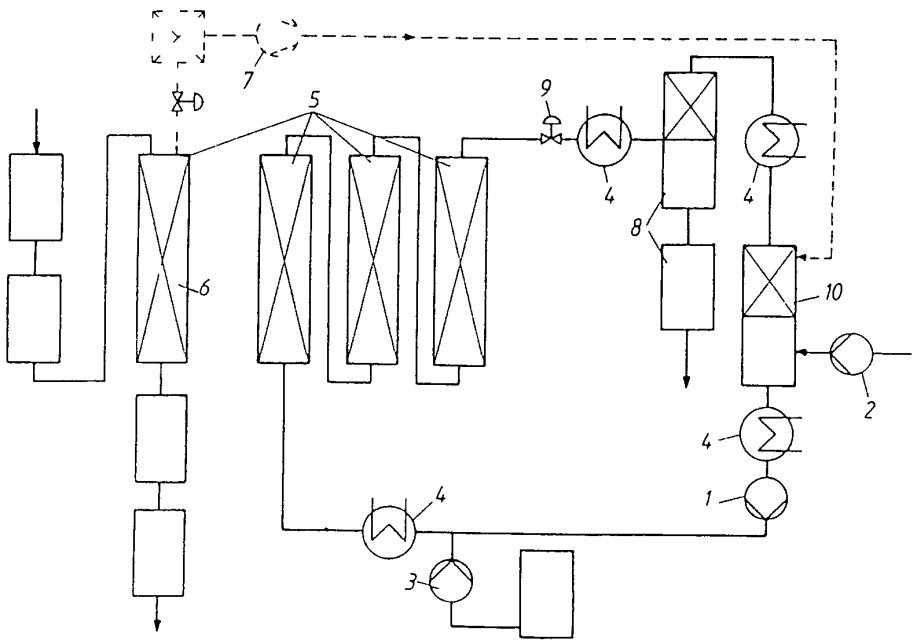

Figure 9 3 Discontinuous extraction process (see text)

extractors 5 is fed with solvent which has been preheated by heat exchanger 4 The extractor (6) is off-line being emptied and then recharged by a system appropriate to the particular application As discussed in section 5 7 1 2 , it can be economic to reuse at least part of the solvent gas discharged from 6 by recompressing with compressor 7 The separation vessels 8 which follow the throttling valve 9 and the heat exchanger 4 are similar to those illustrated in Figure 9 2, and the method of condensing and then repressurising the solvent is also similar

Typical data for the high pressure solvent pumps used in the processes described above are given in Table 9 1

Table 9 1 Typical pump requirements

Application	Discharge pressure (Pressure differential)	Temperature	Capacity
Compression and circulation	100–400 (600) bar 50–300 (600) bar	10–30°C	(0 05)–100 m^3/h
Filling	100–300 bar 50–250 bar	10–30°C	1–200 m^3/h
Circulation (and compression)	100–400 bar 10–100 bar	50–100°C	50–1500 m^3/h

There are a number of other applications of pumps and compressors in supercritical extraction plant The exact nature of these depends on the particular process Examples are

- transport pumps for conveying solvents from storage to the extraction plant (typically 10–50 m^3/h at pressure 50–60 bar),
- transport pumps from tank truck to storage (at low pressure and temperature),
- metering pumps for solvent/entrainer replacement and blending
- metering pumps for water injection,
- transport pumps for the fluids to be extracted or treated
- compressors for recycling gaseous solvent

9 3 Pumps for liquids

9 3 1 Pump characteristics and the selection of the best type of pump

The selection of pumps for extraction plants is based on an evaluation of the optimum design with respect to energy efficiency, characteristics, control pulsation, the net positive suction head which is required safety reliability, lifetime, maintenance, total investment and space requirements In the light of the above it will be necessary to decide whether to use centrifugal or reciprocating pumps As a general rule centrifugal pumps are best for large capacity

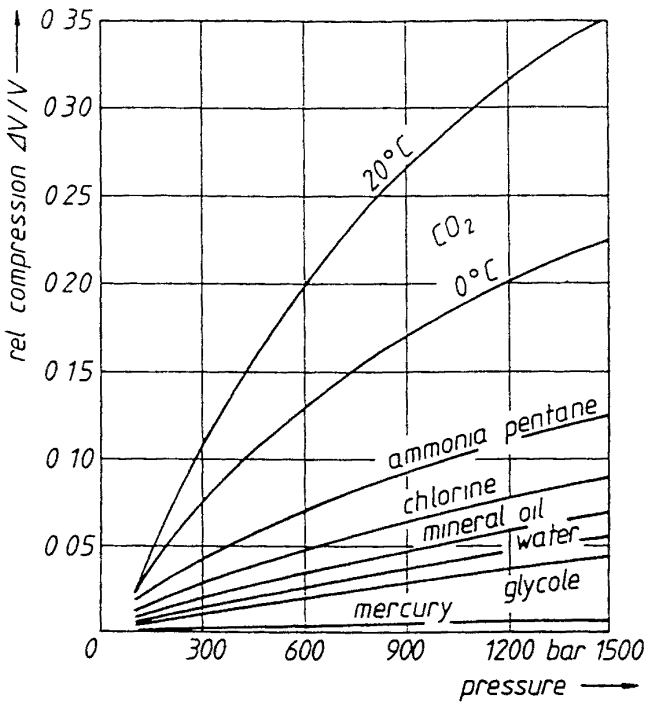

Figure 9 4 Relative volume compressions of various liquids (constant temperature)

applications and reciprocating ones are best for small throughputs For some applications, the decision is clear-cut However, there is an overlapping zone where there is little to choose between the two types of pump on the grounds of efficiency, capacity and costs The final decision may then depend on other factors The solvents (basically CO_2) used in supercritical extraction require pumping under conditions where they show substantial fluid compression (Figure 9 4) and associated with this there will be temperature changes Because of their compact design, high speed and non-pulsating performance, centrifugal pumps show many advantages compared with reciprocating pumps when operating under the above conditions If therefore efficiency calculations of the type outlined below show that if it is at all reasonable to use a centrifugal pump one should be used

9 3 1 1 Head power and efficiency characteristics of pumps The total head (H) generated by a pump in a plant consists of pressure, potential and dynamic components (Figure 9 5)

$$H = \frac{p_d - p_s}{\rho\ g} + z_d - z_s + \frac{v_d^2 - v_s^2}{2g} \qquad (9\ 1)$$

where ρ is the fluid density and g the gravitational constant Other notation is as in Figure 9 5 The power requirement (P) on the shaft (Figure 9 6) is given by

$$P = P_v + P_L + P_{fh} + P_{fm} \qquad (9\ 2)$$

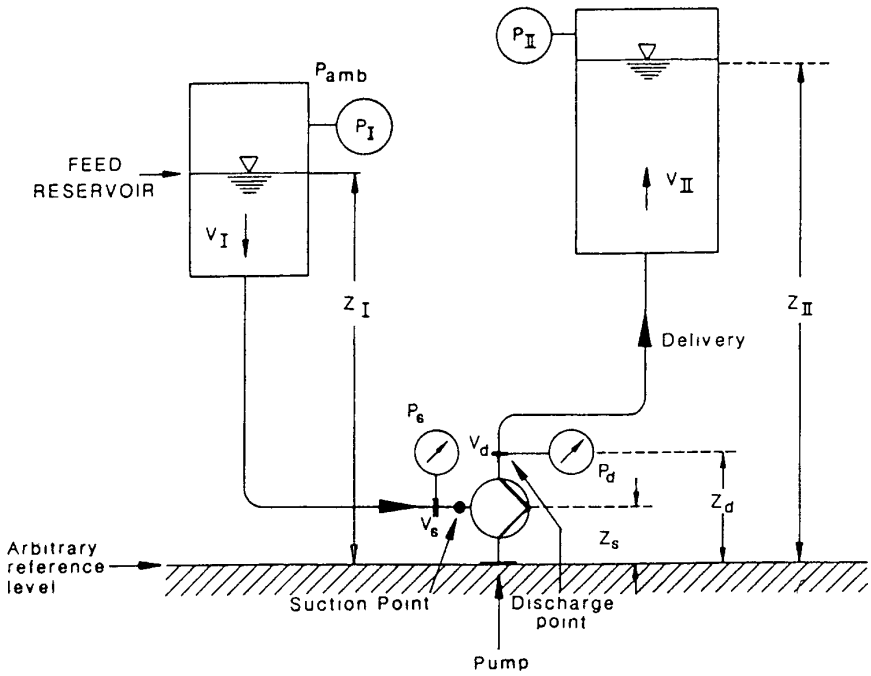

Figure 9 5 Notation used in pressure and head equations for pumps (p z and v are the gauge pressure height and velocity respectively and subscripts d s and I denote the discharge and suction points and the feed reservoir p_{amb} is ambient pressure

P in equation (9 2) is written as the sum of the total hydraulic power (P_v) required to produce the outlet flow the power (P_L) required by leakage flows, and the power required to overcome hydraulic friction (P_{fh}) and mechanical friction (P_{fm}) The pump efficiency η is given by

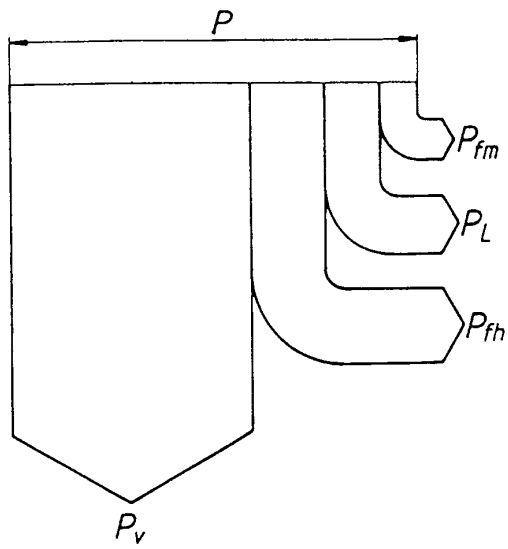

Figure 9 6 Power requirements and energy losses of pumps (see equation (9 2) in text)

$$\eta = \frac{P_V}{P} = \frac{\rho \ g \ H \ V}{P} \tag{9 3}$$

η is largely determined by the method of pressure generation Either a reciprocating or a centrifugal pump may be used for this purpose (Figure 9 7) In order to generate a substantial pressure using a centrifugal pump, a large flow velocity is required, the head per stage being dependent on the square of the rotor circumferential speed u Letting ψ be the pressure coefficient, g the acceleration due to gravity and i the number of stages we can write

$$H_{tot} = i \ \psi \frac{u^2}{2g} \tag{9 4}$$

where H_{tot} is the total head

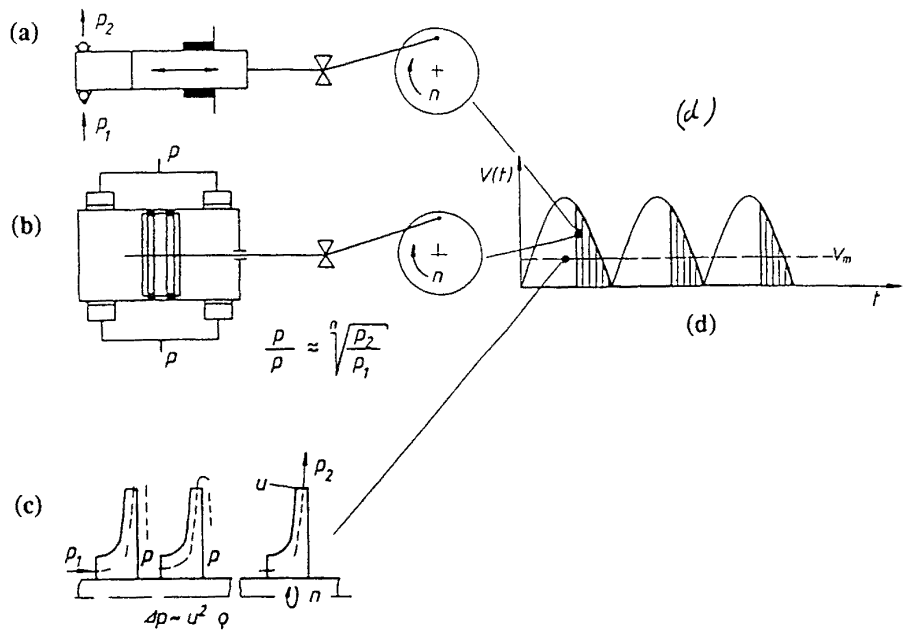

Figure 9 7 Methods of pressure generation (a b) reciprocating pumps/compressors (c) multistage centrifugal pumps (d) Pulsations in volume flow produced by above pumps

Because of the large flow velocities which are required (10–100 m/s) hydraulic friction losses as well as losses due to internal leakage through the rotor clearances are high The total efficiency of centrifugal pumps depends on the specific speed n_q (Figure 9 8) [11 12]
The specific speed n_q, is given by

$$n_q = n \ \frac{\sqrt{V}}{H^{3/4}} \tag{9 5}$$

where n is the rotor speed and V is the volumetric flow rate It may be seen from Figure 9 8 that the efficiency falls as n_q is reduced sharply so at low values of n_q For the flow rates usually encountered in extraction plants

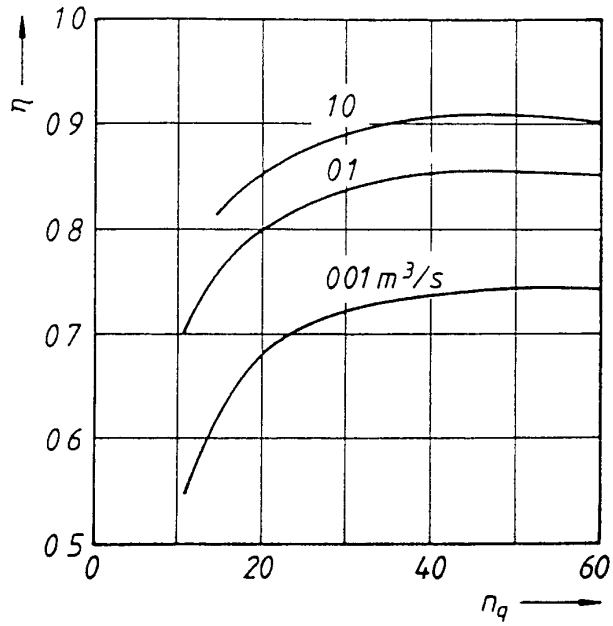

Figure 9 8 Efficiency (η) as function of specific speed (η_q) for typical centrifugal pump [11] volumetric flow rate is given as parameter n_q is given by equation (9 5) in text

($V < 0\ 01 - 0\ 1\ m^3/s$) the specific speed per pump stage should not be less than 10 or 20 depending on pump capacity For specific speeds in this range the pressure coefficient of equation (9 4) ≈ 1 (In calculating n_q, V is expressed in m^3s^{-1}, H in m and n in min^{-1}) For $n_q < 10$ the efficiency decreases rapidly, especially at low volume flows, to values that are not acceptable Increasing the number of stages improves n_q by reducing the head per stage, but the number cannot be increased indefinitely due to the excessive shaft length which results This introduces bearing and vibration problems and also adds to the cost

A reciprocating pump generates hydrostatic pressure by the direct transmission of mechanical forces F from the piston within the working chamber (cross section area A) to the fluid

$$H = \frac{\Delta p}{\rho g} = \frac{F}{A\rho g} \tag{9 6}$$

The flow rate is usually small when a reciprocating pump is used and because of this, the hydraulic friction losses are negligible (i e $P_{fh} \approx 0$) Piston clearances are very small to avoid leakages ($P_L \approx 0$), however mechanical losses P_{fm} are of a similar magnitude to those experienced for centrifugal pumps The head or pressure differential per stage is not influenced by the pump speed and clearance leakages are negligible Reciprocating pumps can generate almost any pressure differential in a single stage with very good efficiency even at low flow rates Internal leakages may be reduced to a

negligible level by periodically statically sealing the checkvalves and sliding piston seals under a high pressure differential

Reciprocating pumps are usually used at comparatively low speed (about one-tenth that for a centrifugal pump) They have the disadvantage of producing a pulsating flow, and this produces an uneven load on the driving mechanism with attendant vibration effects The pump dimensions also tend to be larger than is the case with centrifugal pumps When deciding whether to use a centrifugal pump, a check should be made of the specific speed per stage (n_q) given by equation (9 5) If a centrifugal pump is to be used, n_q should exceed 15 min^{-1} at less than 20 stages for a given V and H_{tot} Furthermore it is necessary to examine the investment cost and the other important factors listed above For example, the efficiency of the centrifugal pump should be evaluated and if this is less than 70%, say, a reciprocating pump must be employed

9 3 1 2 Cavitation, the NPSH criterion For liquid pumps the suction conditions must avoid cavitation in the pump or the piping system Cavitation creates structural damage through pressure shocks and vibrations It also produces noise emission, wear and problems of fatigue This is particularly true of centrifugal pumps The usual and well-tried design method is to work in terms of the net positive suction head at the pump inlet condition (NPSH) The NPSH is the amount by which, at the suction point, the head of the liquid to be pumped exceeds the head equivalent to the vapour pressure of the liquid Pump manufacturers specify the minimum value ($NPSH_r$), which is required if cavitation is to be avoided The design should be such that the actual (or available) value ($NPSH_a$) exceeds this, i e $NPSH_a > NPSH_r$

The design calculations are elaborated further in section 9 3 2 4

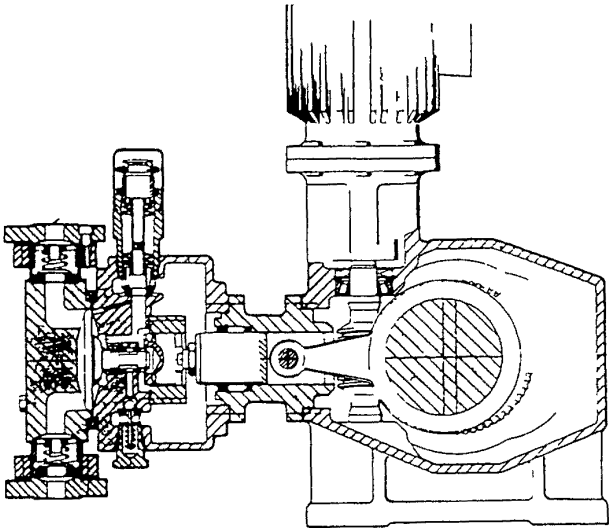

Figure 9 9 Diaphragm pump (LEWA)

9 3 2 Reciprocating pumps [13]

9 3 2 1 Applications Reciprocating pumps are well proven in supercritical extraction plant for pumping and circulating the solvents and entrainers, for conveying or metering the liquid components to be extracted and for blending the solvent/entrainer mixtures used for replacing losses

Reciprocating pumps are available in virtually all the relevant stainless materials that may be required They can be designed to be leak-free and hygienic The main types of reciprocating pumps used in supercritical extrac-

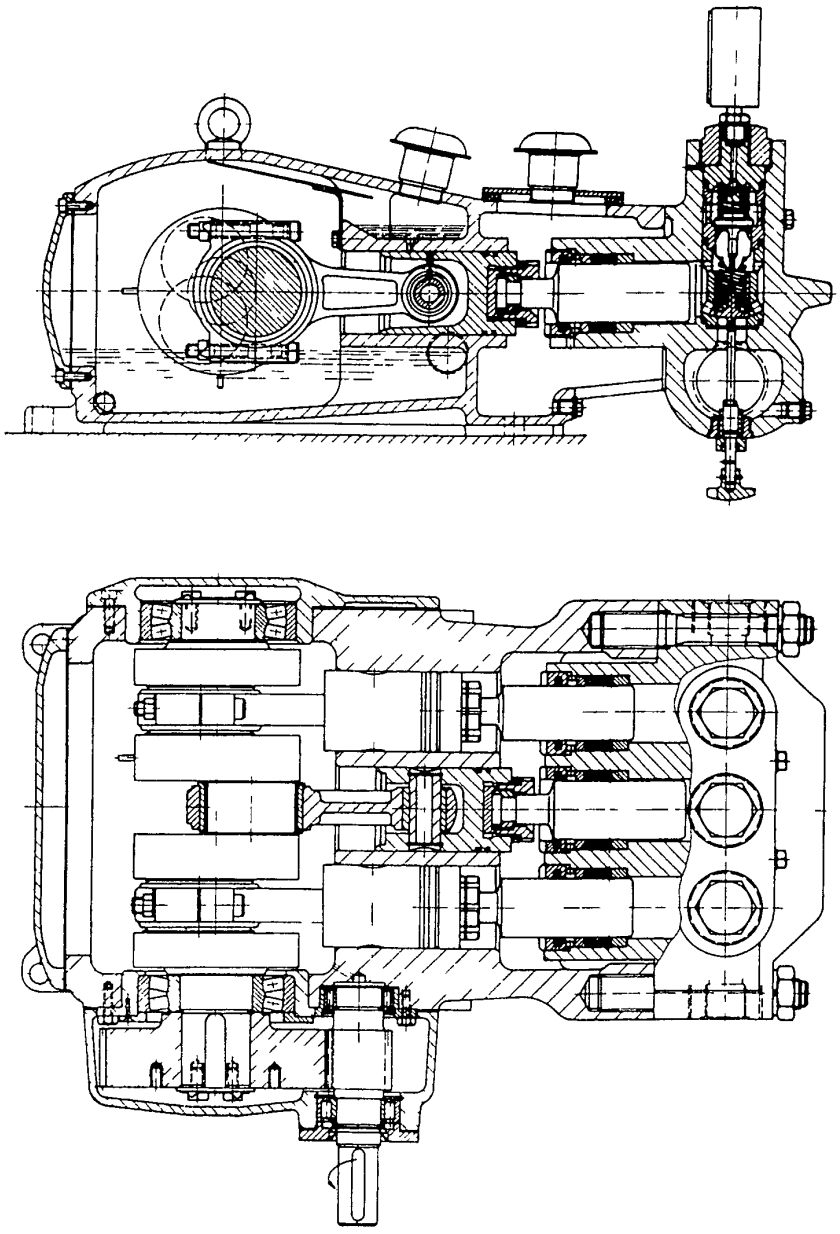

Figure 9 10 Triplex plunger pump (URACA)

tion plant are plunger and diaphragm pumps Cross section views of these are given in Figures 9 9 and 9 10

9 3 2 2 Characteristics

a) Volume flow volumetric efficiency The *piston displacement* in general follows the crank drive mechanism laws and performs approximately harmonic cycles so that v_p (the piston velocity) and b_p (the plunger acceleration) are given by

$$v_p = r\ \omega\ (\sin \omega t + \frac{\lambda_g}{2}\ \sin 2\omega t) \tag{9 7}$$

$$b_p = r\ \omega^2\ (\cos \omega t + \lambda_s \cos 2\omega t) \tag{9 8}$$

n is the stroke frequency t the time r the crank eccentricity, l the rod length and λ_s is the rod ratio ($\lambda_s = r/1$) ω is the angular velocity ($\omega = n\pi/30$)

The piston stroke $h_p = 2r$ can be continuously adjusted with metering pump drive systems, (Figure 9 11) The real fluid displacement is influenced by elasticity effects of the fluid and the working-chamber as well as any leakages during the displacement period through piston seals, valve seals and, in the case of diaphragm pumps, the hydraulic system Taking the above factors into account the actual volumetric flow rate produced by several pump cylinders in parallel is given by

$$V = i\ h_p\ \frac{\pi d_p^2}{4}\ n\ \eta_E\ \eta_s \tag{9 9}$$

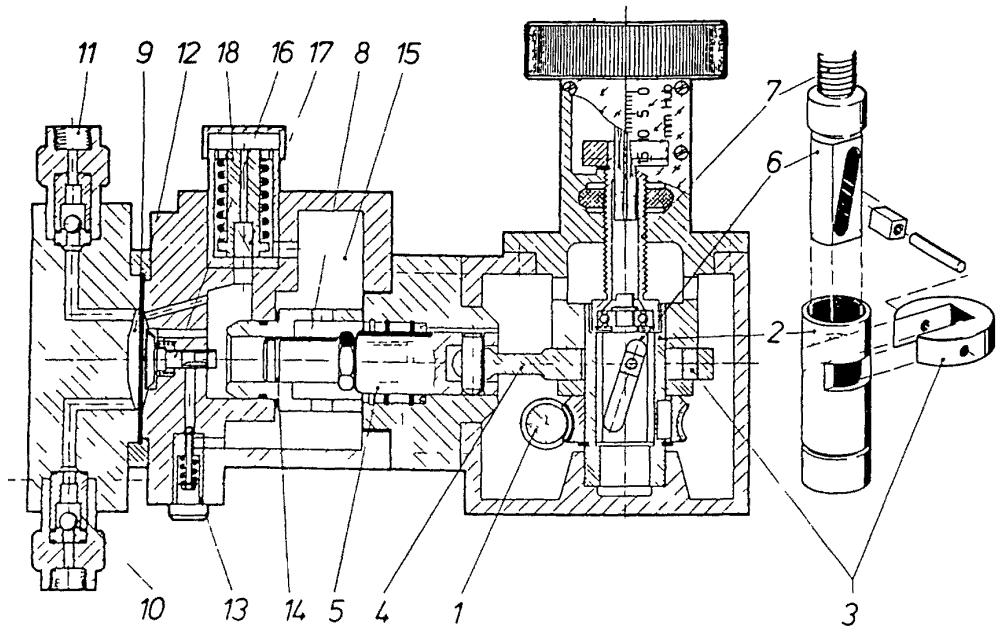

Figure 9 11 Diaphragm pump with stroke adjustment drive (LEWA)

where i is the number of parallel pump cylinders and d_p is the piston diameter

The elasticity factor η_E multiplied by the slip factor η_s is usually called the *volumetric efficiency*

$$\eta_v = \eta_E \quad \eta_s = \frac{V}{V_g} \tag{9 10}$$

η_v is the ratio of the actual volumetric discharge rate to the geometrically displaced volume flow ($V_g = ih_p \pi d_p^3 h/4$)

For drive systems with constant middle-position of the piston when stroke-adjusted η_E can be calculated from the compressibility of the discharge and the hydraulic fluid χ_F and χ_H, the relative dead spaces $\varepsilon_{DF} = V_{DF}/V_p$ and $\varepsilon_{DH} = V_{DH}/V_p$, the modulus of elasticity λ of the working chamber, the pressure differential Δp and the stroke setting h_p [14] (V_p is the chamber volume)

$$\eta_E = 1 - (\varepsilon_{DF} \quad \chi_F + (\varepsilon_{DH} + 0\ 5) \quad \chi_H + \lambda) \quad \frac{\Delta p}{h_p/h_{p100}} - \left(\chi_F - \frac{\chi_H}{2}\right) \Delta p \tag{9 11}$$

where h_{p100} and h_p are the maximum and set values of the stroke length respectively

For a constant stroke length plunger pump

$$h_p/h_{p100} = 1, \ \varepsilon_{DH} = 0, \ \chi_H = \chi_F$$

$$\eta_E = 1 - (\varepsilon_{DF} \chi_F + \lambda) \quad \Delta p \tag{9 12}$$

The fluid compressibility χ_f is related to the relative volume compression $\Delta V/V$ and the modulus of elasticity E (bulk modulus) as follows

$$\chi_F = \frac{1}{\Delta p} \quad \frac{\Delta V}{V} = \frac{1}{E} \tag{9 13}$$

For well designed pumps λ is normally close to zero, i e the pump is of rigid construction so η_E can be calculated directly from pump and fluid data This calculation shows that the relative dead spaces ε_{DF} and ε_{DH} should be minimised to achieve good volumetric efficiency Furthermore as the slip factor should approach $\eta_s \approx 1$ (valves should be tight and operate with no slip [15]) the volumetric efficiency can be obtained directly from the indicator diagram (Figure 9 12) and the table beneath it The diagram shows the relation between the decompression stroke h_1 (from 3 to 4) and the compression stroke h_2 (from 1 to 2) and the table enables Joukowsky-shock volumetric efficiency, shock factor and piston velocity to be calculated

b) Pulsation [6] For volumetric efficiencies less than unity the quasi-harmonic piston displacement curve becomes irregular and velocity jumps Δv occur This results in the excitement of vibrations, an effect which depends directly on volumetric efficiency (Figure 9 13) The fluid in the piping system responds to the vibration excitement with pressure pulsations which have to

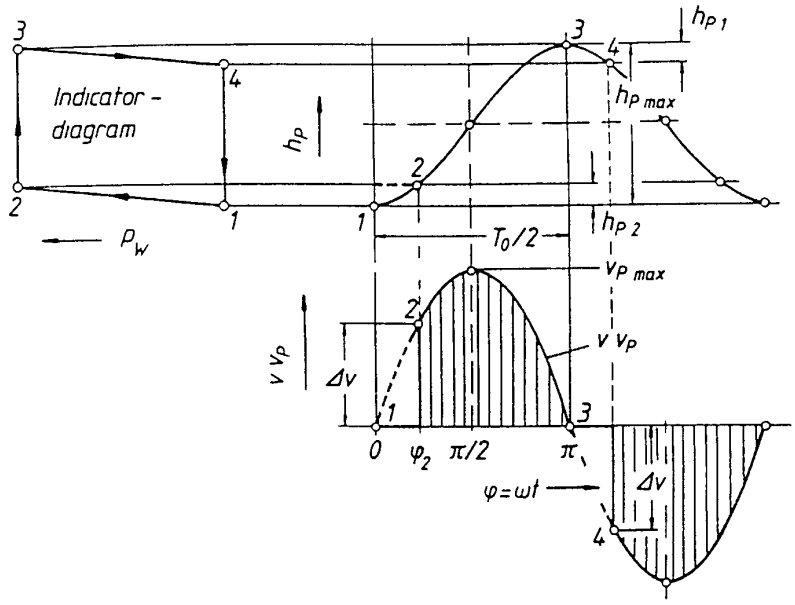

Joukowsky shock	$\Delta p_{jou} = \sigma \; a \; \Delta V = \sigma \; a \; V_{max} \; \Delta_{St}(\eta_V)$
Volumetric efficiency	$\eta_V = \dfrac{h_{max} - h_1}{h_{max}} = \dfrac{1 + \cos \psi_4}{2}$
Shock factor	$\Delta_{St}(\eta_V) = \dfrac{\Delta V}{V_{max}} = \sin \psi_2 = 2\sqrt{\eta_V - \eta_V^2}$
Piston velocity	$v_P = \dfrac{h_{max}}{2} \; \omega \; \sin \omega t \quad v_{max} = \dfrac{h_{max}}{2} \; \dfrac{\pi \; n}{30}$

Figure 9 12 Indicator diagram (table below is for harmonic motion)

meet certain limits and criteria Several different possibilities for reducing the pulsation effects produced by crank-driven reciprocating pumps are shown diagrammatically in Figure 9 14 Reduction in dead space improves volumetric efficiency and thus decreases pulsation and the generation of vibration

c) Thermodynamic effects in the pump chamber and their effect on the required NPSH The change of state which the fluid undergoes during compression, depends on the extent to which adiabatic conditions prevail, i e on whether heat transfer to the pump working chamber is positive, negative or negligible (Figure 9 15) Relatively small dead volumes and short residence times of the fluid result in near-isentropic conditions These conditions are largely met by the piston pump (K) and the diaphragm pump with plastomer diaphragm (M3) in Figure 9 15 The PTFE diaphragm in the latter case insulates the pump chamber from heat transfer to or from the hydraulic system The metal diaphragm in pump M1 (which has a larger dead space) obviously presents less resistance to heat transfer into the working chamber from the hydraulic system As a result, the fluid in the working chamber may warm up

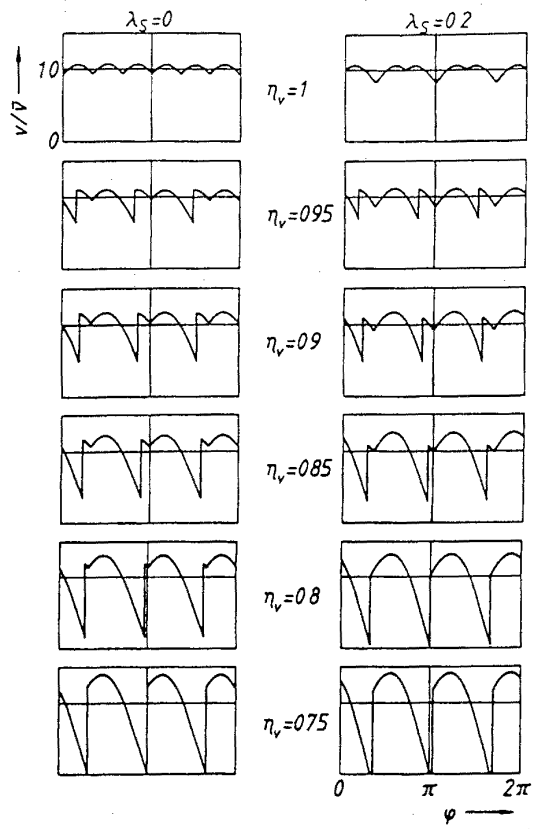

Figure 9 13 Pulsation and volumetric flow rate for a series of values of the volumetric efficiency (η_v) (V and $\bar{V}$ are the instantaneous and average flow rates respectively)

appreciably during its residence time This is undesirable in that it increases the required net positive suction head ($NPSH_r$) Pump M2, a small diaphragm pump shows a very large dead space but negative heat flow producing cooling of the fluid in the working chamber In this case the very large dead space tends to produce isothermal conditions in the pump chamber The volumetric efficiency is low due to the dead space [16, 17] These examples illustrate the need for a small dead space and thermal insulation against positive heat

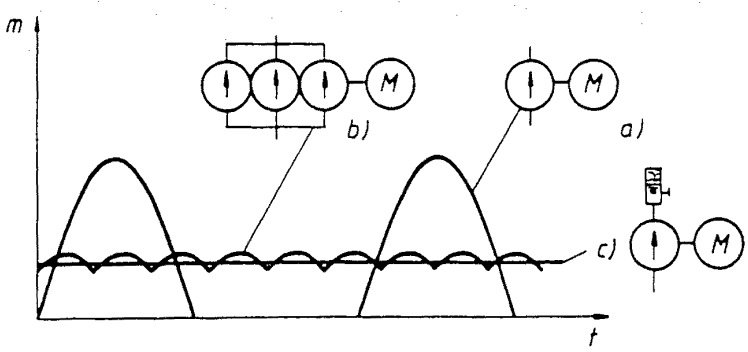

Figure 9 14 Pulsation reduction (a) simplex pump (b) pulsation dampener (c) triplex pump

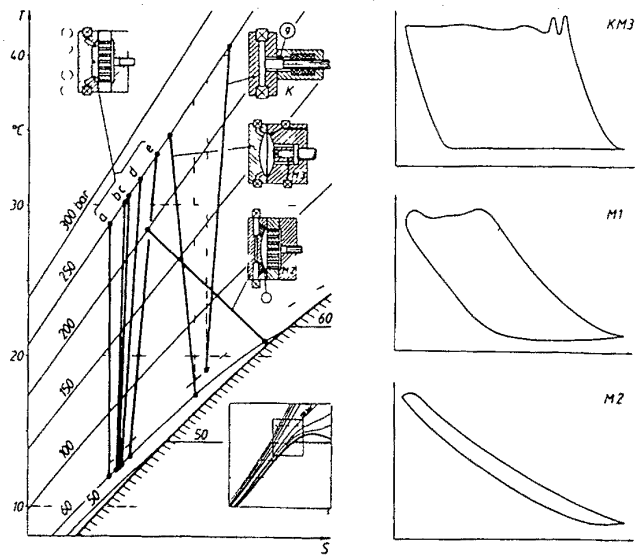

Figure 9 15 Compression stroke for various reciprocating CO_2 pumps shown on a T/S diagram

transfer into the working chamber In general, piston pumps have much smaller dead volumes than do diaphragm pumps and are preferable in this regard

The $NPSH_r$ of reciprocating pumps is usually calculated for incipient cavitation conditions from the maximum entry pressure losses [18, 19], which are largely dictated by the characteristics of the suction check valve The manufacturer s $NPSH_r$ data are in general based on these fluid mechanical effects Typical values for the $NPSH_r$ range between 1 and 3 m for liquid CO_2 (this corresponds to a pressure requirement of between 0 1 and 0 3 bar)

When calculating $NPSH_r$ for the compression of liquefied gases up to supercritical pressures, account should be taken of the real fluid temperature in the working chamber during the suction stroke This can be higher than that of the fluid stream external to the pump, thus increasing $NPSH_r$ above the value calculated from external conditions In addition to the fluid mechanical $NPSH_r$ calculated from the external temperature there is also a thermodynamic NPSH contribution which depends on the fluid temperature in the working chamber Local rises in the temperature can produce two effects which should be considered

1 Due to increased average wall temperature, especially at the discharge end the fluid as it enters undergoes heating at the wall and consequently because of *film cavitation* decreased volumetric efficiency results
2 Positive heat transfer and extended residence time resulting from a large dead space can result in a local temperature increase of the bulk fluid (Figure 9 15 M1 a–e) so the real local evaporation pressure substantially increases (Figure 9 16 and 9 17, I–III) When the transient suction pressure

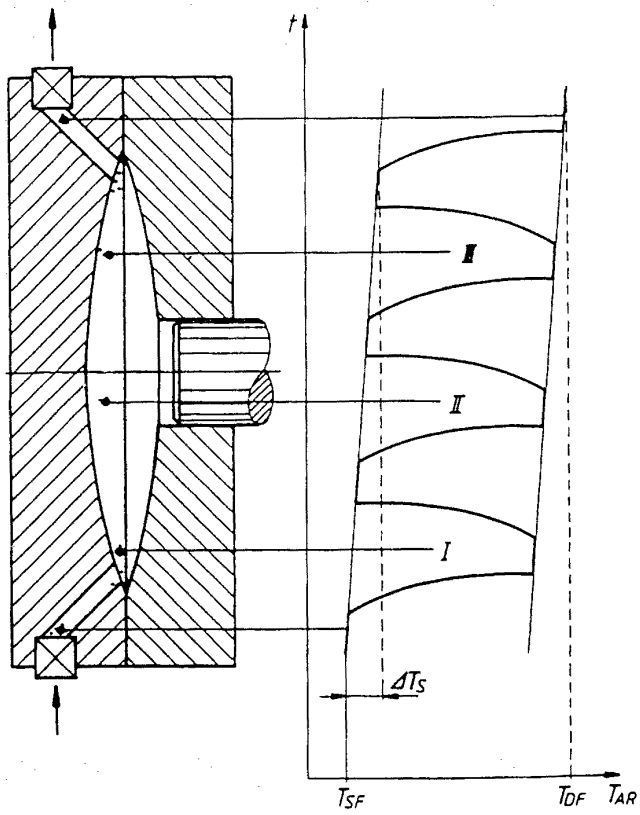

Figure 9 16 Schematic diagram showing temperature of the fluid at three points in the pump chamber as function of time (t) The increase in average temperature as the fluid passes through the chamber is also shown (positive heat transfer) I II III cycles experienced ΔT_s temperature increase T_{SF} T_{DF} temperature at suction and discharge ports respectively

due to entry pressure losses reaches the local evaporation pressure the pump suffers cavitation in the chamber volume (Figure 9 18)

Both film and volume cavitation will be superimposed on each other and it is recommended that the thermodynamic NPSH-criterion is introduced into the $NPSH_a > NPSH_r$ check by calculating the real local evaporation pressure equivalent to the average between the suction flange temperature and the isentropic compression temperature This yields results on the safe side for middle to large capacity pumps

d) Control characteristics In contrast to the centrifugal pumps discussed in section 9 3 3, reciprocating pumps deliver a volume flow which is much less dependent on the pressure differential or head (i e they give a 'rigid' or 'stiff' performance), and which is largely independent of the resistance in the installation It is a consequence of equations (9 8–9 10) (with $\eta_s \approx 1$) that the volume flow delivered should be proportional to the frequency (n) of the piston strokes for a given stroke length or proportional to stroke length (h) for

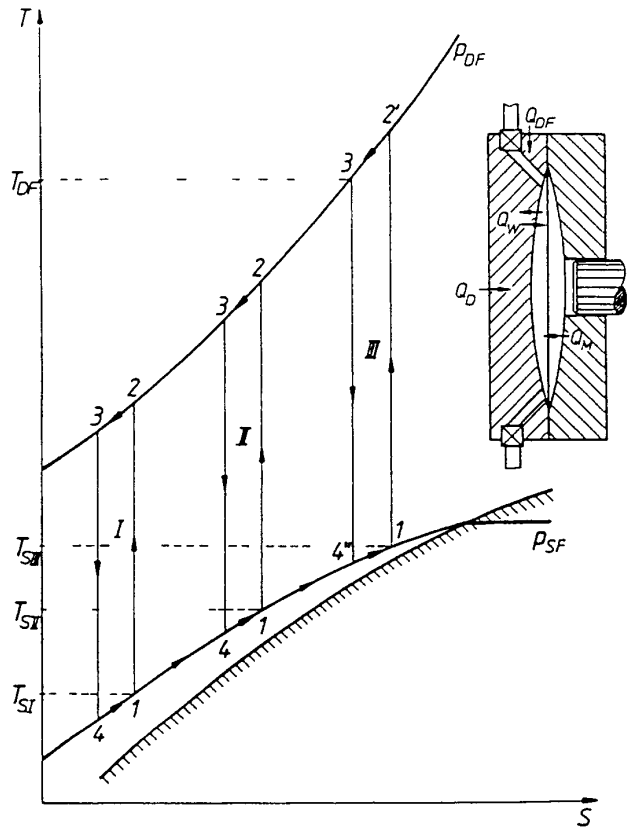

Figure 9 17 Schematic diagram showing change of thermodynamic state of fluid during its residence in the pump chamber (positive heat transfer and extended residence time) p_{SF} p_{DF} pressure at suction and discharge ports respectively T_{SI} T_{SII} T_{SIII} local fluid temperatures at suction in residence cycles I II and III

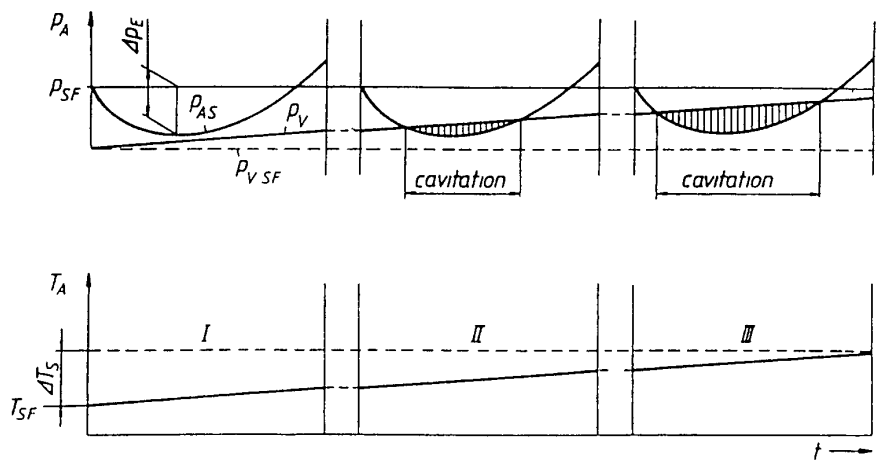

Figure 9 18 Cavitation due to entry pressure losses and increasing fluid temperature (and hence vapor pressure) as fluid passes through the pump chamber p_A p_V working chamber pressure and fluid vapour pressure p_{AS} working chamber pressure at suction Δp_E entry pressure loss I–III pump cycles

a given n (Figure 9 19) For stroke-controlled pumps the stroke length h_{po} at a pressure differential Δp is necessary to overcome the elasticities of the fluid and working chamber The effect of these elasticities on the $(V, n)_h$ curve is to change the slope only The linear correlation between the volumetric flow rate (V) and the set variable (h or n) is very convenient when using the pump for metering or blending or for control in general

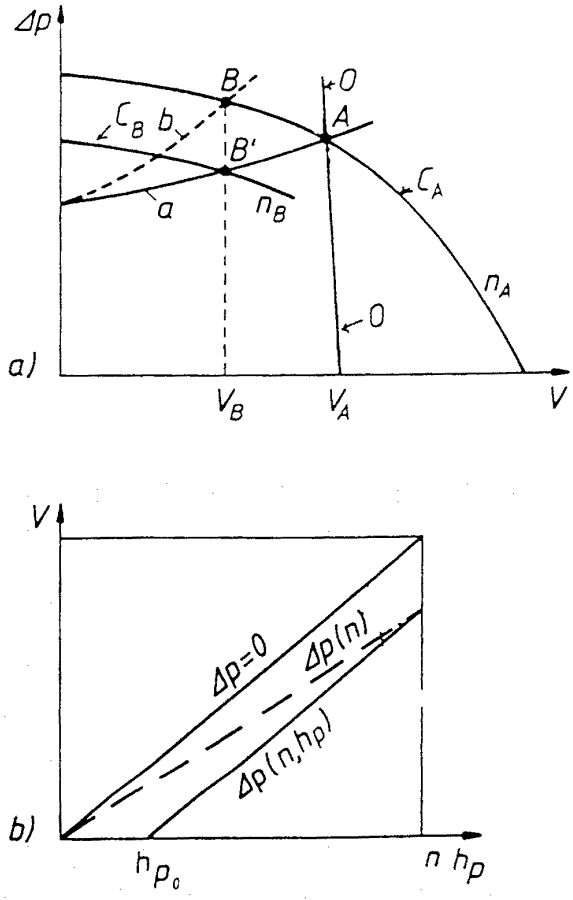

Figure 9 19 Performance curves and control characteristics of pumps (a) Differential pressure Δp as a function of volumetric flow rate V Curves C_A and C_B are performance curves for a centrifugal pump at rotation rates n_A and n_B respectively Curve 0 is for a reciprocating pump Curves a and b give the installation characteristic for the operation points A and B (b) Volumetric flow rate (delivered by reciprocating pump) as a function of stroke frequency n at constant stroke length h_p or of stroke length at constant stroke frequency

If a continuously variable flow rate is required from a constant-speed triplex plunger pump, one low investment possibility is to use bypass control, though this does have the disadvantage of increased power consumption

9 3 2 3 Design of reciprocating pumps The discussion below is limited to the solvent pumps used for high pressure extraction In the range of conditions

for which reciprocating pumps are more suitable than centrifugal pumps, a choice is required between diaphragm and piston pumps (Figure 9 9 and 9 10) In making this choice, safety problems (including ones connected with possible fluid leakage) and investment costs must be considered

*a) Diaphragm pumps** The diaphragm pump with hydraulic diaphragm operation (Figure 9 9) has been extensively used for process applications at high pressure [20] The main advantages of this type of pump are no leakage, no fluid piston seal, good safety features and good reliability (little or no maintenance is required) Diaphragm pumps can produce high pressure differentials and are suitable for handling toxic or dangerous solvents or solvent mixtures (as when entrainers are present) The higher investment cost of diaphragm pumps is usually only justified for small capacities (< 50 kW) In combination with stroke adjustment control these pumps can be very useful for flexible applications and in pilot plants

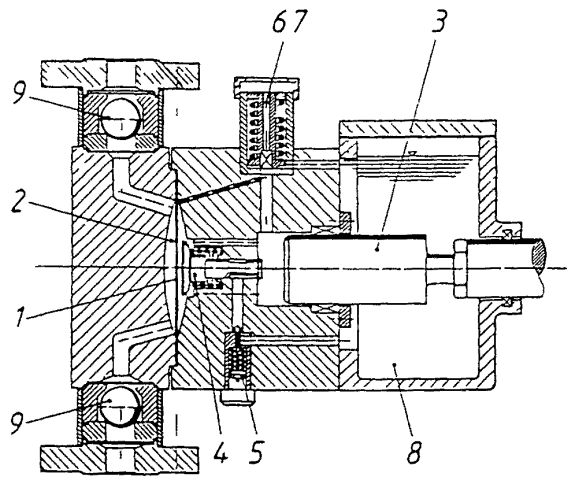

Figure 9 20 Diaphragm pump head with hydraulically actuated position controlled PTFE diaphragm (LEWA)

Position-controlled hydraulically operated PTFE-diaphragms are widely used and are perfectly satisfactory at pressures up to about 300 bar and elevated suction pressures between 50–100 bar Figure 9 20 shows a diaphragm pump head of this type Diaphragm 1 can deflect freely into the working space 2 The space between plunger 3 and the diaphragm is filled with an appropriate hydraulic fluid The supply of this fluid is controlled by gate valve 4 and replenishing valve 5 To bring about replacement of the hydraulic fluid two conditions are necessary (1) the diaphragm has to press on the gate valve thus opening it and establishing a connection from the replenishing valve to the hydraulic chamber (2) the drop in pressure brought

* The author wishes to thank LEWA D7250 Leonberg for help in preparing this section

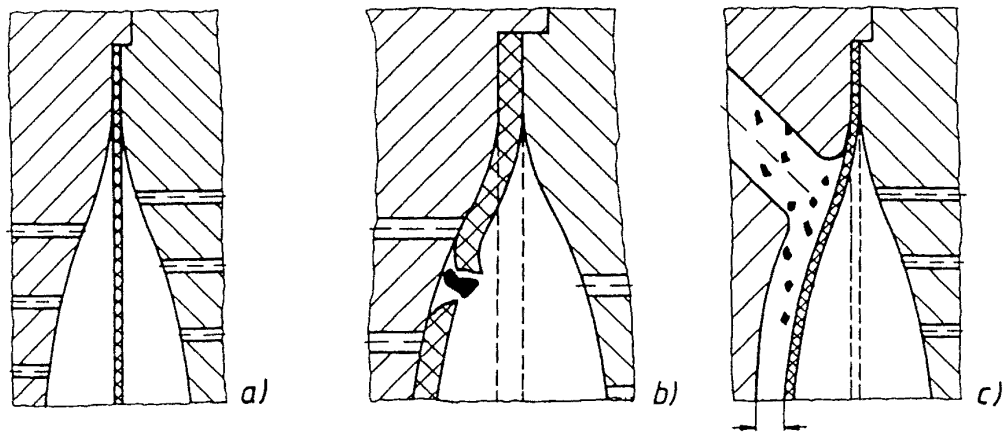

Figure 9 21 Diaphragm motion in the working space (a) between hole plates (b) diaphragm rupture by dumped particles (c) position control (diaphragm prevented from contacting chamber wall)

about by the lack of hydraulic fluid opens the replenishing valve This design prevents the diaphragm from coming into contact with the discharge side working chamber cover thus avoiding diaphragm damage (Figure 9 21) The hydraulic system is equipped with a relief valve 6 for protection against overload and a venting valve 7 to bleed air bubbles automatically (further details are available [13, 14, 21, 22, 23]) PTFE-diaphragms may either be plain discs or may be corrugated Clamping and sealing should be carried out in accordance with the 'restricted compression principle' which implies a geometrically exact 'clamped volume' that is a certain percentage smaller than the original diaphragm volume in the clamping zone (Figure 9 22c) Experience shows that the lifetime of plastomer diaphragms is greater than 10 000 h,

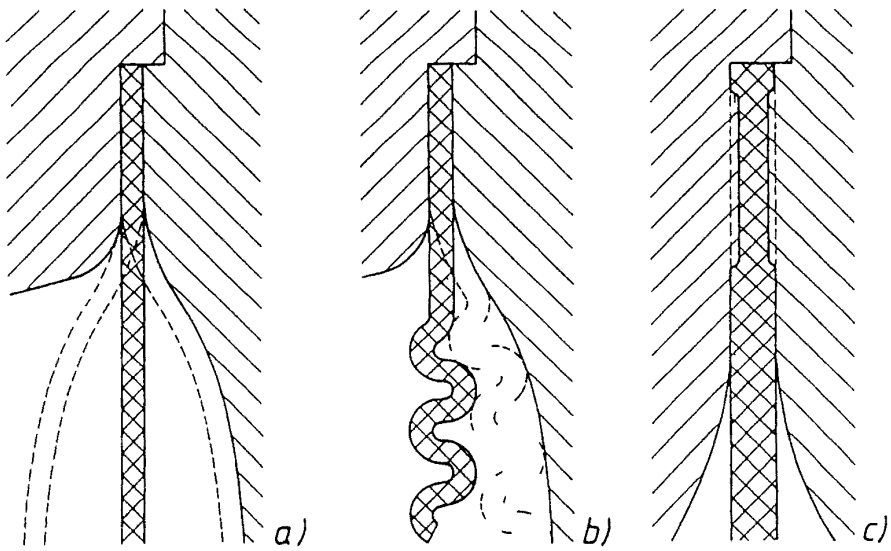

Figure 9 22 Diaphragm design clamping and sealing (a) plane disc diaphragm (b) corrugated diaphragm (c) method of sealing diaphragm showing grooves in clamped region (see text)

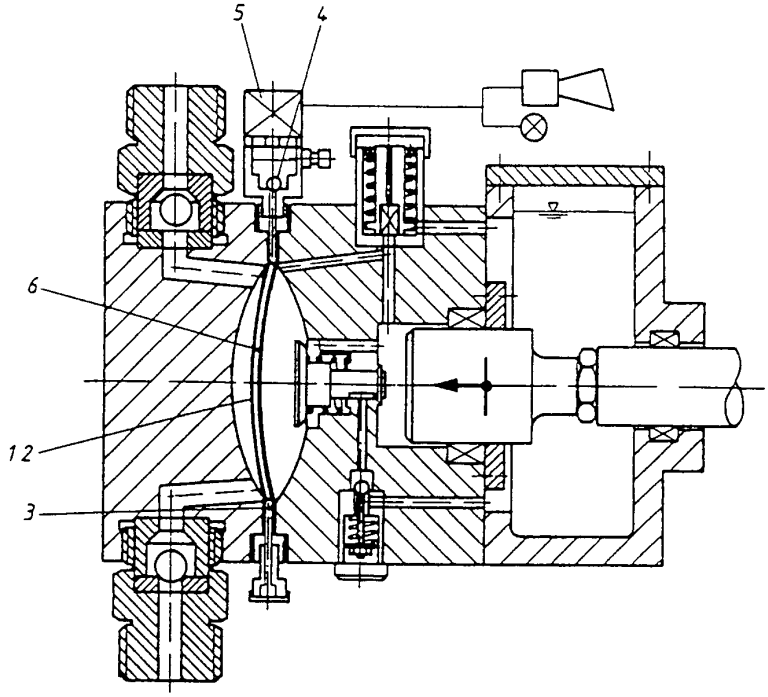

Figure 9 23 Sandwich diaphragm with rupture control

either PTFE or PE may be used for supercritical extraction processes A sandwich design may be employed as a precaution against rupture In this design two diaphragms (1, 2 in Figure 9 23) are hydraulically coupled by a fluid film which communicates via a check valve 4 and an intermediate ring 3 to the differential pressure sensor 5

At discharge pressures above 350 bar plastomer diaphragms become unsatisfactory and it is necessary to use metal diaphragms At low capacities these are quite satisfactory and in high pressure applications they are much easier to seal and clamp than is the case with plastics The correct volume of hydraulic fluid is normally maintained using an underpressure-operated replenishing-valve (Figure 9 24) The diaphragm 1 is protected against being overstrained by situating it between plane and curved perforated plates (or 'hole-plates) 3, 4 In the particular design shown the diaphragm may be pressed, under certain operating conditions, against these plates Dirt particles in the fluid, if trapped between the diaphragm and a 'hole-plate', can therefore damage or even perforate the diaphragm (Figure 9 21b) Dirt should therefore be removed from the fluids by filters on the suction side Recently, metal diaphragm pumps with gate-valve control have appeared on the market In these pumps the diaphragms are prevented from coming into contact with the upper 'hole-plate'

Metal diaphragms have the disadvantage of being sensitive to scratches and surface damage These reduce the fatigue limit of the cold-rolled metal sheets to such a degree that the average lifetime of a metal diaphragm is only around 5000 h At high system and hence suction pressure (> 50 bar) the diaphragms

should be protected by pressure balancing systems [20, 22] Metal diaphragms have the advantage of being totally fluid-tight, whereas plastic diaphragms can show slight porosity

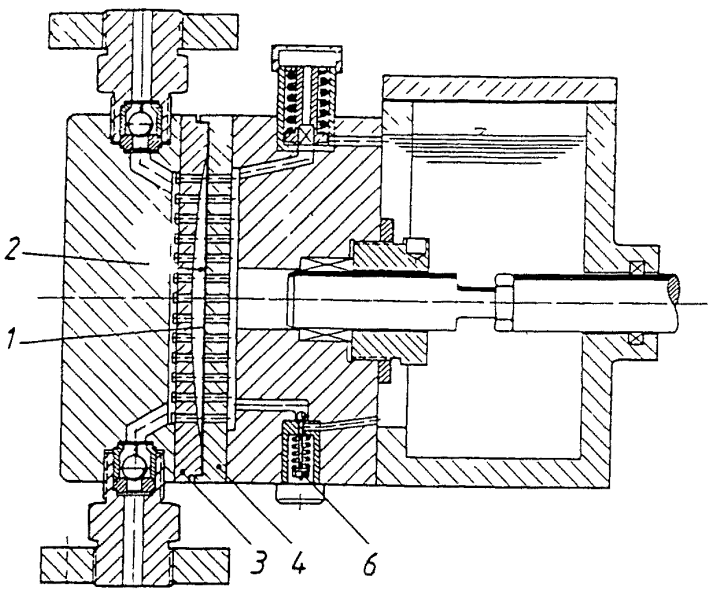

Figure 9 24 Diaphragm pump head with metal diaphragm and hydraulically actuated underpressure control (LEWA)

The hydraulic diaphragm pumps currently available for high pressure applications are partly derived from the development of metering pumps for the process industries There is a wide variety of materials of construction The pumps usually have crank drives with adjustable stroke

Recently *triplex diaphragm* pumps have become available for powers up to 1 MW These can be used to replace plunger pumps if necessary in situations where plunger seal or leakage problems arise [23] The triplex crank drives are similar to those for plunger pumps as may be seen from Figure 9 25 This figure shows some details of the sandwich diaphragm design in the clamping area

The dead space in a diaphragm pump is normally larger than in a plunger pump, so the volumetric efficiency tends to be lower Typical volumetric efficiencies η_v for diaphragm pumps used for pumping CO_2 through a pressure differential of 250 bar are between 0 7 and 0 8 Corresponding values for a plunger pump are between 0 8 and 0 9 Diaphragm pumps also produce more pulsation flow than do plunger pumps Careful piping design and pulsation damping are necessary to counteract this

*b) Plunger pumps [24]** The cost of a plunger pump is usually at most two-thirds that of a diaphragm pump Furthermore, plunger pumps have higher

* The author wishes to thank URACA D7432 Bad Urach for their assistance in preparing this section

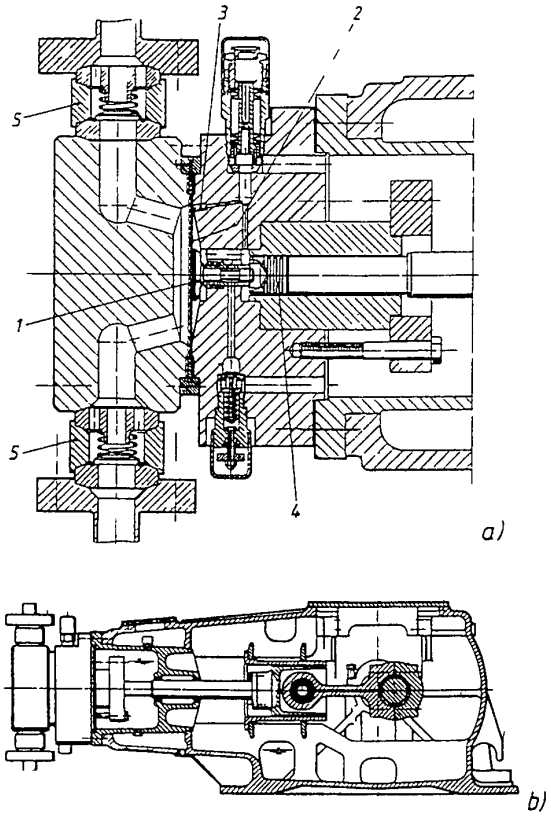

Figure 9 25 Triplex diaphgram pump (LEWA) (a) pump head (b) crank drive unit

volumetric efficiencies than do diaphragm pumps, and are less liable to produce pulsation and vibration problems Particularly for large capacity applications (between 50 and 100 kW) triplex plunger pumps are well-tried and have been found to be economical for pumping supercritical solvent (Figure 9 10) They are available with constant or variable speed drive as well as with bypass control The plunger seal (Figure 9 26) includes two guide bushings 1 and several well restrained compression rings 2 constructed from a PTFE/graphite composite The plunger 8 should be attached to the driving rod with slight

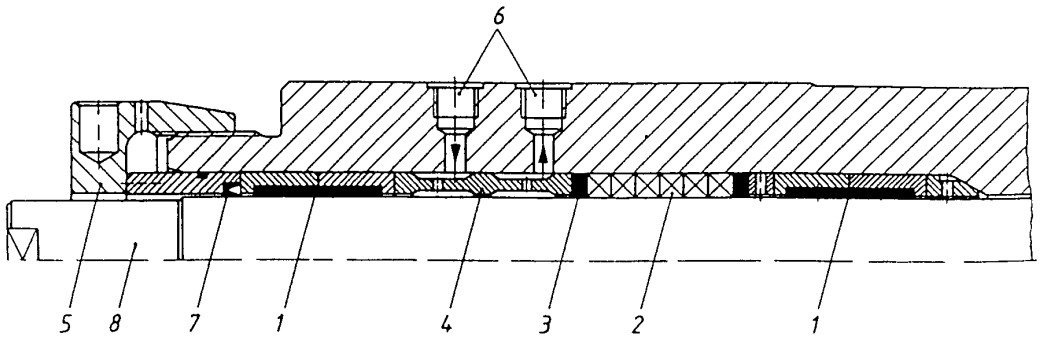

Figure 9 26 Plunger sealing arrangement (URACA)

radial and angular flexibility so that it can move smoothly through the bushings

The above arrangement provides a good seal for CO_2, which has a similar density and viscosity to water, provided dry running is avoided by water flushing in the region of the seal

The pump check valves for reciprocating pumps (whether diaphragm or plunger) should be designed with care They should have a low NPSH requirement, have a good kinematic performance and should be subject to as little wear as possible The last-named condition implies that hard and corrosion resistant materials should be used for the valve cone or plate as well as for the seat A typical valve and pump head design is shown in Figure 9 27

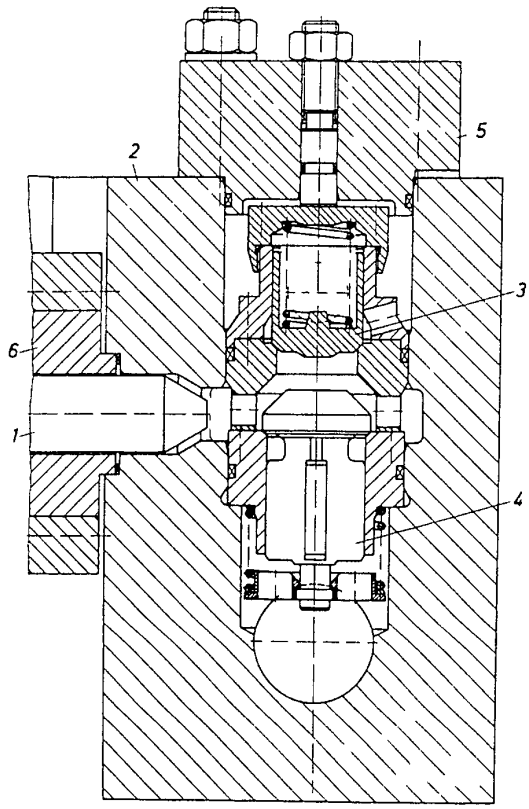

Figure 9 27 Typical valve and pump head design for a high pressure plunger pump (URACA) 1 plunger 2 cylinder 3 discharge valve 4 suction valve 5 cover 6 stuffing box housing

9 3 2 4 Installation When installing reciprocating pumps for use in supercritical extraction plant, care should be taken to ensure that cavitation does not occur in the pump and also that vibration problems are reduced to an acceptable level A special problem which occurs when solvent in liquid form is pumped from the pressure in the solvent recovery unit to the extraction pressure is that the suction pressure will usually be only slightly in excess of the vapour pressure of the solvent This leads to the possibility of cavitation Furthermore, the

solvent will typically have a high compressibility (Figure 9 4) so strongly pulsating flow with attendant vibration problems is possible

a) Cavitation The available 'NPSH can be calculated from the design conditions The appropriate equation is

$$\mathrm{NPSH_a} = \left(\frac{p_I + p_{amb} - p_v}{\rho g}\right) + \frac{v_I^2}{2g} + (z_I - z_s) - H_J \qquad (9\ 14)$$

where ρ is the fluid density and g the gravitational constant, p_v is the fluid vapour pressure at the 'pump temperature' (see section 9 3 2 2 (c)) H_J is the head loss due to friction and non-uniform flow in the piping between the pump inlet and the feed reservoir Other notation is as in Figure 9 5 The head loss H_J can be represented as the sum of components due to friction (H_{Jf}) and acceleration (H_{Ja}) The latter term is important in the case of reciprocating pumps (though it is absent in the case of centrifugal pumps – see section 9 3 3 2) For uniform diameter suction piping the losses can be calculated from the equations

$$H_{Jf} = \left(\frac{\lambda_s l_s}{d_s} + 1 + \sum \xi_{si}\right)\frac{v_s^2}{2g} \qquad (9\ 15)$$

and

$$H_{Ja} = b_s \ \ l_s/g \qquad (9\ 16)$$

l_s is the length of the piping, d_s is its diameter and λ_s is the flow resistance factor The factor ξ_{si} takes account of entry and other losses which do not depend on pipe length

In general both λ_s and ξ_{si} depend on Reynolds number and hence on flow velocity However this dependence is not strong if the flow is turbulent, which is almost always the case in supercritical extraction systems For the present purposes therefore λ_s and ξ_{si} may be taken to be approximately constant Numerical values are available in textbooks [25] The flow velocity v_s and acceleration b_s are directly related to the velocity and acceleration (v_p and b_p) of the pump piston, being given as functions of time by equations (9 7) and (9 8)

From the continuity law

$$v_s(t) = v_p(t)\, A_p/A_s \qquad (9\ 17)$$

and

$$b_s(t) = b_p(t)\, A_p/A_s \qquad (9\ 18)$$

where A_s is the cross-section area of the suction pipe and A_p is the plunger cross-section

The pump parameters v_p, A_p and b_p can either be calculated or taken from manufacturers' documentation For reciprocating pumps the losses H_{Jf} and H_{Ja} both vary in an oscillatory manner with time and are not in phase

For single pumps, a good approximation for the maximum of H_J is obtained by vectorial addition as follows

$$H_{Jmax} = \sqrt{H_{Jfmax}^2 + H_{Jamax}^2} \tag{9 19}$$

For triplex reciprocating pumps, a good approximation is given by

$$H_{Jmax} = H_{Jf} + H_{Ja} \tag{9 20}$$

For turbulent flow and non-pulsating pumps, both $NPSH_r$ and $NPSH_a$ vary as the square of the volumetric flow rate (Figure 9 28)

The acceleration losses for reciprocating pumps increase with the square of the stroke frequency too (see equations 9 8 and 9 16) and normally greatly exceed the friction losses

A value for the available NPSH corresponding to any given layout and component dimensions can be calculated from equations (9 14) to (9 19) The design should be adjusted to provide a reasonable value for this quantity

The required NPSH ($NPSH_r$) is specific to each individual pump design and can normally be taken from the pump specification or manufacturers documentation The $NPSH_r$ values are normally based on the 3% ΔH criterion (Figure 9 29a) For reciprocating pumps they are usually calculated from the pressure drop Δp_E required to actuate the entry check valve (Figure 9 29b) at the onset of cavitation

$$NPSH_r = \Delta p_E/(\rho g) \tag{9 21}$$

In practice it is found that $NPSH_r$ for reciprocating pumps increases with the square of the volumetric flow rate This is because check valve losses are of this form [18]

In practice it is found that the *cavitation criterion*

$$NPSH_a > NPSH_r \tag{9 22}$$

should include a safety factor For reciprocating pumps with positive heat transfer to the liquid in the working chamber $NPSH_a$ has to be evaluated for

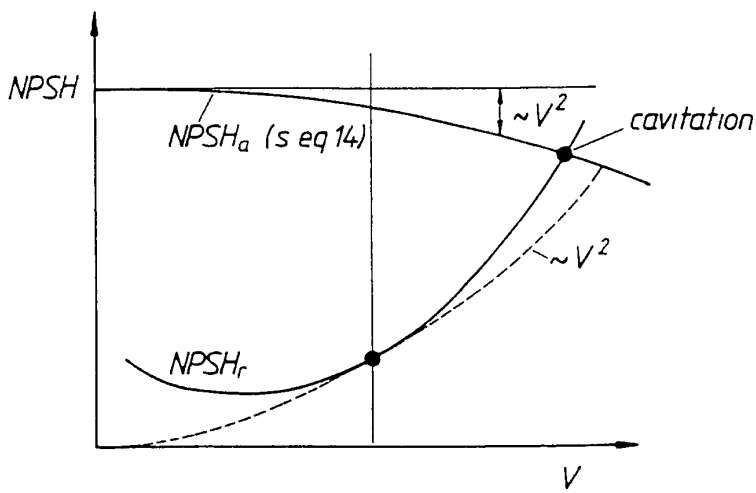

Figure 9 28 The criterion for cavitation (see text)

the highest temperature which the process liquid experiences during the suction stroke (see section 9 3 2 2c)

b) Pressure pulsations and vibrations The pulsations in flow which are characteristic of reciprocating pumps (Figures 9 13 and 9 14) produce pressure pulsations in the piping system It is possible to control the magnitude of these to some degree at the design stage by careful attention to the volumetric efficiency, the number of cylinders used and other factors but they cannot be completely designed out' The pressure pulsations in the piping system depend on the spectrum of excitation frequencies which are produced by the pump Since the fluid-filled piping system is a vibratory system (continuum) with many eigenfrequencies there is usually a risk of resonance conditions being established whereby very large pressure amplitudes may be produced These may result in overloading the pump or the piping system and dangerously intense vibrations in the supporting structure are also possible

This is definitely the case when a large pipe length (> 10 m) is involved Various calculation procedures have been proposed for predicting the magnitude of the pressure pulsations The most accurate is a numerical method which requires either a detailed study [26–28] or consultation with specialists

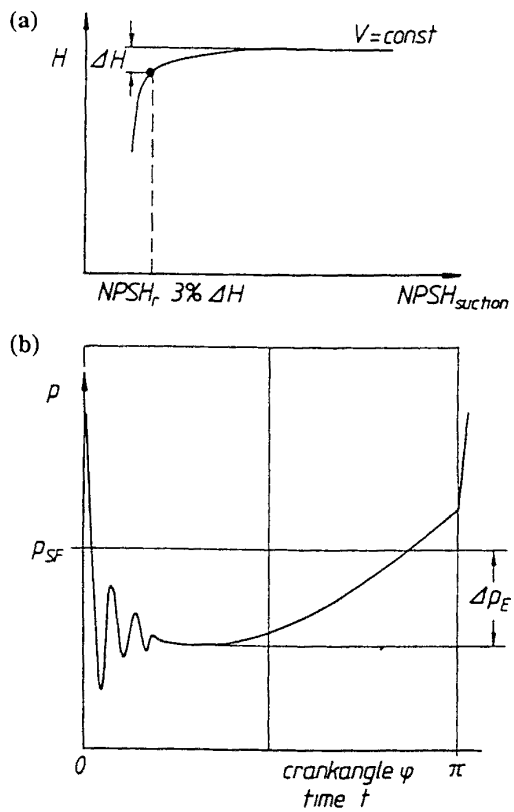

Figure 9 29 Criteria for determining the required NPSH for centrifugal and reciprocating pumps (a) 3% ΔH criterion for centrifugal pumps (b) Δp_E criterion for reciprocating pumps

In order to safeguard the components involved and to avoid overloading the pumps and piping it is necessary to limit the maximum amplitude of the pressure pulsations (the 'superload' criterion) The reduction of the amplitude limits the 'shaking' forces acting on the plant components and their vibration amplitudes [29] Several methods of reducing pressure pulsations are illustrated in Figure 9 30 This shows the results of an experimental and computational study [28] of a triplex pump acting on a long discharge pipe within the resonance range For constant speed pumps it is very useful to shift the eigenfrequencies of the hydraulic piping system (Figure 9 30a) by installing liquid-filled volume dampers Alternatively gas-filled dampers (air-vessels) with diaphragms may be used It is recommended that the piping system should be designed for less than ± 5 – 10% pressure pulsations

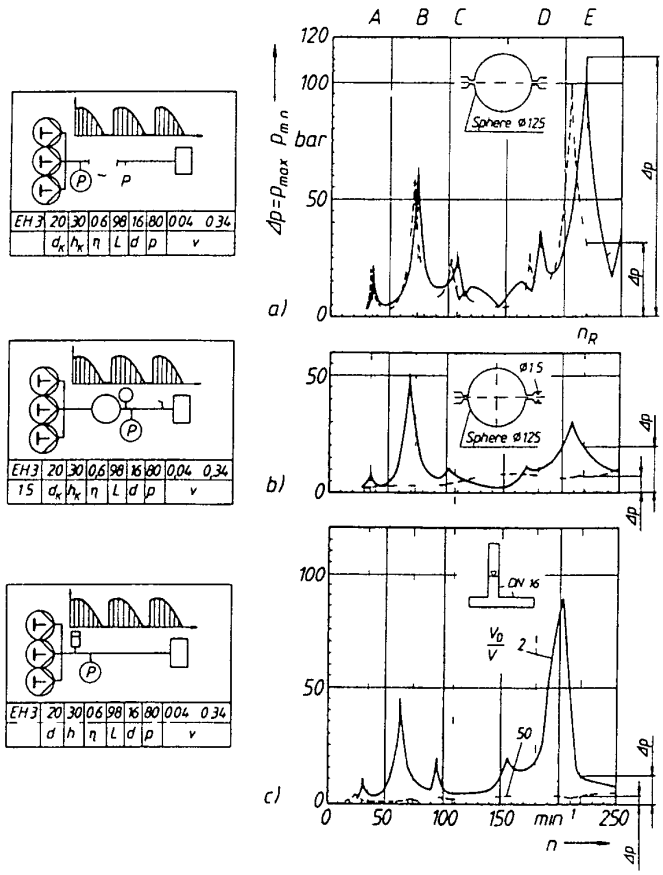

Figure 9 30 Pressure pulsations produced by a triplex piston pump in an installation equipped with various damping devices (see text) (a) with (——) and without (– – – – – –) spherical resonator (b) with orifice directly behind the resonator (—) and at the end of the pipe (c) gas filled (– – – – – –) vessels with small (——) and large gas volume (– – – – – – –)

c) Ancillary components It is recommended that reciprocating pumps should be protected from damage by relief valves and that particles of grit should be excluded from the pumps by suction side filters

*9 3 3 Centrifugal pumps**

9 3 3 1 Applications Centrifugal pumps are used in supercritical extraction plants for pumping the solvent from the truck to storage tank, for replenishing the extraction circuit by pumping solvent from the storage to the working tank(s) and for pumping the solvents round the high pressure extraction circuit

The low pressure pumps used for truck/storage transport are usually of a standard centrifugal type Because of the requirements of the mobile truck service, the shaft seals are normally of a packing type design Transport of the dry liquid solvent (at temperatures between minus 30 and minus 40°C for CO_2) to working tanks, which are typically at a pressure of about 50 or 60 bar is performed with horizontal split case multistage centrifugal pumps, with low temperature tough housing materials and standard mechanical shaft seals As the pumps are permanently under the pressure and temperature of the solvent in the working vessel, they can be started immediately without evaporation effects The use of centrifugal pumps for high pressure circulation (and filling) will be explained in more detail in section 9 3 3 3

9 3 3 2 Operating characteristics Typical performance curves for centrifugal pumps are shown in Figure 9 19a (curves C_A and C_B) At constant pump speed there is a strong influence of pressure differential Δp (or head H) on the volume flow V (the 'elastic characteristic') The working point is given by the intersection of the appropriate performance curve and the 'installation characteristic' (curve a in Figure 9 19a and Figure 9 31)

The 'installation characteristic is the head H which the pump must deliver to perform its duty Typically this is to extract fluid from a vessel at pressure p_I and transfer it to an adjacent vessel at the higher pressure p_{II} The 'installation characteristic' is a function of volume flow rate since it depends in part on the head loss H_{Jf} due to friction in the piping Using equation (9 1) and Figure 9 5 the head or installation characteristic can be calculated

$$H = \frac{p_{II} - p_I}{\rho g} + (z_{II} - z_I) + H_{Js} + H_{Jd} + \frac{v_{II}^2 - v_I^2}{2g} \qquad (9\ 23)$$

H_{Js} and H_{Jd} can be determined from equation (9 15) If the pump is operating across a substantial pressure differential (which is typically the case for circulation pumps in supercritical extraction plant where product recovery is by a throttling expansion) the 'installation characteristic' is not highly sensitive to changes in the volumetric flow rate This is because pressure losses in the piping are then negligible compared to the static differential pressure (Figure 9 31a) If the circulation pump is used to recirculate extractant through equipment in which pressure changes are not substantial (as in the case in extraction plant in which solvent recovery is by absorption or adsorption (see chapter 6)

* The author wishes to thank K L Neumann Grassel D 3260 Rinteln for assisting in the preparation of this section

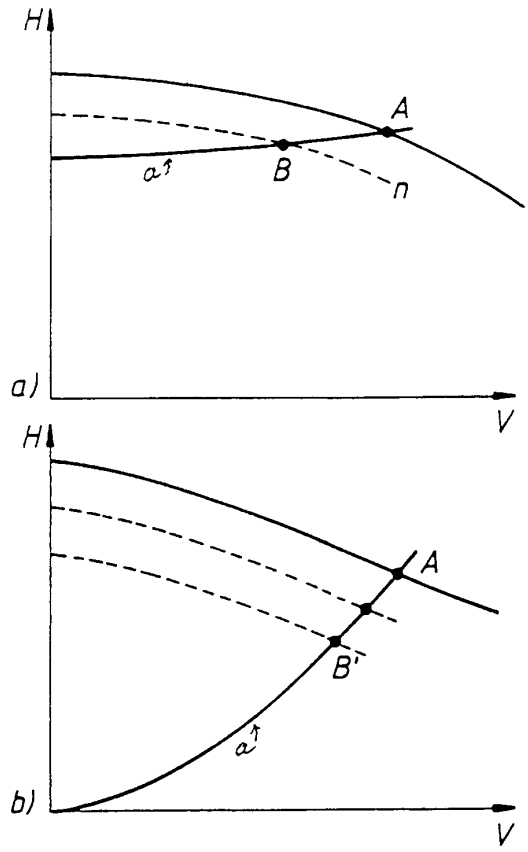

Figure 9 31 Schematic diagram showing pump performance and installation characteristic curves (a) fluid circulation at high differential pressure (low specific speed) (b) fluid circulation at high system pressure but low pressure differential (i e at a higher specific speed) Curve (a) is the installation characteristic curve the remaining curves are pump performance curves for a set of pump speeds

the plant characteristic is dominated by the fluid friction term and accordingly varies approximately as V^2 (Figure 9 31b)

A typical performance chart for a high pressure multistage centrifugal pump suitable for CO_2 is given in Figure 9 32

Control of flow rate Centrifugal pumps deliver a non-pulsating flow, which is a strong point in favour of their application in supercritical extraction plants

For centrifugal pumps, control by throttling or changes in pump speed or bypass control are well-tried possibilities, the choice being strongly influenced by the philosophy of plant operation and by economic considerations Of the regulation methods, speed control involves lowest power consumption This is especially true under conditions where the 'plant characteristic are substantially dependent on the volumetric flow rate The advantage of speed control compared to throttling or bypass control then becomes more important [11] (According to the similarity laws for speed control $V \approx n$ and $H \approx n^2$)

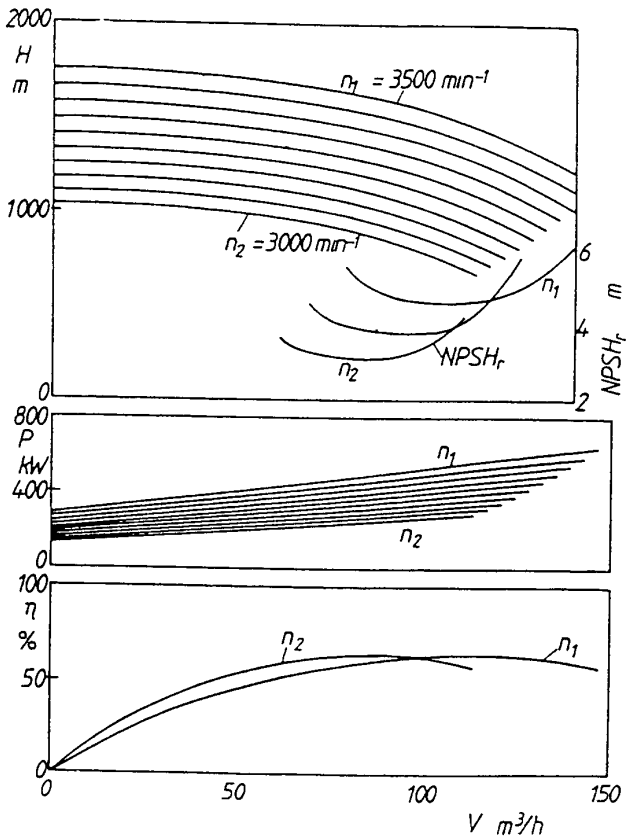

Figure 9 32 Centrifugal pump performance (GRASSEL) The fluid is supercritical CO_2 the suction pressure is 300 bar and the differential pressure is 100 bar The pump may be operated at temperatures between 60 and 120°C and speeds between 3000 and 3900 min^{-1} H = head P = power consumption η = efficiency n = pump speed

Avoidance of cavitation As with reciprocating pumps, the criterion $NPSH_a > NPSH_r$ should be obeyed The available NPSH ($NPSH_a$) for a centrifugal pump may be calculated using equations (9 14) and (9 15) developed in section 9 3 2 4 for reciprocating pumps In this case however $H_{Ja} = 0$ and $NPSH_a$ usually falls with the square of the volume flow rate (Figure 9 28)

The required NPSH ($NPSH_r$) for centrifugal pumps typically, has a square relationship to volume flow (Figure 9 28 and 9 32) It is not usually influenced by changes in the state of the fluid during compression, as the fluid compression occurs in many stages and with only slight temperature increases This is an important difference compared to reciprocating pumps

The $NPSH_r$ characteristics should be requested from the manufacturer who usually evaluates these with water using the well-known 3% ΔH-criterion (Figure 9 29a) For solvent close to their vapour pressure the manufacturer should be asked for special recommendations as general information [30] may not be sufficiently reliable As centrifugal pump cavitation is rather dangerous for pump life, the actual NPSH should include a safety margin A factor between 1 5 and 2 0 is recommended

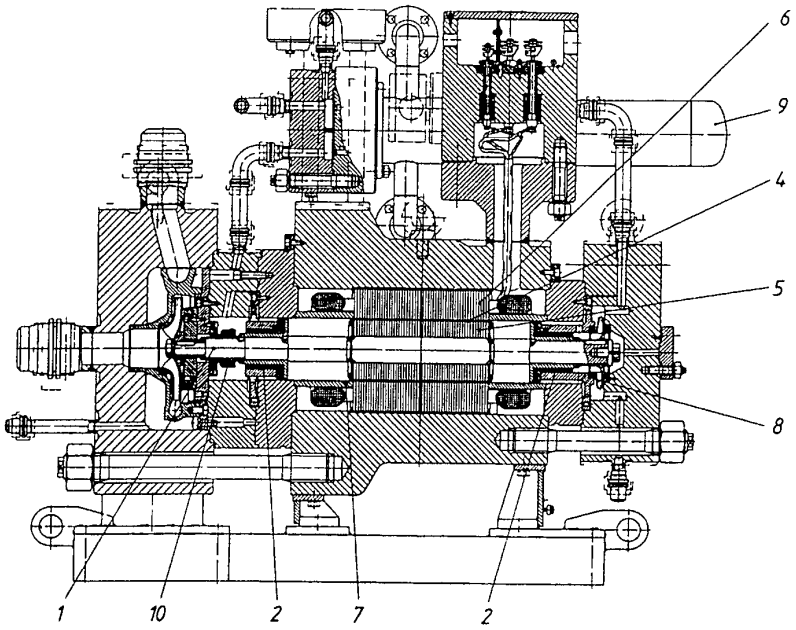

Figure 9 33 Canned motor centrifugal pump (HERMETIC)

*9 3 3 3 Design of centrifugal pumps** As with reciprocating pumps there is a choice between the 'leakfree' (hermetic) and the shaft-sealed designs for centrifugal pumps

The development of *canned motor* and *magnetic drive centrifugal pumps* has been encouraged in the process industries by anti-pollution laws [31–33] and obviously there are also positive arguments on economic grounds for using these designs in certain applications and capacity ranges [34] For applications in supercritical extraction plants there are good reasons to use canned-motor pumps (Figure 9 33) in cases where the system pressure is high and the differential pressure and capacity are low (typical values for the system pressure and differential pressure are 300 bar and 30 bar respectively, a power requirement of less than 200 kW) The rotor 1 in Figure 9 33 has fluid-lubricated sleeve bearings 2 (these would typically be siliconcarbide-based) and the thin sheet austenitic-steel motor can 4 between the stator 5 and rotor 6 of the motor is pressure supported in the radial direction by a specially designed stator core The stator plates are provided with special slots to create space for ceramic bars, capable of bearing high mechanical loads and for insulation, the remaining slots can be filled with incompressible resin for force transmission As this results in radial displacement of the winding slots a reduction of motor power is involved The stator lamination has a clamp at its outer circumference in order to prevent buckling of the plates under high pressure Suitable reinforcement rings 7 support the free ends of the can and also the rotor lamination in the axial direction

* The author wishes to thank R Kramer and R Neumaier Hermetic D 7803 Gundelfinger for assisting in the preparation of this section

For the special purpose of supercritical extraction, a semi-hermetic design has proved satisfactory where the motor cooling system is provided by a separate circuit including an impeller 8 and cooler 9 filled with water so that the lubrication of the bearings and the removal of heat from the motor is ensured The discharge fluid and the water cooling circuit are separated by a mechanical shaft seal 10, which experiences negligible pressure differential as the two systems are connected by a pressure balancing duct The water is controlled and automatically replaced by a small metering pump [35]

Multistage canned-motor centrifugal pumps are also available These deliver a greater head but are limited to powers of 200 kW and less by economic reasons and competition from shaft-sealed centrifugal pumps

In principle magnetic drives could be used with high pressure centrifugal pumps, but as the can between the magnet-coupling rotors has to carry the whole pressure differential it needs to be too thick for this technique to be fully effective this solution is not at all promising

For larger capacity and power requirements than the above, experience derived from centrifugal pump design for the feed to steam boilers, which have similar pressure differentials and high power requirements, is applicable

The *vertical split case multistage centrifugal pump design* is mainly used for maximum pressures below 200 bar with standard balanced mechanical shaft seals Axial thrust balancing can be achieved with a back-to-back rotor arrangement, which is advantageous where many stages and long rotor-shafts are necessary

For a typical application in a large supercritical bulk extraction plant the *multistage cartridge (or barrel) design* (Figure 9 34) might be more suitable since it is more robust with respect to sealing and clamping of the stage-casings The barrel-housing 1 contains the multistage components 2 The rotor is supported in radial and axial bearings 4 and 5 The shaft sealing for pressure differentials of 100–200 bar at a pressure level up to 300 bar requires mechanical seals 6 in a back-to-back double stage design with a blocking pressure system automatically controlled from the system pressure level The blocking

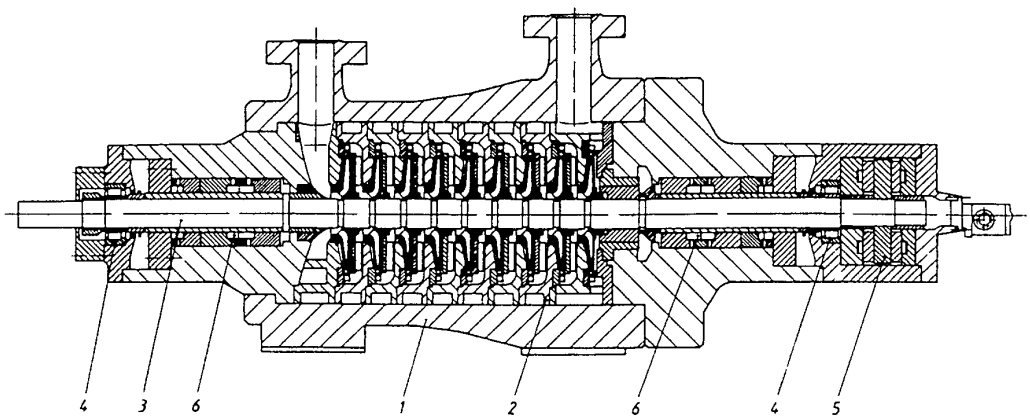

Figure 9 34 Centrifugal pump of the multistage cartridge (or Barrel) design (GRASSEL)

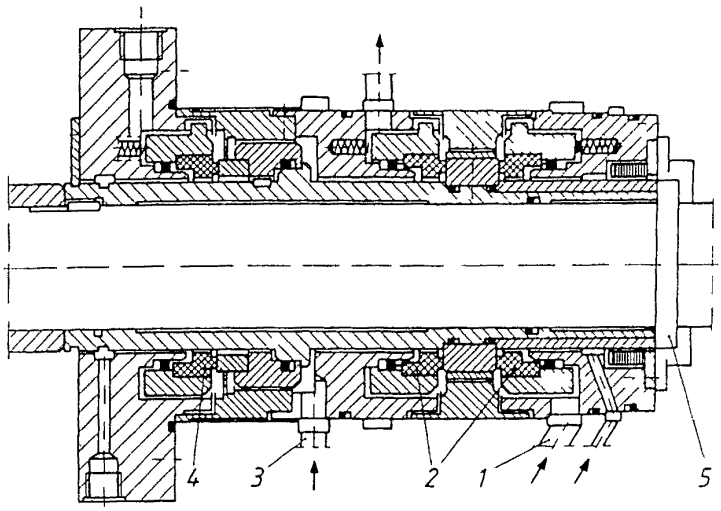

Figure 9 35 High pressure mechanical seal (GRASSEL/BURGANN) 1 blocking circuit I 2 mechanical seals arranged back to back 3 blocking circuit II 4 mechanical seal 5 shaft

pressure should exceed the pressure to be sealed by only a few bar (Figure 9 35) New developments in material and surface-design enable mechanical seals for pressure differentials up to 300 bar to be used with a single-stage blocking-pressure system [36] It is noteworthy that advances in material development, particularly siliconcarbide and silicon-impregnations, have greatly improved the life of high pressure mechanical seals [37]

For the large flow and low head applications which occur in extraction circuits where solvent regeneration is carried out by absorption or by adsorption on activated carbon, *in-line centrifugal pumps* have been found to be very

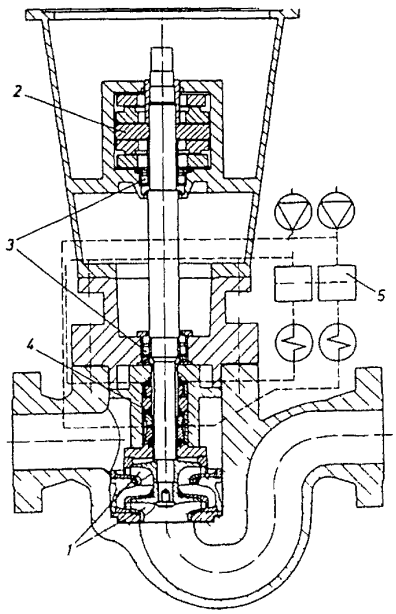

Figure 9 36 In line centrifugal circulation pump (GRASSEL)

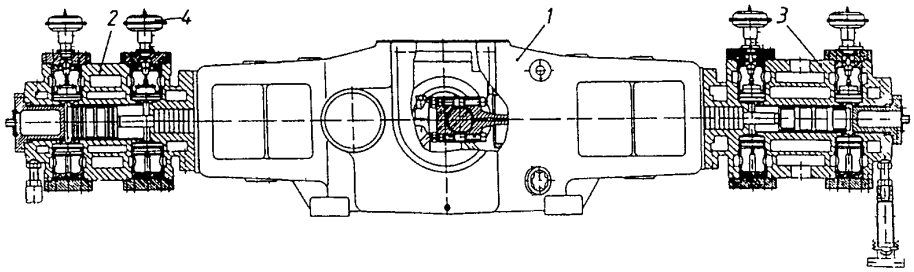

Figure 9 37 Two stage double acting horizontal piston compressor (NEUMAN and ESSER)

satisfactory (Figure 9 36) These pumps have one or two stages, axial thrust sleeves (2 on Figure 9 36) and radial thrust roller bearings (3) The mechanical shaft seal (4) shows the back-to-back double stage blocking pressure (5) design

9 4 Compressors for gas recovery*

The recovery and repressurisation of solvent gas following depressurisation of a section of plant which has already been discussed (section 9 2 2) for discontinuous extraction processes, can be necessary for economic or anti-pollution reasons As the necessary gas compressors do not usually form a very important part of the plant, the discussion below will be limited to some basic considerations

For gas recompression operations *dry-running piston machines* (non-lubricated) must be used The compression ratio during the recompression operation will typically increase from a very low value to about 20 as the inlet pressure progressively decreases Two or three compressor-stages with inter-cooling are therefore usual At the end of the recompression operation the compressor inlet pressure may be as low as 3 bar, while the outlet is at 70 bar The volume flow (measured at NTP) may be as high as 30 000 m^3/h

The solvent gas may contain water and horizontal compressors are therefore recommended (Figure 9 37) The crank drive 1 carries two double-acting compressor heads 2 and 3, the valves 4 provides stepwise regulation of the volume flow The characteristic design of the piston and rod seals is shown in Figure 9 38 for a vertical three-stage compressor It is an important detail that the first stage in these gas recompressors uses standard piston rings, while caught piston rings are employed in the last stage This design is necessary to restrict radial compression and improve machine life The rod seal should drain any gas leakages and prevent contamination by lubricating oil [38 39]

* The author wishes to thank H Gernandt Neuman and Esser D 5132 Ubach Palenberg for assisting in the preparation of this section

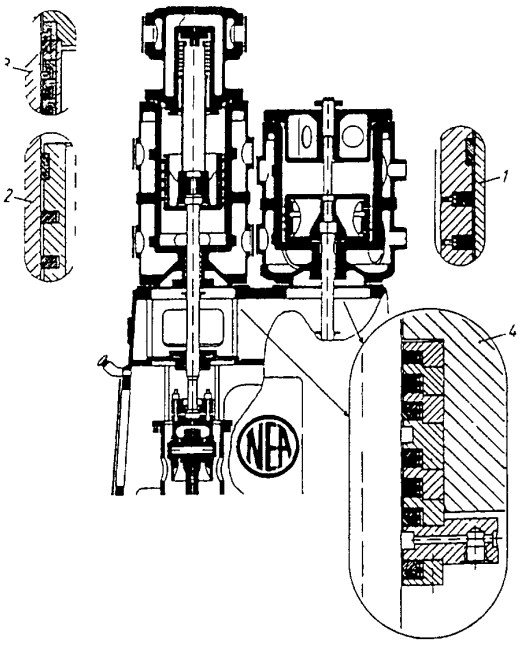

Figure 9 38 Piston and rod seals for a three stage non lubricated piston compressor (NEUMAN and ESSER)

References

1 Siewers V (1987) Variante zum Trennen *Maschinenmarkt Wurzburg* **93** (48) 126
2 Stahl E Quirin K W and Gerad D (1987) *Dense Gases for Extraction and Refining* (English edition translated by M R F Ashworth) Springer Verlag Berlin
3 Matson D W Fulton J L Petersen R C and Smith R D (1987) Rapid Expansion of Supercritical Fluid Solution Solute Formation of Powder Thin Films and Filters *Ind Eng Chem Res* p 2298
4 NN (1990) *Proc 2nd Int Symp on High Pressure Chemical Engineering* (Chairman G Vetter) Erlangen
5 NN (1991) *Proc 2nd Int Symp on Supercritical Fluids* (Chairman M A McHugh) Boston
6 Vetter G (1998) Supercritical Fluids Pumping at High Pressure in *Proc 1st Int Symp on Supercritical Fluids* Nice pp 587–594
7 Weidner E (1991) *The Industrial (Pilot) use of Continuous Supercritical Extraction with Emphasis on Liquid Separations* Handbook of 16th Scandinavian Liquid Symp
8 Weidner E and Peter S (1987) Separation of Lecithin and Soya Oil by near Critical Fluid Extraction in *Int Symp on Supercritical Gas Extraction* NTS INC Tokyo
9 NN Solvant D Extraction dont L Utilisation est Autorisee pour Traitement etc *Journal offic des Communautes Europ* No L 157/32 24688
10 Leyers W E Novak R A and Linning D A (1991) The Economics of Supercritical Coffee Decaffeination in *Proc 2nd Int Symp on Supercrit Fluids* Boston pp 261–263
11 NN (1985) *Sulzer Kreiselpumpen Handbuch* 1 Auflage 1985 Sulzer AG
12 Lobanoff V S and Ross R R (1985) *Centrifugal Pumps Design and Application* Gulf Publishing Co Houston
13 Vetter G (1987) Pumps in *The Theory and Practice in Supercritical Fluid Technology* (eds M Hirata T Ishikawa) NTS Tokyo pp 53–155
14 Muller F and Jarosch J (1987) Dosieren von Flussiggasen mit oszillierenden Verdranger pumpen *3R International* **4** 260–265
15 Vetter G Thiel E and Stork U (1989) Reciprocating Pump Valve Design in *Proc 6th Pump Users Symp* Houston pp 39–52

16 Vetter G Depmeier L and Schlucker E (1990) New Results on Design and Installation of High Pressure Reciprocating Pumps for CO_2 at Supercritical Conditions in *Proc 2nd Int Symp High Pressure Chemical Engineering* Erlangen pp 571–576
17 Vetter G Depmeier L and Schubert W (1991) Design and Installation Conditions of Diaphragm Pumps for High Pressure and Supercritical Fluids in *Proc 2nd Int Symp Super critical Fluids* Boston pp 272–275
18 Fritsch H (1990) Der NPSH Wert bei oszillierenden Verdrangerpumpen aus Vermeidung von Kavitationsschaden *Expert Verlag Band* **193** p 176 ff
19 Vetter G and Schweinfurter F (1989) Computation of Pressure Pulsations in Pumping Systems with Reciprocating Positive Displacement Pumps in *Proc 3rd Joint ASCE/ASME Mech Conf San Diego Pumping Machinery* pp 83–89
20 Vetter G (1988) Reliability and Future Development of High Pressure Diaphragm Pumps for Process Systems in *Proc of the 5th Pump Users Symp* Houston Texas pp 49–64
21 Vetter G (editor) (1990) *Leckfreie Pumpen* Vulkan Verlag
22 Vetter G and Hering L (1980) Leakfree Pumps for Chemical Process Industries *Chemical Engineering* **22** 149
23 Fritsch H (1990) *Prozess membranpumpen aus Leckfreie Pumpen* (ed G Vetter) Vulkan Verlag Essen S 118 ff
24 Stiefel W (1990) Verdrangerpumpen fur die CO_2 Extraktion *Chemie Technik* **19** Nr 8 pp 51–50
25 Idelchic I E (1986) *Handbook of Hydraulic Resistance* Hemisphere New York
26 Vetter G (1988) Zum Kenntnisstand der numerischen Bestimmung von Druckpulsationen durch oszillierende Verdrangerpumpen *3R International* 27 Heft 7 pp 468–475
27 Vetter G Schweinfurter F (1990) Elimination of Disturbing and Dangerous Pressure Oscillation caused by High Pressure Positive Displacement Pumps in *Proc 6th Int Conf on Pressure Surges* BHRA pp 309–324
28 Schweinfurter F (1988) Beitrag zur numerischen Bestimmung von Druckschwingungen in Rohrleitungssystemen bei Erregung durch ein und mehrzylindrige oszillierende Verdranger pumpen Dissertation Universitat Erlangen Nurnberg
29 Wachel J C Morton S J and Atkins K E (1990) Piping Vibration Analysis in *Proc 19th Turbomachinery Symp* Texas A & M University pp 119–134
30 NN (1983) *Hydraulic Institute Standards* 14th Edition Hydraulic Institute Cleveland USA
31 Kramer R and Neumaier R (1990) Hermetic Drive Systems in High Pressure Circuits in *Proc 2nd Int Symp High Pressure Chemical Engineering* Erlangen p 507 ff
32 Neumaier R (1990) Spaltrohrmotorpumpen – ein wesentlicher Beitrag zur leckfreien Forde rung in *Leckfreie Pumpen* (ed G Vetter) Vulkan Verlag Essen pp 74–96
33 Kramer R and Neumaier R (1987) Hermetische Kreiselpumpen fur die chemische und artverwandte Industrie in *Pumpen Bauelemente der Anlagen technik* (ed G Vetter) Vulkan Verlag p 327 ff
34 Richard L (1991) Figuring the relative cost of pumps *Chemical Engineering* p 129 ff
35 Kramer R and Neumaier R (1988) Kreiselpumpen und rotierende Verdrangerpumpen her metischer Bauart Hermetic Pumpen GmbH
36 Victor K H Kontakt und verschleiss frei arbeitende Elasto Hydro Dynamik (EDH) – Glei tring dichtungen fur Hochdruckeinsatz *Pumpentagung Karlsruhe* 88
37 NN (1988) *Burgmann Lexikon – ABC der Gleitringdichtung 1* Ausgabe Burgmann
38 Gernandt H (1990) Kolbenkompressoren fur die Verfahrenstechnik in *Verdichter Handbuch 1 Ausgabe* (ed G Vetter) Vulkan Verlag Essen
39 Gernandt H L (1990) Some Problem Solutions with High Pressure Reciprocating Compres sors in *Proc 2nd Int Symp High Pressure Chem Engineering* Erlangen p 523 ff

Natex Prozesstechnologie GesmbH

Basic-Course

of

Supercritical Fluid Extraction Process

Metal Industries Research & Development Center

Kaohsiung, Taiwan, ROC

Mr TZU-CHEN KUO

Basics and Principles
Of
Heating & Cooling
Systems

1 Heating Systems

1 1 Heating Mediums

In the most cases either water or steam and in special cases thermo-fluids (oils) are used for heating purposes Beside this main mediums various mediums (fluids gases) can be used if they have the necessary temperature and heat capacity (carried out mainly in petrochemical plants)

1 1 1 Water

Water is the common medium for heating below 100 °C Especially for heat sensitive products overheating at the exchange surface can be avoided

1 1 2 Steam

Above heating temperatures of 100 °C up to 200 °C steam is the common medium Because of the higher heat transfer rate (about 1000 W/m² K) smaller heat exchangers in comparison with water (about 300 W/m² K) are necessary

1 1 3 Thermo-Fluids

Thermo-fluids are used for high temperatures (up to 400 °C) and constant heat consumption in special applications E g for heating temperature of 180 °C steam with a pressure of 16 bar would be necessary

1 2 Heat Generators

Steam generators are mainly fired by oil or gas Water and thermo-fluids are also mainly heated by oil or gas in some cases by electricity
The latest thing is there are more and more biomass heated generators coming up because biomass remain neutral for CO2 emissions

1 3 Typical circuit diagrams for heating

1 3 1 Direct heating by hot water

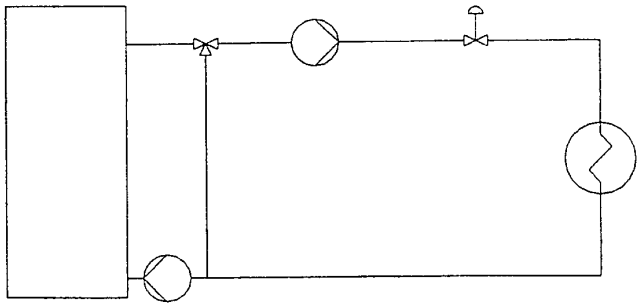

1 3 2 Secondary heating by hot water

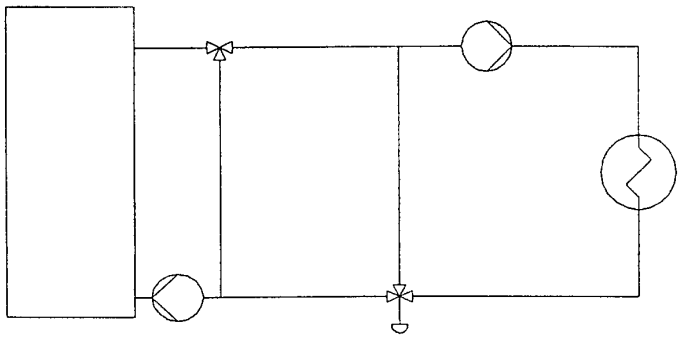

1 3 3 Heating by steam without condensate recovery

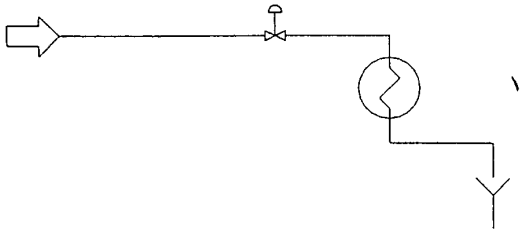

1 3 4 Heating by steam with condensate recovery

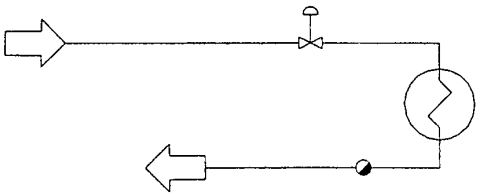

1 3 5 Heating by steam with condensate recovery by pump

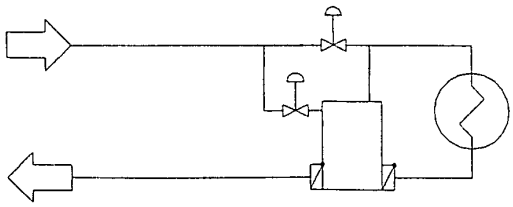

2 Cooling Systems

2 1 Cooling Mediums

In the most cases either water or air and in special cases refrigerants are used for cooling purposes Beside this main mediums various mediums (fluids gases) can be used if they have the necessary temperature and cooling capacity (carried out mainly in petrochemical plants)

2 1 1 Air

Air for cooling is mainly used for air condition systems or to cool very hot mediums (e g waste gas) The usage of air is limited to the climatic conditions of the location (about 35 – 40 °C)

2 1 2 Water

Water has a wide range of applications Fresh water cooling systems use water from rivers and underground water With cooling towers the water consumption can be reduced and through the evaporation effect lower temperatures (25 – 30 °C) than with air can be achieved The usage of water depends on availability of natural resources (e g rivers) climatic conditions (temperature humidity) and last but not least the freezing point (0 °C) especially in regions where during winter season ambient temperatures of minus 30 °C are normal

2 1 3 Water with cooling agent

If water is mixed with a cooling agent the application range can be extended to temperatures below 0 °C On the one hand salts (sodium chloride calcium chloride magnesium chloride) and on the other hand alcohols (ethanol, methanol glycol) are used to reduce the freezing point of water

2 1 4 Refrigerants

Beside the classical refrigerants like sulphur dioxide methyl chloride and ammonia which because of their chemical and physiological effects are disputed and under restriction by laws also the chlorofluorocarbons (CFC) are more and more restricted by laws because of their effects to the global change in climate Nowadays new harmless and save mediums are searched to solve this problems Also systems with carbon dioxide (air condition in cars) will be developed main problem is the high vapour pressure of carbon dioxide (e g 60 bar at 22 °C)

2 2 Cooling Aggregates

2 2 1 Air Cooler

Air cooler are used for cooling of hot cooling water systems (e g diesel engines 90°C) and refrigerants of refrigerating machines

2 2 2 Cooling Tower / open circuit

Cooling towers are used for direct cooling (e g 45 °C) and for water cooled types of refrigerant machines Because of evaporation spraying losses and reducing the concentration of solved matters a make up water consumption of about 10% of the flow rate must be taken into consideration

2 2 3 Cooling Tower / closed circuit

Cooling towers of this type are mainly used like an air cooler only during peaks of cooling power and hot climatic seasons water is sprayed on the exchange surfaces (evaporation effect) to increase the cooling power

2 2 4 Refrigerating Machines

2 2 4 1 Refrigerating Machines air-cooled compact type

At this type the air-cooler for the refrigerant is directly mounted with the machine and the complete machine has to be placed outdoors

2 2 4 2 Refrigerating Machines air-cooled split type

The refrigerating machine is placed indoors and the air-cooler for the refrigerant is placed outdoors (mainly at the roof of the building) If long pipes are necessary they have to be insulated well to avoid temperature losses

2 2 4 3 Refrigerating Machines water-cooled

This type can be cooled by fresh water or cooling water from cooling towers If fresh water is used the installation of a compressor pressure controlled water consumption reducing valve is recommended Also the possibility of energy recovery systems (room heating sanitary water and low temperature heating systems at 40 – 45 °C) should be taken into consideration

2 2 4 4 Refrigerating Machines direct cooling

In some special cases the refrigerant of the machine cools direct the product cooler Problematic items are the pressure (up to 55 bar) leakages (harmful refrigerants) and the low cooling temperatures (minus 40 °C risk of freezing at the exchange surface)

2 3 Typical circuit diagrams for cooling

2 3 1 Direct cooling by refigerating machine air-cooled compact type

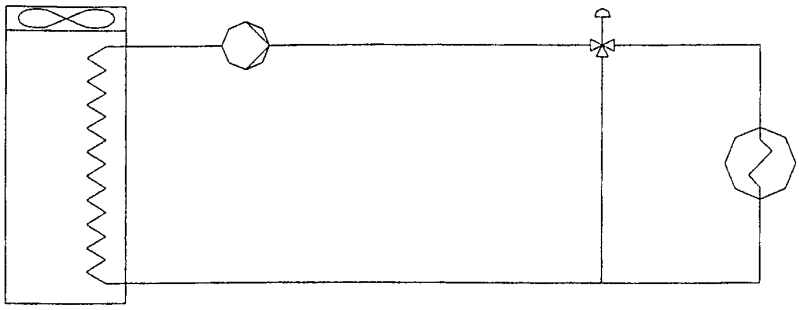

2 3 2 Direct cooling by refigerating machine water-cooled by cooling tower with use of a buffer vessel

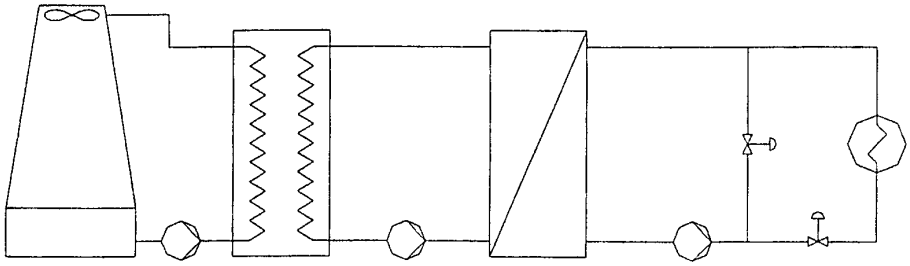

2 3 3 Secondary cooling by refigerating machine air-cooled compact type with use of a buffer vessel

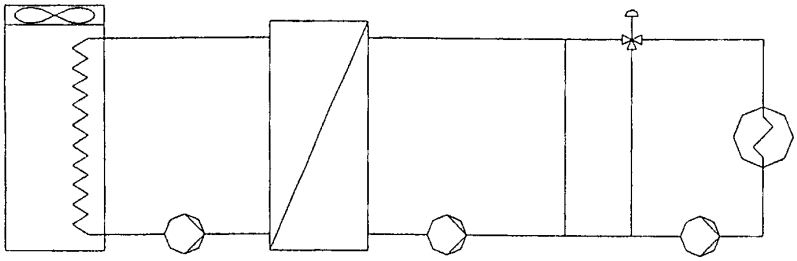

1 3 Typical circuit diagrams for heating

1 3 1 Direct heating by hot water

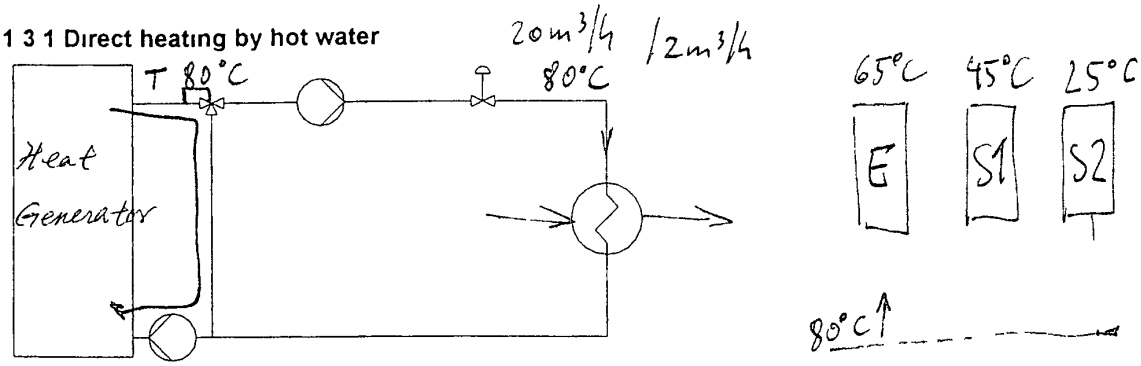

1 3 2 Secondary heating by hot water

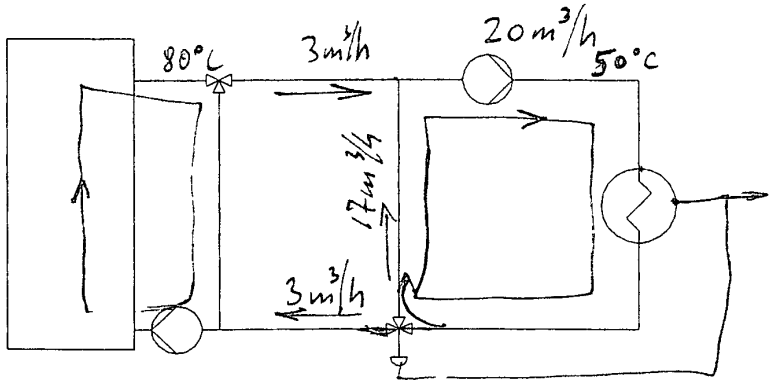

1 3 3 Heating by steam without condensate recovery

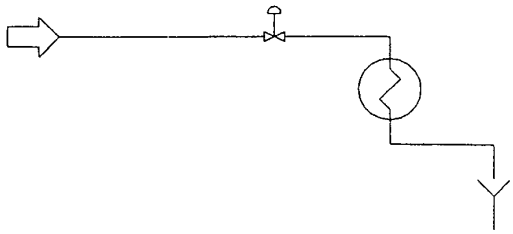

1 3 4 Heating by steam with condensate recovery

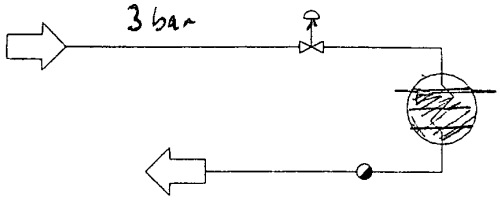

1 3 5 Heating by steam with condensate recovery by pump

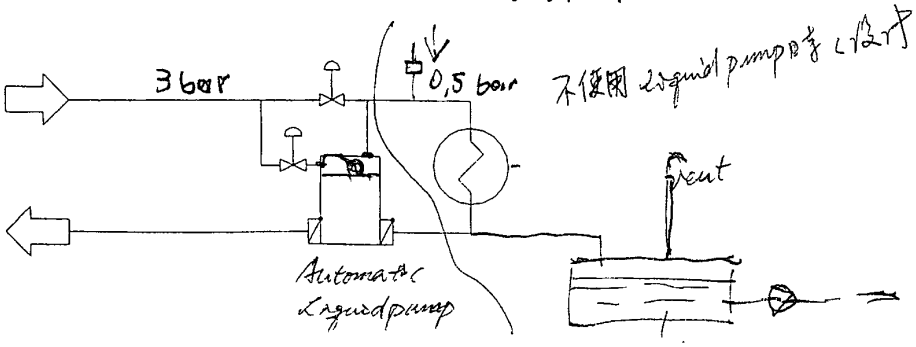

2 3 Typical circuit diagrams for cooling

2 3 1 Direct cooling by refigerating machine air-cooled compact type

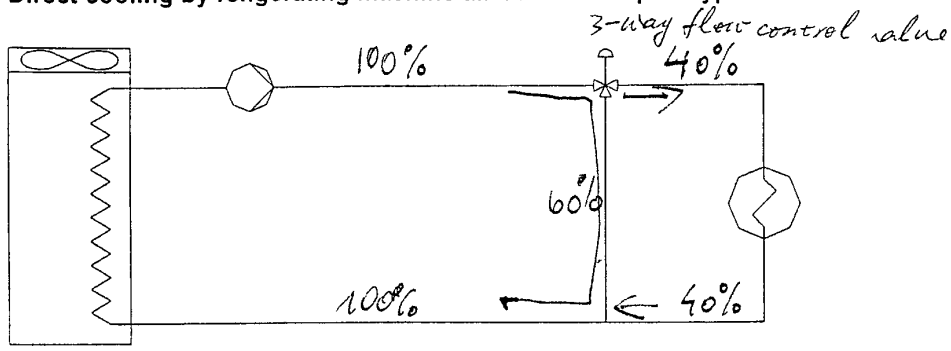

2 3 2 Direct cooling by refigerating machine water-cooled by cooling tower with use of a buffer vessel

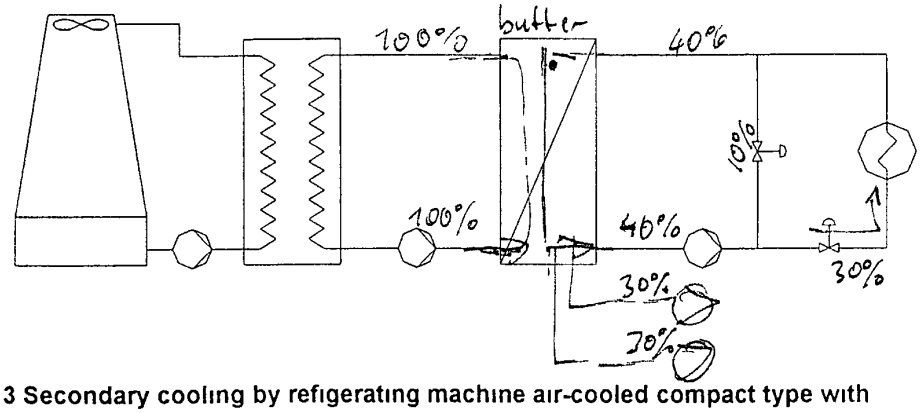

2 3 3 Secondary cooling by refigerating machine air-cooled compact type with use of a buffer vessel

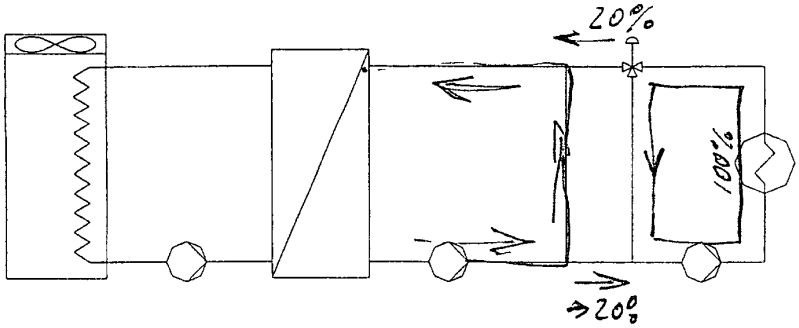

	in / out	Cooling Power	electr Power
Standard	42°C / 7°C	200 kW	50 kW
	-5°C / -10°C	80 kW	50 kW

20% - 30%

75%

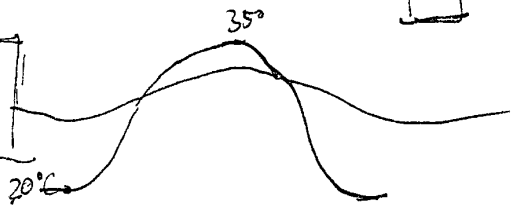

Rhebis

Natex Prozesstechnologie GesmbH

Basic-Course

of

Supercritical Fluid Extraction Process

Metal Industries Research & Development Center

Kaohsiung, Taiwan, ROC

Mr TZU-CHEN KUO

SEPARATION SCIENCE
and
TECHNOLOGY

SEPARATION SCIENCE AND TECHNOLOGY

Executive Editor

J CALVIN GIDDINGS
DEPARTMENT OF CHEMISTRY
UNIVERSITY OF UTAH
SALT LAKE CITY UTAH 84112

Editorial Board

R M BARRER *Imperial College of Science and Technology London*
K D CALDWELL *University of Utah Salt Lake City*
N CATSIMPOOLAS *Boston University School of Medicine Boston*
H FREISER *University of Arizona Tucson*
R B GRIEVES, *University of Texas at El Paso*
E GRUSHKA, *The Hebrew University of Jerusalem Israel*
F G HELFFERICH *347 Knipp Road Houston Texas*
J D HENRY JR *West Virginia University Morgantown*
C HORVATH, *Yale University New Haven Connecticut*
E P HORWITZ *Argonne National Laboratory Illinois*
K KAMMERMEYER *University of Iowa Iowa City*
G KELLER *Union Carbide Corp South Charleston West Virginia*
R A KELLER *State University of New York College at Fredonia New York*
J LEJA *University of British Columbia Vancouver*
N LI *UOP Inc Des Plaines Illinois*
E N LIGHTFOOT, *University of Wisconsin Madison*
A P MALINAUSKAS *Oak Ridge National Laboratory Tennessee*
J K MANGOLD, *H P Kaufman Institute Muenster West Germany*
A MICHAELS, *Stanford University California*
M N MYERS *University of Utah Salt Lake City*
J D NAVRATIL *Rockwell International Golden Colorado*
V PRETORIUS, *University of Pretoria Republic of South Africa*
S RAYMOND *University of Pennsylvania Philadelphia*
L B ROGERS *University of Georgia Athens*
M TISHLER *Wesleyan University Middletown Connecticut*
H WALTON *University of Colorado Boulder*
P C WANKAT *Purdue University Lafayette Indiana*
G H WEISS *National Institutes of Health Bethesda Maryland*
W R WILCOX *Clarkson College of Technology Potsdam New York*
D J WILSON *Vanderbilt University Nashville Tennessee*

Separation Science and Technology

Exploring the range of separation phenomena, **Separation Science and Technology** reviews the newest concepts and techniques for dealing with problems encountered by professionals in this rapidly expanding field It gives authoritative and critical attention—through notes, articles, and reviews—to a wide range of topics, including separation theory, ultrafiltration, chromatography, electophoresis, foam fractionation, flocculation, solvent extraction, field-flow fractionation, ion exchange, adsorption, sedimentation, reverse osmosis, zone melting, thermal diffusion, multi-stage processes, actinide separations, water purification, biochemical fractionation and mineral separation The interdisciplinary coverage of **Separation Science and Technology** enhances and supports the efforts of researchers in biology, chemistry, engineering, and other fields, and will appeal specifically to analytical, physical, and polymer chemists, biochemists, chemical and mechanical engineers, environmental scientists, biologists, and colloid scientists For these and other professionals, **Separation Science and Technology** offers the finest forum for probing the essence of separation phenomena

SEPARATION SCIENCE AND TECHNOLOGY **23**(1-3) pp 63-76 1988

Estimation of the Process Parameter for High-Pressure (supercritical fluid) Carbon Dioxide Extraction of Natural Products

E LACK

VEW TERNITZ
A 8010 GRAZ AUSTRIA

R MARR

INSTITUTE OF CHEMICAL ENGINEERING
TECHNICAL UNIVERSITY OF GRAZ
A 8010 GRAZ, AUSTRIA

Abstract

The objectives of this work were to find a useful concept for the design of high pressure extraction (HPE) plants and to carry out a parameter analysis of various influences on construction and design To evaluate the influence of each parameter on the process better the parameters were subdivided into five groups Experiments were made to determine the solubility and mass transfer of neutral products in CO_2 These results were tested with models in order to establish the possibility of a mathematical description of HPE processes

INTRODUCTION

Since high-pressure extraction (HPE) is important for the production of natural extracts (for example, decaffeination of green coffee beans, production of hop extracts), useful concepts for plant design can reduce the economic risks of a new process

The numerous parameters which influence the process and the design of a plant must be evaluated by many experiments on a laboratory plant This paper tries to reduce this extensive experimental work by a

Copyright © 1988 by Marcel Dekker Inc

subdivision of the main problems (*1*) In an extraction experiment, all parameters act together and it is difficult to recognize the influence of one parameter to the process

The main problem areas are

Nonalterable material specific basic data
Thermodynamic conditions in the extraction and separation steps
Mass transfer
High-pressure extraction process in the *T*,*s* diagram
Special problems in the separation step

DESCRIPTION OF THE EXPERIMENTAL PLANT

Figure 1 shows a general flow sheet of a high-pressure extraction plant as used in our laboratory The experimental plant consists of the following main items extraction vessel, separation vessel, liquid gas storage vessel

The cycle of the solvent CO_2 is as follows A pump draws off liquid CO_2 from the storage vessel (1) and compresses it to extraction pressure (2) Then the CO_2 is heated up to extraction temperature by a heat exchanger In the extraction vessel, the highly compressed supercritical or liquified gas dissolves the soluble substances from the raw material In the throttle

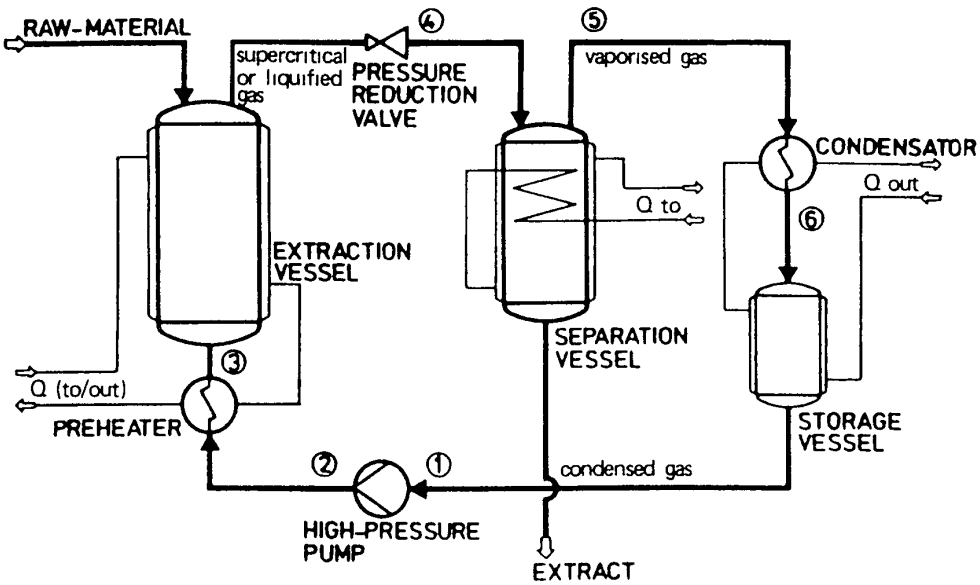

FIG 1 Flow sheet of the experimental plant

section (4) the temperature and/or pressure of the loaded solvent are changed Usually, the pressure is reduced from 150 to about 40–60 bar

The remaining liquid CO_2 is evaporated by means of another heat exchanger At separation conditions the solubility of the extract is completely depressed, the solute and the solvent are separated, and the extract can be drained off through a valve The nearly extract-free gaseous CO_2 is completely liquified in a condenser (6) and fed back into the storage vessel, completing the cycle

It is also possible to use a compressor instead of a pump to increase the pressure In this case the evaporated CO_2 gas flows directly to the compressor, and no condenser or storage vessel is needed However, investment costs and energy demand for the compressor are considerably higher

BASIC DATA

The first main parameters needed for a HPE process are properties of the raw material and the required production rate as well as the concentration of the extractable substances in the feed, kind of raw material for extraction, specific volume of the prepared feed, and the mode of operation For extraction of natural substances, usually only the preparation of the raw material and the specific volume can be varied to some extent For example, it is possible to change the specific volume by milling or pelletizing the raw material This parameter influences mainly the volume of the extraction and separation vessels

THERMODYNAMIC CONDITIONS

The next parameter to be considered is the estimation of the thermodynamic conditions in the extraction and separation steps In the range at the critical point or in the supercritical region the influence of pressure, temperature, and density of the solvent on the distribution equilibrium are much more important than in conventional extraction Therefore, it is possible to vary the solvent properties of a compressed gas by changing the pressure and temperature In the extraction step it is desirable to reach a high solubility and therefore a low solvent consumption In the separation step a very low concentration of the extract in the solvent is required to guarantee a good regeneration of the solvent

Useful models for the description of the experimental equilibrium

concentrations are necessary to enable a fast optimization of this parameter The well-known models in the literature are based on three equation systems

Empirical equations of state
Half-empirical equations of state
Derivations from the association laws and/or from the entropies of the components

Half-empirical equations of state are used to fit binary systems, and thermodynamic data of the solute and the solvent have to be known For systems with more than two components, the mathematical solution is very difficult A useful equation of state for the description of simple binary systems is the Peng-Robinson (*2*) equation This equation is applicable for large pressure and temperature ranges

For unknown solvent data, derivation from the association laws is used to adjust experimental results The most popular equation of this type was published by Chrastil (*3*)

Figure 2 shows the correspondence of measured and, according to Chrastil, calculated equilibrium data for rapeseed oil in CO_2 The dominating influence of gas density on CO_2 loading is significant This

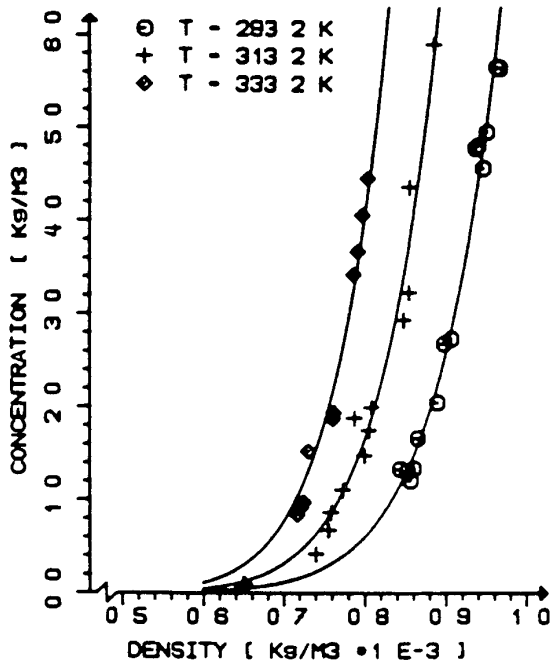

FIG 2 Equilibrium of rapeseed oil in CO_2

equation is very useful to describe the equilibrium distribution of natural substances in compressed gases

MASS TRANSFER

The objective of this investigation is to determine the optimum flow rate The energy consumption is linearly dependent on the mass flow rate of the solvent in any case, involving complete solvent recirculation

In order to study the mass-transfer behavior, several experiments were made to measure the loading of the solvent as a function of extraction time and the height of the bed All experiments were made in the same laboratory plant The flow sheet of this plant is shown in Fig 1

Flaked rapeseed and milled press cake of rapeseed were used as feed To exclude the influence of different feed properties, preparation of the raw material was done in the same way for all experiments

The same thermodynamic conditions were used for all mass transfer investigations

Extraction pressure 290 bar, extraction temperature 40°C
Separation pressure 50 bar, separation temperature 25°C

Some results of these measurements are shown in Figs 3 and 4

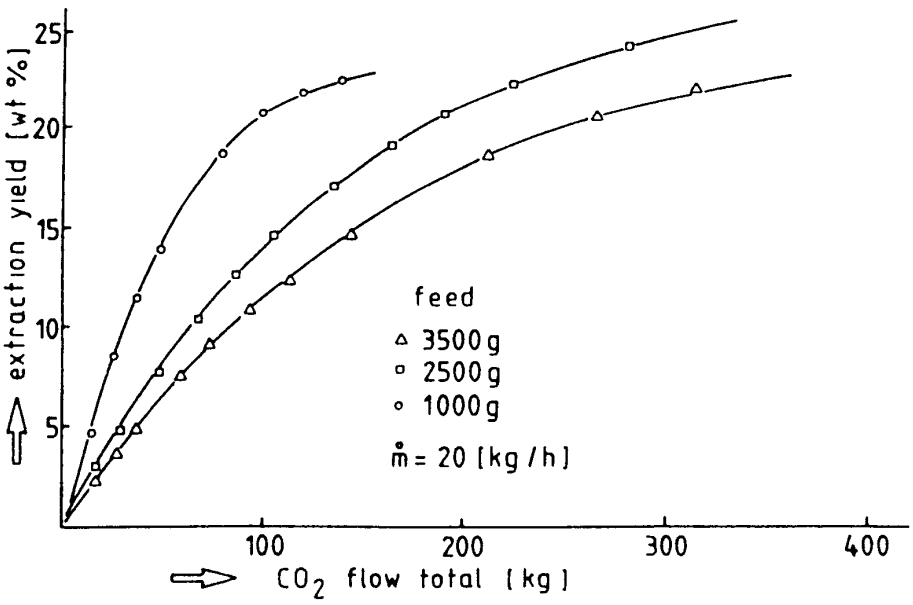

FIG 3 Extraction of rapeseed oil as a function of total CO_2 throughput

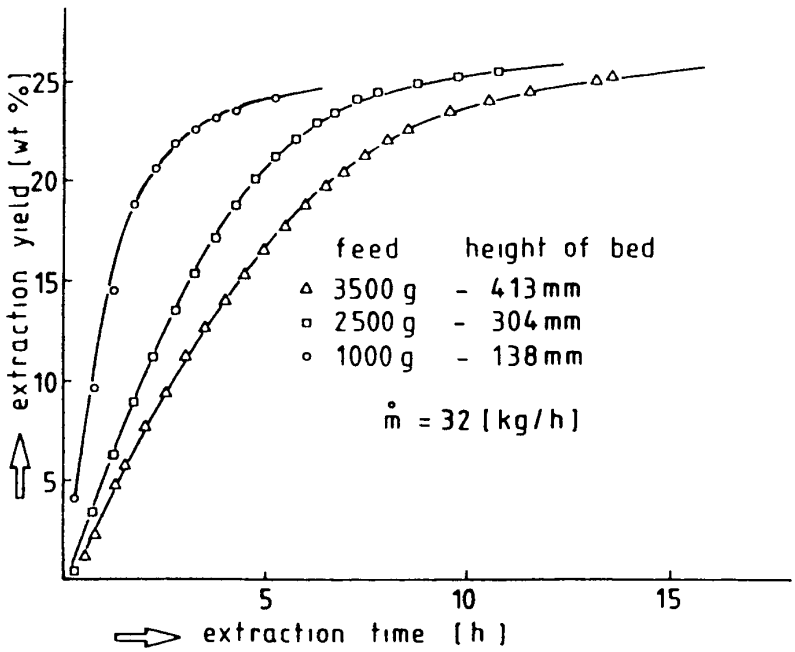

FIG 4 Extraction yield as a function of extraction time

Because it is not possible to get solid samples out of the extraction vessel, it is necessary to make separate experiments for each height This means that it is possible to determine the concentration distribution versus time in one experiment, but it is not possible to determine the concentration distribution versus the height of the bed at the same time The extraction time is very long because of the small solvent velocity in the extractor

At the beginning of an extraction process or at low absolute CO_2 throughput, high solvent loadings are obtained because of the great concentration differences as shown in Fig 5

Extraction in the lower layer is finished after a flow of 120 kg CO_2 Then the mass-transfer area moves to the upper layers The mass-transfer area is that part of the extractor where the concentration gradient is high enough to get an economical mass transfer

Extraction is complete when the boundary of the mass-transfer area reaches the top of the extractor Knowledge of the motion and expansion of the mass-transfer area is very important for optimization of mass transfer

For low solvent throughput the mass-transfer area is much smaller than the height of the bed Therefore, the mass-transfer area is much smaller than the height of the extractor and the extraction time increases For high solvent throughput the mass-transfer area is larger than the

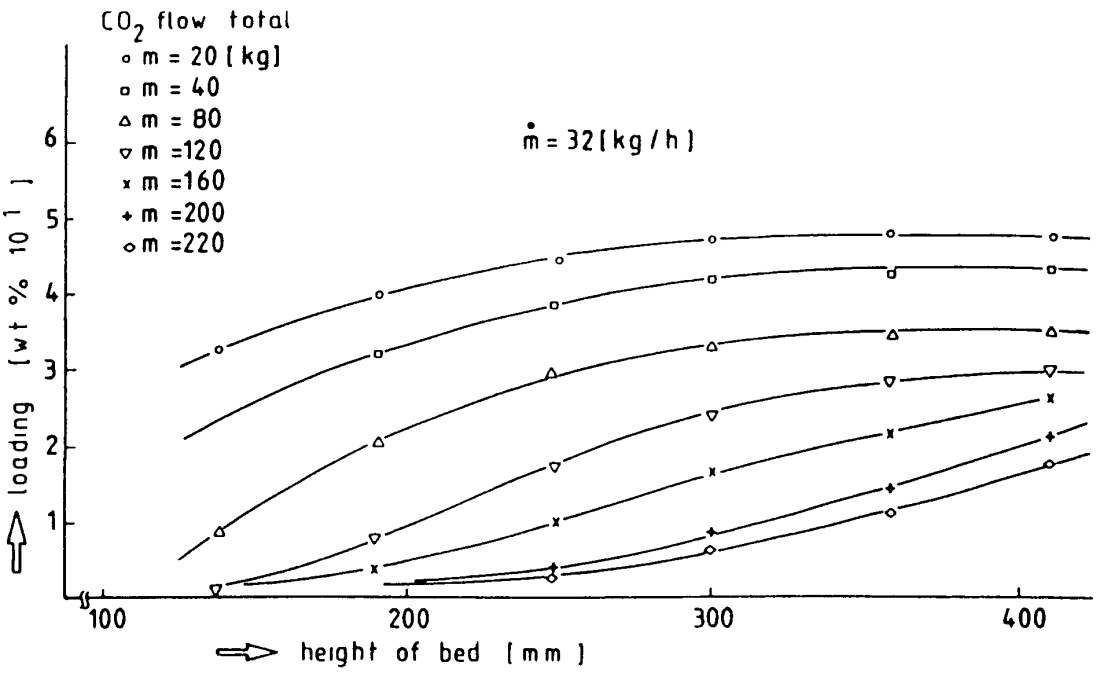

FIG 5 Concentration distribution versus height of bed

height of the bed, the solvent is not completely loaded, and process costs increase

Figures 6 and 7 show the extraction yield versus the height of the bed and the extraction time The logarithmic plot of the extraction time in Fig 7 shows the motion of the mass-transfer area from the bottom to the top of the extractor A three-dimensional projection of Fig 7 in Fig 6 gives a three-dimensional dependence of the extraction yield on extraction time and the height of the bed These relations are important for modeling the mass transfer

MODELING OF MASS TRANSFER

The most popular models for describing mass transfer in high-pressure extraction were published by Brunner and King (*4*, *5*)

Because of the analogy of high-pressure extraction and drying processes, we transformed a drying model into a high-pressure extraction model

There are two main relations between drying and HPE the solubility equilibrium depends on the thermodynamic properties of the solvent and the mass transfer is divided into two sections In the first section the substances to be extracted are removed from the particle surfaces just as in the first drying section In the second part mass transfer is controlled

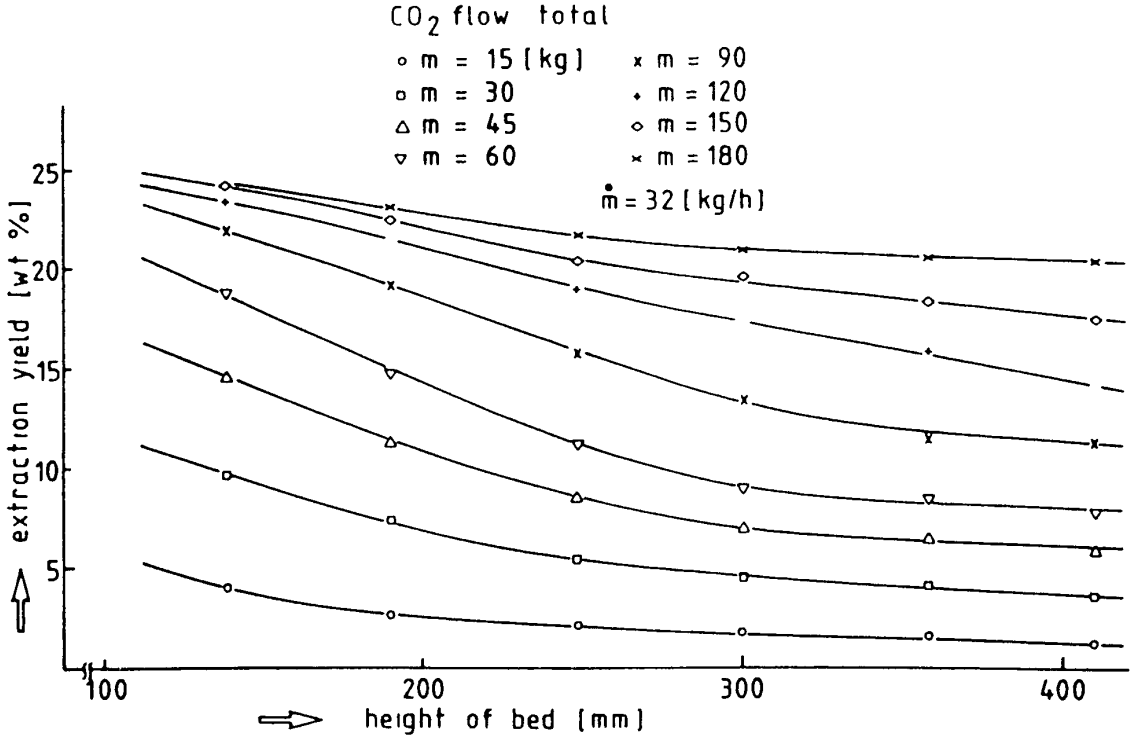

FIG 6 Extraction yield as a function of the height of bed for different total CO_2 throughputs

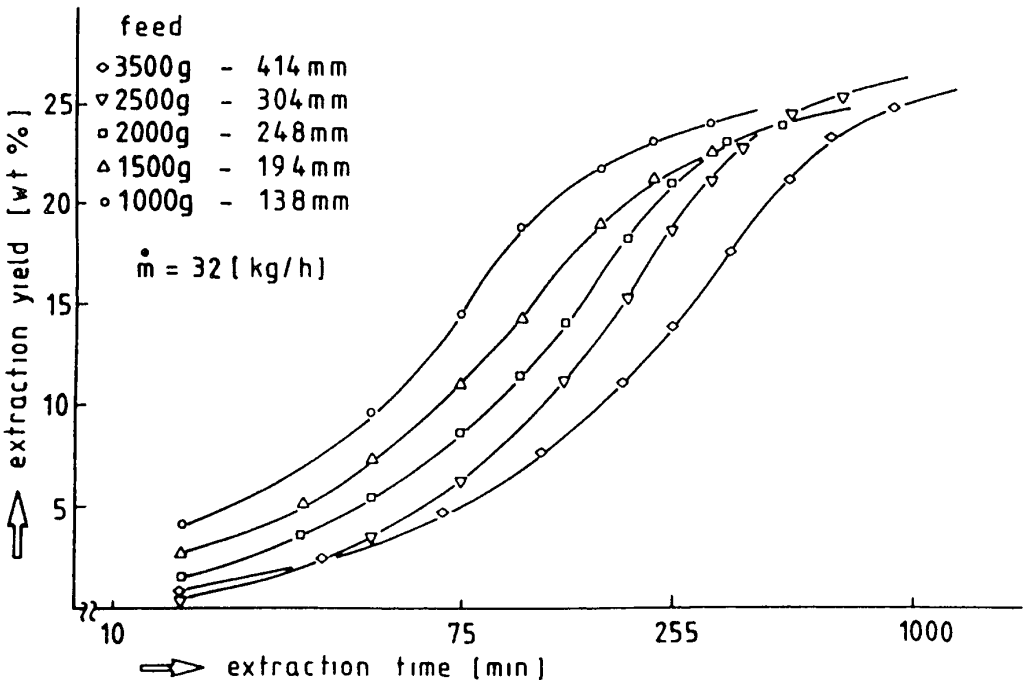

FIG 7 Extraction yield as a function of extraction time for five feed amounts or height of bed

by diffusion or other properties which reduce the mass-transfer velocity (for example, adsorption bondings) A computer program was established to calculate the mass transfer by means of the transformed drying model The results of the calculation show a good correspondence to the experimental results of Fig 8

THE HPE PROCESS CYCLE IN THE *T,s* DIAGRAM

The fourth main parameter is the estimation of the best process cycle in the *T,s* diagram Because of the various possibilities offered in the supercritical region, it is difficult to find the process with the lowest energy consumption as shown in Fig 9 To determine the best process cycle, we used a computer program that enabled us to calculate several process variations

About 250 processes were evaluated with this program The program uses the thermodynamic conditions in the extraction and separation steps as starting points to give the two limits of the process in the *T,s*

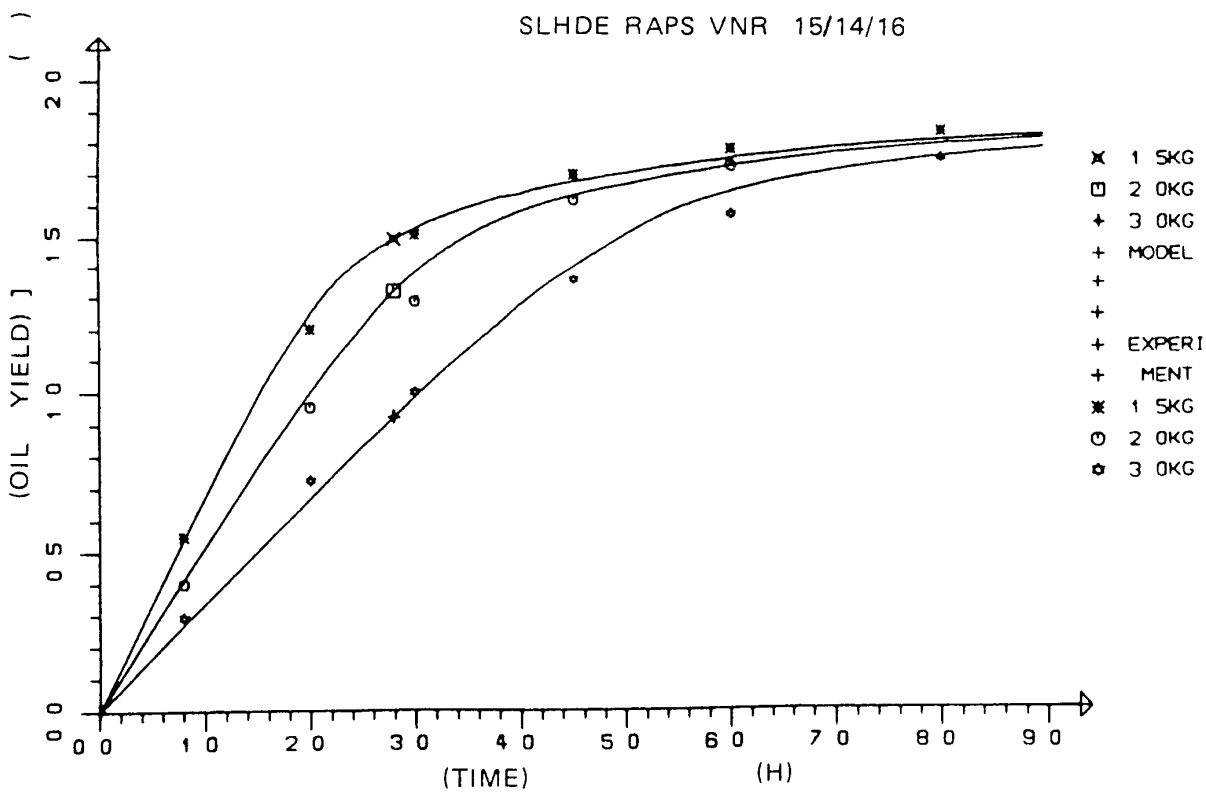

FIG 8 Extraction of rapeseed based on the drying model

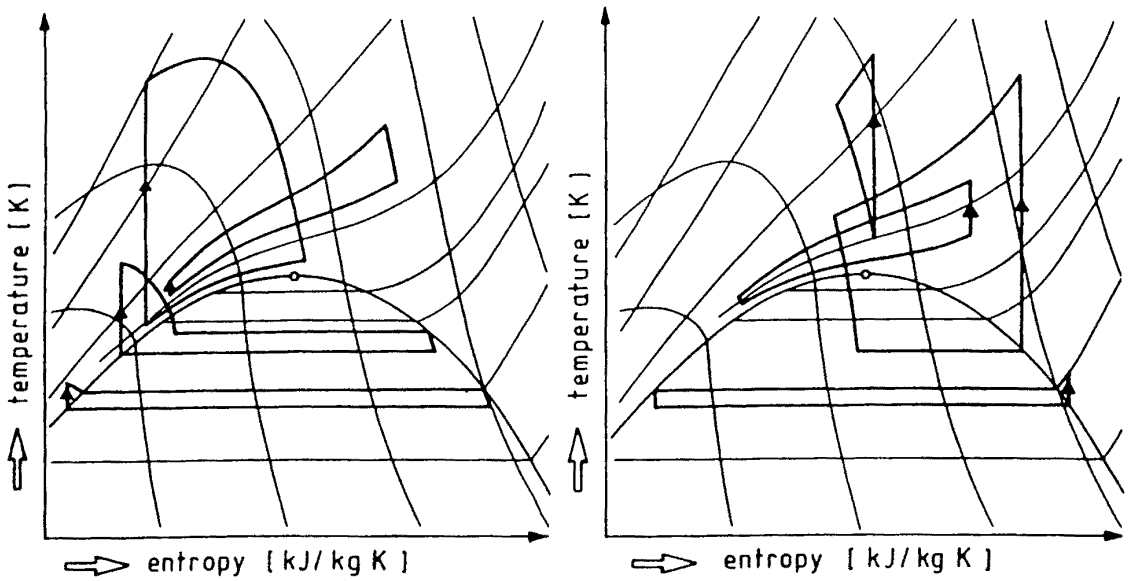

FIG 9 Different possibilities of a process cycle in the HPE extraction

diagram The program then calculates the pump and compressor processes The thermodynamic conditions of CO_2 in each stage of the process are calculated from the JUPAC equation of state The two types of energy required during the process are electric energy for all mechanical equipment, such as pump, compressor, and refrigerator, which is needed for condensing the gaseous CO_2, and thermal energy for the preheater

The energy costs are calculated for 1000 kg CO_2 passing through the process cycle in the T,s diagram The costs for the two types of energy are 0 055 US$ for 1 kWh electric energy and 0 025 US$ for 1 kg of steam with a thermal energy of 2150 kJ/kg

Analysis of the Pump Processes

The main energy consumers of pump processes are the refrigerator for condensing the gaseous CO_2, the circulation pump, and the preheater between the pump and the extractor The electric power consumption of the refrigerator depends only on the separation conditions The cost for the refrigerator varies between 0 1 US$ for a separation pressure of 60 bar and 1 2 US$ for a separation pressure of 30 bar

There is only a small rise in temperature in the pump for low extraction pressures Therefore, the preheater needs more energy When the temperature of the solvent at the delivery side of the pump corresponds to the desired temperature in the extractor, the energy demand is mini-

mized The area of minimum energy costs is situated between 150 and 300 bar, and depends on the extraction temperature

For low separation pressures, as shown in the three-dimensional curve of Fig 10, the cost level is very high This is due to high energy consumption by the refrigerator Minimum process costs are achieved for a separation pressure of about 60 bar and an extraction pressure of 200 bar (about 0 45 US$/t CO_2)

Analysis of the Compressor Process

Plotting of a three-dimensional cost curve is not possible because higher extraction pressures involves more than one compression step The maximum compression ratio for one compression step is about 3 5

The compressor accounts for nearly the entire energy consumption of the process Compressor processes have a low energy consumption for low extraction and separation pressures For a separation pressure of 30 to 40 bar and up to 300 bar extraction pressure, the compressor processes need less energy than the pump processes because of the high costs for the refrigerator

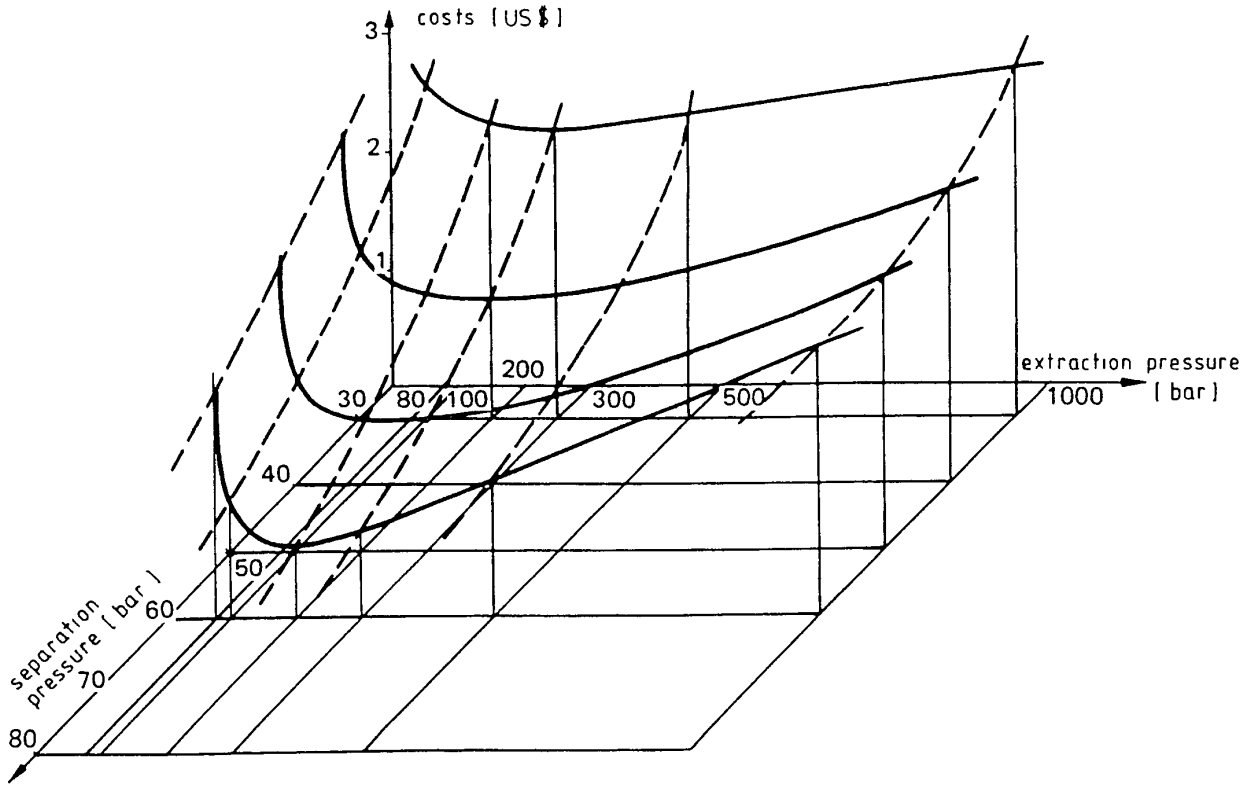

FIG 10 Process costs as a function of extraction and separation pressures for a constant extraction temperature (40°C)

PROBLEMS OCCURRING IN THE SEPARATION STEP

The next group of problems refers to the separation step As mentioned before, energy costs are low if the separation pressure is about 50 to 65 bar But with higher pressure and temperature the concentration of extracts in the CO_2 phase in the separation vessel increases Extracts which contain essential oils and waxes can be fractionated with multistage separation (Fig 11) In the first separation stage, waxes are enriched, and in the second one, which takes place at lower pressure and temperature, a concentrated extract of essential oil is obtained

Significant problems arise when highly volatile substances at low concentrations must be separated To reach a quantitatively high separation in one step, a very low separation pressure and temperature is necessary This involves high energy consumption and the risk that solid material (e g , ice) will block the pipes and the valves

Separation in a multistage distillation column may be a solution to these problems Such columns can operate with a temperature above the freezing point of water The degree of purification is determined by the height of the column and the reflux

Another field of application is the regeneration of activated carbons

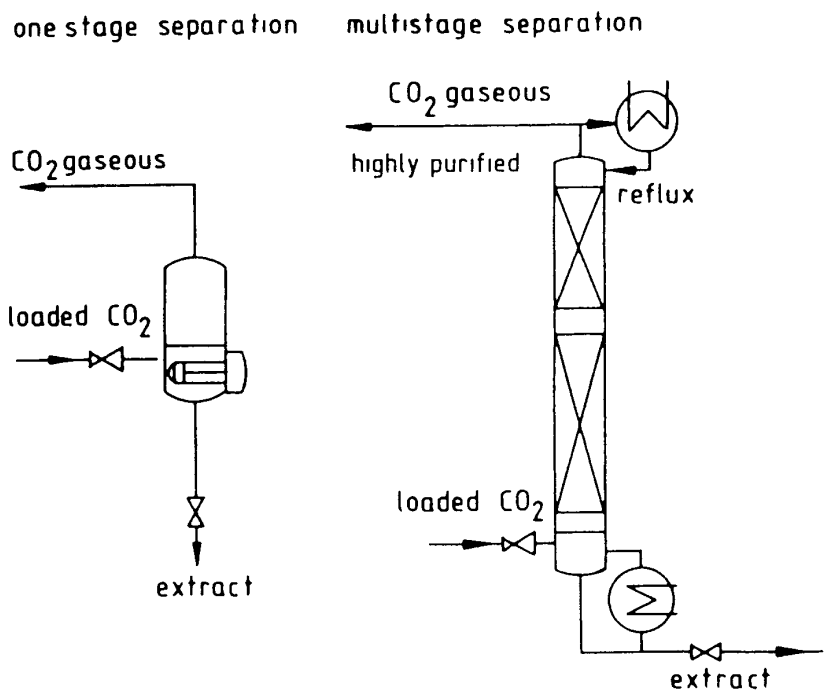

FIG 11 Two examples for separation processes (6)

The degree of regeneration depends on the purity of the CO_2 after separation

SUMMARY

Finally, we discuss the influence of the main parameters on the various parts of the plant Process design data, such as plant capacity, extraction yield, specific volume of the feed, preparation of the feed, mode of operation, etc, mainly influence the volume of the extraction and separation vessels

The thermodynamic conditions determined give the temperatures and pressures in all steps of the process, taking into consideration the desired quality of the product

The optimized mass transfer determines the mass flow of the solvent The HPE process in the T,s diagram determines the change of state in the process steps and therefore the energy level A way of determining the influence of the main parameters on the economy of the process is to combine the results of the mass transfer investigations with the energy demand of the process cycle Determining the extraction yield curves for a defined feed amount and for different solvent flow rates versus extraction time and total throughput of CO_2 enables the extraction time and CO_2 mass flow required for a desired extraction efficiency to be obtained

By multiplying the investment costs of the plant for about 1 h by the extraction time for a desired extraction efficiency and for a constant specific CO_2 mass flow rate, one point of the investment cost curve is evaluated Then, a fixed cost curve can be plotted for several specific CO_2 flow rates The same procedure can be used for the evaluation of the operation costs

For given thermodynamic conditions in the extraction and separation steps, one point of the operating costs curve can be evaluated by multiplying the costs for 1000 kg of CO_2 required for the process cycle by the total throughput of CO_2 required for the desired extraction efficiency

The same can be done for several specific CO_2 flow rates The operating costs curve can then be plotted The addition of the investment costs curve and the operating costs curve yields an approximate answer for the process costs of the desired product

REFERENCES

1 E Lack, G Bunzenberger and R Marr *Preprint High Pressure Chemical Engineering Erlangen* 63 (1984)

2 D U Peng and D B Robinson *Ind Eng Chem Fundam* *15* 59 (1976)
3 J Chrastil *J Phys Chem* *86* 3016 (1982)
4 G Brunner *Ber Bunsenges Phys Chem* *88* 887 (1984)
5 M B King T R Bott K Kassim and M Barr *Preprint High Pressure Chemical Engineering Erlangen* 301 (1984)
6 E Lack, Thesis TU Graz 1985

Received by editor July 14 1986
Revised January 27 1987

Natex Prozesstechnologie GesmbH

Basic-Course

of

Supercritical Fluid Extraction Process

Metal Industries Research & Development Center

Kaohsiung, Taiwan, ROC

Mr TZU-CHEN KUO

CO_2 EXTRACTION

from solids and liquids

6 6 Extraction from solids

The most widespread application of supercritical fluid technology is for extraction purposes

6 6 1 Fundamentals

The basic principles for using a supercritical fluid as an extraction medium are the solubility and phase equilibrium of substances in the compressed gas First, the compounds which have to be extracted must be soluble in the supercritical fluid at moderate pressure and temperature The solubility and phase equilibria can be varied over a wide range by changing the pressure and temperature However, beside the solubility behaviour mass-transfer plays an essential role for extraction processes Fig 6 6-1 shows a typical trend of extraction-yield over extraction-time At the beginning, the extraction efficiency is limited by the solubility in the available amount of fluid Higher solubilities, and therefore shorter extraction times, can be achieved by increasing the extraction pressure, because with a higher fluid density the solvent power also increases The same is normally found also by increasing the extraction temperature, because at higher pressure levels the increase in vapour pressure of the substances to be dissolved is more effective than the reduction in the fluid density at higher temperatures The second phase of extraction is controlled by diffusion, and this, especially, leads to long extraction times Therefore, the aim is to reach the proposed extraction yield within the solubility phase, because otherwise the process will not be economical

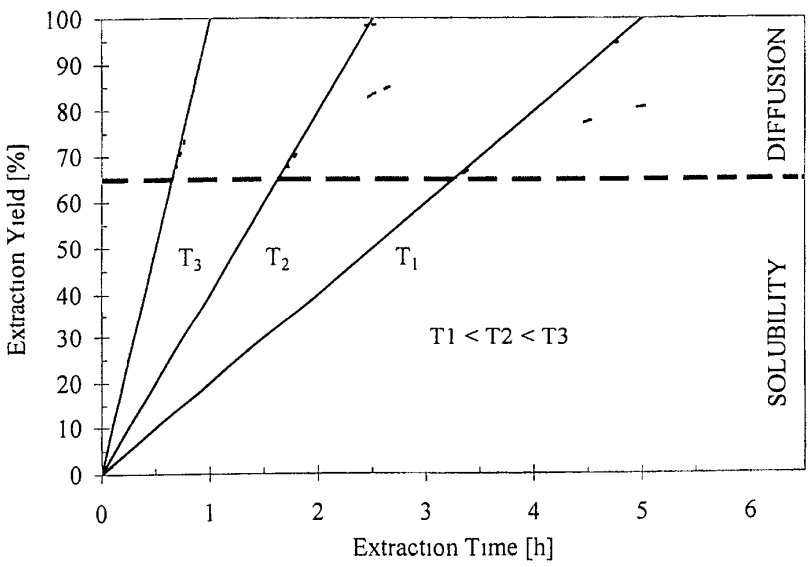

Figure 6 6-1 Typical trend of extraction lines

For calculation of the extraction yield in the solubility phase, Brunner [1] gives the following correlation for solid raw materials

$$E = k_S * a_S * V_t * \Delta c_m \qquad (6\ 6\text{-}1)$$

where k_S is the mass-transfer coefficient (m/s), a_S the specific interfacial area (m^2/m^3) V_t, the bed volume (m^3), and Δc_m, the mean concentration gradient The mass-transfer coefficient, k_S, can be calculated by a correlation with the Sherwood number

$$Sh = k_S * d / D_{12} = 2 + 1{,}1 * Sc^{1/3} * Re^{0\ 6} \qquad \text{for } 3 < Re < 3\ 000 \qquad (6\ 6\ 2)$$

It is obvious that the mass-transfer coefficient, k_S, can be influenced by the diffusion coefficient, D_{12}, which is also included in the Sherwood number, Sh, as in the Schmidt number, Sc Diffusion can be increased by shortening the diffusion length For solid materials this is achieved by smaller particle sizes, which further leads to a higher specific interfacial area, a_S However, there is a limit for reducing the particle size because if the particles are too fine, the problem of channelling arises, so an optimum has to be found

A further possibility for increasing extraction yields is to use higher flow-rates This causes an increase of the Reynolds number, Re, which is defined as

$$Re = \frac{v * d}{\upsilon}, \qquad (6\ 6\text{-}3)$$

because at same extractor diameter, d the velocity v, is increasing Higher flow-rates also give a larger mean concentration gradient, Δc_m, because the equilibrium concentration is constant at a given pressure and temperature, and the loading of the extraction fluid is lower Increasing the velocity, v, also gives a better mixing effect in the extractor which results under certain conditions, in a fluidized bed

If pure supercritical solvents have too low a solubility for substances of interest, the addition of small amount of entrainers to the extraction gas is another possibility for increasing the extraction efficiency by reducing the extraction time The effect of the entrainer has to be considered On the one hand, the entrainer may influence the polarity of the fluid and therefore dramatically increase the solubility of the more polar substances Supercritical CO_2 is a particularly non-polar solvent Adding small amounts of alcohol or even water, for example, changes the polarity much more than increasing the pressure to high levels On the other hand, so called matrix modifiers are used which influence the availability of compounds in the solid matrix so that they can be extracted An example is caffeine, which is soluble in pure CO_2, but for the decaffeination of coffee and tea, water saturated CO_2 has to be used Otherwise, the caffeine is incorporated too strong in the matrix of the raw material and cannot be extracted The negative effect of using a modifier is that no solvent-free products are achieved, because both the extract and the entrainers are collected in the separator Either the product is useful in this form, or a subsequent separation step has to be included to provide solvent-free extracts and to recover the entrainer and recycle it in the extraction process

After sufficient extraction the dissolved substances have to be separated from the fluid in a following step *Decreasing the pressure* at constant temperature reduces the fluid-density, and therefore the solvent-power of the fluid The extracted substances are collected at the bottom of the separator, as shown in Fig 6 6-2 To close the solvent cycle, the fluid has to be recompressed to extraction pressure

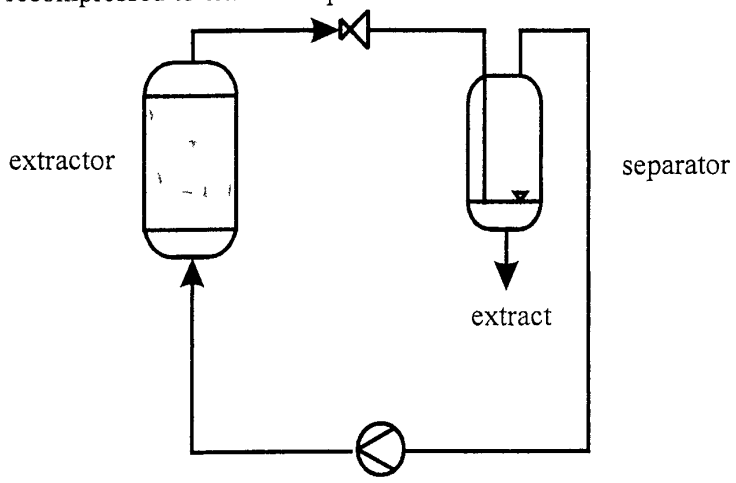

Figure 6 6-2 Separation by pressure reduction

A density reduction of the extraction gas can also be achieved by *increasing the temperature* (see Fig 6 6 3) However, for this kind of separation the solubility behaviour of the dissolved substance has to be taken into account A temperature increase also results in a higher vapour pressure, which may result in higher solubility so that no separation can occur No further complete separation is achieved, which results in a residual loading of the extraction gas and in longer extraction times and higher residual concentrations because of the smaller concentration difference between the entering fluid and the extractive material The advantage of this separation method is that the process can be operated under isobaric conditions so that no compression step is necessary after separation and the pump only cycles the fluid at a constant pressure level

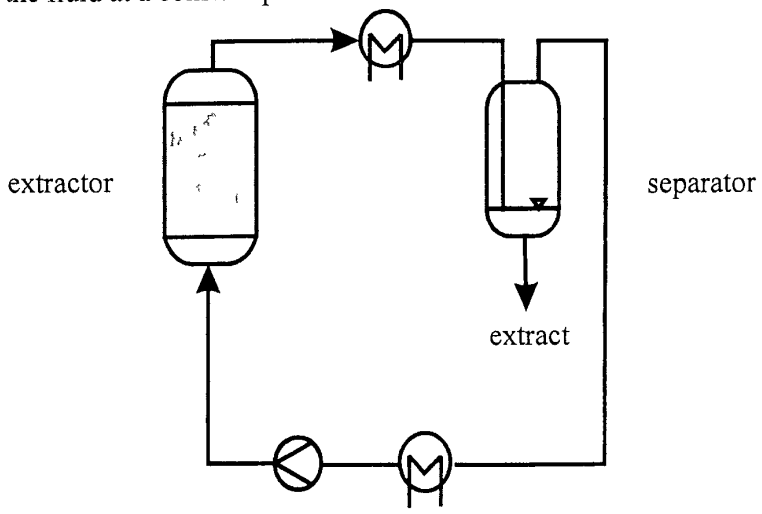

Figure 6 6-3 Separation by temperature change

Most applications use a *combination of pressure and temperature change* After pressure-reduction the extraction gas is heated so that it reaches the gaseous state In this phase, no solvent-power of the extraction gas is present for any substances and therefore complete separation of extracted substances takes place In cycling the extraction gas after separation, it has to be condensed, undercooled to prevent cavitation of the pump, and recompressed and heated up to extraction temperature

A further method separates the extracted substances by *absorption* Basic for this method is that there should be a high solubility of extracted substances in the absorption material, and that the solubility of absorption substance in the circulation solvent should be as low as possible Further, the absorption material must not influence the extract in a negative way and a simple separation of extract and absorption material has to be available An ideal absorption material is therefore a substance which is present in the raw material Most plant-materials contain water, which can act as a very successful absorption material An ideal example is the separation of caffeine for the decaffeination of coffee and tea On the one hand, water has a low solubility in CO_2, and on the other, water saturated CO_2 is necessary for the process The extracted caffeine is dissolved into water in the separator and caffeine can be produced from this water-caffeine mixture by crystallization One advantage of this separation method is that the whole process runs under nearly isobaric conditions

Analogous to above mentioned method, the *adsorption* of extract on a suitable solid material, is possible (see Fig 6 6-4) The disadvantage of adsorption is that regeneration of the adsorbent is difficult or impossible Therefore no extract is produced and adsorption can only be used if the residual material is the product and not the extract

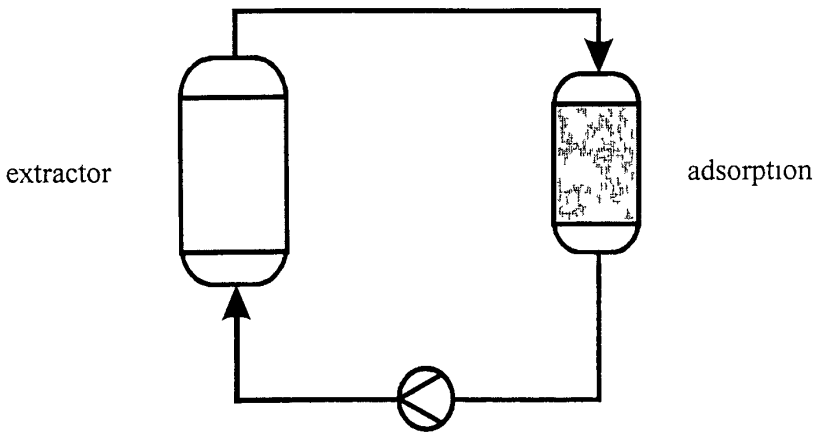

Figure 6 6-4 Separation by adsorption

An industrial-scale application is the decaffeination of coffee and tea where a direct separation of the extracted caffeine in the extractor is realized A layer of activated carbon follows a layer of raw material, and so on In this way, the loaded extraction fluid is directly regenerated in the adsorption layer and enters as pure solvent into the next stage of raw material The great advantage of this method is that no further high-pressure vessel is necessary for separation, which reduces investment costs dramatically

Adding a substance with low solvent power can also reduce the solvent power of a supercritical gas Adding nitrogen, for example, reduces the solubility of caffeine

dramatically, and lasts to a separation In a subsequent step this substance has to be removed from the extraction gas before entering the extractor again and this can be achieved by membrane techniques

6 6 2 Design criteria [1,2,3]

In this Chapter, fundamentals of design criteria in relation to processes and equipment are reviewed for dense gas-extraction from solid matrices Although, as mentioned in previous chapters numerous dense gases can be used as solvents In the following discussion we concentrate on the most extensively used gas-carbon dioxide The reason for this is its non-toxic, non-flammable and inert nature, the possibility of gentle treatment of thermally sensitive materials, and the fact that it is inexpensive and an environmentally acceptable material

Successful engineering design presupposes knowledge of reliable data on mass transfer including thermodynamic properties, such as phase-equilibrium data and solubility, within a technically and economically possible range of pressure and temperature

For the development of a new process or application, or the design of a plant, the following main parameters must be known or obtained from the engineer concerned

- Specific basic data,
- Thermodynamic conditions for extraction and separation,
- Mass transfer,
- Energy consideration/consumption by means of the TS-diagram,
- Specific separation problems,
- Selection and design of proper plant components

As will be explained later, the first two factors influence mainly the size of extractors and separators, while mass-transfer determines the CO_2 circulation system, and consequently the energy consumption and the size of heat exchangers and the piping system

6 6 2 1 Specific basic data

The design engineer must have a clear picture of the service requirements of the plant, which presuppose knowledge of

- Raw material specifications,
- Desired plant size,
- Final product specification,
- Plant location, with local prevailing conditions

The extraction of vegetable plant-material requires careful selection of raw materials in connection with chemical analysis, because the content of the vegetables to be extracted can vary substantially Also the possibility of high concentrations of undesired substances - either contained within them, or contaminations such as pesticides can influence the product quality enormously Exhaustive extraction is not always possible with acceptable effort, owing to the vegetable structure, and the extraction efficiency using low-quality raw materials may be too poor to allow economic processing

A more detailed review in Chapter 8 shows that the plant size can have a strong effect on its feasibility

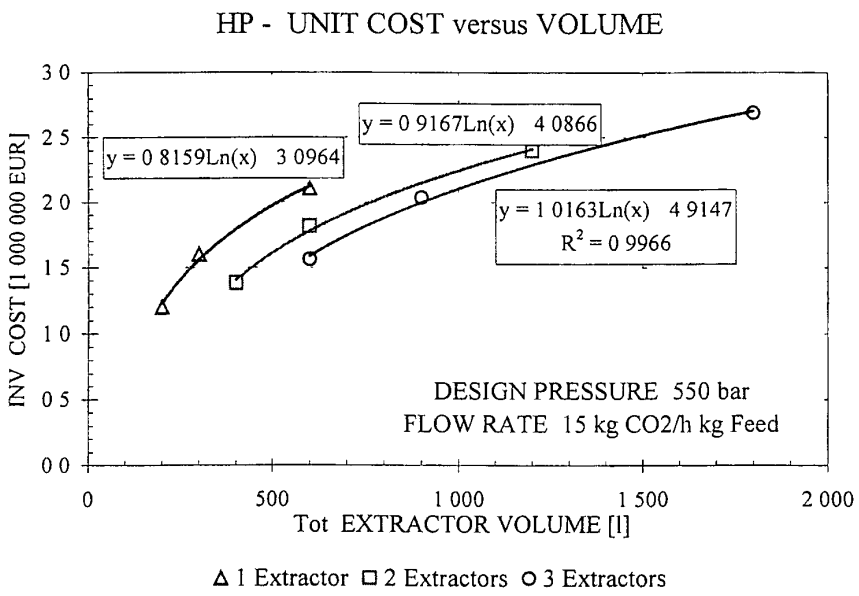

Figure 6 6-5 Investment cost for multi-purpose plants designed for 550 bar

It is obvious from Fig 6 6-5 that the investment costs for a specific type of plant can be determined accurately enough from the following equation

$$\text{Investment Cost} = C \ \ln V_T - A \qquad (6\ 6\text{-}4)$$

With A and C = Plant Specific Constants
V_T = Total Extraction Volume [lit]

The final product specification can influence the process with regard to processing conditions (pressure, temperature, pretreatment of feed material), and may require fractionated separation or further treatment such as concentration, purification or demoisturization

The plant location can determine the mechanical construction - for example, in case earthquake factors are to be considered, and climatic conditions can have an impact on machinery sizing and dimensions particular for cooling machines and electrical drives

Extractable substances

Natural material to be extracted can be divided into two categories

A Raw materials, whose geometry must be maintained during the process, and/or only undesired substances are removed

This group represents the largest one in terms of tonnage and comprises the following applications

- Decaffeination of green coffee, black- and green tea,
- Defatting of cocoa press cake and nuts,

- Removal of plant protective materials from cereals, particularly rice and pharmaceuticals (for example, ginseng),
- Reducing the alcohol content in beverages

Such processes require a high selectivity for the substances to be removed, in order to maintain the flavour, appearance, smell, and shape of the treated feed material which represents the main product Because CO_2 has selective solubility properties, which can be altered to some extent, its use may often be feasible By-products, such as caffeine can if recovered - improve the economics

B Materials which allow pretreatment and where the extracted substances represent the main product

For such processes the extract's revenues must cover the raw-material's treatment cost and therefore only highly valuable extracts with a corresponding yield justify the application of the CO_2 technology Furthermore, it must be remembered that extracts produced using different solvents, can vary in their chemical composition and appearance, owing to the different selectivities

Table 6 6-1
List of bulk densities for various feed materials

Pepper, ground	470 kg/m³	Camomile	175 kg/m³
Paprika, ground	450 kg/m³	Laurel, ground	130 kg/m³
Caraway, ground	400 kg/m³	Vanilla, ground	350 kg/m³
Coriander, ground	400 kg/m³	Mace, ground	450 kg/m³
Clove, ground	450 kg/m³	Nutmeg, ground	470 kg/m³
Juniper ground	400 kg/m³	Ginger, ground	450 kg/m³
Cardamom, ground	370 kg/m³	Rice	820 kg/m³
Rosemary, ground	360 kg/m³		

Pretreatment of raw materials

Higher extraction volumes in high-pressure processes represent higher costs and attention must be paid to limiting them as far as possible The main impact comes from the bulk density of the feed material (see Table 6 6-1)

The ground feed-material should have average particle sizes of 0 4 to 0 8 mm Smaller particles, although better for mass transfer, reduce the fluidized bed velocity, can cause clogging of filters, and tend to channelling Ground raw materials with bulk densities below 200 to 250 kg/m³ should, if possible, be pelletized Such pretreatment can be advantageous in the destruction of cell matrices, thereby possibly lowering mass transfer resistances For example, the pelletizing of hops increases the bulk density from about 150 to 500 kg/m³ and improves the yield

The extraction result is further influenced by the moisture content For spices and herbs this concentration should be in general between 8 and 15 % At higher values the water is extracted preferentially and/or the co-extraction of polar substances is at a low level Low

moisture contents cause shrinking of the cell structure and consequent hindrance to diffusion, which reduces the yield The optimum moisture levels should be determined by means of extraction tests The best moisture content for black tea is between 20 and 27 %, for green coffee between 35 and 45 %, and for the removal of pesticides from rice, between 15 and 20 % For paprika extraction the moisture should be as low as possible, to avoid water enrichment at the opposite side of the CO_2 entrance, which results in agglomeration and clogging of filters at the CO_2 exit

For rosemary, a high moisture content yields a solid, crystalline extract while the raw material with a high essential-oil content yields a viscous, brownish and homogenous product Essential oils act as entrainers for other valuable substances in other biomaterials also

6 6 2 2 Thermodynamic conditions

No other solvent extraction process other than the CO_2 technology allows such a strong influence on loading, phase equilibrium, and selectivity Unfortunately, the solubility of extracted substances in CO_2 is relatively low, compared with the usual solvents which give absolute miscibility with the extracted valuable materials in most cases The determination of solubility and solvent ratios is therefore important for the economy of the process

The target for the design engineer is to obtain the highest possible loading, with consideration of the selectivity and product quality, within the extraction step, and the lowest possible one for the separation to ensure optimum precipitation and to avoid carry-over of extract with the solvent

The solubility is mainly dependent on the density of the dense gas whereas the extraction pressure is limited for technical and economic reasons Industrial-scale plants use pressures between 45 and 60 bar for the separation step Lower pressures would increase the energy consumption substantially, especially in the pump-driven process, because condensation is to be performed at lower temperature levels

The separation temperature should be chosen to be at least 5 to 10°C above saturation temperature to prevent floating with the liquid CO_2 and to ensure that the precipitated extract is under liquid conditions

For the modelling of thermodynamic conditions, many useful models have been published in the literature [4] to describe the experimental equilibrium data and to enable fast optimization of the parameters The well-known models are based on the three equation systems empirical equations of state, semi-empirical equations of state and derivations from the association laws and/or from the entropies of the components

Semi-empirical equations of state are used to fit binary systems, and thermodynamic data for the solute and the solvent have to be known For systems with more than two components, the mathematical solution is very difficult A useful equation of state for the description of simple binary systems is the Peng Robinson equation [5], applicable for large pressure and temperature ranges

For unknown solute properties, a derivation from the association laws is used to adjust experimental results, Chrastil has published the most popular one [6] An example is given in Fig 6 6-6, comparing measured and calculated equilibrium data for rapeseed oil in CO_2, showing the dominating influence of the solvent density This equation is very useful for describing the equilibrium distribution of natural substances in dense gases

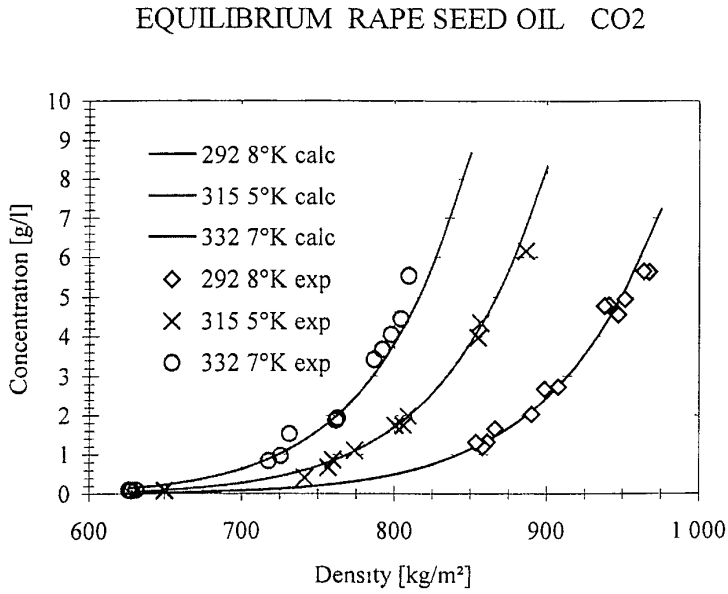

Figure 6 6-6 Comparison of measured and calculated equilibrium data (Chrastil) for rapeseed oil

6 4 2 3 Mass transfer [1]

The target of this investigation is to find the optimized specific solvent mass-flow-rate, in order to obtain the highest extraction efficiency, that means, the highest possible yield in the shortest time, with the lowest energy input The investigation should yield the amount of CO_2 per kg of raw material and hour, the extraction time, and the length to-diameter ratio of the extractor

As in conventional processes the mass transfer at HPE is determined from diffusion and hydrodynamic data

Diffusion

The diffusion depends on the size of particles and the initial distribution of the substances to be extracted within a solid matrix The valuable substance can be located within the plant cell, on the surface, or absorbed in the solid matrix First, the location of the substances must be determined Further, it is necessary to know if the desired substance is bound in any chemical reaction to the matrix or bound to a complex Literature searches are necessary to find out more information about how the substance is embedded in the matrix

For non chemically bonded substances the diffusion can be influenced by the following processes

- Changing the particle size to shorten the diffusion paths and destruction of the plant cells
- Breaking of the cell walls through pelletizing
- Swelling of the cell structure through moisturizing of the raw material
- Breaking of complex bonding through moisturizing or changing the pH-value

Hydrodynamics

The hydrodynamics are mainly influenced by the size and form of the particles and by the particle size distribution, which in most cases should be in a range between 0 4 and 0 8 mm Too small particle sizes can cause channelling which, for example, can occur during the extraction of paprika powder egg yolk powder, cocoa powder, and algae powder Fibrous feed materials such as ginger, black- and green tea, and paprika have a tendency to swell and block the filters at the outlet of the extractor The mechanism of transport in the solid phase proceeds in the following parallel and consecutive steps

- Absorbing the solvent in the plant matrix, swelling the cell structure, and dissolving the soluble substances
- Transport of dissolved substances to the outer surface by means of diffusion and passing through
- Transport from the surface layer into the solvent

The particle size distribution and the shape of the particles also influence the ratio of length-to-diameter of the extractor As the costs for extractors depend not only on volume, but mainly on the diameter, the proper selection of the extractor height/diameter ratio must be made, with a preference for slim vessels So far, only for the decaffeination of coffee beans with a particle size of about 7 mm can large ratios of 9 1 (length to diameter) be applied For large particle sizes it is of advantage to feed the solvent from top to bottom, in order to avoid back mixing For the usual particle-size distribution, ratios of 6 1 should be used For raw material which tends to swell, like black tea or paprika, the ratio should be only 3 1, or if the extractor is equipped with baskets the baskets should be equipped with multiple distribution

Increasing the mass-transfer through agitation is, in most technical applications, not feasible

6 6 2 4 Process optimization by means of the TS-Diagram

The fourth main parameter deals with the estimation of the optimized process cycle There are various possibilities for running the cycle in the TS-diagram

For the energy- and cost-calculation of the HPE-process a program has been developed, allowing the determination of the various cycle processes under selected conditions for extraction and separation In principle, the cycle is either in the pump- or in the compressor-mode

Pump process

The pump process commences (see Fig 6 6 7) in the storage tank, with dense gas under liquid conditions (1) To avoid cavitation, the solvent is precooled (2) ahead of the circulation pump, where compression to the required extraction pressure (3) takes place The temperature for extraction is adjusted by means of a heat exchanger (4) The dissolved substances in the solvent leaving the extractor are to precipitate in the separator, in our case by changing the pressure and temperature by means of a control valve, according to an isenthalpic expansion The liquid part of the solvent (5 to 7), which is now in the two-phase region (5), is evaporated and the complete gaseous phase superheated (8) The solvent power is substantially reduced and the dissolved substances can be separated The gaseous solvent is condensed afterwards, thereby closing the cycle process

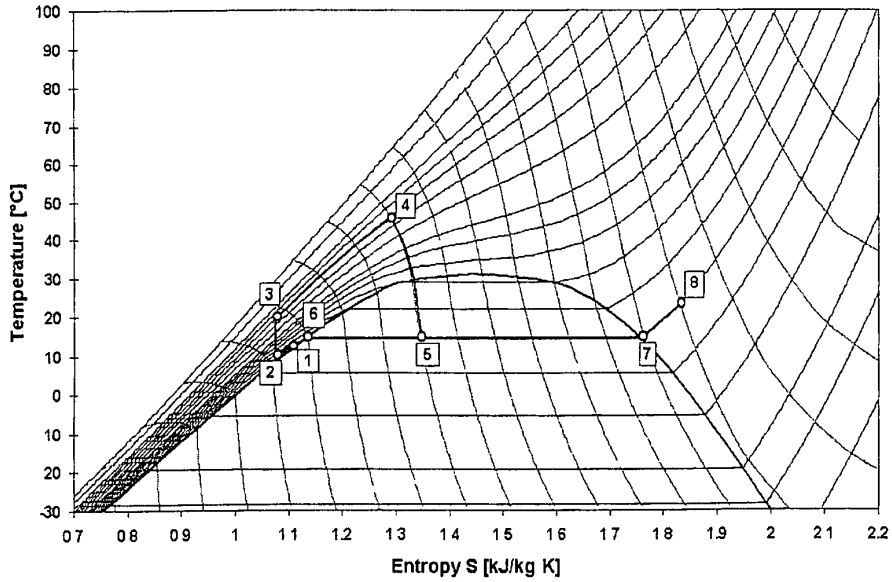

Figure 6 6-7 Pump process in the temperature-entropy diagram

The main energy consumers in the pumping mode are the cooling unit, with the highest demand for electrical energy, the circulation pump, the CO_2 pre-heater, and the evaporator

The electrical power consumption of the refrigerator depends only on the separation condition The pumping mode is optimal for high extraction pressures (more than 150 bar), low extraction temperatures (40 to 80°C), and separation pressure between 45 and 60 bar

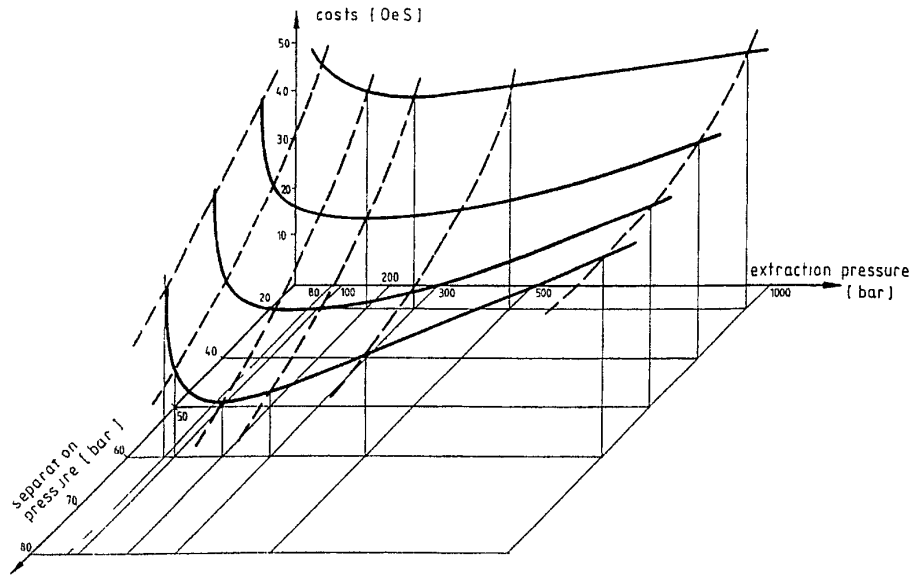

Figure 6 6-8 Energy consumption of pump process

Compressor process

The starting point for the compressor process (see Fig 6 6-9) is the condition prevailing within the separator, that means, the gaseous solvent enters directly into the compressor (1) and is pressurized to the extraction pressure (2) The use of intermediate cooled compressors is necessary, otherwise low efficiency and extremely high outlet temperatures would be reached After compression, the extraction fluid has to be cooled to the extraction temperature (3), and under these conditions extraction takes place Analogous to the pump process the loaded fluid is expanded in the two phase region (4) and heated up to gaseous conditions (1) where separation takes place

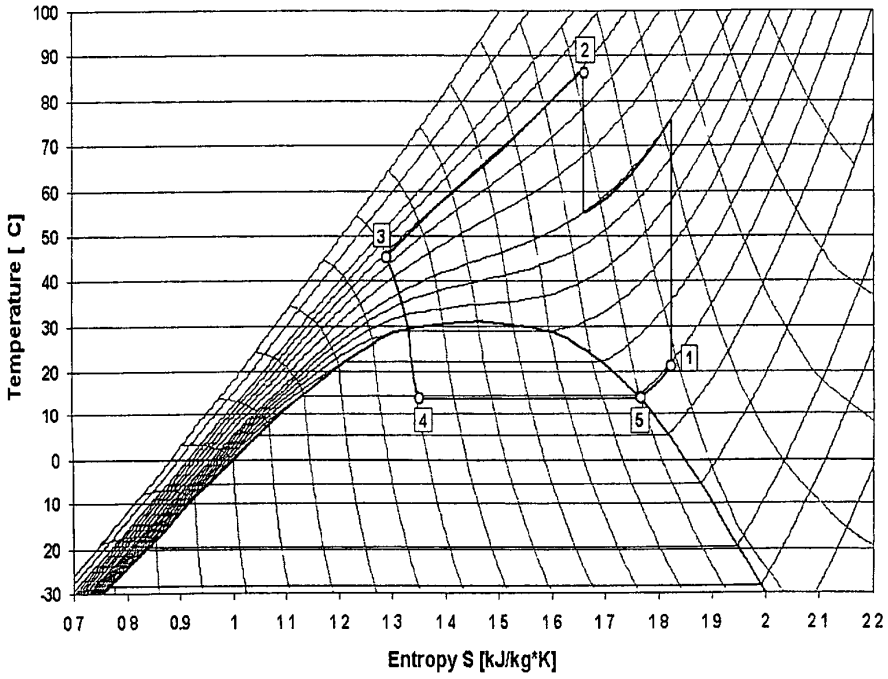

Figure 6 6-9 Compressor process in the temperature entropy diagram

The advantages of using compressors are that for the solvent circulation no condenser and undercooler are necessary, which reduces investment and running costs

For this process, almost all of the energy is provided from the compressor Compression ratios greater than 3 5 require multistage compressors, where intermediate cooling steps must be installed Compressor processes have low energy consumption for low extraction pressures (80 to 200 bar) and low separation pressures (30 to 40 bar) Owing to the high temperature after the compressor (80 to 120°C) it is also recommended for high extraction temperatures In the food industry bone dry compressors are normally used, in which the discharge pressure is limited to 200 bar Also high separation pressures - above 60 bar - can be maintained with the compressor process Under these conditions CO_2 cannot be compressed with a pump, owing to the high compressibility In the case where a single-stage compressor is sufficient the investment costs are lower as well

Isobaric process

Processes with high mass flow rates, for example more than 40 t/h, have energy demands of a very high level Especially for the decaffeination processes, in which several hundred up to a thousand tons of CO_2 are in circulation, isobaric processes were developed In these processes, the extraction step and the separation step have nearly the same pressure and temperature The separation of the dissolved substance from the CO_2 in circulation is maintained by adsorption on activated charcoal, with an ion-exchanger, or by absorption in a washing column

6 6 2 5 Separation of dissolved substances

Most of the industrially applied separation processes use precipitation by means of reduced solvent power by changing the pressure/temperature in one or more steps In most cases, as for the production of oleoresins from spices, or the extraction of hops a single step separation is sufficient Double- or triple-step separations are applied for spice extraction, in case enrichment of pungency, colour or essential oils are desired as, for example, with pepper, with precipitation of piperin, the pungent substance of the pepper, in the first step, and essential oil in the second step

For highly volatile aromas of fruits or wine, the single or double step separation based on pressure is not sufficient, and needs expensive precipitation at very low temperatures About minus 50°C are necessary for sufficient recovery of aroma components For this application an aroma rectification, with multiple withdrawal at different temperatures, is appropriate

The separation in the isobaric decaffeination processes is executed with absorption of caffeine, that means, the caffeine dissolved in CO_2 is carried over into water by means of a packed washing column, or by adsorption with activated charcoal, but without recovery therefrom Other separation methods under investigation are the use of membranes, since the difference in molecular weight between extract and solvent is high enough, or by the addition of substances of low solvent power It is questionable whether the advantage of the possible isobaric process can compensate for the investment for the additional process steps required

6 6 3 Cascade operation and multi-step separation

Up to now, no appropriate methods are available for continuous feeding and emptying devices for solid materials which are applicable for high pressure plants In different research studies the possibility of screw presses or moving cells through a high pressure vessel are described, but the technical realization for industrial plants is too difficult Therefore, solid materials are extracted by cascade operation which means that more than one extractor is installed (see Fig 6 6 10) In this way a quasi continuous flow of the solid material can be achieved because the extractors are connected in series The compressed extraction gas passes through the extractors in the sequence 1 2-3-4 until extraction in extractor 1 is finished This extractor is switched off from the cycle, decompressed, emptied, refilled with fresh material, and added as the last one to the sequence which is now 2 3-4-1 In the next step, extraction in extractor 2 is finished and this one will be added again as last one in the sequence, and so on This sequence has the advantage that extremely high extraction yields are achieved because the pure solvent-flow is contacted with pre extracted material so that a concentration difference is present, and on the other side the pre-loaded solvent flow enters the extractor with fresh material, so the maximum solvent capacity is used

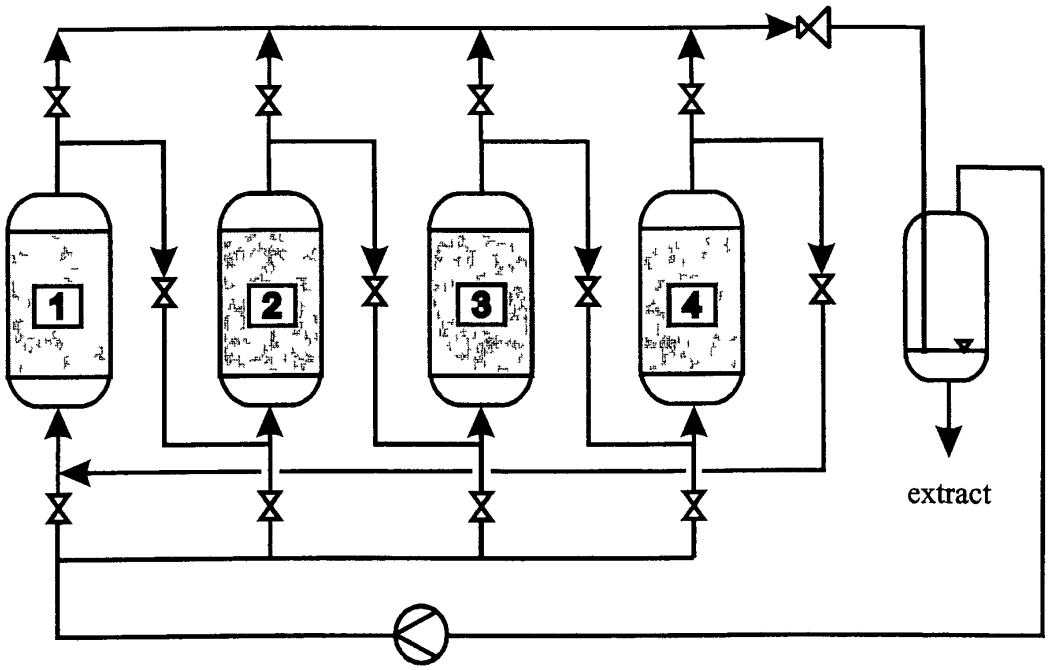

Figure 6 6-10 Cascade operation for extraction of solid materials

The number as well as the volume of extractors has to be optimized and fitted to the extraction problem Larger extractor volumes result in lower separation times from the sequence, but the investment costs increase with increasing extractor volume Extractors which are too small cause longer dead-times because the number of separations from the sequence increases

The basis of a multi-step separation (see Fig 6 6-11) is, that the solvent power of the compressed fluid can be influenced by changing pressure and temperature This is one of the advantages of the high-pressure technology, that in the down-stream phase a simple fractionation of the product can be achieved Normally, little pressure reduction is performed in the first separator, together with temperature change, to remove this fraction with the lowest solubility in the compressed fluid All other substances have to remain in the compressed gas and enter the next separator where, again, change in pressure and/or temperature takes place The last separator must guarantee that all light volatile substances are separated, and leave at the outlet a pure extraction fluid which is recycled Further loading of the fluid will cause a reduction in extraction efficiency In this way different fractions of the total extract are produced so that different products can be obtained from one raw material in a single process This becomes more and more common because in most cases certain fractions are of interest but not the total extract

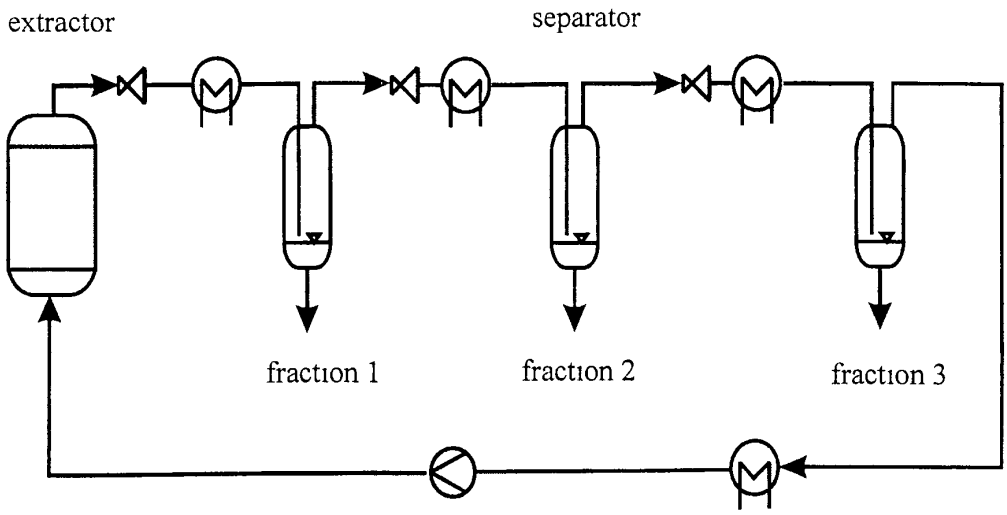

Figure 6 6-11 Multi-step separation

6 6 4 Main applications

With the permission of the Author Schutz Consulting, D-83308 Trostberg, 2000

As one can see from Table 6 6-2 the decaffeination of coffee and tea is the largest application for supercritical fluid extraction, in terms of annual capacities and investment costs Since the beginning of the 1970s, to the early 1990s, nearly 50% of the whole production capacity for decaffeination of coffee and tea changed to the supercritical extraction process As the market for decaffeinated coffee is stable, no further plants have been installed within the past eight years

The second largest application is in the extraction of hops In the last twenty years nearly all producers of hop extracts have changed to the supercritical extraction process Even in the Eastern European countries the methylene chloride process was stopped several years ago

The extraction of spice oleoresins is relatively new, and industrial plants have been in operation for about the last ten years Because the CO_2 extracts are different to the conventional processed oleoresins, the acceptance in the food industry is growing slowly The spice plants are much smaller than the decaffeination and hop plants, and use extractors of between 200 and 800 l The same is true for medical herbs and high value fats and oils which are more or less at the beginning of development

One of the latest industrial applications is the reduction of plant protectives from cereals, which started commercial production at the end of 1999 in Taiwan

Table 6 6-2
Commercial Plants for Supercritical Fluid Extraction

Product Group	Total Number of plants	America	Asia/ Australia	Europe	Total Capacity [1000 t Input/ Year]
Coffee and tea decaffeination	5	1	0	4	100
Hops (including coca defatting)	7	4	1	2	60
Nicotine from Tobacco	3	1	1	1	n a
Chemistry	5	3	1	1	n a
Environmental purposes including cleaning of foodstuff and medicinal plants	5	2	3	0	n a
Spices	12	1	5	6	9
Fats and oils including Lecithine	8	0	3	5	3
Medicinal plants	7	0	1	6	3
Flavours	7	0	3	4	3
Total	59	12	18	29	>178

Explanation Of the caffeine-extraction plants, most of the commercial plants produce at least two different products Plants were consolidated to what is thought to be the main product Capacities are estimated on a twelve months' operation basis, which is - at least for hops - higher than reality The order of product groups is in terms of decreasing total extraction volume The product groups "Chemistry" and "Environmental Purposes' contain both products from natural and artificial origins Several plants with the same product at one site are counted as one

6 6 5 Specific application processes

Beside the typical extraction purposes, different applications using supercritical fluids mainly carbon dioxide are tested in the laboratory as well as on an industrial scale

Decontamination of soils using supercritical fluids is an attractive process compared to extraction with liquid solvents because no toxic residue is left in the remediated soil and, in contrast to thermal desorption, the soils are not burned In particular, typical industrial wastes such as PAHs, PCBs, and fuels can be removed easily [7 to 21] The main applications are in preparation for analytical purposes, where supercritical fluid extraction acts as a concentration step which is much faster and cheaper than solvent-extraction The main parameters for successful extraction are the water content of the soil, the type of soil, and the contaminating substances, the available particle-size distribution, and the content of plant material, which can act as adsorbent material and therefore prolong the extraction time For industrial regeneration, further the amount of soil to be treated has to taken into account, because there exists, so far, no possibility of continuous input and output of solid material for high pressure extraction plants, so that the process has to be run discontinuously

The neutralization and impregnation of paper is of great interest for all libraries, because acid degradation results in a reduction in the pH and weakening of the mechanical properties of the paper For this reason, in the first step the degradation products are extracted with supercritical carbon dioxide, which increases the pH In the following step, neutralizing substances are dissolved in the CO_2 stream, and impregnation of the paper takes place [22]

Supercritical CO_2 is used in a process for bone-tissue treatment to obtain a novel bone substitute for human surgery The supercritical extraction step results in de-lipidation of

bones, and therefore reduces infection effects Then efficient enzymatic deproteination can be performed [23,24]

As halogenated solvents are widely banned, either for health or environmental reasons, the degreasing and cleaning of mechanical and electronic parts becomes a worldwide issue Carbon dioxide, mainly in the liquid state, is becoming one of the most attractive substitutes for chlorinated solvents [25,26]

In the field of polymer recycling and/or disposal new techniques are required Most of the electronic waste contains flame retardants, mainly halogenated organic substances In many recycling processes, plastics are incinerated and the formation of halogenated dibenzodioxins and dibenzofurans cannot be avoided One promising way to separate halogenated flame retardants from polymer matrices uses the extraction with supercritical carbon dioxide The advantage of this process is that the polymer as well as the flame retardant can be recycled, especially because flame retardants are relatively high priced products [27]

References

1 G Brunner, Ber Bunsenges Phys Chem 88 (1984) 887
2 R Eggers, R Tschiersch, Chem Ing Techn 50 (1978) Nr 11, 842
3 R Eggers, Chem -Ing Techn 53 (1981) Nr 7, 551
4 E Lack, Theses, TU Graz, (1985)
5 D V Peng u D B Robinson, Ind Eng Chem Fundam 15 (1976) 59
6 J Chrastil, J Phys Chem 86 (1982) 3016
7 B O Brady, C P C Kao, K M Dooley F C Knopf, R P Gambrell, Ind Eng Chem Res 26(2), (1987) 261
8 I J Barnabas, J R Dean, W R Tomlinson, S P Owen, Anal Chem 67(13), (1995) 2064
9 J Puiggene, M A Larrayoz, E Velo, F Recasens, Proc 3rd Int Symp Supercrit Fluids, Strasbourg, (ed G Brunner, M Perrut), (1994) Vol 2, 137
10 G K C Low, G J Duffy, S D Sharma, M D Chensee, S W Weir, A R Tibbett, Proc 3rd Int Symp Supercrit Fluids, Strasbourg, (ed G Brunner, M Perrut), (1994) Vol 2, 275
11 G Markowz, G Subklew, Proc 3rd Int Symp Supercrit Fluids, Strasbourg, (ed G Brunner, M Perrut), (1994) Vol 2, 505
12 L Barna, J M Blanchard E Rauzy, C Berro Proc 4th Meeting Supercrit Fluids, I N S A Villeurbanne (ed D Barth, J M Blanchard, F Cansell), (1997) 63
13 R Zaragoza, J M Blanchard, L Barna, Proc 4th Meeting Supercrit Fluids, I N S A - Villeurbanne (ed D Barth, J M Blanchard, F Cansell), (1997) 145
14 J Thauront, J C Fontan, R Zaragoza, S Ruohonen, L Parvinen J M Blanchard L Barna, M Carles, C Perre, Proc 4th Meeting Supercrit Fluids, I N S A Villeurbanne (ed D Barth, J M Blanchard, F Cansell), (1997) 151
15 L Barna, J M Blanchard, E Rauzy, C Berro, Proc 4th Meeting Supercrit Fluids, I N S A -Villeurbanne (ed D Barth, J M Blanchard, F Cansell), (1997) 157
16 J Hawari, A Halasz, L Dusseault, J Kumita, E Zhou, L Paquet, G Ampleman, S Thiboutot, Proc 5th Meeting on Supercrit Fluids Materials and Natural Products Processing, Nice, (ed M Perrut, P Subra), (1998) 161

17 A Izquierdo, M T Tena, M D L de Castro M Valcarcel, Chromatographia 42 (3/4), (1996) 206
18 W Sielschott, C Frischkorn, M Schwuger, Chem -Ing Tech 65 (4), (1993) 434
19 A Schleussinger, I Reiss, S Schulz, Chem -Ing Tech 68 (12), (1996) 1602
20 Y Yang, S B Hawthorne, D J Miller, J Chromatogr A, 699, (1995) 265
21 D R Gere C R Knipe, W Pipkin, L G Randall, Int Environ Techn 5 (4) (1995) 20
22 C Perre, A Beziat, M Carles, A C Brandt, Proc 3rd Int Symp Supercrit Fluids, Strasbourg, (ed G Brunner, M Perrut), (1994) Vol 2, 19
23 J Fages, A Marty, J S Condoret, Proc 3rd Int Symp Supercrit Fluids, Strasbourg, (ed G Brunner, M Perrut), (1994) Vol 2, 253
24 J Fages, A Marty, D Combes, J S Condoret, French Patent 2 699 408, European Patent EP 0603920 A 1
25 N Dahmen, J Schon, H Schmieder, E Dinjus, Proc Int Meeting GVC-Fachausschuß "Hochdruckverfahrenstechnik", Karlsruhe, (1999) 293
26 V Perrut M Perrut, Proc Int Meeting GVC-Fachausschuß "Hochdruckverfahrenstechnik", Karlsruhe, (1999) 289
27 F Steinkellner, T Gamse, R Marr, P Alessi, I Kikic, Proc 5th Int Symp Supercrit Fluids, Atlanta, cd rom 5340939 PDF

6 7 Extraction from liquid mixtures

6 7 1 Introduction

The extraction of liquid mixtures with supercritical fluids is comparable to liquid-liquid extraction, with the compressed gas acting instead of an organic solvent While in liquid-liquid extraction the pressure influence is negligible, it plays an important role in high pressure extraction, changing as well the physical properties of the fluid like density, viscosity, surface tension, etc as the phase equilibria One advantage is that depending on the feed material the density difference between the two countercurrent flowing phases can be adjusted, which can be done by liquid liquid extraction only by changing the temperature and/or the solvent

Another advantage of high pressure extraction is the simple solvent regeneration For liquid-liquid extraction solvent regeneration includes, in most cases, a re-extraction or distillation step, which is energy consuming and therefore cost intensive, and causes problems if heat sensitive materials have to be treated For a high pressure extraction plant the solvent regeneration is achieved by changing pressure and/or temperature after the extraction step thus changing the density and with it the solvent power of the extraction gas, which can be easily recycled after separation closing the solvent cycle

Extraction of liquid feed materials has the great advantage, compared to solid materials, that liquids can be continuously introduced in and withdrawn from the high pressure separation unit This gives the benefit of a continuous operating process which is easier to handle and to design than a discontinuous one, in addition, higher throughputs can be achieved because of no dead times, which are required by the discontinuous process (vessel emptying and refilling)

The basic for developing a high pressure liquid extraction unit is the phase equilibrium for the (at least) ternary system, made up of compound A and compound B, which have to be separated by the supercritical fluid C Changing pressure and temperature influences on one hand the area of the two phase region, where extraction takes place, and on the other hand the connodes, representing the equilibrium between extract and raffinate phase

6 7 2 Operation methods

Compared to liquid liquid extraction different operation methods for a continuous supercritical extraction are available Among others, note that the possibility of adsorption-desorption of compounds of the liquid feed mixture on a supporting material will not be treated in this chapter

6 7 2 1 Single stage extraction

We refer to Fig 6 7-1 Reaching once equilibrium between the supercritical fluid *SCF1* and the feed in the extractor *E1* is enough for separation By changing pressure and temperature the produced extract *EX1* and raffinate *R1* concentrations can be varied following the ternary phase equilibrium The supercritical solvent to-feed flow rate ratio affects the amounts of products obtained from a given feed The apparatus required to apply this method are a normal stirred reactor, where contact of the two phases takes place, followed by a separator eliminating the extract from the extraction gas which is recycled back to the extractor

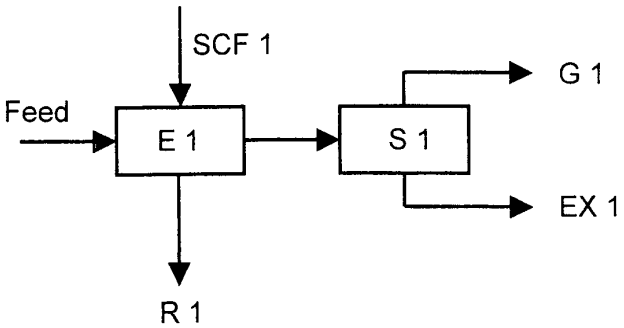

Figure 6 7 1 Single stage extraction

6 7 2 2 Multistage cross-flow extraction

For this kind of extraction (fig 6 7-2) the number of extraction steps can be varied In the first extraction step *E1* the feed is contacted with the supercritical fluid *SCF1* The supercritical fluid - extract mixture enters the separator *S 1* and the extract of the first extraction step *EX1* is separated from the gas *G1* The raffinate *R1* enters the next extraction step *E2* where it is contacted with new supercritical fluid *SCF2* and so on The raffinate *Rn* leaves the last extraction step *En* and the extract *Exn* the separator *Sn*, as well

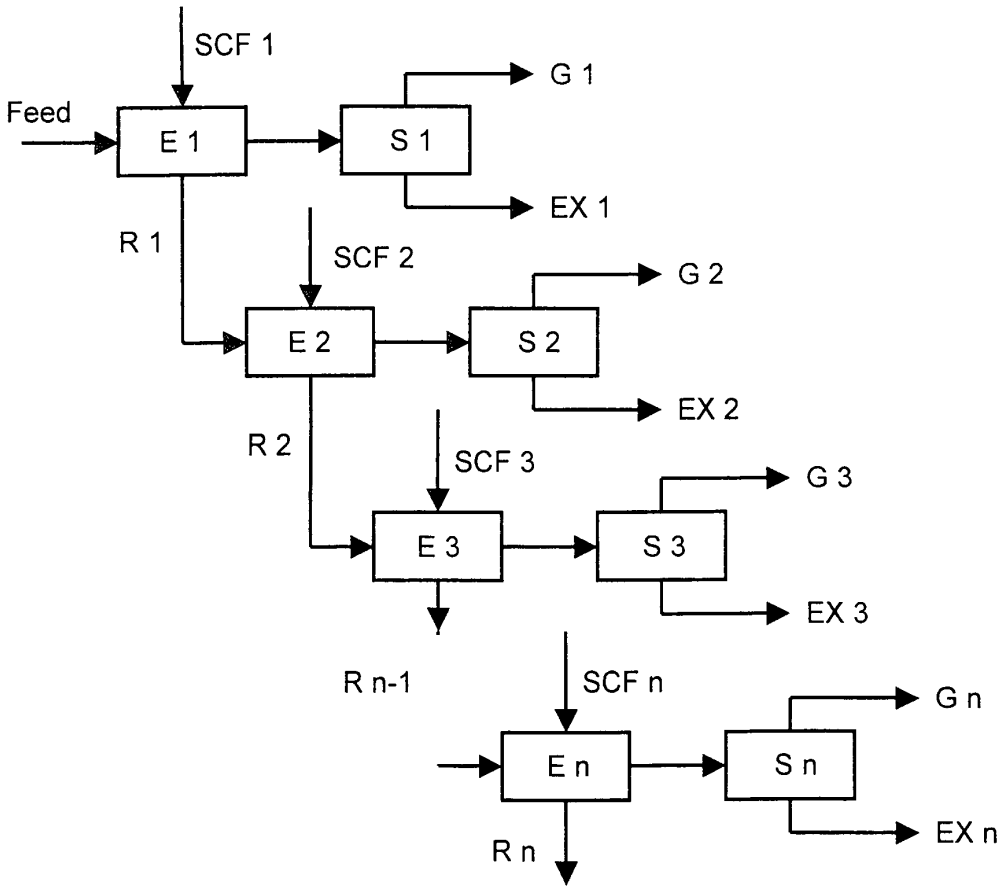

Figure 6 7-2 Multistage cross-flow extraction

The advantage of this extraction method is that the parameters pressure, temperature and solvent to feed ratio can be varied in each extraction step By this way a very accurate fractionation of the different compounds included in the feed can be achieved The solubility of the compounds in the supercritical fluid, depending on pressure and temperature, can be changed in each extraction step The highly soluble substances are extracted in the first step at low fluid density Increasing the density in the following extraction steps leads to the removal of the less soluble substances Further, the flow rate of the supercritical fluid can be adjusted in each extraction step, either constant flow for each step or different flow rates, depending on the separation to be achieved
At the industrial scale this extraction method is not installed yet for supercritical fluids The reason is that the investment costs are relatively high because of the needed number of high pressure vessels, in addition, for the case of different pressure levels and flow rates, in each extraction step one high pressure pump or compressor is necessary

6 7 2 3 Multistage countercurrent extraction
The countercurrent extraction method is the most common one for separation of liquid mixtures with supercritical fluids as solvents The extraction is performed in pressure columns where the liquid feed and the supercritical fluid flow in countercurrent way

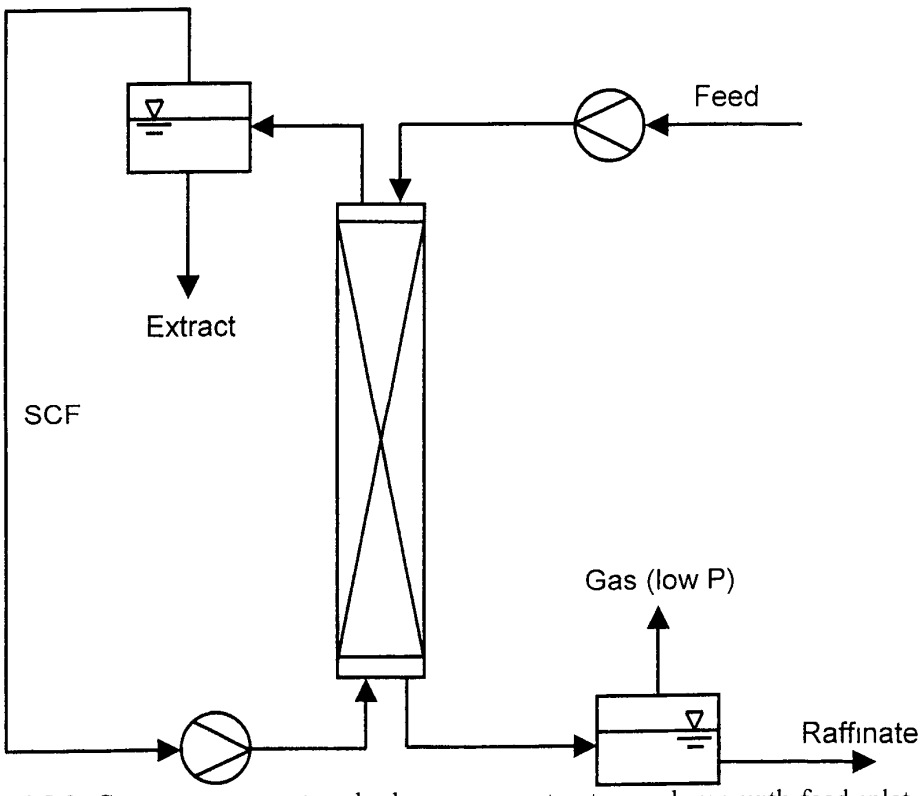

Figure 6 7-3 Continuous operating high pressure extraction column with feed inlet at the top of the column

Normally the supercritical fluid phase is the light one and enters therefore at the bottom of the column The liquid phase the heavy one, can be inserted either at the top or somewhere in the

middle of the column For the case of liquid feeding at the top (fig 6 7-3) the extraction column operates as a stripping column at given pressure and temperature The raffinate is withdrawn at the bottom and separated from the solved gas by pressure reduction to atmospheric pressure in a separator The supercritical fluid with the extracted substances leaves at the top of the column and enters a separator, where pressure and temperature are changed to separate the extract from the supercritical fluid

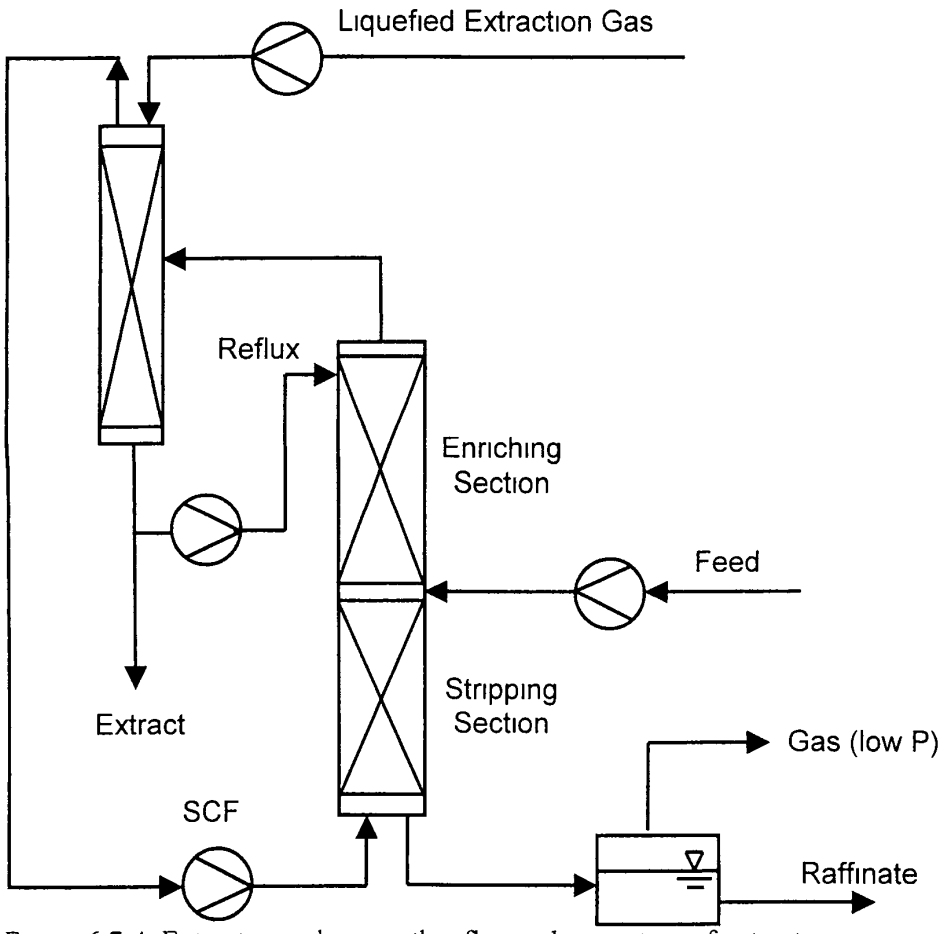

Figure 6 7-4 Extraction column with reflux and separation of extract in regeneration column

In laboratory scale units an enrichment can be achieved by changing the temperature over the column height and producing by this way an internal reflux This method is not adopted for large scale columns, because a heating or cooling from the wall side is not sufficient enough for temperature change of the whole content For columns of industrial size an external reflux has to be used, as given in figure 6 7-4 For this case the column is divided into an enrichment and a stripping section, separated by the entrance of the feed material At the top of the column the supercritical fluid together with the solved substances exit and enter a separator The separator can be designed either like the apparatus for separation in high pressure extraction plants for solid materials or a second countercurrent column, a regeneration column, can be used Extraction gas in liquefied form can be introduced at the top of the

regeneration column to increase separation efficiency and to produce a absolutely pure fluid at the outlet, which is recycled
A specified part of the separated extract, the reflux, is pumped back to the top of the extraction column and the rest of the extract is withdrawn as top product of the extraction column

6 7 3 Modelling of countercurrent high pressure extraction

The gas extraction column can be calculated according to the basic equations on phase equilibria, mass and energy balance and the kinetic equations for mass transfer Based on these equations the number of theoretical steps or the number of transfer units can be determined for a given separation problem Then, having the height of a theoretical plate or of a transfer unit allows to calculate the height of the column needed for separation Calculation of compound concentration along the extraction columns is also possible For more details on the modelling of high pressure extraction columns from liquids, we refer to the extensive book by Brunner [1]

6 7 4 Types of extraction columns

For a good separation efficiency an intensive contact of both phases along the column height is necessary to ensure good mass and heat transfer In general the columns can be divided in four groups

- columns without internals
- plate columns
- packed columns
- columns with energy input

6 7 4 1 Extraction columns without internals

In this case the column operates as a bubble column Either the heavy phase forms droplets (dispersed phase) moving countercurrent to the continuous supercritical phase from the top to the bottom or the supercritical phase is dispersed in form of drops or bubbles moving going up in the continuous liquid phase For both cases the drop sizes and the drop size distribution is essential for separation efficiency The smaller the drop sizes the larger is the mass transfer based on the higher specific surface area
From the viewpoint of construction, devices for producing fine, uniform drop sizes are necessary

6 7 4 2 Plate columns

In plate columns the two phases are intensively mixed on each plate and separated between each plate (Fig 6 7-5) For the distribution of the light phase through the liquid a lot of devices were developed The simplest one is a perforated sieve tray, where the supercritical phase can pass through To avoid weeping of the liquid through the holes different devices like bubble caps or valves (Fig 6 7-6) were developed

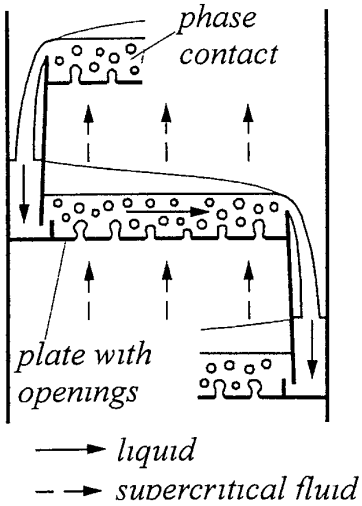

Figure 6 7 5 High-pressure extraction plate column

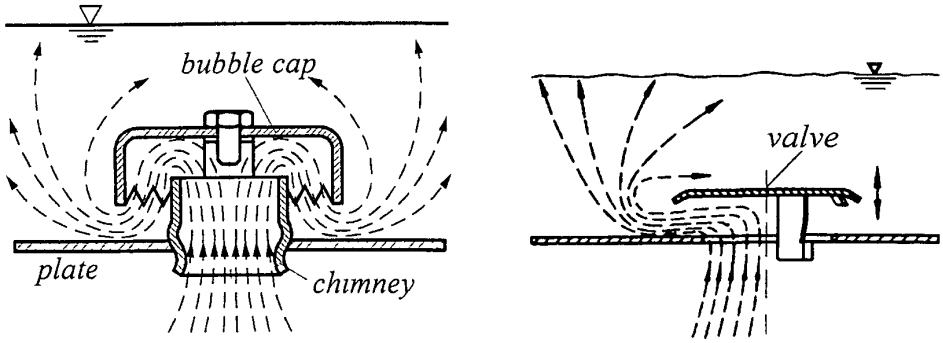

Figure 6 7 6 Bubble cap tray (a) and valve tray (b)

6 7 4 3 Packed columns

A large number of packings of different forms are used for packed columns either as random or structured packings (Fig 6 7-7) The liquid feed wets the surface of the packings and the supercritical gas passes over this thin liquid film By this way a very large phase boundary area is available where mass transfer takes place The material of the packings (plastic, metal, ceramic, steal or glass) influences the degree of wetting

The packing cannot be higher than a maximum value because the liquid has the tendency to pass to the wall of the column Therefore at given sections the liquid has to be collected and re distributed to the next layer of packings A maldistribution of the liquid results in low separation efficiency

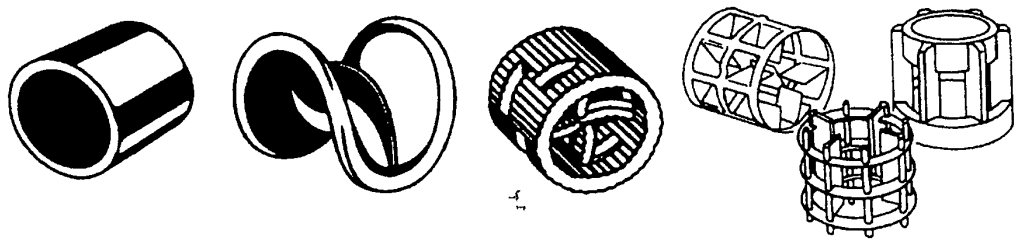

Figure 6 7-7 Examples of different random packings

6 7 4 4 Columns with energy input

The energy input can be performed either by rotation or by pulsation

Extraction columns with rotating internal parts are divided into mixing and separation zones On a vertical shaft stirrers are mounted in the mixing zones giving an intensive contact of the countercurrent flowing phases In the separation zones the phases coagulate before entering the next mixing zone

Pulsed columns are either sieve tray or packing columns The content of the column is brought into vibration so that the moving phases are finely distributed on the sieve trays or on the packings This pulsation causes a higher separation effect compared to the same columns without pulsation For producing the vibration either extra devices are used or the pulsation of the high pressure pumps is great enough to produce the vibration For sieve tray columns another possibility is to move the trays up and down

6 7 5 Applications

Most of the application are up to now in laboratory scale, but the interest in this separation method shows that this process is a very promising way for the future

Brunner et al [1, 2] investigated separations of fatty acids according to chain length, using methyl esters of different carbon chain length from C14 to C18, separation of tocopherols from a by-product of the edible oil production and separation of fish oil esters [3] Stahl et al [4] proposed the supercritical fractionation of orange peel oil and Reverchon et al [5,6] of an orange flower concrete Different authors treated citrus peel oil [7,8] and citrus oil [9-12]

The separation of alcohol from different raw materials like cider [13] wine fermentation broth [14], alcohol water mixtures [15-18] and wine [19-22] is an interesting alternative to distillation processes especially if heat sensitive substances are present Separex company separated the aroma substances out of whisky and cognac, which gives a very interesting product for food industry

Further investigations were done for cleaning of wastewater For an industrial scale the high pressure extraction will only be sufficient if a high contamination in a relatively low waste water stream is available Otherwise this separation method is too expensive, as for flow rates in the range of some m^3/h the investment and operation cost for such a plant become uneconomic

References of section 6 7

1 G Brunner, Gas Extraction, Steinkopf Darmstadt Springer New York, 1994

2 G Brunner, T Malchow, K Sturken, T Gottschau, J Supercrit Fluids 4 (1991) 72

3 V Riha, G Brunner, J Supercrit Fluids 17 (200), 55
4 E Stahl, K W Quirin, D Gerard, Verdichtet Gase zur Extraktion und Raffination, Springer, Berlin, 1987
5 E Reverchon, G Della Porta, G Lamberti, R Taddeo, Proceedings 4th Italian Conference on Supercritical Fluids and their Applications Capri, (1997), 47
6 E Reverchon, G Della Porta, G Lamberti, J Supercrit Fluids 14 (199), 115
7 C Perre, G Delestre, L Schrive, M Carles, in M Perrut, G Brunner (Eds), Proceedings 3rd International Symposium on Supercritical Fluids, Strasbourg, vol 2, (1994), 465
8 M Sato, M Goto, A Kodama, T Hirose, Proceedings 4th Italian Conference on Supercritical Fluids and their Applications, Capri, (1997), 39
9 M Sato, M Goto, T Hirose, in M Perrut, G Brunner (Eds), Proceedings 3rd International Symposium on Supercritical Fluids, Strasbourg, (1994), vol 2, 83
10 M Sato, M Goto, T Hirose, Ind Eng Chem Res 34, (1995), 3941
11 G Brunner, M Budich, T Wesse, V Leibkuchler Proceedings 4th Italian Conference on Supercritical Fluids and their Applications, Capri (1997), 27
12 M Sato, M Kondo, M Goto, A Kodama, T Hirose, J Supercrit Fluids 13, (1998), 311
13 I,Medina, J L Martinez, in M Perrut, G Brunner (Eds), Proceedings 3rd International Symposium on Supercritical Fluids Strasbourg, (1994), vol 2, 401
14 S Fernandes, J A Lopes, A S Reis Machado, M Nunes da Ponte, in M Perrut, G Brunner (Eds), Proceedings 3rd International Symposium on Supercritical Fluids Strasbourg (1994) vol 2 491
15 M Randosz, Fluid Phase Equilibria 29 (1986), 515
16 M Randosz, J Chem Eng Data 31 (1986), 43
17 G Brunner, K Kreim, Ger Chem Eng 9 (1986), 246
18 G Brunner, K Kreim, Chem Ing Tech 57(6) (1985), 550
19 T Gamse I Rogler, R Marr Proceedings 4th Italian Conference on Supercritical Fluids and their Applications, Capri (1997), 191
20 T Gamse, I Rogler, R Marr, J Supercrit Fluids 14 (1999), 123
21 T Gamse, F Steinkellner, R Marr, Proceedings International Meeting of the GVC Fachausschuß "Hochdruckverfahrenstechnik" on High Pressure Chemical Engineering, Karlsruhe, (1999), 255
22 T Gamse, R Marr, in M Perrut and E Reverchon (Eds), Proceedings 7th Meeting of Supercritical Fluids, Antibes / Juan-Les-Pins, vol 2, 579